

UNCLASSIFIED

AD NUMBER

AD890303

LIMITATION CHANGES

TO:

Approved for public release; distribution is unlimited.

FROM:

Distribution authorized to U.S. Gov't. agencies only; Test and Evaluation; NOV 1971. Other requests shall be referred to Air Force Weapons Lab., Kirkland AFB. NM.

AUTHORITY

AFWL ltr 16 Mar 1972

THIS PAGE IS UNCLASSIFIED

AD 890303

AFWL-TR-71-137

AFWL-TR-
71-137

A CALCULATION OF THE BLAST WAVE FROM THE CONSTANT VELOCITY DETONATION OF AN EXPLOSIVE SHEET

Gerald G. Leigh
Major USAF

TECHNICAL REPORT NO. AFWL-TR-71-137

November 1971

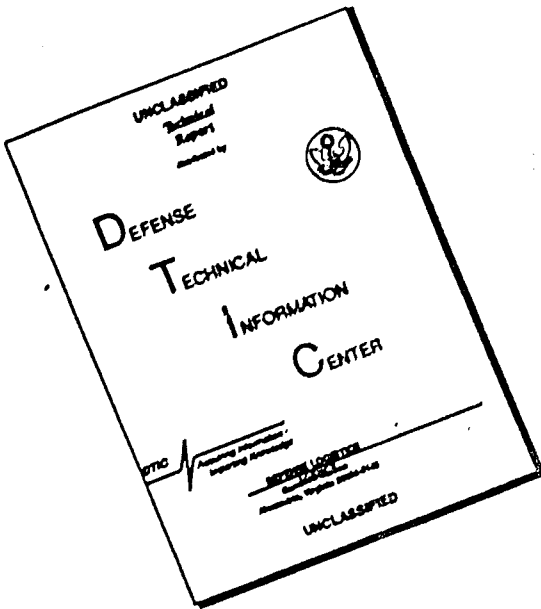
AIR FORCE WEAPONS LABORATORY
Air Force Systems Command
Kirtland Air Force Base
New Mexico



Distribution limited to US Government agencies only because test and evaluation information is discussed in the report (Nov 71). Other requests for this document must be referred to AFWL (DEV), Kirtland AFB, NM, 87117.

274

DISCLAIMER NOTICE



**THIS DOCUMENT IS BEST
QUALITY AVAILABLE. THE COPY
FURNISHED TO DTIC CONTAINED
A SIGNIFICANT NUMBER OF
PAGES WHICH DO NOT
REPRODUCE LEGIBLY.**

AIR FORCE WEAPONS LABORATORY
Air Force Systems Command
Kirtland Air Force Base
New Mexico 87117

When US Government drawings, specifications, or other data are used for any purpose other than a definitely related Government procurement operation, the Government thereby incurs no responsibility nor any obligation whatsoever, and the fact that the Government may have formulated, furnished, or in any way supplied the said drawings, specifications, or other data, is not to be regarded by implication or otherwise, as in any manner licensing the holder or any other person or corporation, or conveying any rights or permission to manufacture, use, or sell any patented invention that may in any way be related thereto.

This report is made available for study with the understanding that proprietary interests in and relating thereto will not be impaired. In case of apparent conflict or any other questions between the Government's rights and those of others, notify the Judge Advocate, Air Force Systems Command, Andrews Air Force Base, Washington, DC 20331.

DO NOT RETURN THIS COPY. RETAIN OR DESTROY.

REF ID: A	
PER	UNIT NUMBER C
NAME	BUA REPORT
INVESTIGATOR	
REPORT DATE	
II	
REF ID: A	
PER	NAME ON R. SHEET
B	

AFWL-TR-71-137

**A CALCULATION OF THE BLAST WAVE FROM THE
CONSTANT VELOCITY DETONATION OF AN
EXPLOSIVE SHEET**

**Gerald G. Leigh
Major USAF**

TECHNICAL REPORT NO. AFWL-TR-71-137

Distribution limited to US Government agencies only because test and evaluation information is discussed in the report (Nov 71). Other requests for this document must be referred to AFWL (DEV), Kirtland AFB, NM, 87117.

FOREWORD

This research was performed under Program Element 62601F, Project 06CB.

Inclusive dates of research were July 1969 through June 1971. The report was submitted 13 October 1971 by the Air Force Weapons Laboratory Project Officer, Major Gerald G. Leigh (DEV).

This report was presented to the Arizona State University Engineering Department in partial fulfillment of the requirements for the degree of Doctor of Philosophy.

The author is deeply grateful to the members of his academic committee and particularly to his advisor, Dr. Donovan L. Evans, for the guidance, suggestions, and encouragement provided throughout this study. Acknowledgement is extended to Mr. Charles E. Needham of the Air Force Weapons Laboratory for his assistance in working with the SHELL and SHPLOT codes. Further acknowledgement is given Captain Gregg Canavan and Lieutenant Stephen Rockwood for their guidance and help in understanding the postdetonation combustion reactions. Acknowledgement is also due Arizona State University and the Air Force Institute of Technology for the opportunity to pursue these studies.

This technical report has been reviewed and is approved.

Gerald G. Leigh

GERALD G. LEIGH
Major, USAF

Chief, Facilities Survivability Branch
Project Officer

William B. Liddicoet

WILLIAM B. LIDDICOET
Colonel, USAF
Chief, Civil Engineering Research
Division

ABSTRACT

(Distribution Limitation Statement B)

Predictions of the blast wave from the constant velocity detonation of a thin explosive sheet have not previously considered the contribution of the post-detonation combustion of the detonation products. This problem is simplified by first considering the explosive material as releasing only energy into an ideal gas medium. This is solved for several energy densities and velocities of detonation. An expression that can predict the shape and location of the shock front from a line source of energy in a hypersonic flow is then developed. The problem is more realistically modelled by considering the explosive sheet to release six distinct mass species, as well as energy, into a mixture of nitrogen and oxygen. Results of this study shift the shock front to a position inside the previously determined shock front. Using the dissociation of molecular oxygen as the determinant for the reaction rate of combustion, and models for material mixing, the contribution of postdetonation combustion (PDC) to the total energy is determined. The mass and energy addition problems were then recomputed with PDC included. Results indicate that while significant amounts of energy are released by PDC, they are small compared to the energy released by the detonation, and there is essentially no contribution from PDC in the early time formation of the blast wave.

CONTENTS

<u>Section</u>	<u>Page</u>
I INTRODUCTION	1
Background	1
Statement of the Problem	3
Approach	7
II THE IDEALIZED PROBLEM	9
Analytic Solution	9
Numerical Solution	21
Results of Numerical Solution	28
Empirical Fit to Numerical Solution	37
III MASS AND ENERGY ADDITION	41
Multi-Material Hydrodynamic Code	41
Multi-Material Equation of State	47
The Computational Problem	52
Computed Results	55
IV POSTDETONATION COMBUSTION	65
Estimate of PDC Energy Release	66
Mixing of Mass Species in SHELTC7	72
Postdetonation Combustion Scheme	93
Computed Results Including PDC	100
V CONCLUSIONS AND RECOMMENDATIONS	105
APPENDIXES	
A. The SHELTC Code	115
B. Additional Plots for the Idealized Problem	170
C. The SHELTC7 Code	198
D. Additional Plots for the Mass and Energy Addition Problem	250
REFERENCES	262

ILLUSTRATIONS

<u>Figure</u>		<u>Page</u>
1	Detonation of Explosive Sheet	5
2	Two-Dimensional View of Detonation of Explosive Sheet	6
3	Line Source of Energy in Hypersonic Flow	10
4	Computational Grid	23
5	Pressure Contour	25
6	Comparison of One-Dimensional Blast Wave Solutions	27
7	Shock Front Location in the XY Plane	29
8	Constant Pressure Contours (Isobars)	30
9	Constant Energy Contours	31
10	Constant Density Contours	32
11	Velocity Vector Field	33
12	Velocity Vector Field with Background Velocity Subtracted	34
13	Numerical Solution for Four Energy Values	36
14	Numerical Solution for Three Velocity Values	38
15	Comparison of Numerical Solution and Empirical Fit	40
16	Equilibrium Constant versus Temperature, K	44
17	Shock Front Location in the XY Plane	57
18	Constant Pressure Contours (Isobars)	58
19	Constant Energy Contours	61
20	Constant Density Contour	62
21	Constant Temperature Contours (Isotherms)	63
22	Comparison of Solutions (Idealized versus Mass and Energy Addition)	64
23	Material Zones behind the Blast Wave	67
24	Constant Mass Contours--Species A (Nitrogen)	79
25	Constant Mass Contours--Species B (Oxygen)	80

ILLUSTRATIONS (cont'd)

<u>Figure</u>		<u>Page</u>
26	Constant Mass Contours--Species C (Carbon Monoxide)	81
27	Constant Mass Contours--Species D (Carbon Dioxide)	82
28	Constant Mass Contours--Species E (Water)	83
29	Constant Mass Contours--Species F (Hydrogen)	84
30	Constant Mass Contours--Species G (Carbon)	85
31	Mass Distribution--Species A (Nitrogen)	86
32	Mass Distribution--Species B (Oxygen)	87
33	Mass Distribution--Species C (Carbon Monoxide)	88
34	Mass Distribution--Species D (Carbon Dioxide)	89
35	Mass Distribution--Species E (Water)	90
36	Mass Distribution--Species F (Hydrogen)	91
37	Mass Distribution--Species G (Carbon)	92
38	Shock Front Location in the XY Plane	94
39	Shock Front Location in the XY Plane	102
40	Shock Front Location in the XY Plane	103
41	Shock Front Location in the XY Plane	104
42	Constant Pressure Contours (Isobars)	107
43	Constant Density Contours	108
A1	SHELL Zoning--Two-Dimensional Axisymmetric Case	119
A2	The SHELL Mesh	122
A3	SHELL Zoning--Two-Dimensional Planar Case	135
A4	Variation of Parameter S_1	137
A5	Variation of Parameter S_2	138
A6	Variation of Parameter S_3	139
A7	Results of S Parameter Study	140
B1	Shock Front Location in the XY Plane	170

ILLUSTRATIONS (cont'd)

<u>Figure</u>		<u>Page</u>
B2	Constant Pressure Contours (Isobars)	171
B3	Constant Energy Contours	172
B4	Constant Density Contours	173
B5	Velocity Vector Plot	
B6	Plot of Velocity Vector with Background Velocity Subtracted	175
B7	Shock Front Location in the XY Plane	176
B8	Constant Pressure Contours (Isobars)	177
B9	Constant Energy Contours	178
B10	Constant Density Contours	179
B11	Velocity Vector Plot	180
B12	Plot of Velocity Vector with Background Velocity Subtracted	181
B13	Shock Front Location in the XY Plane	182
B14	Constant Pressure Contours (Isobars)	183
B15	Constant Energy Contours	184
B16	Constant Density Contours	185
B17	Plot of Velocity Vector with Background Velocity Subtracted	186
B18	Shock Front Location in the XY Plane	187
B19	Constant Pressure Contours (Isobars)	188
B20	Constant Energy Contours	189
B21	Velocity Vector Plot	190
B22	Plot of Velocity Vector with Background Velocity Subtracted	191
B23	Shock Front Location in the XY Plane	192
B24	Constant Pressure Contours (Isobars)	193
B25	Constant Energy Contours	194

ILLUSTRATIONS (cont'd)

<u>Figure</u>		<u>Page</u>
B26	Constant Density Contours	195
B27	Velocity Vector Plot	196
B28	Plot of Velocity Vector with Background Velocity Subtracted	197
D1	Constant Pressure Contours (Isobars)	250
D2	Constant Energy Contours	251
D3	Constant Density Contours	252
D4	Constant Temperature Contours (Isotherms)	253
D5	Velocity Vector Field with Background Velocity Subtracted	254
D6	Mass Distribution--Species A (Nitrogen)	255
D7	Mass Distribution--Species B (Oxygen)	256
D8	Mass Distribution--Species C (Carbon Monoxide)	257
D9	Mass Distribution--Species D (Carbon Dioxide)	258
D10	Mass Distribution--Species E (Water)	259
D11	Mass Distribution--Species F (Hydrogen)	260
D12	Mass Distribution--Species G (Carbon)	261

TABLES

<u>Table</u>		<u>Page</u>
I	Detonation Products from TNT	42
II	Revised Material Accountability List	46
III	Specific Heats for Six Gases and Solid Carbon	48
IV	Molecular Weights of Mass Species	53
V	Mass of Each Species Deposited	53
VI	Internal Energy of Detonation Products	54
VII	Letter Designators for Mass Species	55
VIII	C, H, O, N Reactions with Third Body	95

SECTION I

INTRODUCTION

The problem of predicting the blast effects from explosions has been of interest ever since the use of explosive materials began. Historically, the approach has been one of "trial and error." This has not been very successful until recent years when adequate electronic instrumentation became available. Calculational efforts were rare. Only in the last thirty years have calculations taken any degree of sophistication. Calculations of the blast effects from various explosive materials in several geometric arrays have been completed in the past ten years. Of particular recent interest are the blast effects from a large, relatively thin sheet of explosive material when the detonation is initiated uniformly along one edge and permitted to propagate along the length of the sheet. It is toward the theoretical determination of the blast effects from such an explosive arrangement that this work is directed.

BACKGROUND

Perhaps the most significant early calculation of air-blast phenomena was accomplished by G. I. Taylor in 1941 (1). He considered an instantaneous release of a point source of energy in an ideal gas and was able to find a similarity solution by making a strong shock approximation. Sedov (2) and Von Neumann (3) later confirmed Taylor's results. Lin (4) and Sakurai (5) applied Taylor's technique to the line and

sheet source of energy. The development of an artificial viscosity concept by Richtmyer and Von Neumann (6) provided a means for numerically integrating across shock discontinuities, opening the way for use of modern numerical computation techniques in blast wave calculations. Brode (7) used this technique in his numerical treatment of the point source in ideal gas and was able to extend the solution to much lower overpressures where the strong shock approximation could not be applied. The same problem was addressed independently by Goldstine and Von Neumann (8) using a different numerical computation scheme. A repeat of the point source problem by Brode using a real equation of state for air (9) provided the first realistic calculation of a blast wave in air. Other calculations by Brode, such as the detonation of a sphere of TNT in air (10) and the expansion of a high-temperature, high-pressure sphere of hot gases in air (11), soon followed. All work described thus far has been one-dimensional, generally with spherical symmetry, and has led to the development of numerous one-dimensional hydrodynamic computer codes (12, 13, 14).

In the late 1950's, considerable interest in two-dimensional calculations began to appear. A major contribution by Harlow (15) was his development of the particle-in-cell (PIC) computing method wherein distinct particles of mass are permitted to move through an Eulerian grid in a manner satisfying the conservation equations. From this work have evolved several families of sophisticated two-dimensional

hydrodynamic computer codes useful in solving a variety of problems including hypervelocity impact, supersonic flow, blast wave propagation, etc. The SHELL family of hydrodynamic codes (16, 17) is representative. In the SHELL codes the basic computational scheme is similar to the PIC codes except that the mass distributed throughout the Eulerian grid is considered to be continuous with mass transport from cell to cell being accomplished as a continuum rather than as discrete particles. Numerous blast-wave calculations have been performed using the SHELL codes (18, 19, 20), and development to encompass a greater variety of problems continues.

Perhaps the most sophisticated family of two-dimensional computer codes is AFTON, developed by Trulio (21). These codes can be used for solving problems in continuum mechanics including the blast load deformation and motions of elasto-plastic materials such as soil.

STATEMENT OF THE PROBLEM

In recent years large quantities of explosive materials have been used in the simulation of nuclear blast effects (22, 23). One simulation method of considerable interest utilizes detonating cord wrapped around a flat wooden rack and detonated in an earth cavity (24). It has been proposed to replace the detonating cord with large, relatively thin sheets of explosive materials. The blast-wave properties of sheet explosives are thus of immediate interest.

Consider a sheet of explosive material a few centimeters thick having an infinite length and width. A detonation is

initiated uniformly along one edge and allowed to proceed evenly along the sheet at the inherent velocity of detonation of the explosive material (Figure 1). Viewed along one edge, the sheet approaches a line, and the detonation becomes a point moving along this line. The problem is thus two-dimensional with a plane of symmetry along the center line of the explosive sheet (Figure 2).

The detonation proceeding along the explosive sheet is considered to be a classical Chapman-Jouguet detonation process (37). After proceeding some distance from the point of initiation, the process becomes essentially steady state. As a result of the detonation process, detonation products are produced and a large quantity of explosive energy is released. These hot, primarily gaseous, detonation products expand and compress the surrounding medium, which in most cases is air, resulting in the formation of a shock wave and a particle flow behind the shock. The shock waves moves with the point of detonation and when steady state is reached the shock wave assumes a fixed shape such that the properties behind the wave do not vary with time.

At the onset of expansion of the detonation products a distinct interface exists between these products and the surrounding air. However, as expansion proceeds, this interface becomes less distinct as mixing and diffusion take place. Finally, at considerable distance from the point of detonation, wholesale mixing has occurred and an essentially uniform mixture of gases exists over a large volume.

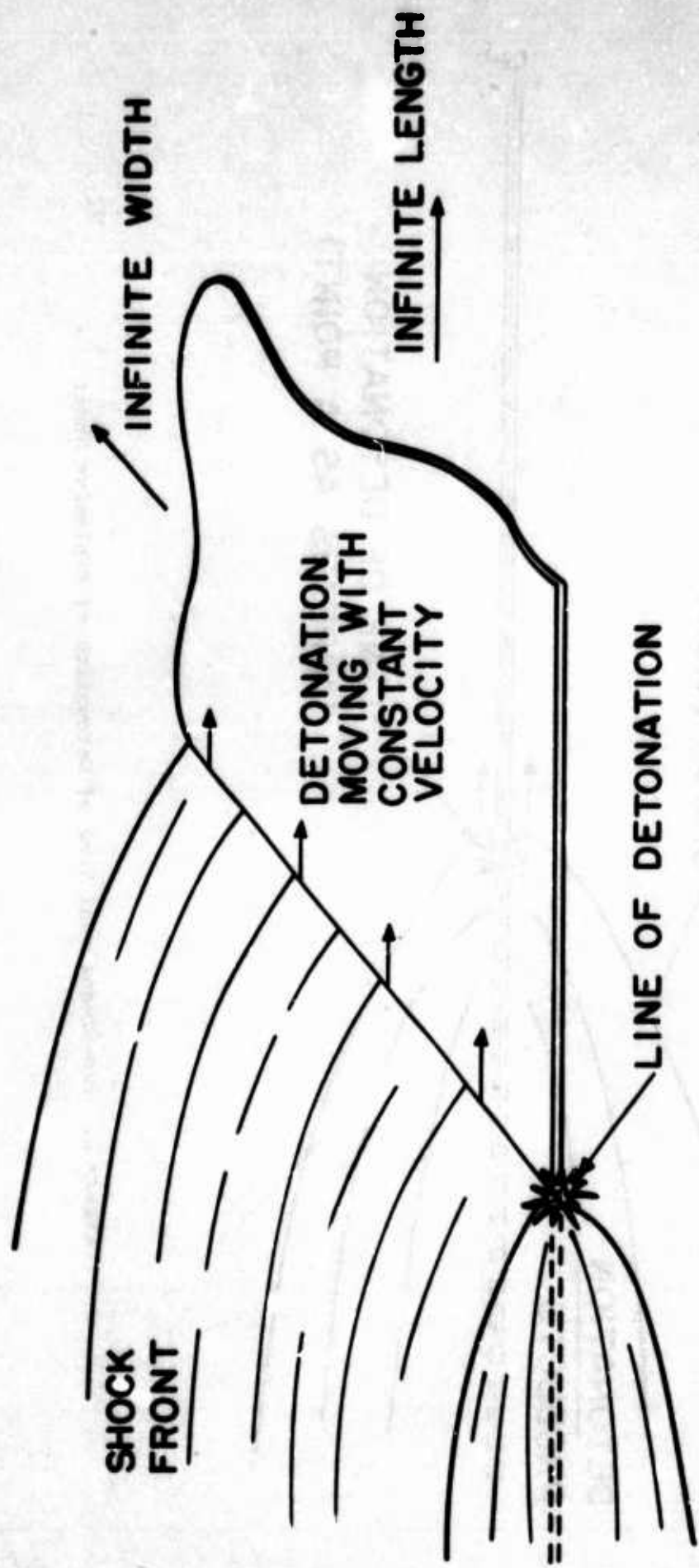


Figure 1. Detonation of Explosive Sheet

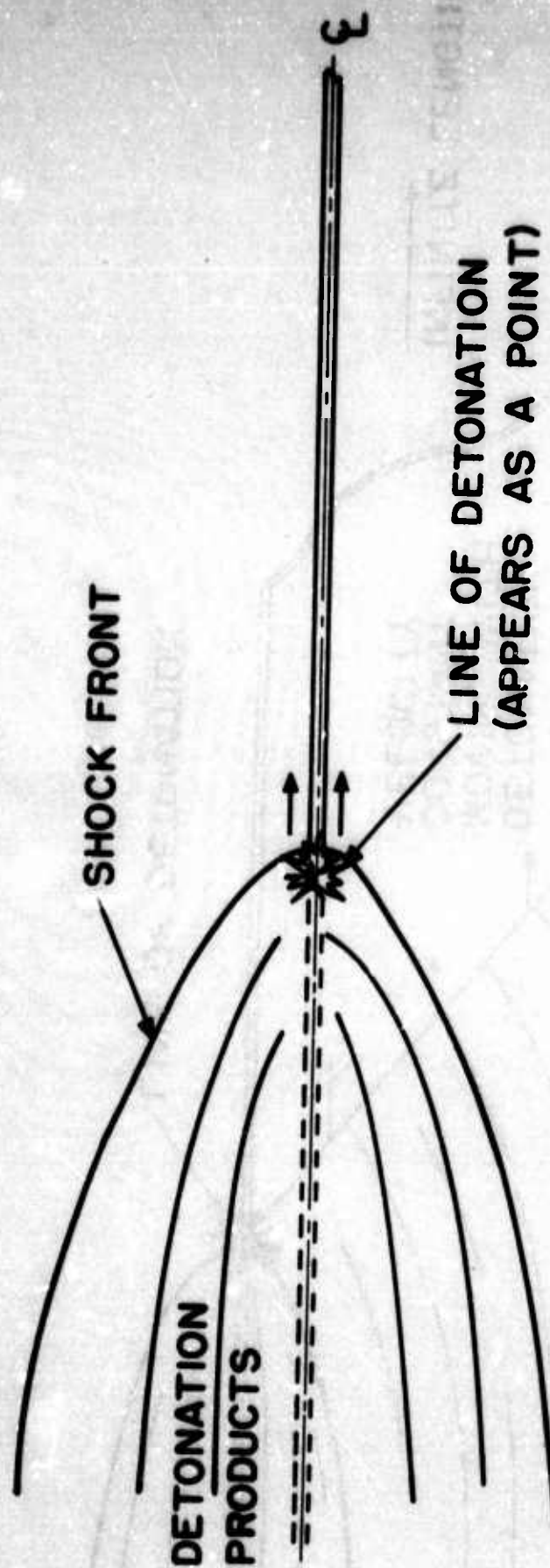


Figure 2. Two-Dimensional View of Detonation of Explosive Sheet

Most explosive materials (TNT, PETN, RDX, etc.) are highly oxygen negative, i.e., all available oxygen is consumed in the detonation reaction and excess combustible materials are released as detonation products. As these hot detonation products mix with the surrounding air, a post detonation combustion (PDC) process occurs and additional energy is released. However, the blast contribution from this PDC energy release is low because the release is distributed over a large spatial volume and over a long period of time. The extent to which this PDC affects the blast wave and the properties behind the shock front is not well known and of considerable interest.

APPROACH

Determining the blast wave properties associated with this explosive arrangement is first approached by idealizing the problem. The sheet of explosive material is considered to have no mass such that the line of detonation becomes a constant line source of energy. The surrounding medium is considered to be an ideal gas. Consideration is given to a closed form analytical solution but little hope of finding such a solution exists. The idealized problem is then solved by using a finite difference computational technique (a SHELL hydrodynamic code). An empirical fit to the numerically obtained solution is obtained.

Next, a more realistic approach to the problem is taken. The explosive sheet is considered to be insignificantly thin, but to have finite mass and energy. A multimaterial

computational code is developed using a multimaterial equation of state. The properties and detonation products from a TNT detonation are used with this code to obtain a solution which accounts for the release of mass from the detonation process.

Finally, the post-detonation combustion of the detonation products by the oxygen in the surrounding air is considered. A simplified combustion scheme is incorporated into the multimaterial code above, and the previous problems are solved with PDC included.

The results of the above three computational schemes are compared and the effect of PDC on the shape and location of the blast wave is determined.

SECTION II

THE IDEALIZED PROBLEM

To examine the blast wave from a sheet explosive in its simplest form we make several idealizing assumptions. Looking at the sheet along one edge (2 dimensions), we first consider the explosive to have no mass and to be a pure source of energy concentrated along a line. The line of detonation becomes a line source of energy perpendicular to the x-y plane (see Figure 3) and appears as a point moving along the plane of symmetry at a fixed velocity and releasing a constant amount of energy for each unit of length that it traverses. The medium through which this point source moves is considered to be an ideal gas. Further clarification can be gained by changing coordinates, fixing the line of detonation in space, and letting the background flow past this point. Since most velocities of detonation (10,000 to 20,000 fps) well exceed the sonic velocity in the surrounding medium the flow produced by the change of coordinates is hypersonic ($M > 10$). The problem is thus reduced to the two-dimensional plane symmetric case of a constant line source of energy in a steady hypersonic flow.

ANALYTIC SOLUTION

The surrounding medium is considered to be an inviscid, compressible ideal gas having a specific heat ratio of 1.4. Heat conduction and gravitational effects are ignored. The governing equations for steady flow are

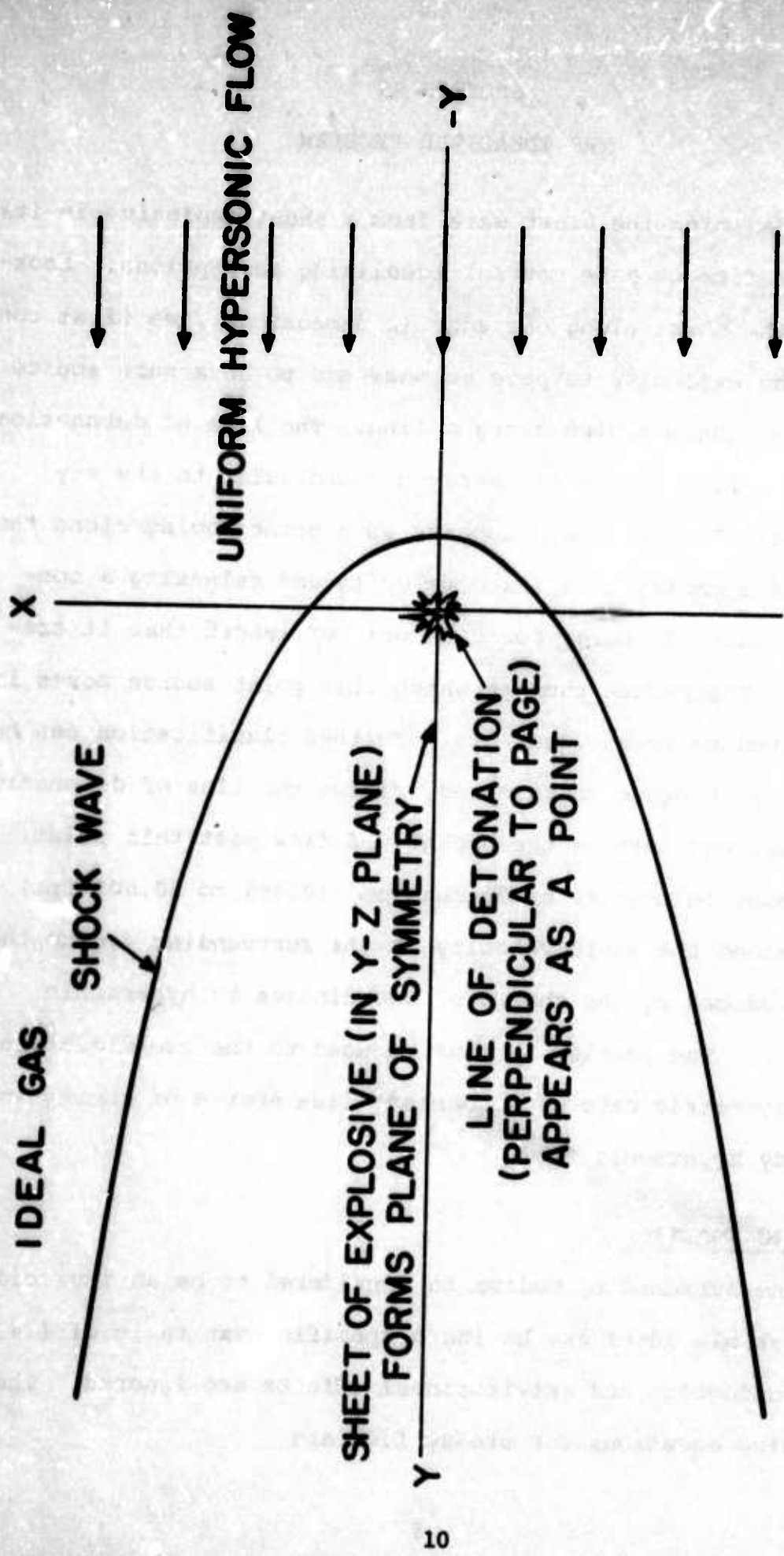


Figure 3. Line Source of Energy in Hypersonic Flow

Continuity

$$\frac{\partial(\rho u)}{\partial x} + \frac{\partial(\rho v)}{\partial y} = 0 \quad (1)$$

Momentum

$$u \frac{\partial u}{\partial x} + v \frac{\partial u}{\partial y} + \frac{1}{\rho} \frac{\partial p}{\partial x} = 0 \quad (2)$$

$$u \frac{\partial v}{\partial x} + v \frac{\partial v}{\partial y} + \frac{1}{\rho} \frac{\partial p}{\partial y} = 0 \quad (3)$$

Energy

$$\rho u \frac{\partial e}{\partial x} + \rho v \frac{\partial e}{\partial y} + p \frac{\partial u}{\partial x} + \frac{\partial v}{\partial y} = E \quad (4)$$

State

$$\bullet = \frac{P}{(\gamma - 1)\rho} \quad (5)$$

where

E is the energy deposited per unit volume per unit time

u and v are the velocities in the x and y directions

P is the pressure

ρ is the density

e is the specific internal energy.

These equations can be combined and reduced to the following form:

$$u^2 - \frac{\gamma P}{\rho} \frac{\partial u}{\partial x} + uv \frac{\partial u}{\partial y} + \frac{\partial v}{\partial x} + v^2 - \frac{\gamma P}{\rho} \frac{\partial v}{\partial y} = (1 - \gamma) \frac{E}{\rho} \quad (6)$$

This is a nonlinear, inhomogeneous, 1st order differential equation with four dependent variables (u , v , P , ρ) and two independent variables (x , y).

Numerous approaches to finding an exact or a nonnumerical approximate solution to these equations have been attempted, but so far without success. The methods tried are described below.

Similarity Approach -- The 1-D, unsteady flow resulting from the instantaneous release of a fixed quantity of energy at a point, along a line, or on a plane is self-similar during the early times when the blast pressures are large compared to the ambient pressure. Numerous investigators (1, 2, 3, 4, 5) have utilized this characteristic to reduce the number of independent variables and thus obtain solutions to blast-wave problems. A similarity solution to the present problem was considered. Following the method of Sedov as described by Korobeinikov (26), the dimensionality of all the variables and parameters in this problem was considered. The number of constants with independent dimensions which could be formed was found to be three. The problem was not self-simulating, then, according to the criteria defined by Korobeinikov, and further consideration of a similarity solution was abandoned.

Hypersonic Flow - Point Explosion Approach -- During the literature search several papers describing the use of point source explosions to simulate hypersonic flow past various bodies were encountered (27, 28). Consideration was given to

using one of these methods with the present problem. Hypersonic flow simulation is based on an "equivalence principle" stated by Hayes and Probstein (29, pg. 37) as the "the equivalence of a 3-D physical problem to a 2-D unsteady problem with a parameter or a 2-D or axisymmetric physical problem to a 1-D unsteady problem with a parameter." Stated in another way, the "equivalence principle" is

"The flow as viewed in any transverse plane is independent of the flow in any other transverse plane. In the 2-D physical case we may liken the flow in a given transverse plane to the flow in a cylinder driven by a piston."

Thus, in the 2-D hypersonic flow over a body, the flow in any transverse plane can be considered as a function of one space dimension and time; the flow in this plane is self-similar. Therefore, it is the same as the flow outward from a point or line source of energy and different energy sources can be used to simulate different bodies in hypersonic flow.

When these concepts were brought to bear on the present problem, it was apparent that the flow in any transverse plane in the present problem is not self-similar and is not independent of any other transverse plane, at least not near the origin or the region between the origin and the forward-most portion of the shock wave.

Hodograph Transformation Approach -- A method in common use for solving compressible flow problems is that of the hodograph transformation as explained by Von Mises (30). In this method, the dependent and the independent variables are interchanged by using a Jacobian of the form

$$J = \frac{\partial x}{\partial u} \frac{\partial y}{\partial v} - \frac{\partial x}{\partial v} \frac{\partial y}{\partial u} \quad (7)$$

When this Jacobian is applied to a homogeneous equation similar to the equation

$$(u^2 - \frac{Y_P}{\rho}) \frac{\partial u}{\partial x} + uv \left(\frac{\partial u}{\partial y} + \frac{\partial v}{\partial x} \right) + (v^2 - \frac{Y_P}{\rho}) \frac{\partial v}{\partial y} = 0 \quad (8)$$

one obtains

$$(u^2 - \frac{Y_P}{\rho}) \frac{1}{J} \frac{\partial y}{\partial v} - \frac{1}{J} uv \left(\frac{\partial x}{\partial v} + \frac{\partial y}{\partial u} \right) + (v^2 - \frac{Y_P}{\rho}) \frac{\partial x}{\partial u} \frac{1}{J} = 0 \quad (9)$$

and since the equation is homogeneous one can multiply out the Jacobian to obtain a linear equation

$$(u^2 - \frac{Y_P}{\rho}) \frac{\partial y}{\partial v} - uv \left(\frac{\partial x}{\partial v} + \frac{\partial y}{\partial u} \right) + (v^2 - \frac{Y_P}{\rho}) \frac{\partial x}{\partial u} = 0 \quad (10)$$

When this approach is tried with the present problem the Jacobian cannot be multiplied out since equation 6 is not homogeneous. One obtains

$$(u^2 - \frac{Y_P}{\rho}) \frac{\partial y}{\partial v} - uv \left(\frac{\partial x}{\partial v} + \frac{\partial y}{\partial u} \right) + (v^2 - \frac{Y_P}{\rho}) \frac{\partial x}{\partial u} = J(1 - \gamma) \frac{\epsilon}{\rho} \quad (11)$$

where $J = J(x, y)$ and is unknown.

We consider the possibility of evaluating the term $J(1 - \gamma)\epsilon$ realizing that ϵ is very small at all locations except near the origin.

$$J = \frac{1}{J} = \frac{1}{\frac{\partial u}{\partial x} \frac{\partial v}{\partial y} - \frac{\partial u}{\partial y} \frac{\partial v}{\partial x}} \quad (12)$$

Consideration of the physics of the problem leads to the conclusion that near the origin

$$\frac{\partial v}{\partial x} = 0 \quad \frac{\partial v}{\partial y} = \text{some finite number}$$

(13)

$$\frac{\partial u}{\partial x} = 0 \quad \frac{\partial u}{\partial y} = \text{some finite number}$$

which results in $j = 0$ and the term $J(1 - \gamma) \frac{E}{\rho}$ goes from essentially zero at all points not near the origin to an infinite value near the origin. The reasoning behind the conclusion that $\partial u / \partial x = 0$ near the origin is that along the x-axis the x-component of velocity drops from the hypersonic value before the shock to a subsonic value immediately behind the shock. Then, since it is flowing against an increasing pressure gradient as it approaches the point source of energy, it continues to decrease in magnitude until it reaches the origin where the line source of energy is located. Then beyond the origin, the x-component of velocity begins to increase because the pressure is now decreasing with increasing x. Thus, $\partial u / \partial x$ must be zero near the origin.

From the above analysis it was concluded that the hodograph transformation could not be used to solve the presented problem.

Von Mises' Approach for a Nonisentropic Hypersonic Flow Around a Body -- Consideration was given to solving the problem of hypersonic flow about a point source using a nonisentropic method described by Von Mises (30). In this method, Von Mises uses the continuity equation and the equation for

the y-component of momentum. He introduces a stream function and then converts these equations to natural coordinates (s , n) that follow the streamlines. That is, the s coordinate is tangent to the streamline and the n coordinate is normal to the streamline at any point in the flow field. He is thus able to obtain an expression relating ψ , P , q , ρ_0 , s and n where q is the component of velocity tangent to the streamline (magnitude of the velocity vector), ψ is the stream function, and ρ_0 is a constant density at some point in the flow field. He then recognizes that while behind a curved shock the entropy is not constant, it is constant along any streamline (for flow around a body) and he uses this fact to obtain an expression relating P and n . After much algebra he is able to obtain an expression of the form

$$\left[1 - \frac{q_x^2}{A^2}\right] \frac{\partial^2 \psi}{\partial x^2} - \frac{2q_x q_y}{A^2} \frac{\partial^2 \psi}{\partial x \partial y} + \left[1 - \frac{q_y^2}{A^2}\right] \frac{\partial^2 \psi}{\partial y^2} = \frac{\rho^2}{\rho_0^2} G^1 - \frac{\rho F^1}{\rho_0^2} \left[\rho_T + \frac{M^2}{\partial S / \partial P}\right] \quad (14)$$

where

q_x , q_y are the respective components of velocity
 A is the local speed of sound
 M is the local Mach number
 G^1 and F^1 are known functions depending on the boundary conditions at the shock.

For a known material (such as a perfect gas) and for flow around a defined body this equation can be solved to obtain the entire flow field.

In attempting to apply this approach to the present problem difficulty was immediately encountered with the entropy equation. Whereas entropy may be constant along a streamline for some of the flow field, there is at least one streamline (at least the one passing through the origin) where entropy is not constant, therefore, this concept could not be applied. It was then decided to try the energy equation (equation 4) to obtain relations between P and n in a manner similar to Von Mises'. However, the energy equation could not be converted to natural coordinates because of the inhomogeneous term containing E which is a function of the spatial coordinates and not of the velocity field.

Approximate Method of Integral Representations -- During the literature search, a Soviet paper by P. I. Chushkin and Li Li-kan (31) was discovered in which they used an approximate method of integral representation to determine the 2-D hypersonic flow of gas about a body. Their method consisted of consolidating the continuity equation, the y -component of momentum equation and the entropy equation ($Ds/Dt = 0$) into a single expression.

$$\frac{\partial p_i}{\partial x} + \frac{\partial q_i}{\partial y} = T_i \quad (i = 1, 2, 3) \quad (15)$$

where

$$P_1 = y^v \rho u \quad Q_1 = y^v \rho v \quad T_1 = 0$$

$$P_2 = y^v \rho u v \quad Q_2 = y^v (\rho v^2 + p) \quad T_2 = v \rho$$

$$P_3 = y^v \rho u s \quad Q_3 = y^v (\rho v s) \quad T_3 = 0$$

and $S = p/\rho^2$ and $v = 0, 1$ for plane or axisymmetric flow, respectively.

$$\xi = \frac{y - y_o(x)}{y_N(x) - y_o(x)} = \frac{y - y_o(x)}{\epsilon(x)}$$

where $y_o(x)$ is the y distance to the body surface at any x and $y_N(x)$ is the y distance to the shock wave at any x and $\epsilon(x) = y_N(x) - y_o(x)$ is the distance between the body and the shock wave and is a function of x only. The result of this transform applied to equation 15 is

$$\frac{\partial}{\partial \xi} [Q_i - P_i(\Sigma \epsilon' + y'_o)] + \frac{\partial (P_i \epsilon)}{\partial x} = T_i \epsilon \quad (i = 1, 2, 3) \quad (16)$$

They next divide the flow region between $y_o(x)$ and $y_N(x)$ into bands of equal width designated by $\xi_0, \xi_1, \xi_2 \dots \xi_N$ where ξ_0 is the body surface and $\xi_N = 1$ is the shock wave. They then integrate equation 16 over these bands to obtain

$$\frac{d}{dx} \epsilon \int_0^{\xi_1} P_i d\xi - P_{i1}(\xi_1 \epsilon' + y'_o) + Q_{i1} + P_{io} y'_o - Q_{io} = \epsilon \int_0^{\xi_1} T_i d\xi \quad (17)$$

and

$$\begin{aligned} \frac{d}{dx} \varepsilon \int_{\xi_{n-2}}^{\xi_n} p_i d\xi &= p_{in}(\varepsilon' \xi_n + y'_o) + Q_{in} + p_{i,n-2}(\varepsilon' \xi_{n-2} + y'_o) \\ - Q_{i,n-2} &= \varepsilon \int_{\xi_{n-2}}^{\xi_n} T_i d\xi \quad (i = 1, 2, 3) \quad (n = 2, 3, \dots, N) \end{aligned} \quad (18)$$

In the above they have used Leibnitz' rule to obtain

$$\int_{\xi_{n-2}}^{\xi_n} \frac{\partial}{\partial x} (p_i \varepsilon) d\xi = \frac{d}{dx} \varepsilon \int_{\xi_{n-2}}^{\xi_n} p_i d\xi - p_i(x, \xi_n) \frac{d\xi_n}{dx} + p_i(x, \xi_{n-2}) \frac{d\xi_{n-2}}{dx} \quad (19)$$

and have assumed the last two terms to be approximately equal for $n-2$ close enough to n .

They then approximate the integrands in the above expressions with 2nd-order polynomials and perform the designated differentiation with respect to x . They thus arrive at a series of ordinary differential equations which can be solved for the slopes of the various flow variables.

In attempting to apply this method to the present problem it was first discovered that the governing equations could not be consolidated into the same general form as equation 15 because $Ds/Dt \neq 0$. The energy equation introduces additional terms in equation 15 (for $i = 3$). Nevertheless, an expression similar to equation 15 is obtained, differing only for $i = 3$.

The transformation, $\xi = (y - y_0)/\epsilon$ was applied and an equation similar to equation 16 obtained. For $i = 3$ it has the form

$$\begin{aligned} \frac{\partial}{\partial \xi} [Q_3 - P_3(\xi \epsilon')] + (\gamma - 2) \frac{P}{\rho} \frac{\partial}{\partial \xi} [(u \xi \epsilon') - v] + \frac{\partial}{\partial x} (P_3 \epsilon) \\ + (\gamma - 2) \frac{P}{\rho} \frac{\partial}{\partial x} (u \epsilon) - 2(\gamma - 2) \frac{P}{\rho} u \epsilon' = \epsilon(\gamma - 1) E \quad (20) \end{aligned}$$

while for $i = 1, 2$, it was identical with equation 16.

In studying the approximation made by dropping the last two terms of equation 19, it can be seen that this approximation is only valid at some distance away from the head of the body. In the region immediately behind the curved shock this approximation is not valid because $d\xi_n/dx$ and $d\xi_{n-2}/dx$ are both large and different. Thus, in the present problem where we are interested in determining the flow immediately behind the curved portion of the shock, we cannot use the approximation. Chushkin and Li-kan avoid this problem by picking up the solution some distance downstream after some other method has been used to obtain the flow around the nose of the body. Even then, an attempt was made to integrate equation 20 in a manner similar to Chushkin and Li-kan. In so doing, one obtains a series of integrals of the form

$$\int_{\xi_{n-2}}^{\xi_n} \frac{P}{\rho} \frac{\partial}{\partial \xi} [(u \xi \epsilon') - v] d\xi$$

$$\int_{\xi_{n-2}}^{\xi_n} \frac{p}{\rho} \frac{\partial}{\partial x} [u \epsilon] d\xi \quad (21)$$

$$\int_{\xi_{n-2}}^{\xi_n} \frac{p}{\rho} u \epsilon' d\xi$$

No method of solving these integrals was discovered and methods of approximating them soon became too cumbersome to be practical.

Termination of Search for Exact Solution -- In view of the fact that this idealized problem was only an introductory portion of the planned dissertation study, it was decided that numerical methods and computerized solutions were the only practical way to proceed.

NUMERICAL SOLUTION

The idealized problem (line source of energy in a hypersonic flow) was next addressed numerically using a hydrodynamic computer code named SHELLTC. In this code the 2-D hydrodynamic equations of continuity, momentum and energy for an inviscid compressible fluid plus an ideal gas equation of state are converted to finite difference form and utilized in a computation algorithm which, in essence, integrates these equations in a time-marching sequence. Pressure, internal energy, mass and two components of velocity are the variables accounted for throughout the flow. (See Appendix A for detailed discussion of SHELLTC.)

The computational solution is started by establishing a grid in cartesian coordinates into which an initial quantity of mass is placed. The mass is distributed uniformly throughout all the cells of the grid and an initial velocity, density and internal energy is assigned to the mass in each cell. This initial loading of the grid represents the background hypersonic flow of the line source problem where the plane of symmetry of the grid represents the center of the infinitely thin sheet of explosive energy (Figure 4). An auxiliary generator code titled CLAMTC is used to construct the grid and to establish the initial flow conditions. The code records this information as the zero cycle on a magnetic tape (the problem tape) which is then used by SHELLTC throughout the computation.

In the computational scheme of SHELLTC, time moves forward in small increments and a small amount of mass transport is accomplished with each time step. Thus, in the background flow, mass moves uniformly from right to left, with the incoming flow from the right being reestablished in the first two rows of cells at the beginning of each time step. Mass is permitted to flow out the left and top boundaries of the grid as dictated by the flow computations.

After the satisfactory background flow is established, deposition of energy begins at the point of detonation. The amount of energy deposited is determined by the strength of the energy source (energy content of the explosive sheet), the detonation velocity and the length of the time step.

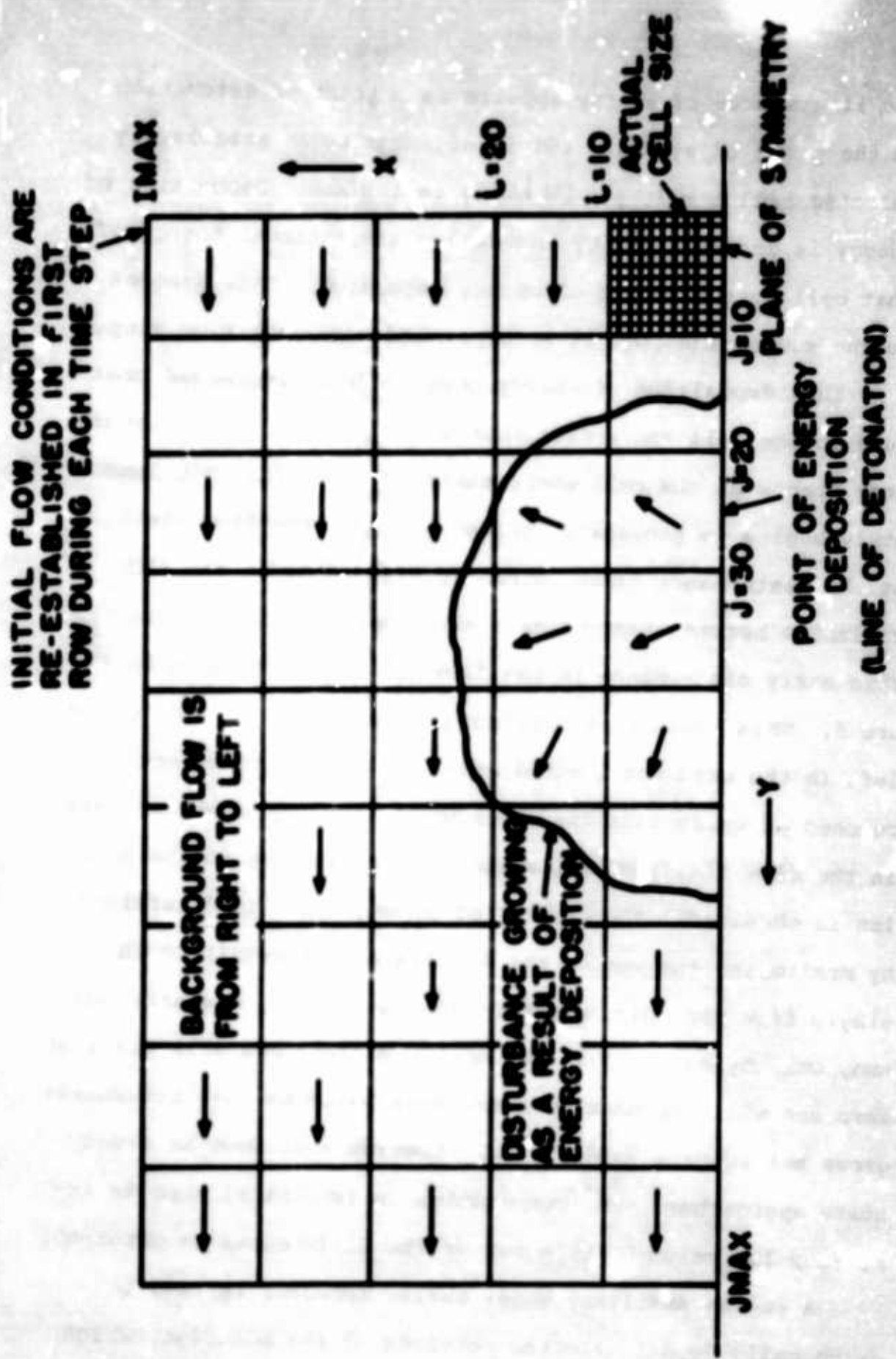
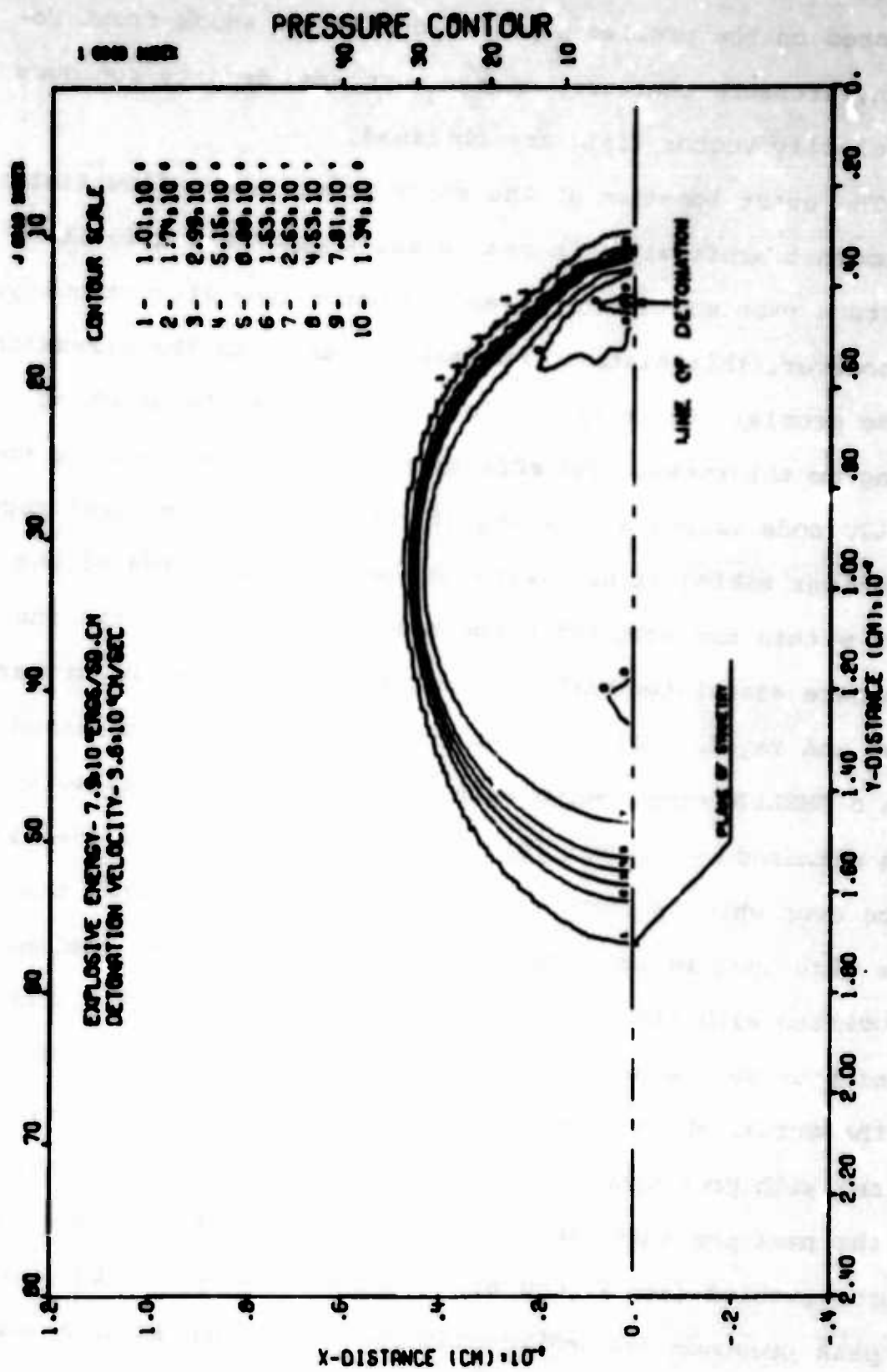


Figure 4. Computational Grid

The line source of energy appears as a point of detonation on the plane of symmetry and is adjacent to an arbitrarily selected cell ($i = 1, j = 15$) along that plane. Deposition of energy is accomplished by increasing the internal energy of that cell by the amount of energy deposited. This process, in the subroutine CDT, is accomplished once each time step.

This deposition of energy results in an increased pressure in the cell and a disturbance in the flow. The disturbance starts at the cell where energy is deposited but immediately begins to propagate farther out into the flow field. As the disturbance grows, dramatic variations in the flow variables become apparent as a shock wave begins to form. This early disturbance in the flow is clearly visible in Figure 5. This shock wave continues to move outward and to the left in the grid until steady-state flow conditions are reached at which time the shock wave becomes a standing wave in the flow field and the steady-state solution to the problem is obtained. The arrival of steady state is determined by monitoring the sum of the differences in magnitude in a single flow variable (pressure was used) along one grid column, cell by cell. This sum of the differences will start at zero and will increase to some large value as the disturbance grows but returns exponentially towards a minimum as steady state approaches. The computation is terminated when an arbitrary low value of this sum of the differences is obtained.

A second auxiliary code, called SHPIOTL, is used to graphically depict selected portions of the solution, which



SHELLTIC CALCULATION OF POINT SOURCE IN HYPERSONIC FLOW
TIME .000160 SEC CYCLE 2185 PROBLEM 21.000

Figure 5. Pressure Contour

is stored on the problem tape. Plots of the shock front location, pressure contours, energy contours, density contours and velocity vector field are obtained.

The exact location of the shock front in the flow field is somewhat arbitrary. In real gases a shock has a finite structure over some distance and is not a true discontinuity. If, however, this distance is small relative to the dimensions of the problem, it is appropriate to consider the shock as having no thickness. The effective viscosity inherent in the SHELLTC code causes a smearing of the shock over several zone dimensions making it necessary to specify a position of the shock within the computed structure. In a study of the shock structure associated with a one-dimensional planar blast wave, Leigh and Yagala (32) compared the shock structure obtained from a SHELLTC computation with the planar similarity solution obtained by Sakurai (5). This work showed that the distance over which a shock was spread was dependent upon the zone size used in the computation and the effective viscosity associated with the code. The location of the shock discontinuity as determined from the similarity solution was chosen as the actual shock location and occurred at positions associated with pressures of between 60 percent and 80 percent of the peak pressure for cell dimensions suitable to the line source problem (see Figure 6). A shock location at 80 percent of peak pressure was arbitrarily chosen for use in this work. The plotting code (SHPLOTL) was adapted to search for the 80 percent of peak pressure point normal to the pressure gradient

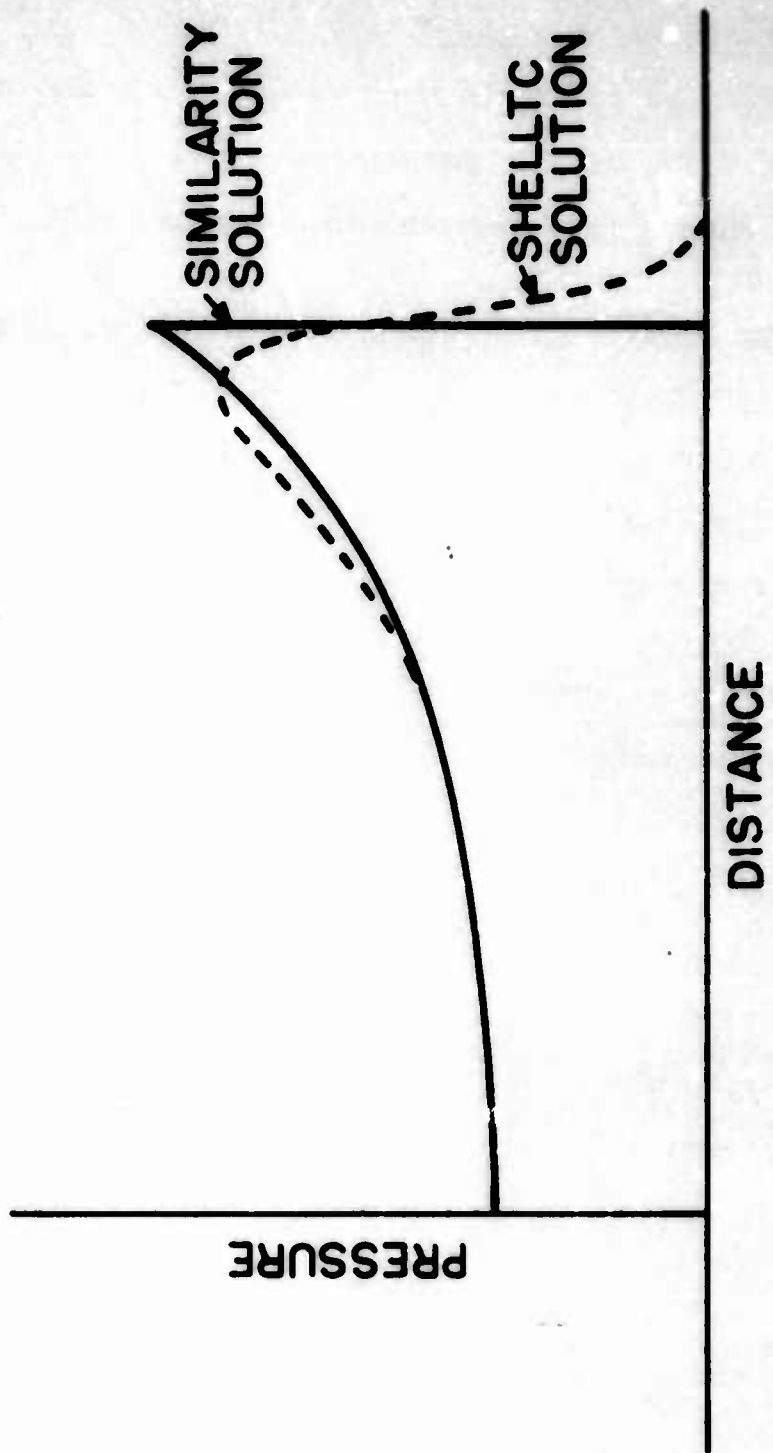


Figure 6. Comparison of One-Dimensional Blast Wave Solutions

and form all such points into a smooth curve. This curve is considered to be the location of the shock front.

RESULTS OF NUMERICAL SOLUTION

In order to solve the point source in hypersonic flow problem, four values of source energy and detonation velocities were chosen for computational solutions.

<u>Energy (ergs/cm²)</u>	<u>Detonation Velocity (cm/sec)</u>
7.9×10^6	7.2×10^5
7.9×10^7	3.6×10^5
7.9×10^8	2.4×10^5
7.9×10^9	1.8×10^5

The selection of velocity was based on an assumed velocity of available detonating sheet explosives (7.2×10^5 cm/sec) and fractions thereof. The explosive energy values were obtained by considering sheets of explosive material 1/4-inch thick having energy densities of 10^7 through 10^{10} ergs per gram and a density of 1.25 gram per cubic centimeter. These choices were quite arbitrary but were influenced by the required computation time, the greater the energy deposition the larger the computation time required. The computer runs were made using a CDC-3400 for the low energy levels and a CDC-6600 for the higher energy levels.

The results for the energy value of 7.9×10^8 ergs/cm² and velocity of 3.6×10^5 cm/sec are shown in Figures 7 through 12. A 240-cm long by 60-cm high grid having cell sizes 3 cm long by 1.5 cm high was used in this computation.

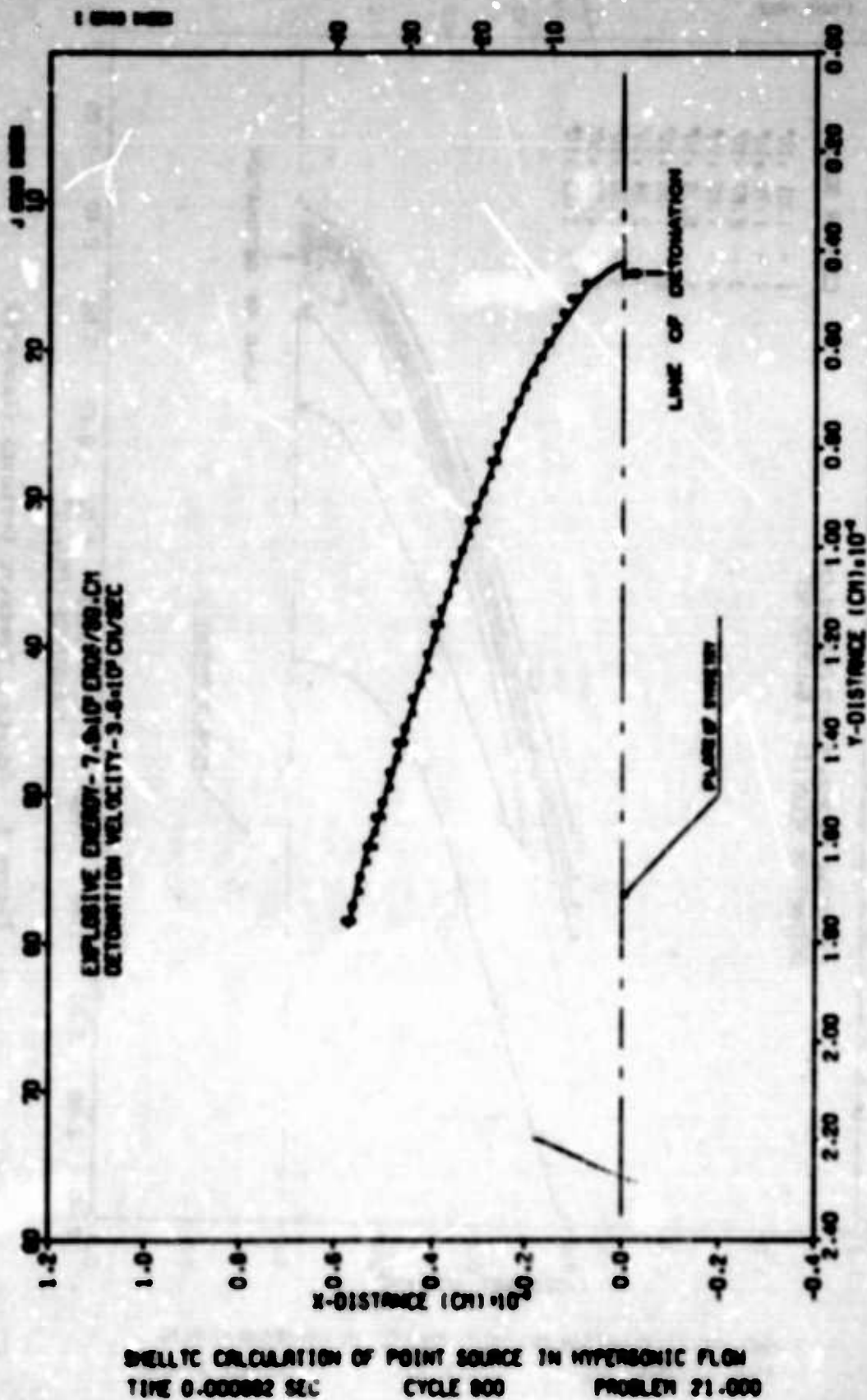


Figure 7. Shock Front Location in the XY Plane

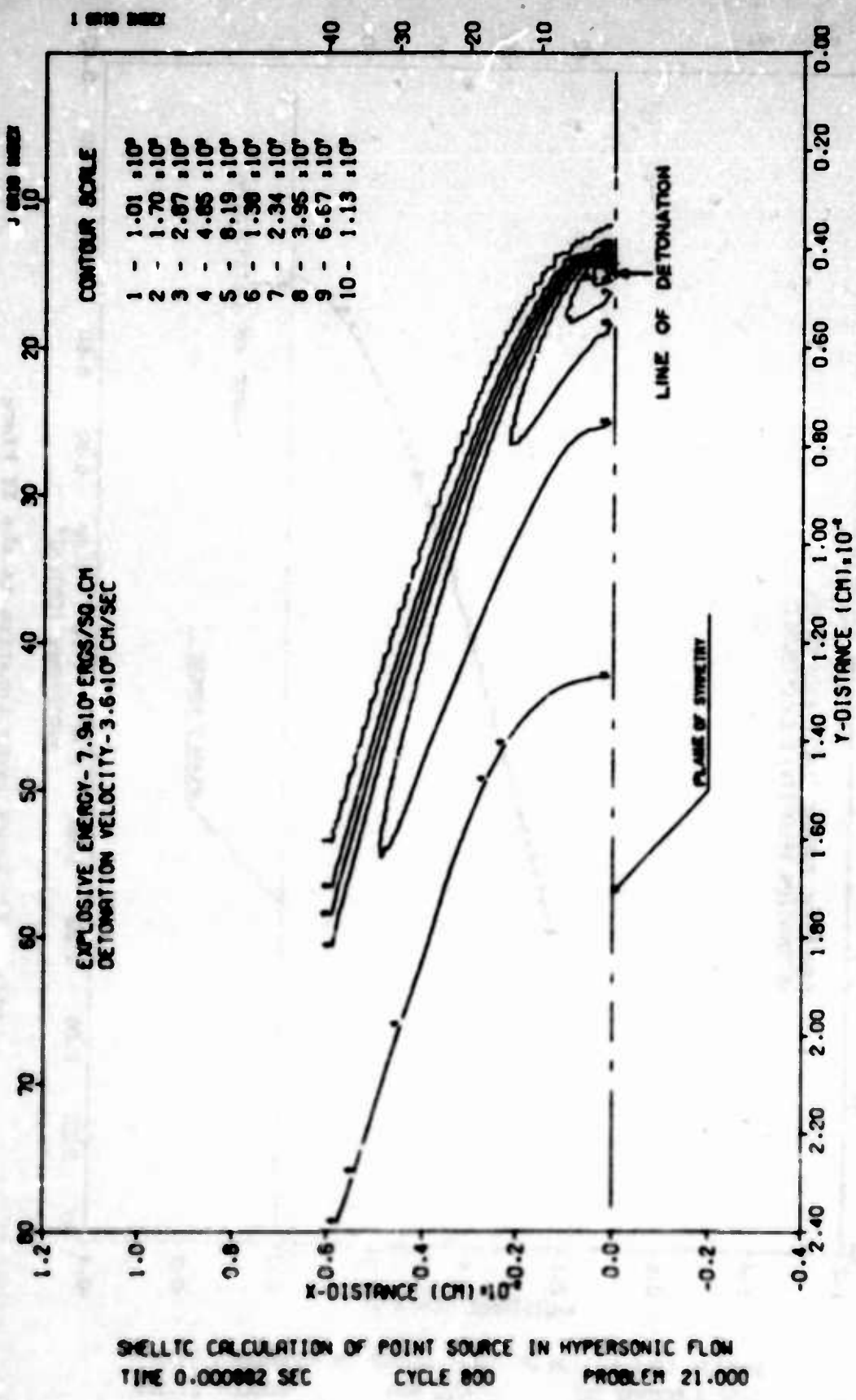


Figure 8. Constant Pressure Contours (Isobars)

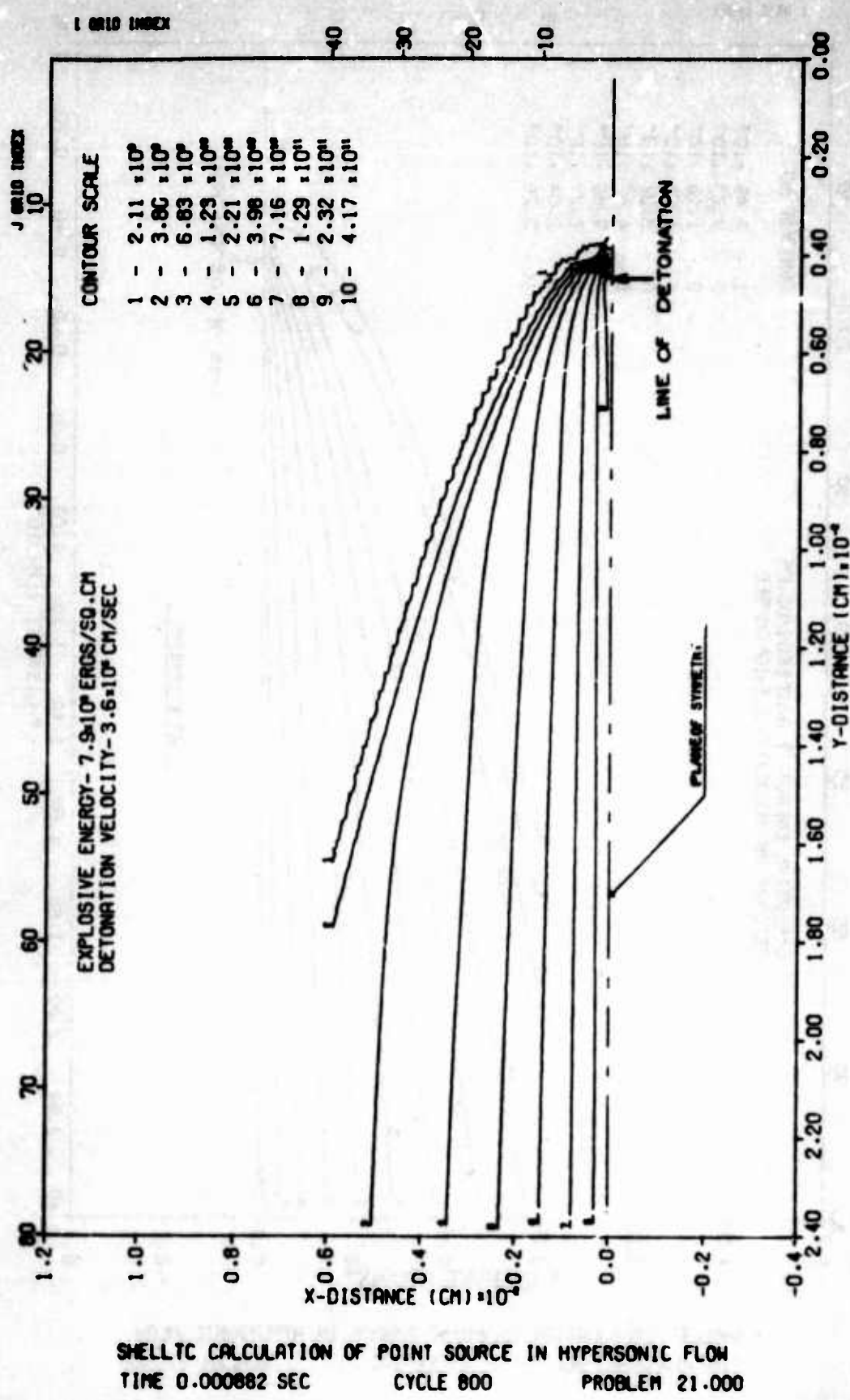
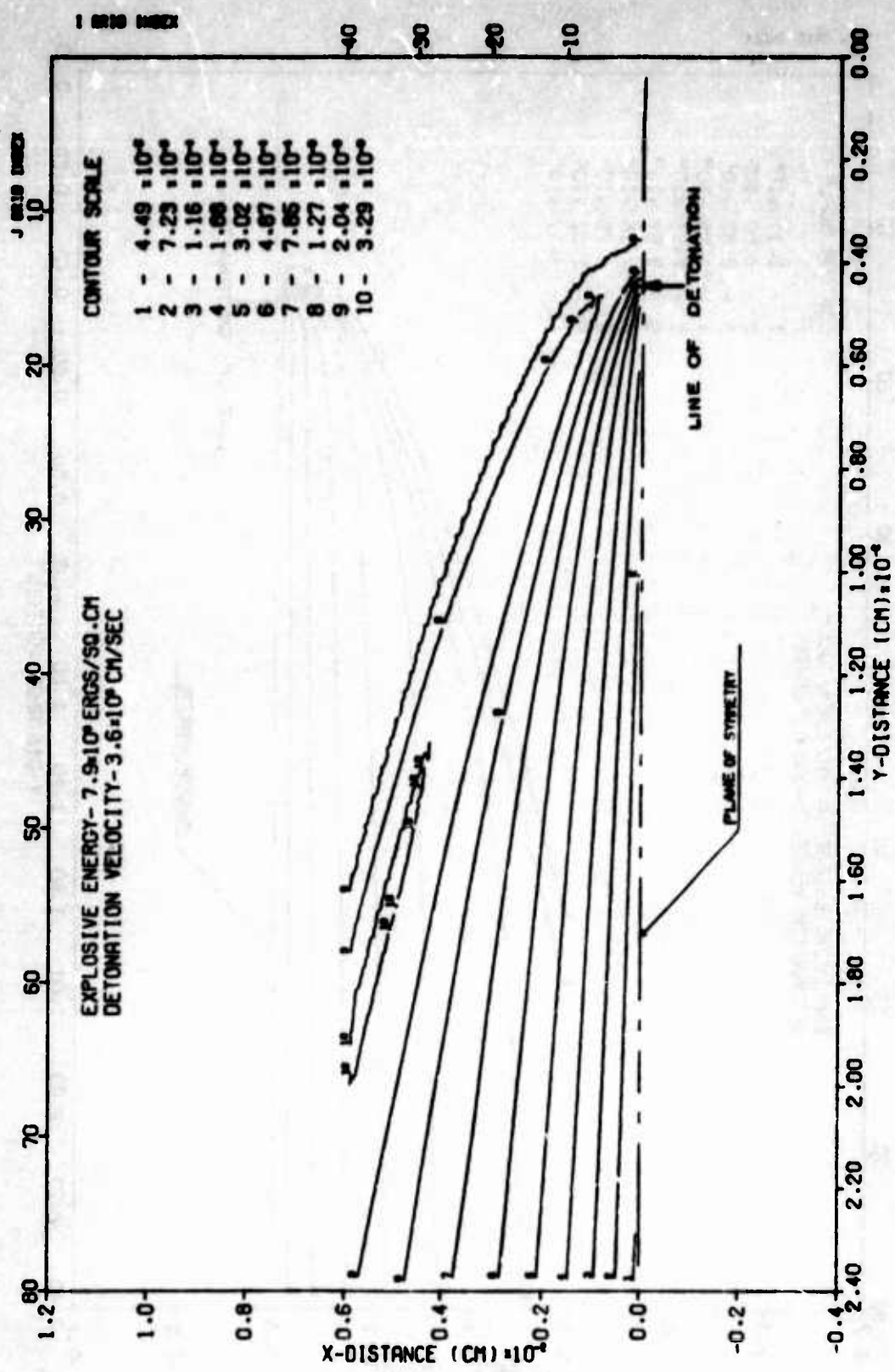
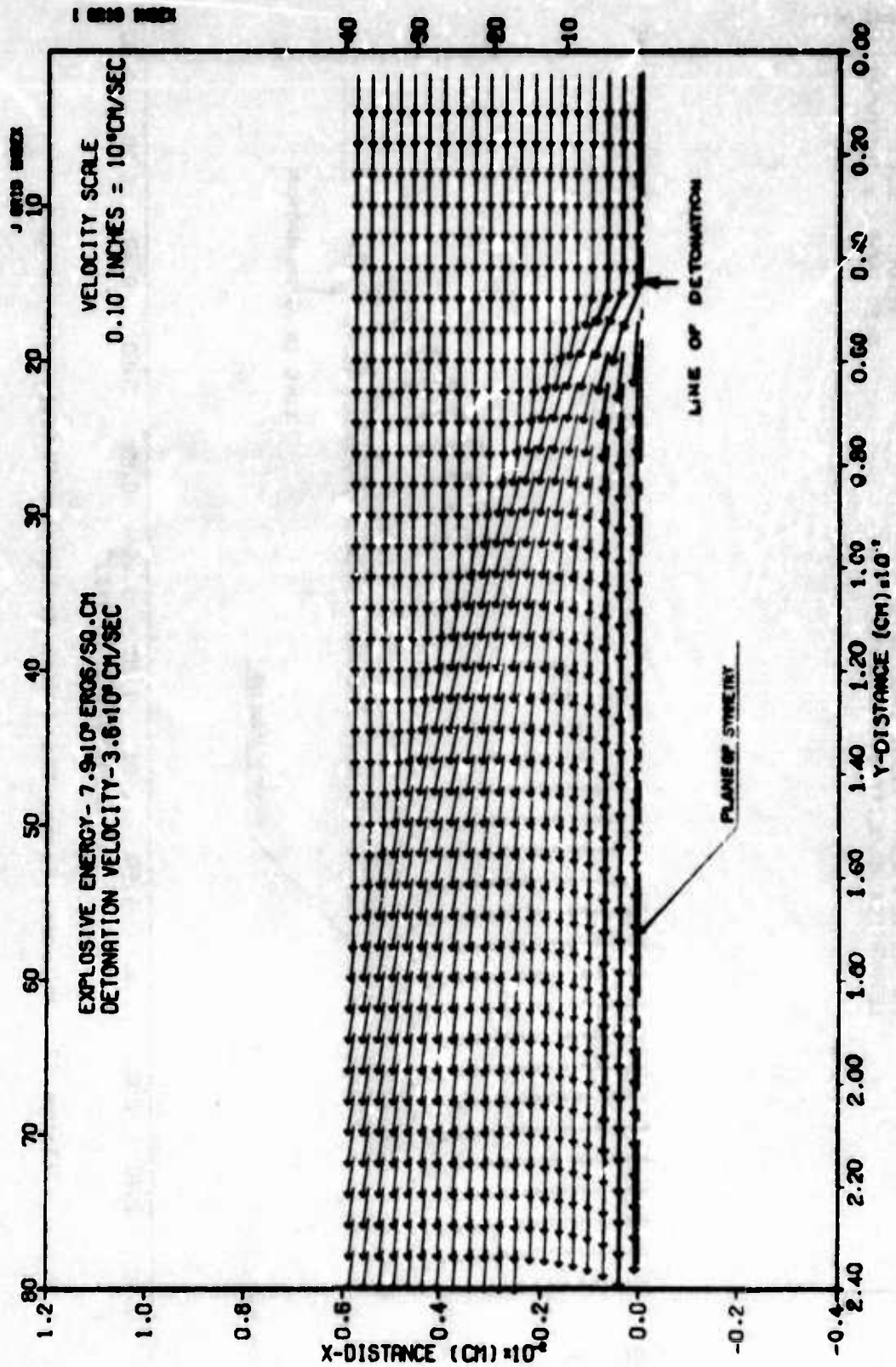


Figure 9. Constant Energy Contours



SHELLTC CALCULATION OF POINT SOURCE IN HYPERSONIC FLOW
TIME 0.000882 SEC CYCLE 800 PROBLEM 21.000

Figure 10. Constant Density Contours



SHELLTC CALCULATION OF POINT SOURCE IN HYPERSONIC FLOW
TIME 0.000882 SEC CYCLE 800 PROBLEM 21.000

Figure 11. Velocity Vector Field

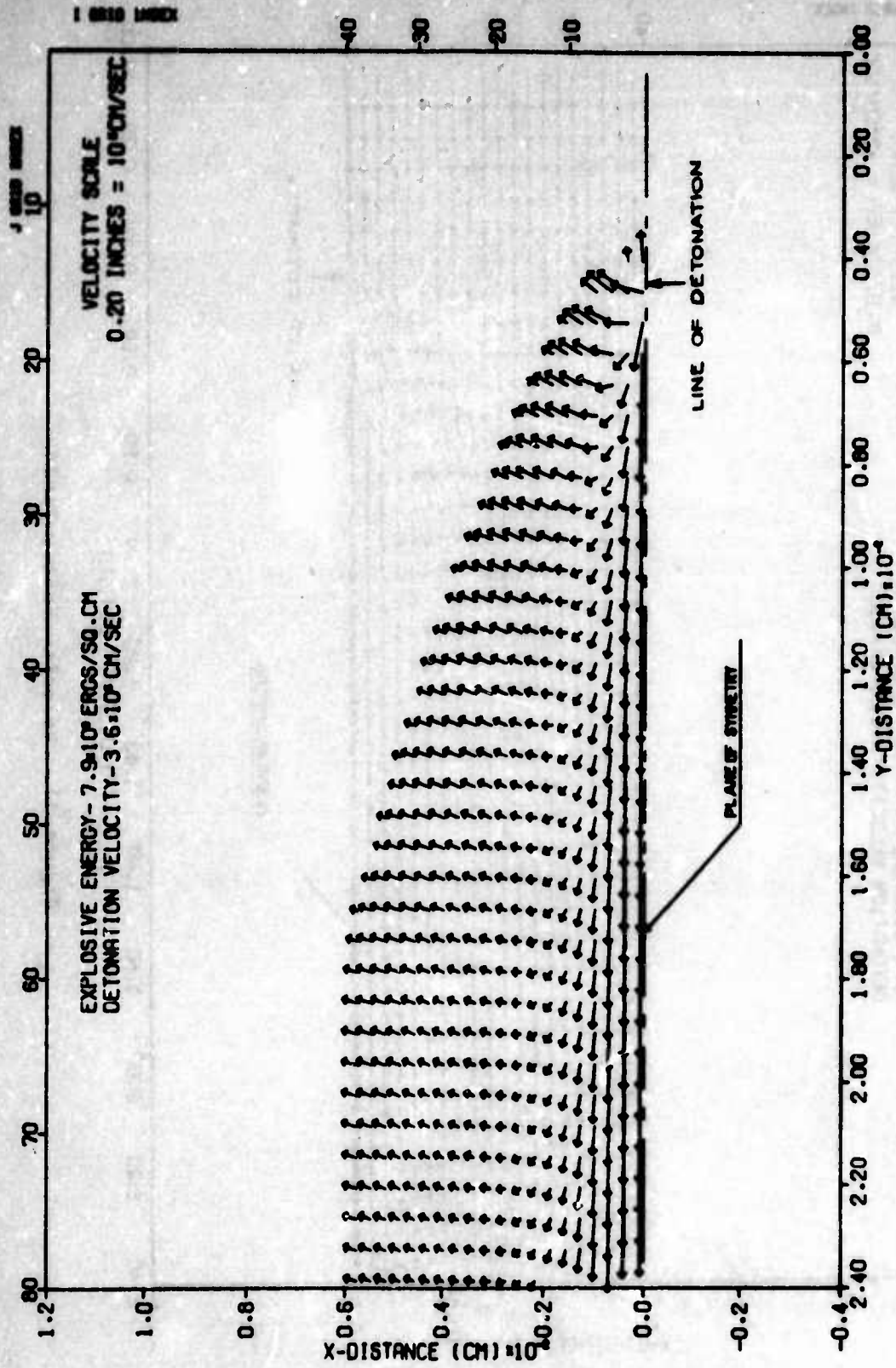


Figure 12. Velocity Vector Field With Background Velocity Subtracted

SHELLTC CALCULATION OF POINT SOURCE IN HYPERSONIC FLOW
 TIME 0.000882 SEC CYCLE 800 PROBLEM 21.000

The solution exceeds the upper grid boundary for χ distances greater than 180 cm. The small oscillations on the pressure, energy and density contours (Figures 8 through 10) are due to the contouring scheme in the SHPLOTL code and do not represent oscillations in the flow field. The disturbance of the uniform flow field is apparent in the velocity vector field of Figure 11. By subtracting the background velocity (uniform flow velocity) one can see in Figure 12 the instantaneous velocity field produced by a line source moving along the plane through still gas. This vector field corresponds to a change of coordinates back to a fixed sheet of explosives with a detonation moving along the sheet.

The shock front locations for the four energy values, all at 3.6×10^5 cm/sec, are superimposed in Figure 13. We observe that the shock forms out in front of the line of detonation in the incoming uniform flow and is normal to the plane of symmetry of the problem. The shock front bends quite dramatically in its departure from the plane of symmetry moving backwards past the line of detonation giving a shock front shape not unlike that formed by a blunt body in hypersonic flow (33). The shock then tends to curve less dramatically, approaching the Mach angle for the free stream hypersonic flow at large distances downstream from the point of detonation. The Mach angle, μ , is defined by Reference 39

$$\sin \mu = \frac{1}{M} \quad (22)$$

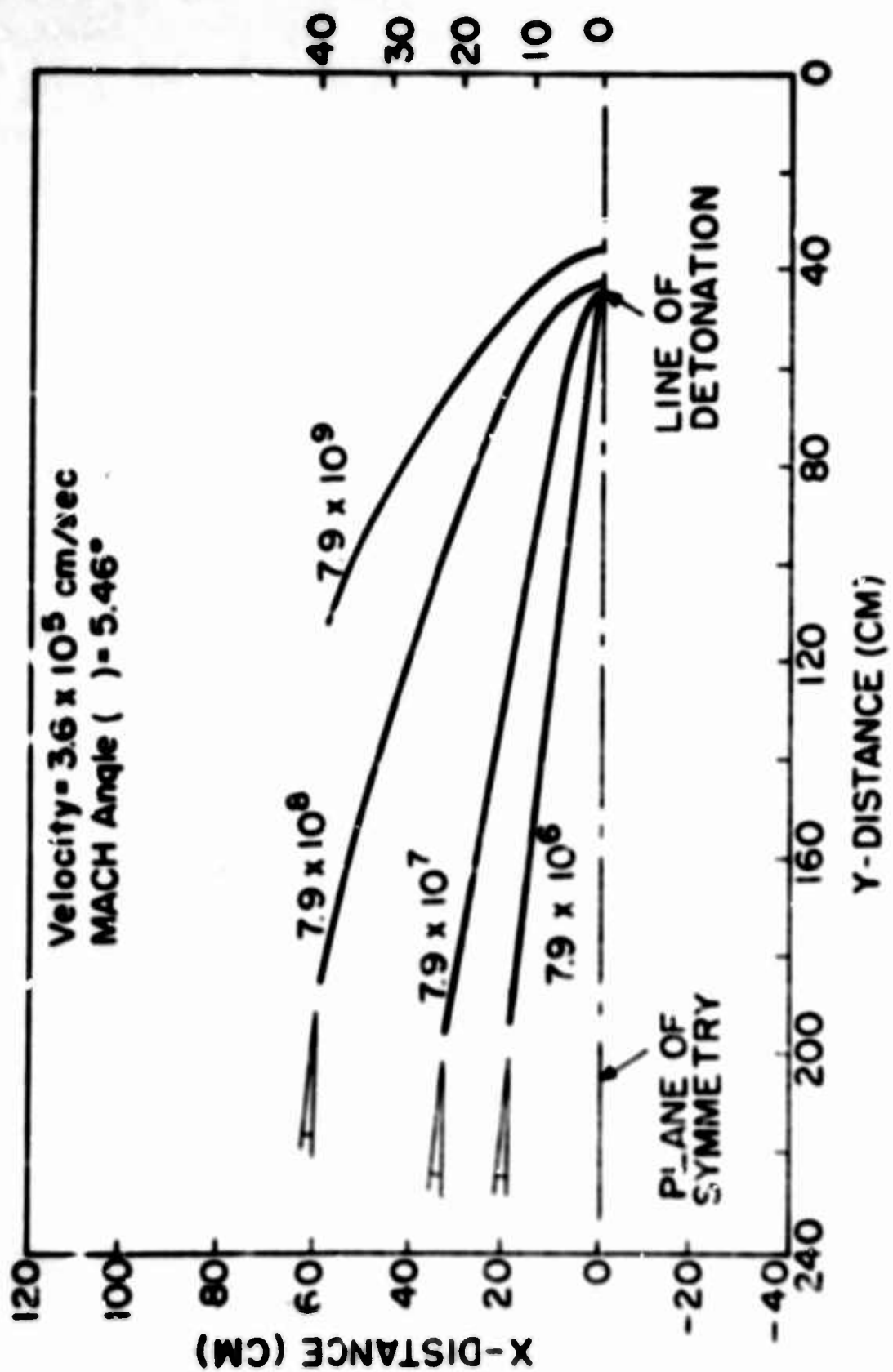


Figure 13. Numerical Solution for Four Energy Values

where M is the Mach number of the free stream flow. The shock front locations for three detonation velocities, all at the energy level 7.9×10^7 ergs/cm², are superimposed in Figure 14. One can observe that a slower hypersonic flow velocity (velocity of detonation) results in a slight shift of the shock upstream and a fuller shock profile.

EMPIRICAL FIT TO NUMERICAL SOLUTION

Several approaches to finding an empirical equation for shock location curves were tried. An attempt at normalizing the numerically obtained curves to find a single curve normalized by energy and velocity was not successful. Polynomials and exponentials did not prove satisfactory. A reasonably satisfactory fit was obtained using

$$Y = A + BX^n \quad (23)$$

where A , B and n are functions of the energy and velocity of detonation. Solution of this relationship for the numerically obtained data points provides the following functional relationships:

$$A = -\left(\frac{E}{a}\right)^{\frac{8}{3}}$$

$$B = 10(\gamma - 0.1 \log_{10} E) \quad (24)$$

$$n = C + \epsilon \log_{10} \left(\frac{E}{10}\right)$$

where

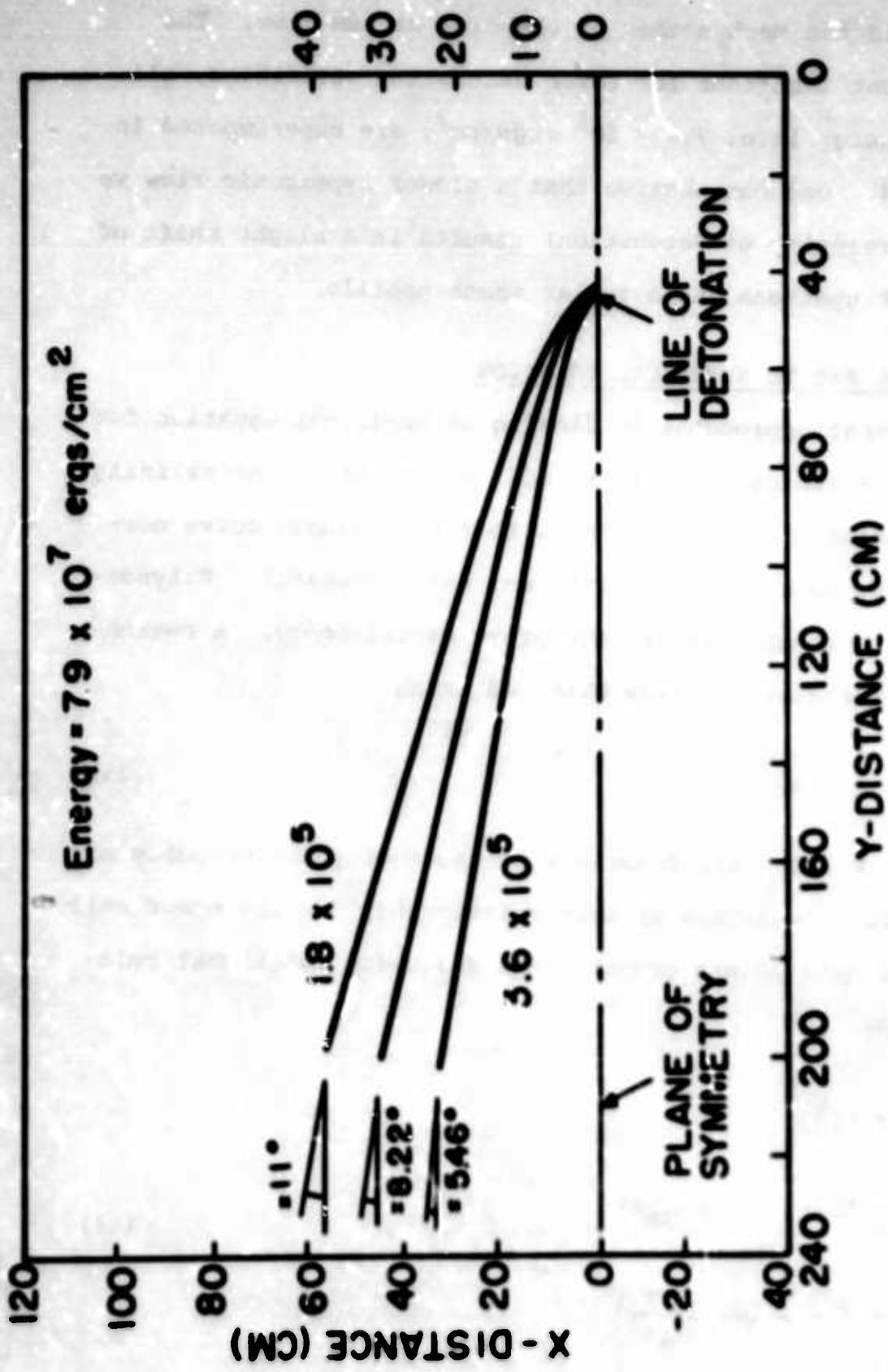


Figure 14. Numerical Solution for Three Velocity Values

E = detonation energy (ergs/cm^2)

V = detonation velocity (cm/sec)

and

$$a = 30.45V - 3.175 \times 10^6$$

$$b = 0.368 - 3.28 \times 10^{-7}V$$

$$\gamma = 1.8 + V \times 10^{-5}$$

$$\theta = 0.315 + V \times 10^{-6}$$

$$\xi = 1.36 - 9.0 \times 10^{-7}V$$

$$\phi = 5.12 \times 10^{-7}V$$

A comparison of the numerically obtained curves with this empirical fit is shown in Figure 15.

Additional plots from solution of the idealized (energy-only) problem for other values of energy and velocity of detonation are provided in Appendix B.

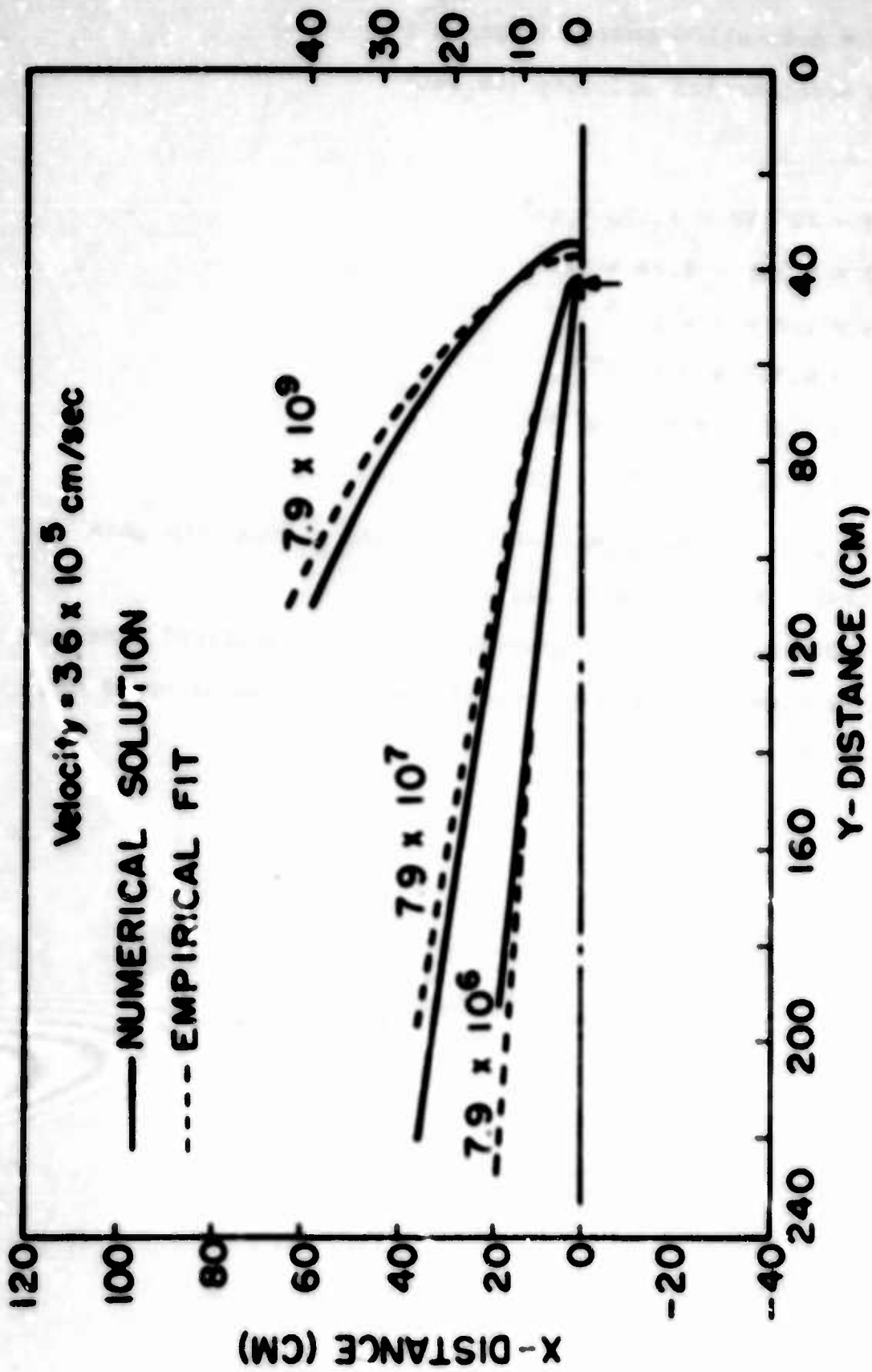


Figure 13. Comparison of Numerical Solution and Empirical Fit

SECTION III

MASS AND ENERGY ADDITION

The results obtained in the previous section are obviously limited by the idealizing assumptions used. A more realistic solution is obtained by recognizing that in the detonation of an explosive material, mass in the form of detonation products is released as well as energy. A further improvement is obtained by treating the gases in the surrounding medium and the gaseous detonation products as ideal gases while recognizing the ratio of specific heats (γ) for each gas as being a temperature-dependent parameter. A method of accounting for several distinct mass species is required in anticipation of the post-detonation combustion problem addressed in the next section. Obviously an analytical solution is not possible and a more sophisticated numerical approach is required.

MULTI-MATERIAL HYDRODYNAMIC CODE

In developing a computer code suitable for the solution of the real sheet-explosion problem, the first order of business is to determine how many different mass species must be accounted for. A review of the detonation products from explosive materials (34) indicates that TNT, one of the most common explosive materials, is also one of the most oxygen negative explosives (i.e., detonation products contain a large amount of combustible materials) and thus should provide a substantial post-detonation combustion effect. The

quantity of each species of detonation product produced is dependent upon the initial density of the explosive material. An initial density of 1.47 gr/cm³ was arbitrarily selected resulting in the release of the nine species of detonation products listed in Table I.

TABLE I
Detonation Products from TNT
(moles of each/kg of TNT)

CO - 1.8	H ₂ - 5.9	CH ₃ OH - 4.29
CO ₂ - 9.5	CH ₄ - 0.1	C(s) - 14.2
H ₂ O - 1.3	NH ₃ - 0.4	HCN - 1.1

By including the oxygen from the surrounding air, ten mass species are involved in the problem (air considered as containing only oxygen and nitrogen). At the detonation temperature (approximately 4000 °K) substantial dissociation occurs, but a short distance from the detonation point the temperature is markedly reduced and much recombination has occurred. It is therefore a reasonable approximation to assume no dissociation throughout the entire blast-wave problem. The quantities of CH₄ and NH₃ are so small that they may be ignored as separate species for which accountability must be maintained. However, the mass associated with the CH₄ and NH₃ must be accounted for. A way of accomplishing this is to assume that these two species dissociate into carbon, hydrogen, and nitrogen, and increase the quantities of each of these species an appropriate amount so that the total mass

remains constant. Thus, the following increase in the quantities of carbon, hydrogen, and nitrogen is made to account for the ignored CH_4 and NH_3 :

$$\text{C} = 0.1 \text{ moles/kg of TNT}$$

$$\text{H}_2 = 0.8 \text{ moles/kg of TNT}$$

$$\text{N}_2 = 0.2 \text{ moles/kg of TNT}$$

By using a similar approach, a further reduction in the number of mass species can be obtained by considering the equilibrium curves (41) for HCN and CH_3OH (Figure 16). At temperatures below 4000 °K these materials dissociate into H_2 , N_2 , CO and solid carbon. Realizing that the temperature will be much less than 4000 °K in all but one or two cells, it is reasonable to assume that this dissociation has occurred at all locations in the flow field. The amounts of H_2 , N_2 , CO, and C(s) are increased an appropriate amount to account for the dissociation of HCN and CH_3OH ; thus keeping the total mass constant.

$$\text{HCN: } \text{H}_2 = 0.55 \text{ moles/kg of TNT}$$

$$\text{N}_2 = 0.55 \text{ moles/kg of TNT}$$

$$\text{C} = 1.1 \text{ moles/kg of TNT}$$

$$\text{CH}_3\text{OH: } \text{CO} = 4.29 \text{ moles/kg of TNT}$$

$$\text{H}_2 = 8.58 \text{ moles/kg of TNT}$$

The total number of species to be accounted for can then be reduced to the seven listed in Table II.

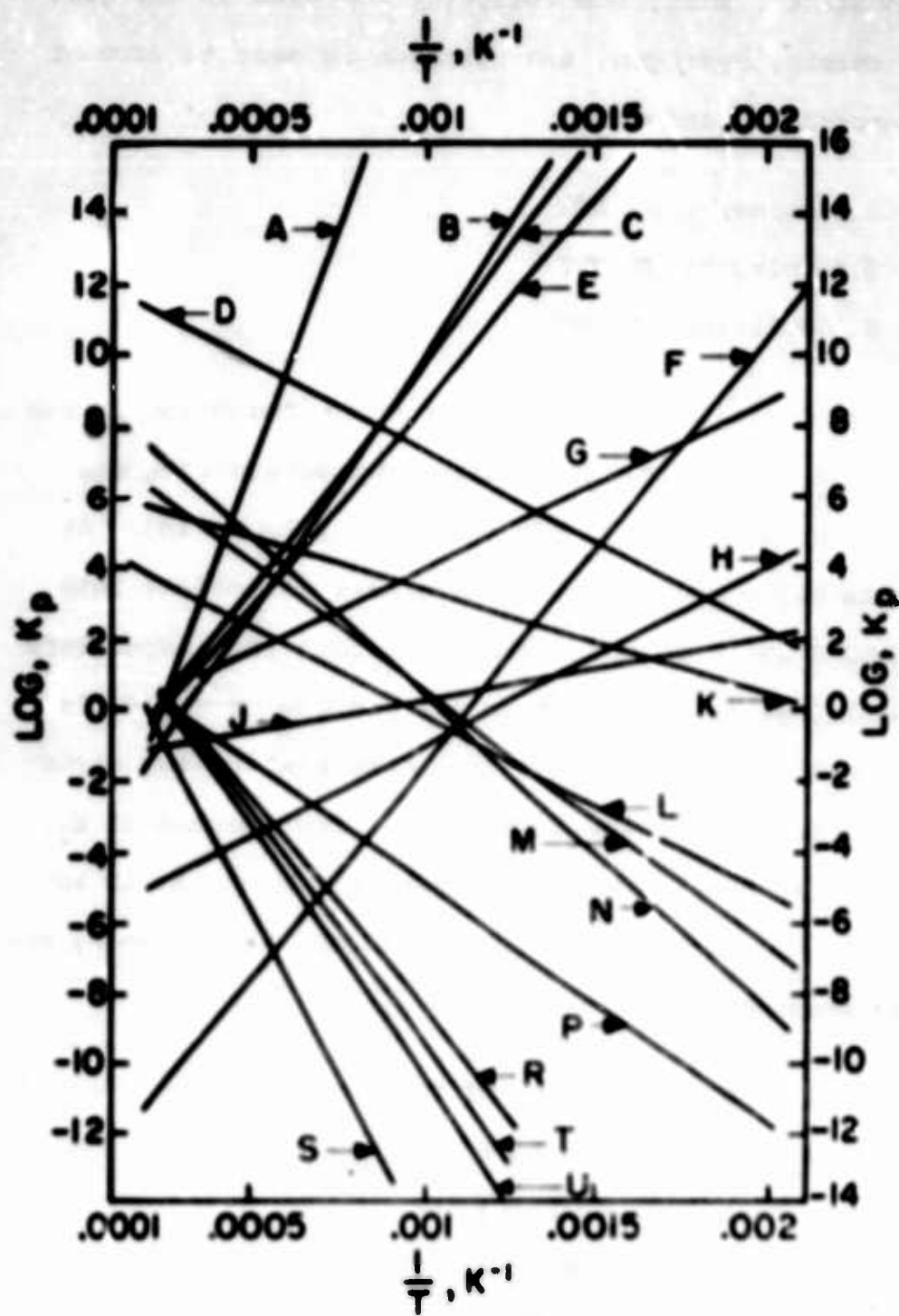


Figure 16. Equilibrium Constant versus Temperature, K

See Key, page 45.

KEY:

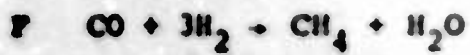
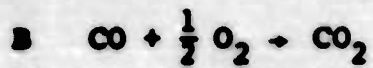


TABLE II
Revised Material Accountability List
(moles/kg of TNT)

$\text{CO} = 6.05$	$\text{H}_2\text{O} = 1.3$	O_2 (background flow only)
$\text{CO}_2 = 9.5$	$\text{N}_2 = 6.65$	
$\text{H}_2 = 9.93$	$\text{C(s)} = 15.4$	

Thus, a seven-material hydrodynamic code could be used, within limitations, to approximate a more realistic solution of the blast wave formed by the explosion of a TNT sheet.

A multi-material version of the SHELL code, called RADISH 5, was already in existence at the start of this work (35). This code has the capability of determining the inviscid, compressible hydrodynamic behavior of five distinct mass species and includes effects of radiation diffusion. It is limited to axisymmetric coordinates as was SHELL OIL but includes temperature as another dependent variable for which accountability is maintained in each cell (in addition to pressure, mass, internal energy, and two components of velocity as in SHELL OIL).

In developing a computer code for the sheet explosion problem, RADISH 5 was used as the basic vehicle. The radiation diffusion portions were deleted and the code modified to operate in either axisymmetric or cartesian coordinates. It was expanded to accommodate seven materials, and a mass and energy deposition scheme was included. This revised code, titled SHELTC7, is the primary tool for use in this and the following section (see Appendix C for details of SHELTC7).

MULTI-MATERIAL EQUATION OF STATE

In using SHELTC7, a multi-material equation of state is required which will provide the pressure and temperature of the mixture of detonation products and air when the internal energy and quantity of each type of mass are known. Such an equation of state was developed, assuming the mixture to consist of six gases and solid carbon where the gases obey the ideal gas equation

$$P = \frac{nRT}{V} \quad (26)$$

where

P = pressure

n = number of moles

R = ideal gas constant

T = temperature

V = specific volume

and whose ratios of specific heats are functions of temperature.

$$\gamma = C_p/C_v = \gamma(T) \quad (27)$$

C_p and C_v data for the six gases listed in Table II are provided in the JANAF Thermochemical Tables (38) for temperature ranges of interest. C_v data for solid carbon are available in Reference 37. A polynomial fitting routine was used to obtain the expressions for C_p and C_v as functions of temperature listed in Table III. These C_p and C_v expressions were

TABLE III

Specific Heats for Six Gases and Solid Carbon

N_2	$C_p = 6.393 + (1.7789 \times 10^{-3})T - (4.102 \times 10^{-7})T^2 + (3.1875 \times 10^{-11})T^3$
	$C_v = 4.4163 + (1.7675 \times 10^{-3})T - (4.034 \times 10^{-7})T^2 + (3.0933 \times 10^{-11})T^3$
O_2	$C_p = 6.6046 + (1.8603 \times 10^{-3})T - (3.6125 \times 10^{-7})T^2 + (2.5902 \times 10^{-11})T^3$
	$C_v = 4.608 + (1.8774 \times 10^{-3})T - (3.6968 \times 10^{-7})T^2 + (2.6853 \times 10^{-11})T^3$
CO	$C_p = 6.4114 + (1.8637 \times 10^{-3})T - (4.4326 \times 10^{-7})T^2 + (3.5074 \times 10^{-11})T^3$
	$C_v = 4.4239 + (1.8638 \times 10^{-3})T - (4.4233 \times 10^{-7})T^2 + (3.4856 \times 10^{-11})T^3$
CO_2	$C_p = 7.8268 + (5.9678 \times 10^{-3})T - (1.5678 \times 10^{-6})T^2 + (1.3213 \times 10^{-10})T^3$
	$C_v = 5.8423 + (5.9368 \times 10^{-3})T - (1.5217 \times 10^{-6})T^2 + (1.2629 \times 10^{-10})T^3$
H_2	$C_p = 6.5548 + (8.6152 \times 10^{-4})T - (2.7312 \times 10^{-8})T^2 - (3.1196 \times 10^{-12})T^3$
	$C_v = 4.5507 + (9.0598 \times 10^{-4})T - (4.9424 \times 10^{-8})T^2 - (3.1041 \times 10^{-12})T^3$
H_2O	$C_p = 6.7245 + (3.9967 \times 10^{-3})T - (7.4975 \times 10^{-7})T^2 + (4.9546 \times 10^{-11})T^3$
	$C_v = 4.7832 + (3.9428 \times 10^{-3})T - (7.9342 \times 10^{-7})T^2 + (5.4627 \times 10^{-11})T^3$

Solid Carbon

$$\begin{array}{ll} T < 1600 & \bar{C}_v = 0.8 + 0.002556T \\ T \geq 1600 & \bar{C}_v = 4.2 + 4.09 \times 10^{-4}T \end{array}$$

Units are calories
gm-°K

formed into computational subroutines to the main equation of state subroutine so that for any temperature, gamma can be computed for each mass specie.

$$\gamma(T) = \frac{C_p(T)}{C_v(T)} \quad (28)$$

The governing equations used in the equation of state subroutine are

$$P = (\gamma_i - 1) \frac{I_i}{V_i} \quad (i = 1, 2, \dots, 6) \quad (29)$$

$$P = n_i \frac{RT}{V_i} \quad (i = 1, 2, \dots, 6) \quad (30)$$

$$V_i = \frac{V_i}{m_i} \quad (i = 1, 2, \dots, 6) \quad (31)$$

$$P_i = n_i \frac{RT}{V} \quad (i = 1, 2, \dots, 6) \quad (32)$$

$$P = \sum_{i=1}^6 P_i \quad (i = 1, 2, \dots, 6) \quad (33)$$

$$I = \sum_{i=1}^6 m_i I_i \quad (i = 1, 2, \dots, 6) \quad (34)$$

$$m = \sum_{i=1}^6 m_i \quad (i = 1, 2, \dots, 6) \quad (35)$$

$$n_i = \frac{m_i}{M_i} \quad (i = 1, 2, \dots, 6) \quad (36)$$

where

P = cell pressure

P_i = partial pressure of i th gas specie

v_i = specific volume of i th gas specie

V = cell volume

v_i = partial volume of i th gas specie

I = total internal energy of cell

I_i = specific internal energy of i th gas specie

M = total cell mass

m_i = mass of i th specie

M_i = molecular weight of i th gas species

γ_i = specific heat ratio of i th gas specie

Combining equations 28, 29, and 30 to eliminate $P V_i$ we obtain

$$I_i = \frac{n_i RT}{(\gamma_i - 1)m_i} \quad (37)$$

Using this in equation 33 along with equation 35 we obtain

$$I = \sum_{i=1}^6 I_i m_i = \sum_{i=1}^6 \frac{n_i m_i RT}{(\gamma_i - 1)m_i} \quad (38)$$

$$I = RT \sum_{i=1}^6 \frac{m_i}{M_i (\gamma_i - 1)} \quad (39)$$

Finally

$$T = \frac{I}{R \sum_{i=1}^6 \frac{m_i}{M_i (\gamma_i - 1)}} \quad (40)$$

The temperature being found, the partial pressure for each specie is found by

$$P_i = \frac{n_i RT}{V} \quad (i = 1, 2, \dots, 6) \quad (41)$$

then,

$$P = \sum_{i=1}^6 P_i \quad (i = 1, 2, \dots, 6) \quad (42)$$

provides the cell pressure.

The computation of the pressure and temperature using the multi-material equation of state subroutine (called STATE 7) is accomplished on a cell-by-cell basis throughout the entire grid, once during each time step. In each cell the volume of solid carbon is computed and, if significant, subtracted from the volume of the cell. Then the specific heat ratio (γ) is computed for the six gases at the present cell temperature using the formulations in Table III. The denominator for equation 39 is computed and a new temperature for the gas mixture is determined. Then the gas mixture and the solid carbon are brought into temperature equilibrium to obtain a new cell temperature. With the new cell temperature new gammas are computed and the above process repeated until the temperature converges. When temperature convergence has been obtained, the partial pressure for each gas specie is computed using equation 40. Finally the partial pressures are summed to obtain the new cell pressure.

THE COMPUTATIONAL PROBLEM

From previous experience with the idealized problem (point source in hypersonic flow), an energy value of 7.9×10^8 ergs/cm² was chosen as one not requiring excessive computer running time and that still could provide a substantial shock wave. From this energy value a thickness for the explosive sheet was determined. Using the following values

$$\text{density} = 1.47 \text{ gr/cm}^3$$

$$\text{energy} = 1.13 \text{ kcals/gr}$$

$$\text{conversion} = 4.186 \times 10^{10} \text{ ergs/kcal}$$

a thickness of 1.136×10^{-2} centimeters is obtained. Note that this is the thickness of material deposited above the axis of symmetry and corresponds to an actual sheet thickness of 2.272×10^{-2} centimeters.

With the thickness known the amount of explosive material (W) deposited into the computational grid per unit length of detonation travel can be determined

$$\begin{aligned} W &= (\text{density}) \cdot (\text{thickness}) \cdot (\text{length}) \cdot (\text{width}) \\ &= (1.47)(1.136 \times 10^{-2})(1)(1) \\ W &= 1.67 \times 10^{-2} \text{ gr/cm} \end{aligned} \tag{43}$$

Returning to the revised list of detonation products (Table II) and using the molecular weights assigned in Table IV, the amount of each specie provided by the detonation of a unit length of explosive can be determined.

TABLE IV
Molecular Weights of Mass Species

CO - 28	H ₂ - 2	H ₂ O - 18
CO ₂ - 44	O ₂ - 32	N ₂ - 28
C - 12		

$$\text{Amount of Each Specie Deposited (per unit length)} = \left(\frac{\text{Total Mass Deposited Per Unit Length}}{\text{Total Mass}} \right) \cdot \left(\frac{\text{Moles of Each Specie Per Unit Length}}{\text{Total Mass}} \right) \cdot \left(\frac{\text{Mole Weight of Specie}}{\text{Mole Weight of Species}} \right)$$

The amount of each specie that is deposited by a detonation of a unit length (cm) of explosive is listed in Table V.

TABLE V
Mass of Each Specie Deposited (gr/cm)

CO - 2.85×10^{-3}	H ₂ - 3.32×10^{-4}
CO ₂ - 6.98×10^{-3}	H ₂ O - 3.91×10^{-4}
C - 3.09×10^{-3}	N ₂ - 3.11×10^{-3}

The computational grid was initially loaded with a uniform mixture of N₂ (75.5%) and O₂ (24.5%) representing air with an ambient density of 1.2×10^{-3} gr/cm³, temperature of 292 °K and pressure of 14.7 psi. A modified CLAMTC code was used to establish and load this grid and to generate the zero cycle on the problem tape. The specific internal energy for each of the detonation products and the background flow gases were computed for ambient temperature using

$$I = \phi \frac{RT}{M} \quad (44)$$

where

$\phi = 5/2$ for diatomic gases

$\phi = 3$ for triatomic gases

and are listed in Table VI.

TABLE VI

Internal Energy of Detonation Products
(ambient temperature) (ergs/gr)

$N_2 - 2.165 \times 10^9$	$CO - 2.095 \times 10^9$	$H_2 - 29.3 \times 10^9$
$O_2 - 1.895 \times 10^9$	$CO_2 - 1.656 \times 10^9$	$C(s) - 0$
	$H_2O - 4.05 \times 10^9$	Air - 2.0×10^9

The explosive detonation energy deposited with each deposition of mass was 4.72×10^{10} ergs per gram.

A background flow regeneration scheme (used to simulate incoming flow conditions) was devised and incorporated into the subroutine CDT of SHELTC7. The initial background flow conditions are reestablished in the first two rows of the grid (right edge - Figure 4) with appropriate adjustments to total problem mass, total problem energy and the mass of each species.

A mass and energy deposition scheme was devised and incorporated into subroutine CDT of the SHELTC7 code. A letter designator was assigned to each mass specie as listed in Table VII and used to account for that specie throughout the computation.

TABLE VII
Letter Designators for Mass Species

A - N ₂	D - CO ₂	G - C(s)
B - O ₂	E - H ₂ O	
C - CO	F - H ₂	

The length of material detonated (which establishes the amount of mass deposited) is determined by the time step and the detonation velocity. A momentum balance is performed between the material in the detonation cell and the material deposited, and new cell velocities are determined. Conservation of energy then determines how much kinetic energy is converted to internal energy. The mass of each specie and the total mass in the detonation cell are adjusted by the amount of mass deposited, and the internal energy of the cell is increased by the amount of explosive energy deposited. Finally, the total mass and the total energy in the grid are increased by the amount of each deposited during the detonation sequence.

COMPUTED RESULTS

Two solutions were obtained by using this more sophisticated computational scheme. Energy values of 7.9×10^8 and 7.9×10^9 ergs/cm², both at a detonation velocity of 3.6×10^5 cm/sec, were used corresponding to previously obtained solutions for the idealized (energy addition only) problem. The corresponding half thicknesses for a TNT sheet are 1.136×10^{-2} and 1.136×10^{-1} centimeters, respectively.

These problems were run on the CDC-6600 computer and required several hours of computation time for each.

The plotting code (SHPLOTL) was modified to accommodate the multi-material results obtained from the SHELTC7 computations and was then titled SHPLOT7. Plots of the temperature distribution (isotherms) are provided by this modified plotting code in addition to the plots of other variables (pressure, energy, velocity, etc.) mentioned previously in Section II.

The location in the x-y plane of the shock front, as determined by the SHELTC7 computation for the energy value of 7.9×10^8 ergs/cm² is shown in Figure 17. The shock again forms out in front of the line of detonation and then curves downstream, approaching the Mach angle at some distance downstream from the line of detonation. Contours of constant pressure (isobars) are shown in Figure 18. A high pressure zone occurs along the shock front with the highest pressures immediately adjacent to the line of detonation. In the region downstream from the line of detonation and along the plane of symmetry a low-pressure zone exists which causes a partial reversal of the initial outward flow of the mass. The inward-moving mass then converges on the plane of symmetry causing a new high-pressure region. Hence, high- and low-pressure regions alternate downstream along the plane of symmetry until the oscillations damp out and become insignificant. This same effect was observed in solutions of the idealized problem.

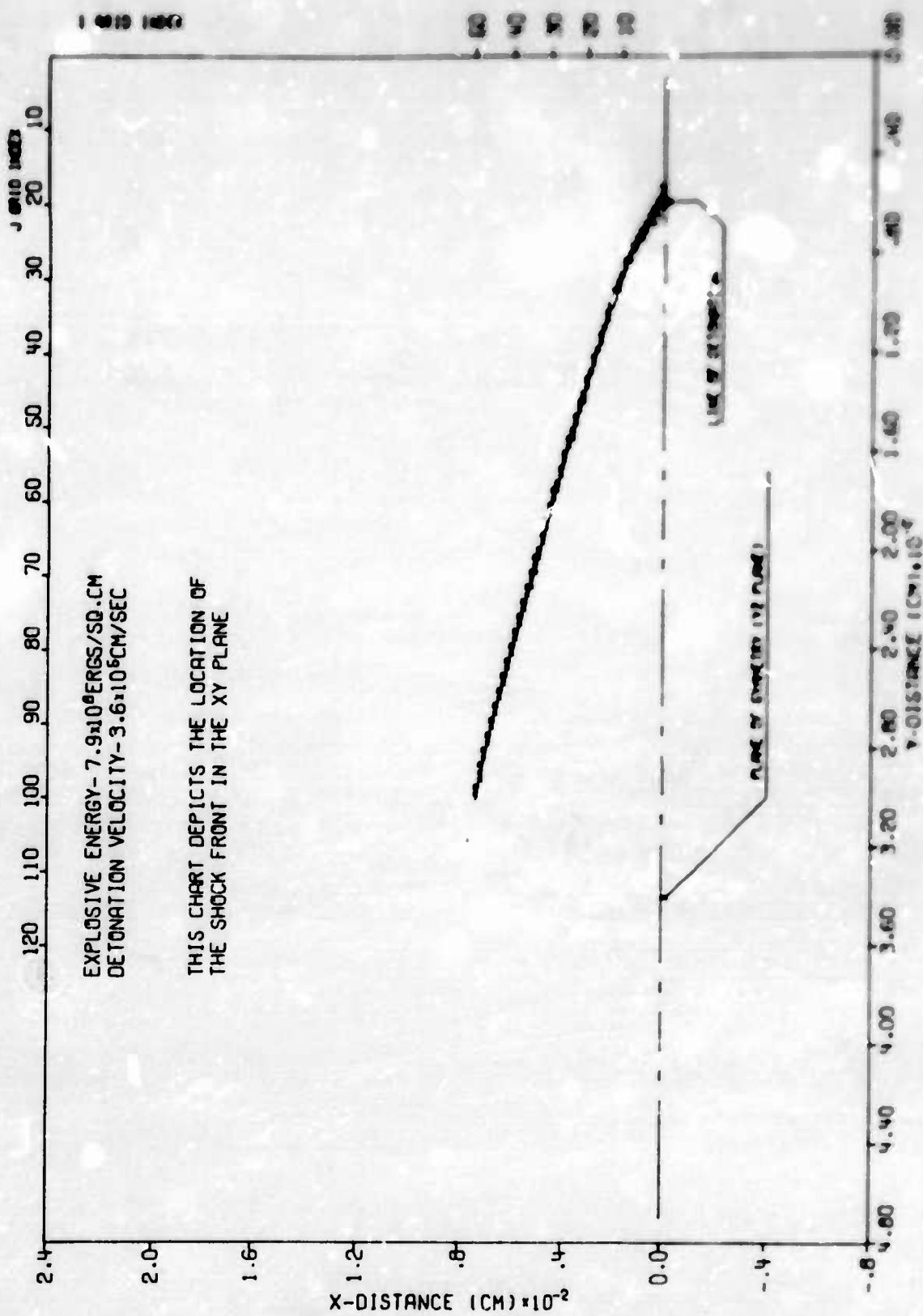
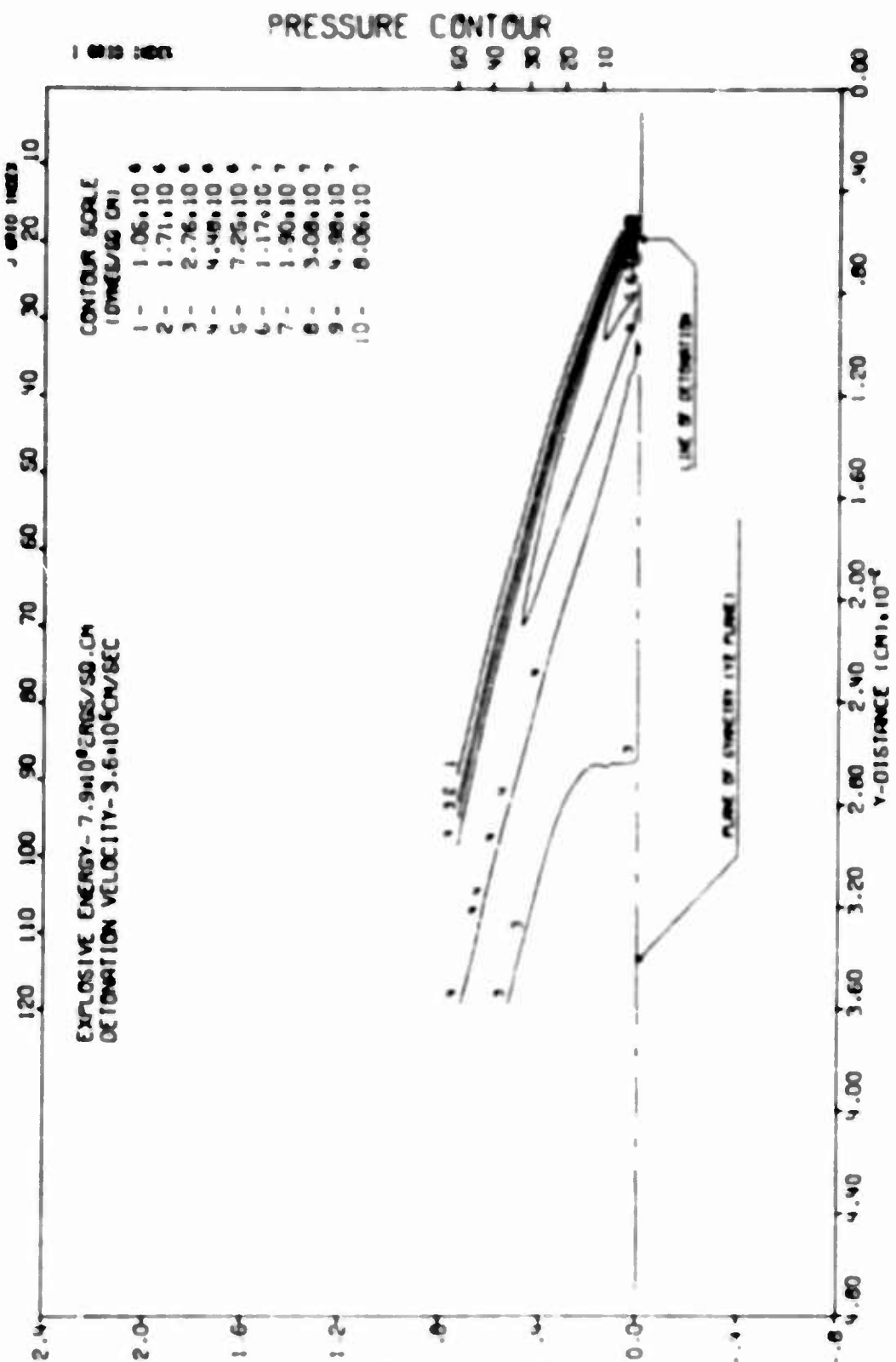


Figure 17. Shock front locations in the XY plane.



SIMPLY CALCULATION OF EXPLOSIVE SOURCE IN HYPERSONIC FLOW (NO PDC)
TIME .000006 SEC CYCLE 700 PROBLEM 30.000

Figure 19. Constant Pressure Contours (inobars)

Contours of constant energy are shown in Figure 19 and constant mass density in Figure 20. The concentration of a large percentage of the total mass involved in the blast wave in a narrow region close to the shock front can be seen. Figure 21 shows contours of constant temperature (isotherms) behind the blast wave. One may observe that the highest temperatures are located near the line of detonation and drop to below 3000 °K a short distance from that point. Hence, the assumption made earlier concerning the temperature distribution and the shift of chemical equilibrium is shown to be valid providing the time required for attaining equilibrium is short compared to the time it takes the mass to move from the line of detonation out to the cooler cells.

A comparison was made of the shock front locations determined from the idealized solution (energy addition only - Section II) and from the solution produced here (mass and energy addition). The comparison for the two energy levels, 7.9×10^8 and 7.9×10^9 ergs/cm², is shown in Figure 22. The shock front from the mass and energy addition solution forms slightly farther out in front of the line of detonation than the shock front from the idealized solution but it curves back more sharply. Thus, the shock front from the mass and energy addition solution crosses under the shock front from the idealized solution and continues beneath the idealized solution at all locations downstream from the line of detonation. In other words, the x-coordinate of the shock front from the mass and energy addition solution (x_{me}) is smaller

than the x-coordinate of the shock front from the idealized solution (x_i) by approximately the same amount for all values of y beyond the line of detonation.

$$x_i - x_{me} = \text{constant} \quad \text{for } y > y_{\text{detonation}} \quad (45)$$

This compressed outline of the shock front from the mass and energy addition solution is caused by the detonation products having only y-momentum when they enter the flow field. In the transformed coordinate system used in solving these problems, the mass of the explosive material is moving in the same direction and at the same rate as the background gas. When this mass is injected into the background flow along the line of detonation (injected with no x-component of velocity), the same amount of detonation energy cannot accelerate and compress this increased mass as far in the x-direction as in the idealized (energy addition only) solution. Hence the shock front for the mass and energy addition solution will not have moved as far in the x-direction for any y-distance as will the shock front from the idealized solution.

No attempt was made to obtain an empirical fit for the mass and energy addition solution. Additional plots from mass and energy addition solution for other energy values and velocities of detonation are provided in Appendix D.

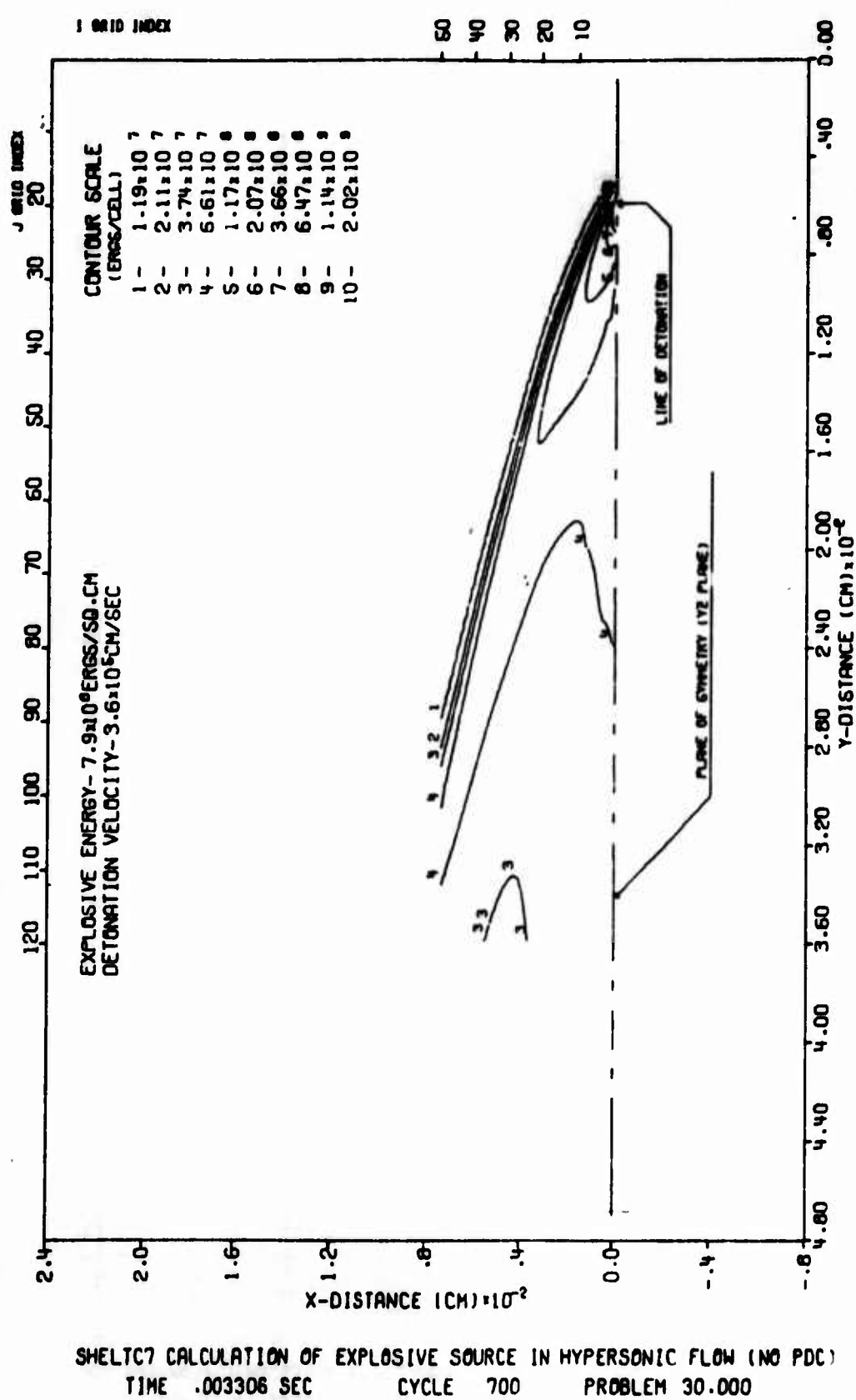
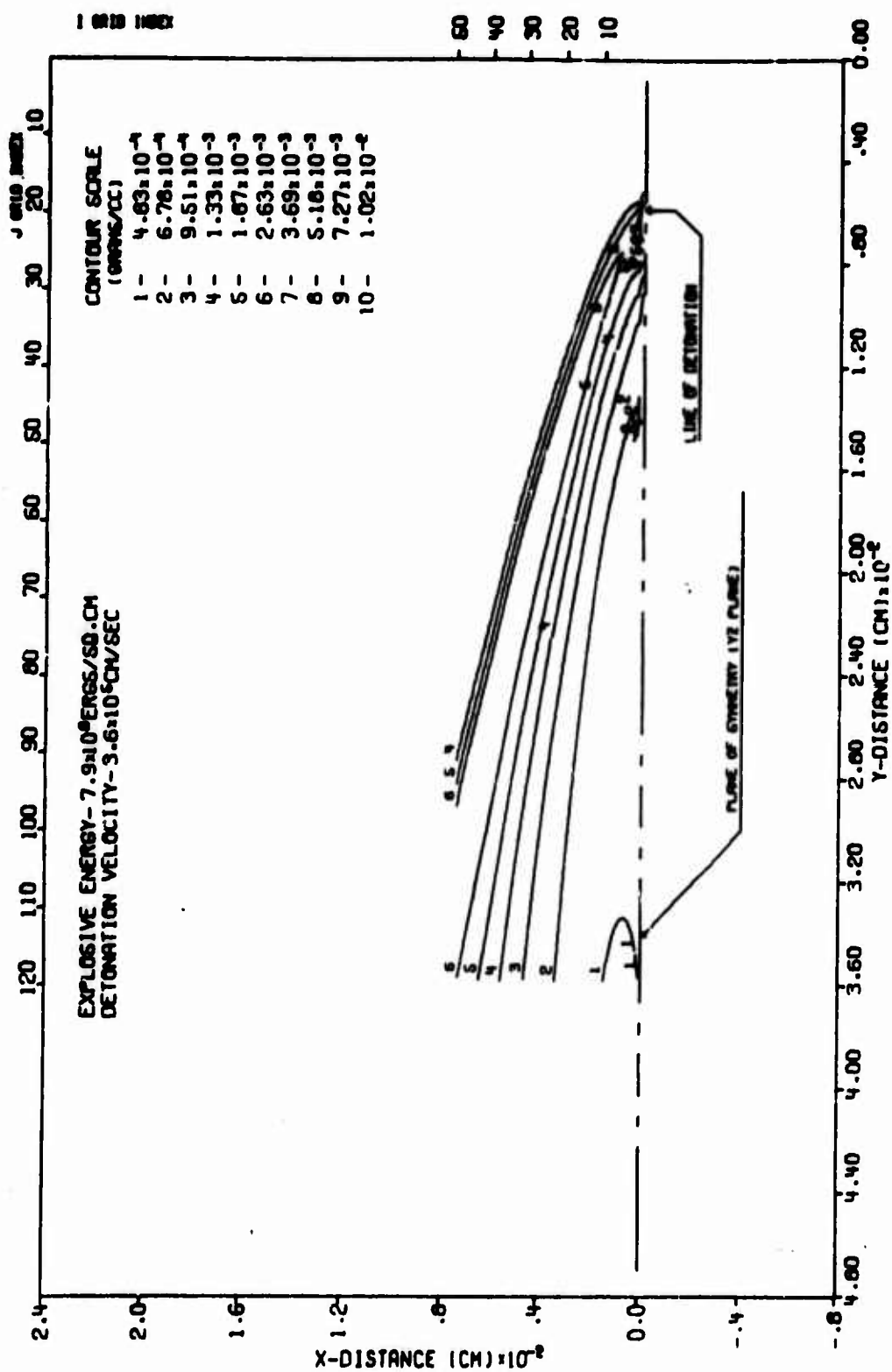


Figure 19. Constant Energy Contours



SHELTC7 CALCULATION OF EXPLOSIVE SOURCE IN HYPERSONIC FLOW (NO PDC)
TIME .003306 SEC CYCLE 700 PROBLEM 30.000

Figure 20. Constant Density Contour

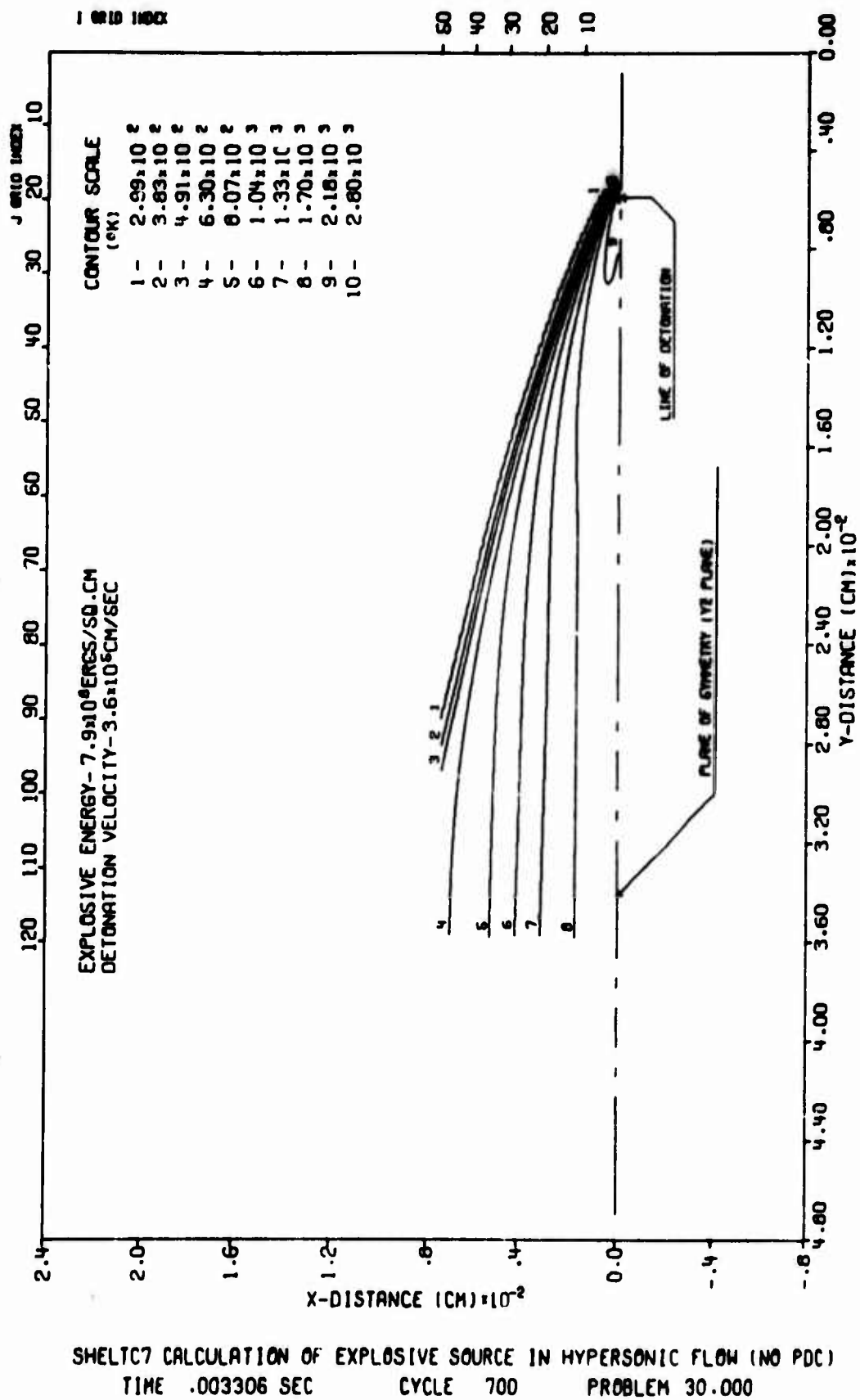


Figure 21. Constant Temperature Contours (Isotherms)

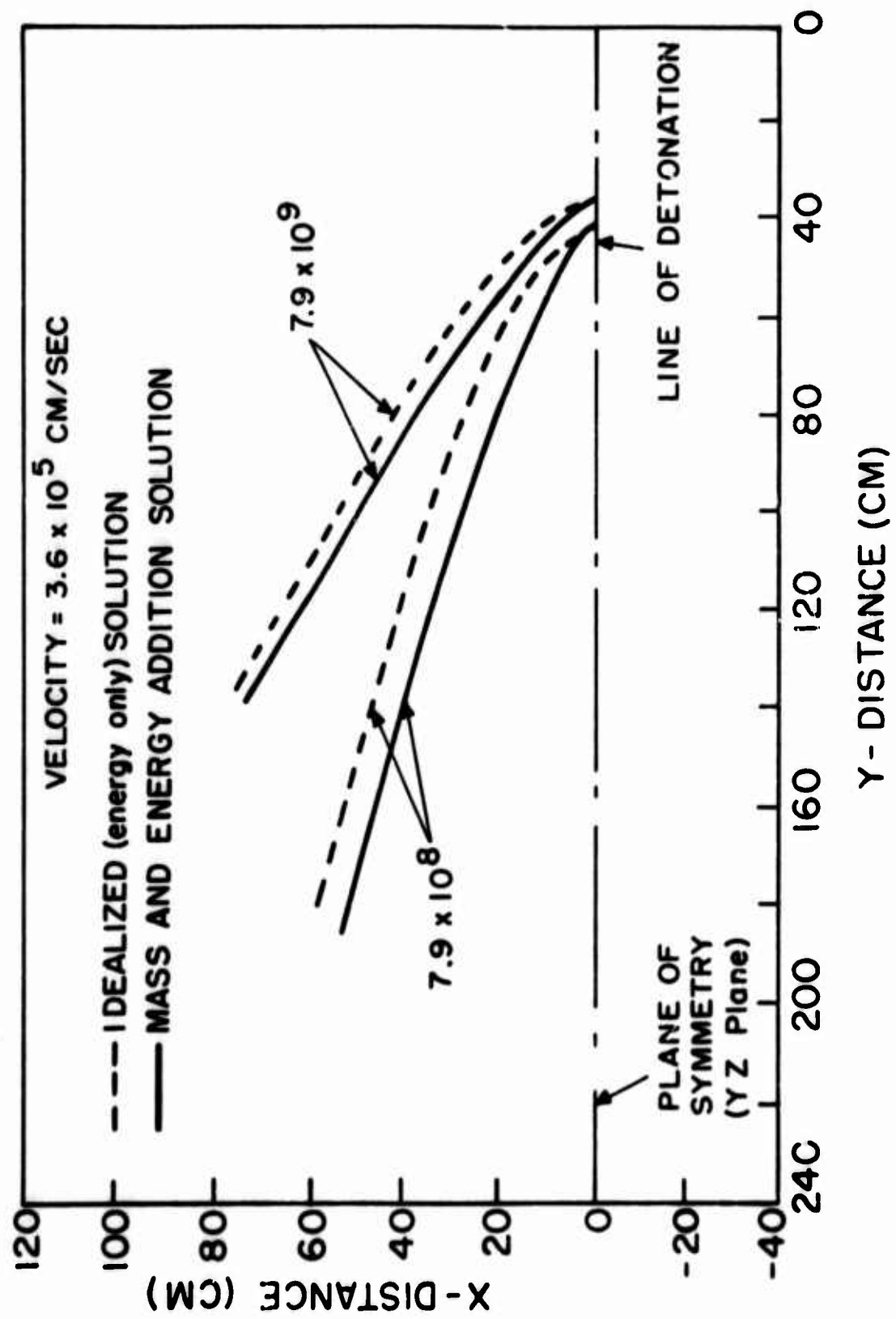


Figure 22. Comparison of Solutions (Idealized versus Mass and Energy Addition)

SECTION IV

POST-DETONATION COMBUSTION

Most explosive materials are highly oxygen negative. That is, in the basic detonation reaction (usually a decomposition of some complex molecule) all of the oxygen in the explosive material is consumed and substantial amounts of hot, combustible detonation products are produced. As these detonation products flow outward from the line of detonation, a material interface is formed between the detonation products and the surrounding medium. At first this interface is distinct with good material separation across the interface. The interface is not stable, however, and as outward flow continues, turbulent mixing and mass diffusion occur and an expanding zone of mixed materials (detonation products and surrounding air) is formed. Thus, the hot detonation products are provided with a source of oxygen, and combustion occurs to release an additional quantity of energy. This process is known as post-detonation combustion (PDC) or "after burning" and is a potential source of error for calculations where it is not included. Hence, the flow field behind the blast wave from the detonation of an oxygen negative explosive consists of (1) a region adjacent and downstream to the point of detonation filled only with products of detonation where no PDC occurs, (2) a mixed zone of detonation products and air where PDC occurs, and (3) an outlying zone of shocked air with no detonation products to be burned. This

distribution of materials through the different zones is depicted in Figure 23.

ESTIMATE OF PDC ENERGY RELEASE

An estimate of the total amount of energy which is available for release by PDC can be obtained by burning to completion all combustible detonation products in an abundance of oxygen. Using the detonation products from TNT listed in Table II, the following amounts of combustible materials are available:

$$C - 15.4 \text{ moles/kg of TNT}$$

$$CO - 6.09 \text{ moles/kg of TNT}$$

$$H_2 - 9.93 \text{ moles/kg of TNT}$$

The combustion reactions are



The heats of combustion for these reactions (36) are

$$\Delta H_1 = -26,620 \text{ cals/mole of C}$$

$$\Delta H_2 = -68,320 \text{ cals/mole of } H_2$$

$$\Delta H_3 = -67,410 \text{ cals/mole of CO}$$

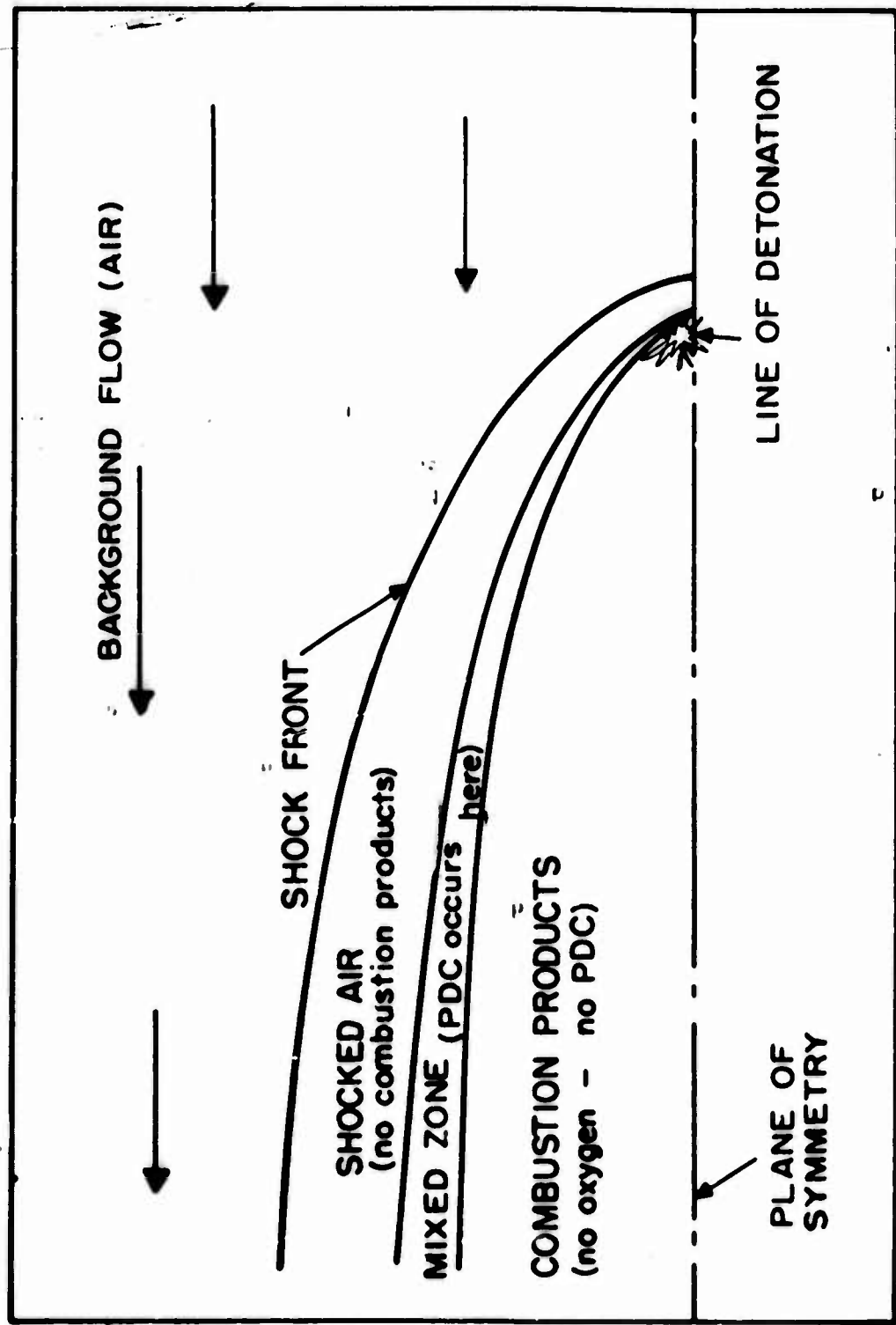
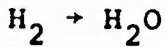


Figure 23. Material zones behind the Blast Wave

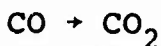
The calculation of energy release, per kg of explosive material, follows:



$$(15.4)(26,620) = 410,000 \text{ cals/kg} \quad (49)$$



$$(9.93)(68,320) = 678,000 \text{ cals/kg} \quad (50)$$



$$(6.09 + 15.4)(67,410) = 1,450,000 \text{ cals/kg} \quad (51)$$

The explosive energy released by a kg of TNT ($\rho = 1.47$) is
(Reference 34)

$$Q_D = (1.13) \frac{\text{kcal}}{\text{gr}} (1000) \frac{\text{cal}}{\text{kcal}} (1000) \frac{\text{gr}}{\text{kg}}$$
$$= 1.13 \times 10^6 \frac{\text{cal}}{\text{kg}} \quad (52)$$

The ratio of PDC energy to detonation energy is

$$\text{ratio} = \frac{2.538 \times 10^6}{1.13 \times 10^6} = 2.245 \quad (53)$$

Thus, it would appear that more than twice as much energy can be produced by the PDC than is produced by the basic detonation of the TNT and that the contribution to the blast wave is substantial. Experimental evidence, however, indicated this is not true, because the detonation products are not all burned to completion and the burning which occurs does so over a long period of time. In fact, photographic evidence and post-detonation examination of large high-

explosive experiments indicate a substantial amount of unburned carbon is deposited around the vicinity of the detonation. The contribution of PDC to the early-time (under 10 milliseconds) formation of blast waves is not known and thus has been ignored in previous blast wave calculations. Some experimental evidence exists (43) which suggests that this may be a source of error, particularly at late times (several hundred milliseconds) after the detonation of a large explosive charge.

It was intended at the start of this study to develop an understanding of the post-detonation combustion process and to incorporate a combustion scheme into an existing hydrodynamic code so that some quantitative information on the role of PDC in the formation of a blast wave could be obtained without a several-year development of a completely new computer code. During the course of this work it has become apparent that this goal is difficult to achieve.

Post-detonation combustion is a complicated process involving mass transport, mixing of different mass species, and chemical reaction kinetics. The quantities of combustible materials and oxygen at any point in the flow field at any time depends both upon the overall hydrodynamic flow and upon the amount of mixing and diffusion which has occurred across the air-detonation product interface. There are several competing reactions occurring simultaneously. The reaction rate for a particular reaction depends upon the concentration of the reactants and upon a reaction rate coefficient which is,

in turn, dependent upon temperature. An exact determination of the PDC reaction requires the simultaneous solution of a series of differential rate equations of the form

$$\frac{dx_i}{dt} = (v_i^p - v_i^r)k \prod_{j=1}^n (x_j)^{v_j^r} \quad (i = 1, \dots, n) \quad (54)$$

where

x_i = molar concentration of i^{th} specie (moles/cm³)

v_i^p = stoichiometric coefficient of i^{th} specie in products

v_i^r = stoichiometric coefficient of i^{th} specie in reactants

k = reaction rate coefficient for the specified reaction

n = number of mass species

for each incremental volume (grid cell) in the flow field.

Solving these equations for the three simplified combustion reactions used in determining the amount of PDC energy available (Equations 46, 47, and 48) will not provide correct results because the actual combustion process involves many other molecular and atomic species and several chemical reactions. Accurate results are obtained only if all of the reactions are included and the correct reaction rate constants are known. These equations have previously been solved for certain mixtures and computer programs for solving such reaction-rate problems have been developed (37). However, these programs depend upon iterative integration

schemes and require several seconds of computer running time to determine the progress of a reaction over some small period of time. To incorporate such an exact reaction rate subroutine into a hydrodynamic code (such as SHELTC7) would require the execution of that subroutine for every cell once during each cycle. Most blast-wave problems require several thousand grid cells and run several hundred cycles to obtain a solution. Hence, the computer time required for solving a hydrodynamic combustion problem would be several hundred hours on the fastest computers currently available. In addition, it would be necessary to maintain accountability of at least twelve distinct mass species in each cell of the computational grid (only seven species are stored in SHELTC7) which would greatly increase the amount of computer memory required.

A further difficulty was encountered in attempting to determine the mixing and diffusion which occur in the flow behind a blast wave. When study of the available hydrodynamic codes suitable for blast-wave calculations was started, it appeared that mixing and diffusion had been considered in their development and computation of the mixing in a multi-material flow field would not present a problem. During the course of the study it was discovered that such was not the case--all the codes suitable for two-dimensional blast-wave calculations had been originally developed for a single material and later adapted for multi-material operation. In the adaptation no means had been specifically provided for

computing the mixing and diffusion of one mass specie through another. Thus, it became apparent that no mathematically rigorous method for computing the mixing and diffusion of mass species which accompany the hydrodynamic flow behind a blast wave was available.

There was little hope, then, of performing an exact calculation of the PDC. The development of a new computer code to accomplish this would take several years and was beyond the scope of this study. It was discovered, however, during the study of SHELL hydrodynamic codes that mixing of the different mass species does occur in the multi-material versions of SHELL, even though no specific mechanism had been incorporated in the code to cause it to happen. This mixing, sometimes called "artificial diffusion," is inherent in all multi-material Eulerian codes and is an accidental rather than a planned occurrence.

With this discovery in mind it was decided to pursue the development of a scheme to approximate the contribution from PDC in a blast-wave calculation, realizing that experimental correlation would be required before good confidence in the approximation scheme could be obtained.

MIXING OF MASS SPECIES IN SHELTC7

Previous studies using the SHELL codes (16, 17) have referred to mass transport across a material interface, called an "artificial diffusion," as a disadvantage inherent in all Eulerian codes. However, for the approximation that is being developed it may be an advantage if satisfactory comparison

with experiment can be obtained. The basic equations from which SHELTC7 was developed (see Appendix A) are the equations for 2-D inviscid compressible flow and do not contain any terms which would provide mixing or diffusion. Hence, the code should produce only laminar flow. However, in the computational algorithm at the conclusion of the mass transport phase (subroutine Phase II in the code), all the mass species in any cell are considered to be uniformly distributed throughout the cell. This instantaneous dispersion or "diffusion" causes any new mass specie which has been introduced into the cell to be instantaneously transported across and throughout the cell. By this means, mass species are propagated from cell to cell and mixed with other species somewhat like the mixing and diffusion in real gases. But since this "effective mixing" does not result from the basic equations, it must be considered entirely artificial being caused directly by the computational scheme. Nevertheless, it does accomplish mixing and diffusion (superimposed upon the basic hydrodynamic flow), and may be useful much as the artificial or "effective viscosity" which is inherent in SHELL (see Appendix A for SHELL effective viscosity).

The mixing and diffusion in SHELTC7 occur only when there is a flow of mass and only in the direction of the flow velocity (i.e., when there is no component of velocity in a given direction, there is no mixing in that direction). The amount of mixing which occurs in a given time (i.e., the mixing rate) is governed by the magnitude of the flow velocity,

the concentration gradient of the various mass species, and the cell size of the computational grid. Expressed in another way, the time rate of change of the concentration of a mass specie in any direction is a function of the magnitude of the component of velocity in that direction and of the concentration gradient of that specie in that direction.

$$\frac{d(C_i)}{dt} = F \left(|V|, \frac{d(C_i)}{dR} \right) \quad (i = 1, 2, \dots, n)$$

where

(C_i) = mass concentration of i^{th} species (gm/vol)

V = component of velocity in specified direction
(cm/sec)

R = distance in specified direction (cm)

t = time (sec)

n = number of mass species

The functional relationship has not been determined but is undoubtedly influenced by cell size. A literature search was conducted for a suitable experiment which could be calculated using SHELTC7, to permit comparison of the mixing in that code with experimental data. Recent work by McArtor (44) involving 2-D transverse injection of mass into supersonic flow offered hope but a preliminary single-material calculation using SHELLTC revealed that boundary layer effects dominate that experiment making it unsuitable for correlation with SHELTC7. Other experimental work (45, 46) was considered but none proved suitable for this purpose.

Realizing the need for a more detailed investigation and definition of the mixing in SHELTC7, if one accepts this mixing as a suitable approximation for the turbulent mixing and diffusion which occur during the propagation of a blast wave, then further work in the study of PDC can be accomplished. (Substantial discussion of the suitability of this approximation with others who are using and modifying multi-material versions of SHELL has, in general, resulted in agreement with the approximation.) It was decided that continuing the post-detonation combustion study using this approximation of material mixing would be meaningful, particularly if correlation with specifically designed experiments could later be obtained.

After some preliminary computer runs were attempted, it was discovered that an obvious excess of mixing was occurring near the line of detonation as a result of the mass deposition scheme incorporated into SHELTC7 (deposition of the detonation products into the flow field--described in Section III). In that scheme the amount of each of the mass species to be deposited is computed and then added to the mass of the cell immediately adjacent to the line of detonation. In so doing, each mass specie is instantaneously dispersed throughout the volume of that cell and thus is uniformly mixed with all the other mass species already in the cell. This results in an unrealistically large amount of mixing and precludes a sharp interface between the background flow of air and the incoming flow of detonation products. It can be argued that

the most distinct material interface in the entire flow field from an actual detonation will be found close to the line of detonation before significant mixing or diffusion has had time to occur. Thus, the mixing which occurs as a result of the mass-deposition scheme is not realistic and does not very well represent that which happens near an actual line detonation.

To correct this deficiency, a special subroutine called INTFACE was incorporated into SHELTC7 which creates a more distinct material interface near the line of detonation. INTFACE is executed once each cycle after the mass transport phase (subroutine Phase II) is completed. The subroutine begins in a cell adjacent to the plane of symmetry and a few cells upstream from the line of detonation ($i = 1, j = 16$ was chosen). The next cell adjacent to the beginning cell in the direction of increasing i index ($i = 2, j = 16$) is examined to see if it contains any detonation products. If it does, equal quantities of air (nitrogen and oxygen) and detonation products are exchanged between the two cells until either there is no air remaining in the first cell or no detonation products remaining in the second cell. The second cell is then designated as the new first cell and the next adjacent cell in the increasing i direction ($i = 3$) is designated the new second cell. The mass trading sequence is then repeated. This process is continued along the row (increasing i index) until cells with no detonation products are encountered. The j index is then increased by one and the

above sequence is repeated starting with the i index at the value of the last cell encountered in the previous sequence. The progression in the direction of increasing j index is continued for an arbitrary number of rows (14 was used). By this means the material interface between air and detonation products is reduced to essentially one or two cell widths for the first several rows near the line of detonation and the excess mixing associated with the mass deposition scheme is greatly reduced. Here again, experimental verification is required before real confidence in this interface preservation scheme can be attained.

The mass and energy addition solution for the energy value of 7.9×10^8 ergs/cm² and detonation velocity of 3.6×10^5 cm/sec (described in Section III) includes the distribution of the seven material species throughout the computational grid which results from the mixing which is inherent in SHELTC7 as influenced by subroutine INTFACE. The multi-material plotting code SHPLOT7 was constructed to depict this distribution in two ways. First, contours linking locations where equal quantities of a selected specie exist are drawn for each mass specie as shown in Figures 24 through 30. The units of the contour scale are grams and refer to the number of grams of that specie in the cell at that location in the grid. The second method of depicting the mass distribution consists of assigning a symbol and a size for that symbol for increments of the mass fraction of the specie being plotted. The mass fraction of that specie in the cell is determined

at selected cells in a pattern throughout the grid. The appropriate symbol is then drawn (with the corresponding size) at the location of each of the selected cells. Thus, a graphic representation of how each mass specie is distributed through the grid is provided as shown in Figures 31 through 37. One can observe in Figures 24, 31 and 32 the distribution of N_2 and O_2 in the background flow (air) and within the blast wave. The concentration of O_2 within the blast wave is low, most of it having been deflected around the blast wave. The plot of constant mass contours for O_2 , Figure 25, is not very satisfactory since extremely low concentrations of O_2 (associated with locations very near to the line of detonation) dominate that plot. Although the bulk of the N_2 from the background flow is deflected around the blast wave, the concentrations within the wave are somewhat higher than the amount which would correspond to the concentration of oxygen within the blast wave because N_2 is one of the products deposited from the detonation.

The distribution and concentration of the remaining five detonation products are shown in Figures 26 through 30 and 33 through 37. In particular, the distribution and concentration of CO_2 are shown quite clearly in Figure 34.

This approximate distribution of the material species within the blast wave is the foundation on which a post-detonation combustion scheme can be built.

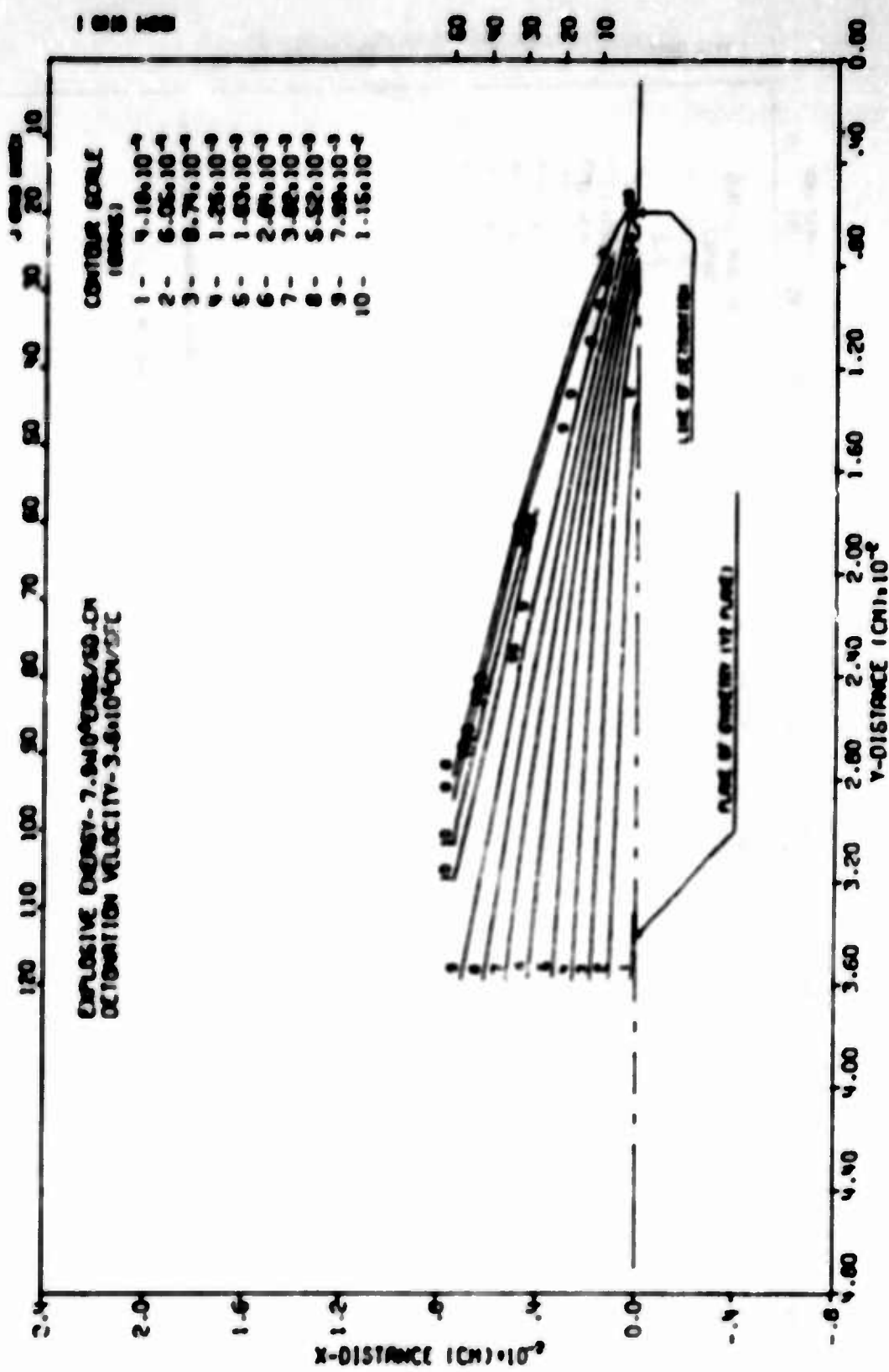
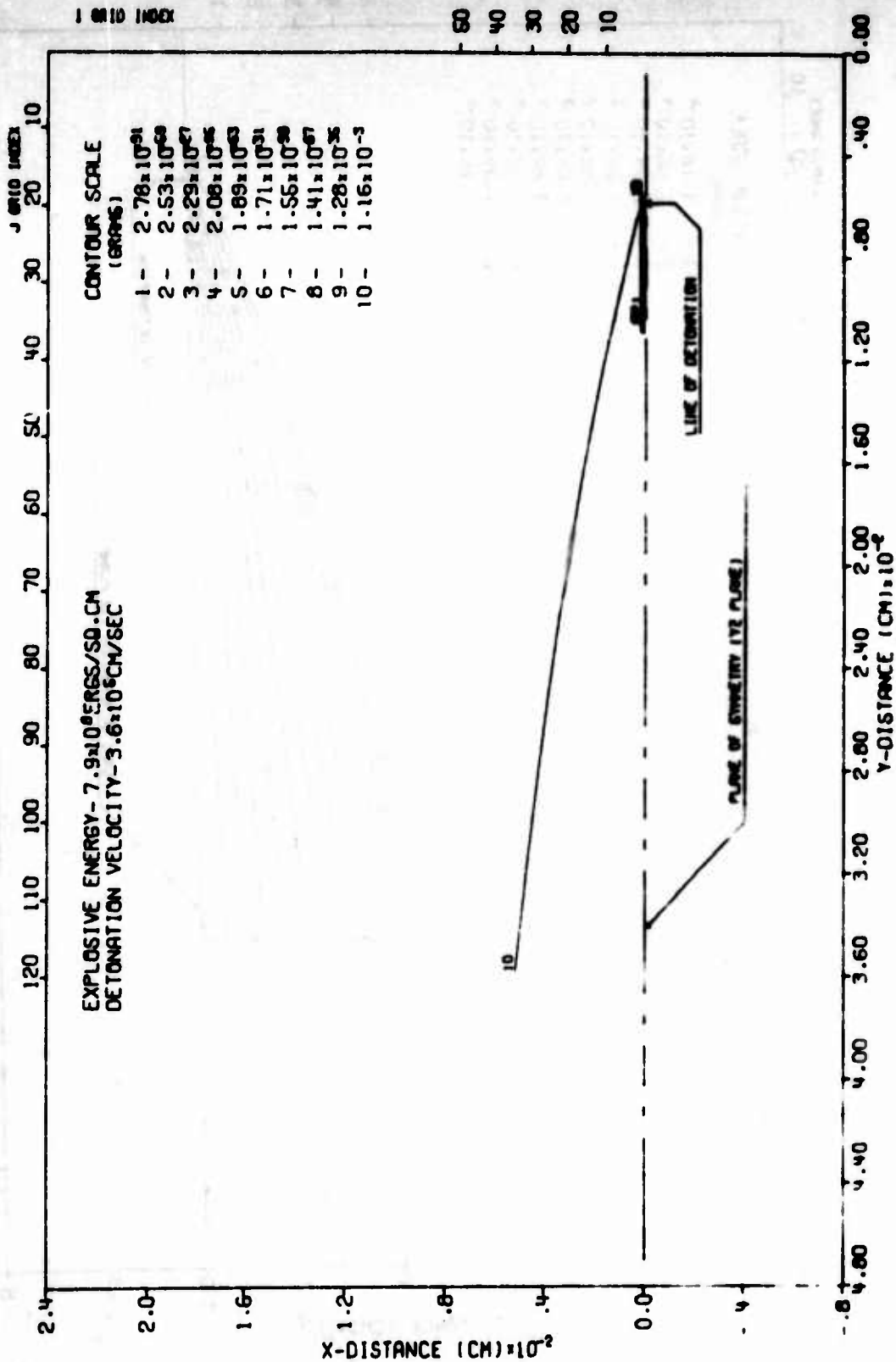


Figure 24. Constant Mass Contours—Species A (Nitrogen)



SHELTC7 CALCULATION OF EXPLOSIVE SOURCE IN HYPERSONIC FLOW (NO PDC)
 TIME .003306 SEC CYCLE 700 PROBLEM 30.000

Figure 25. Constant Mass Contours--Species B (Oxygen)

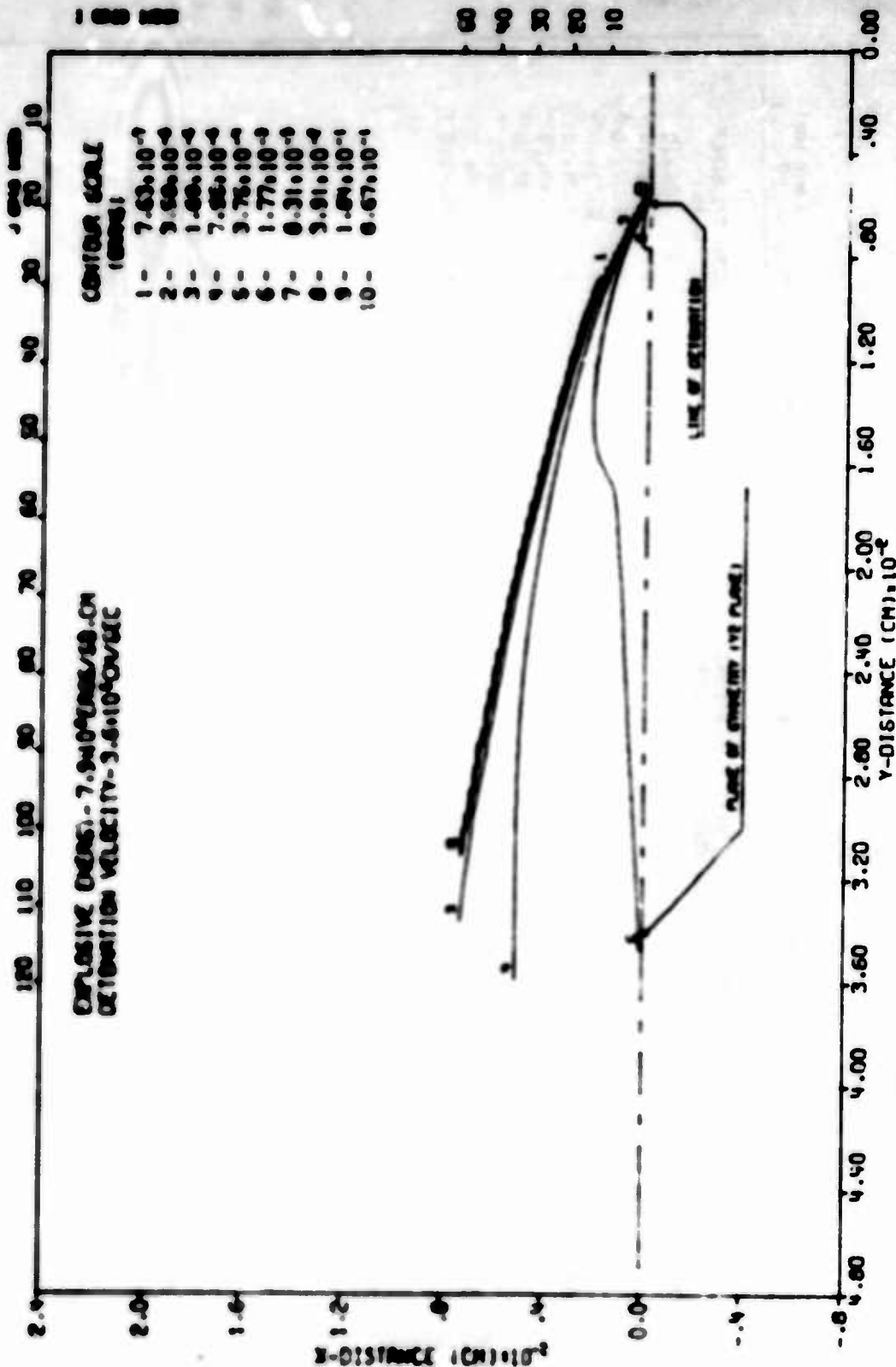


Figure 26. Constant Mass Contours--Species C (Carbon Monoxide)

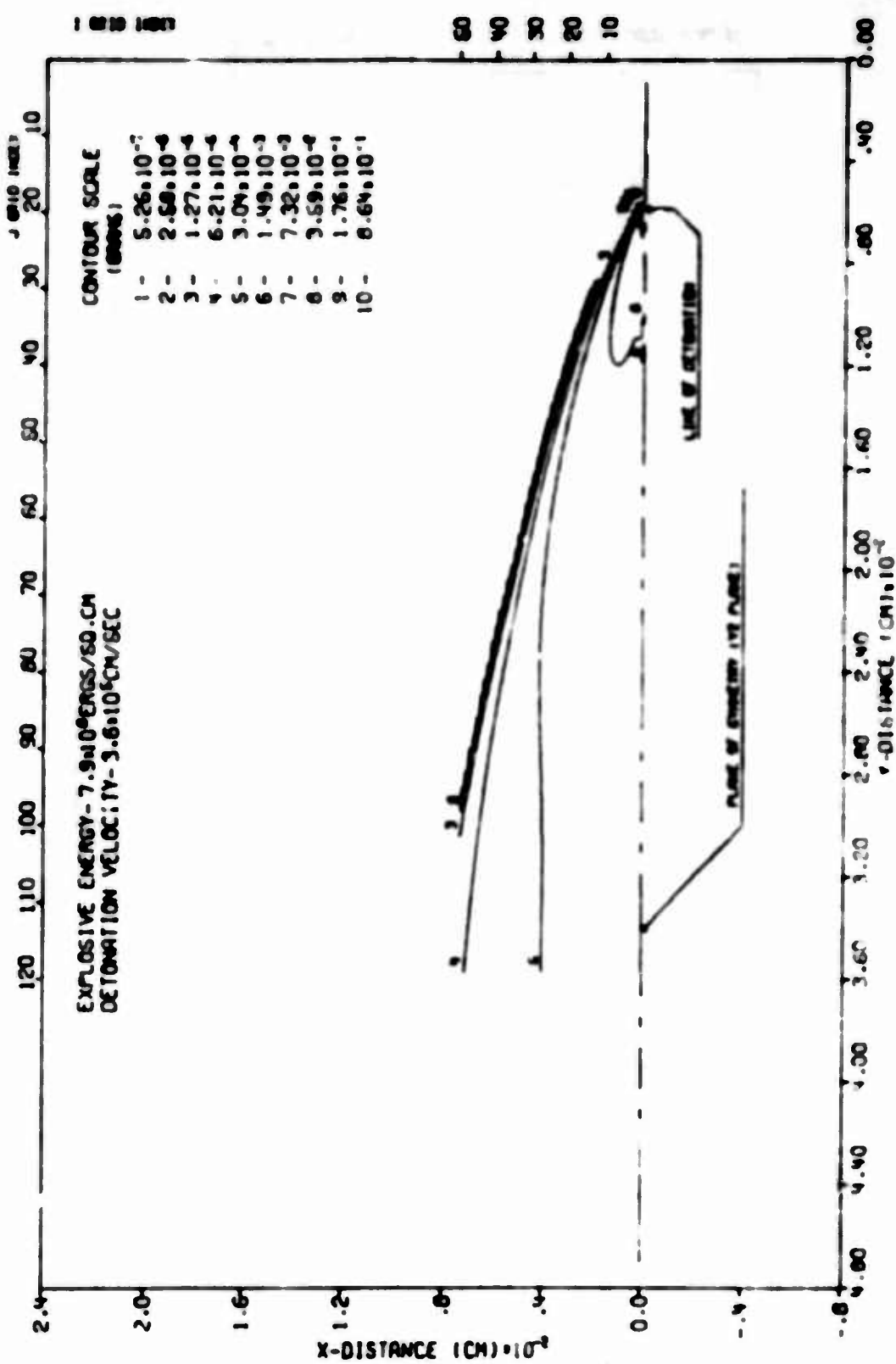
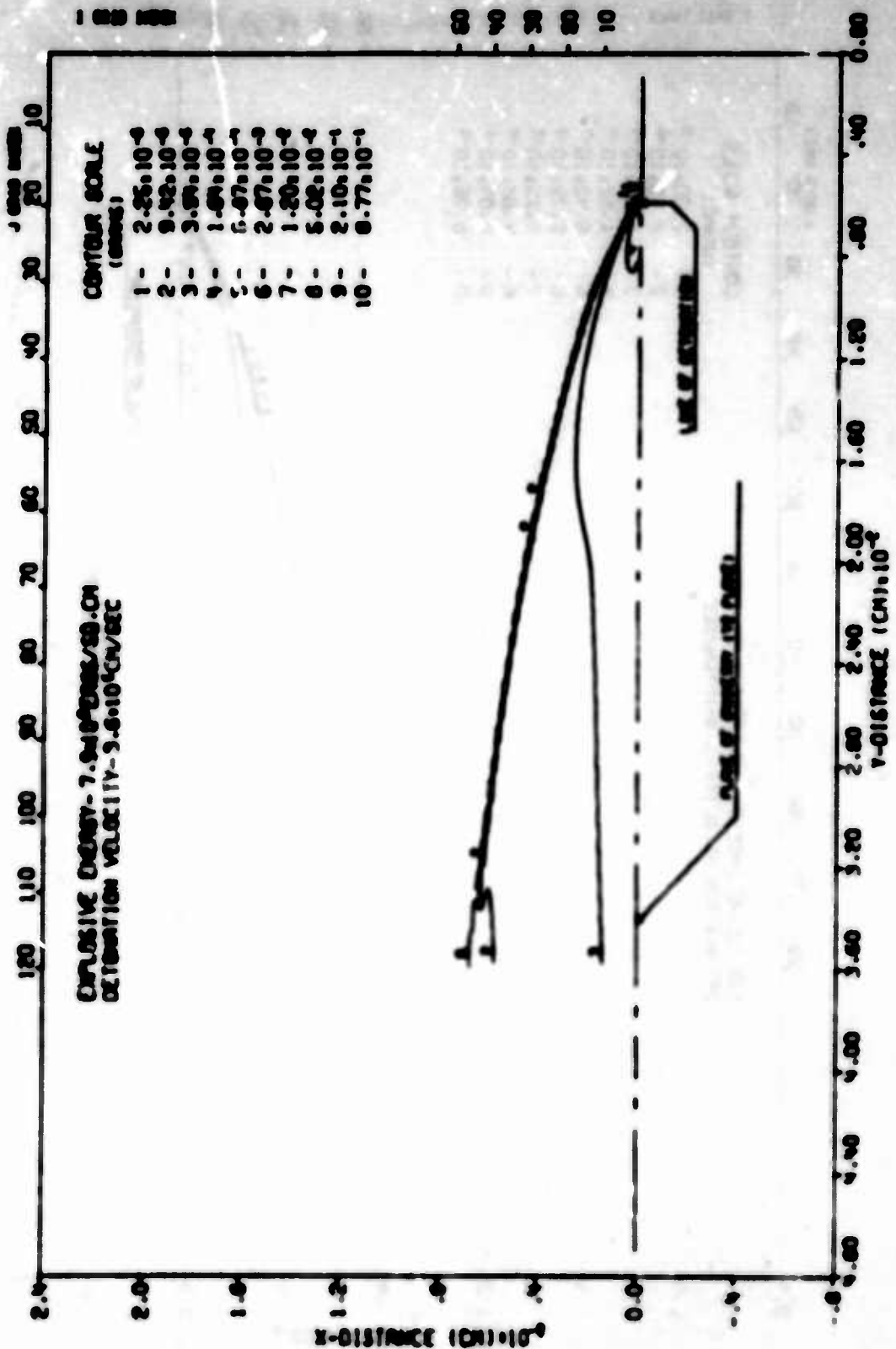


Figure 27. Constant Value Contours--Species D (Carbon monoxide)



SMELIC7 CALCULATION OF EXPLOSIVE SOURCE IN HYDROSTATIC FLUID (NO FOC)
TIME .003308 SEC CYCLE 700 PROBLEM 30.000

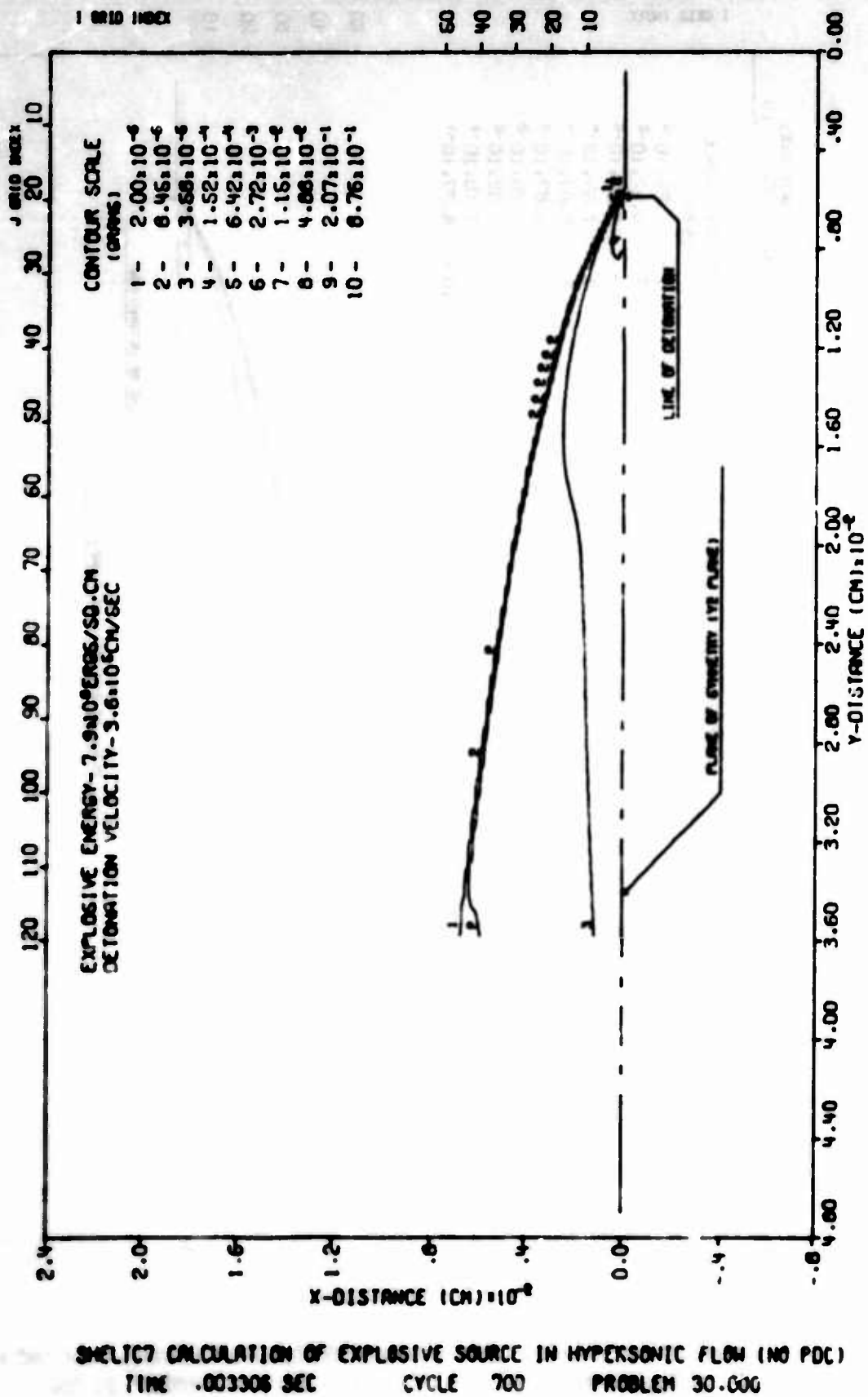
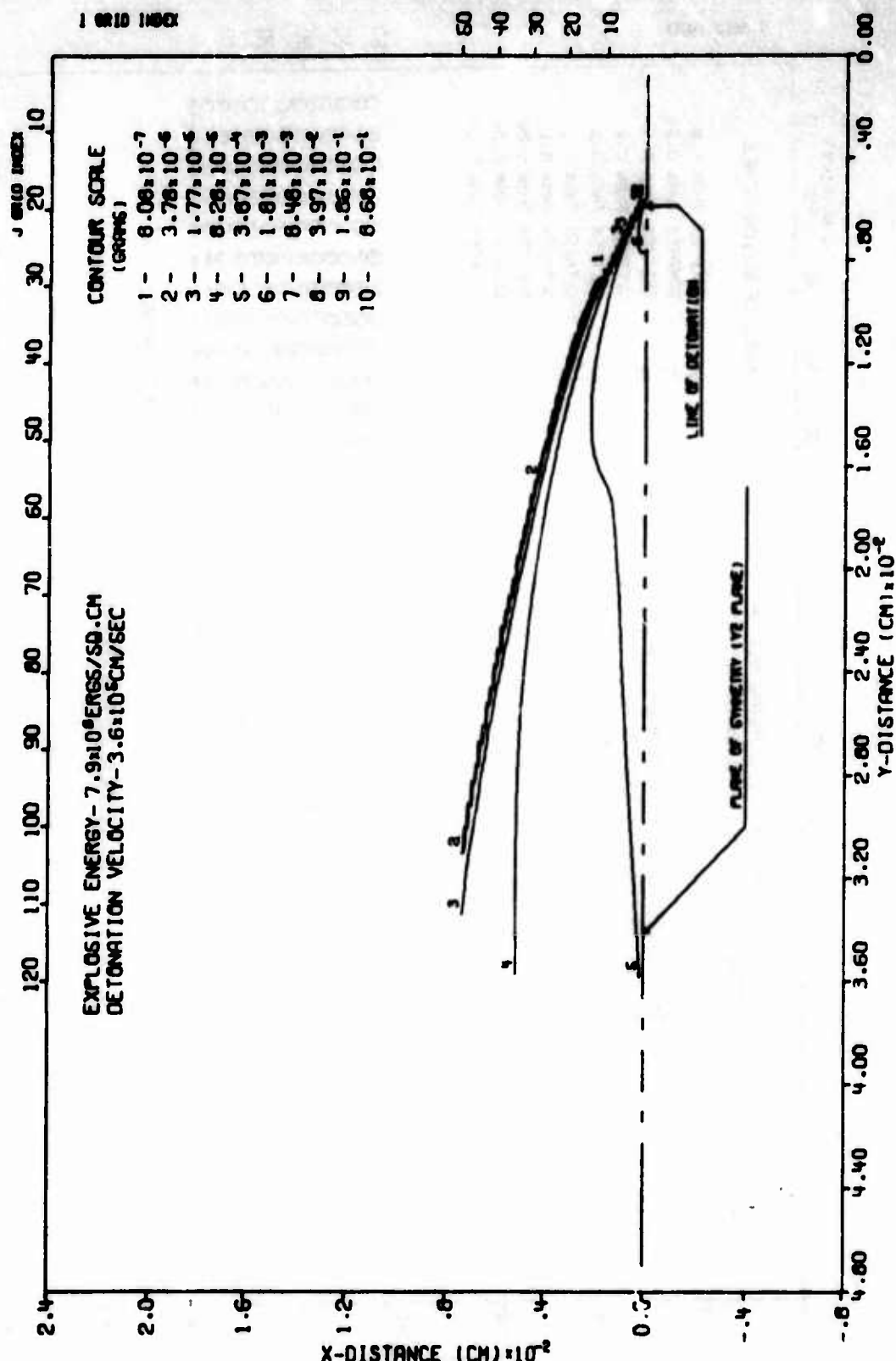
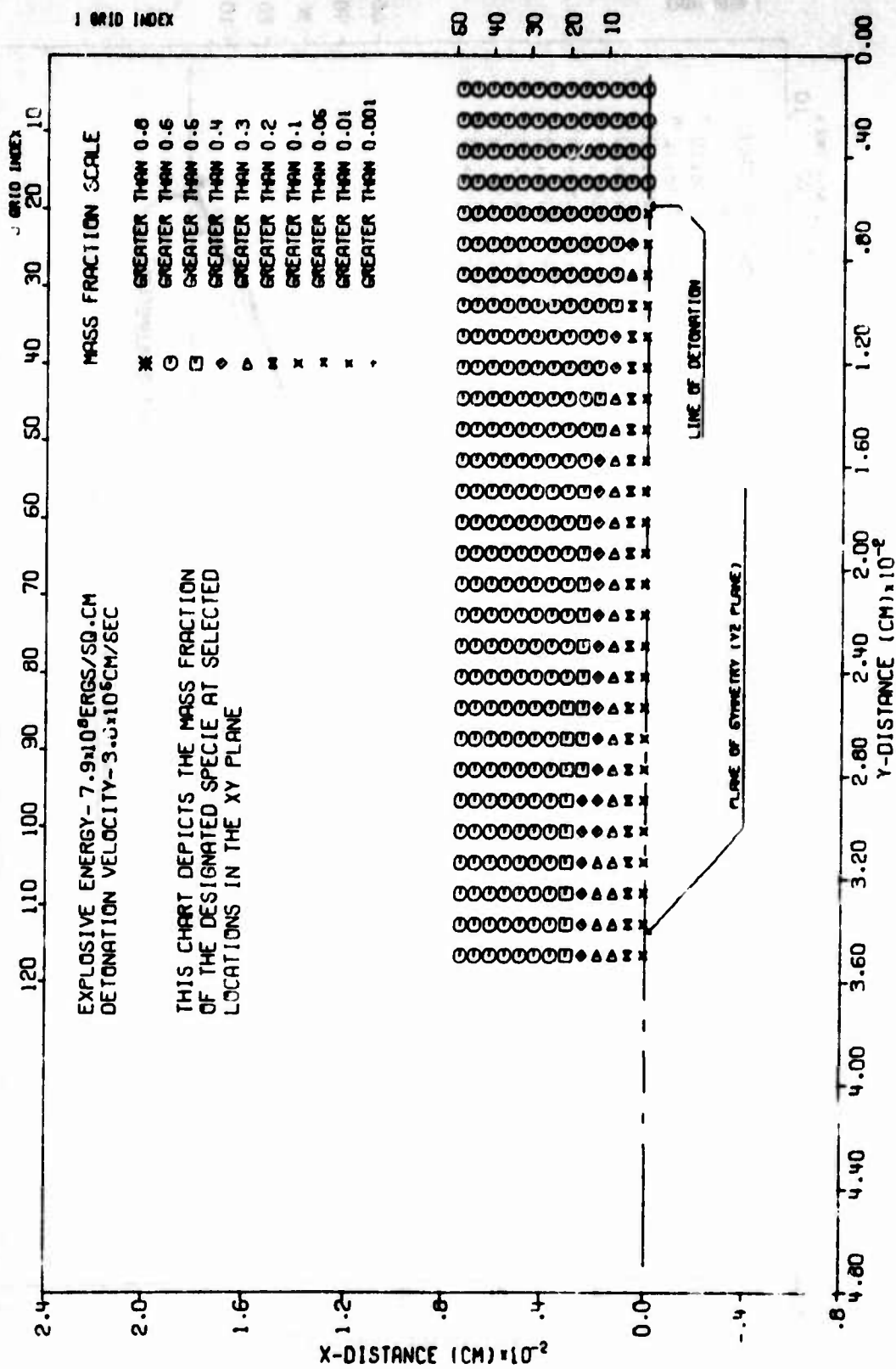


Figure 29. Constant Mass Contours—Species F (hydrogen)



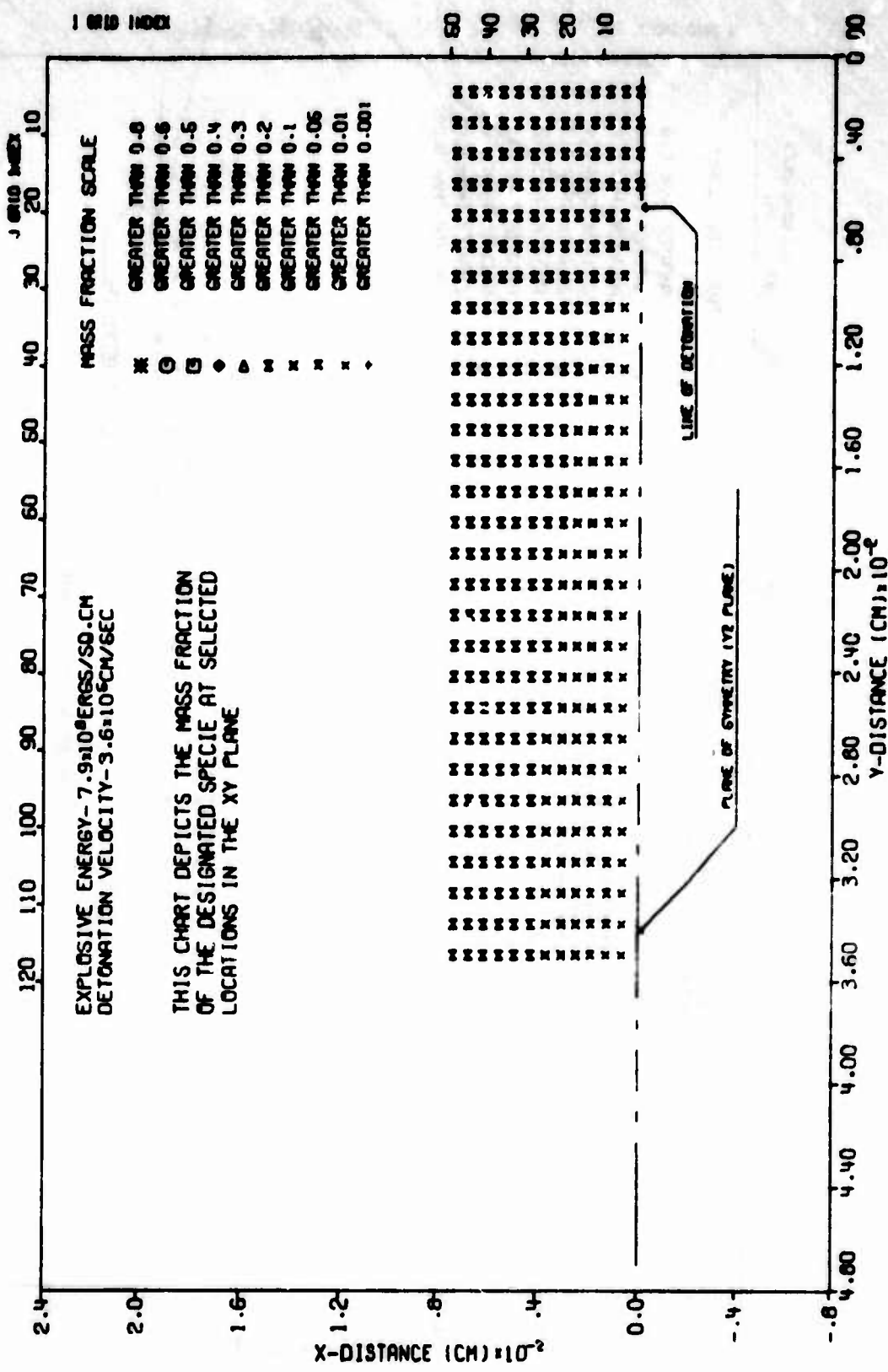
SHELTC7 CALCULATION OF EXPLOSIVE SOURCE IN HYPERSONIC FLOW (NO PDC)
 TIME .003306 SEC CYCLE 700 PROBLEM 30.000

Figure 30. Constant Mass Contours--Species G (Carbon)



SHELTC7 CALCULATION OF EXPLOSIVE SOURCE IN HYPERSONIC FLOW (NO PUC)
TIME .003306 SEC CYCLE 700 PROBLEM 30.000

Figure 31. Mass Distribution--Species A (Nitrogen)



SHELTC7 CALCULATION OF EXPLOSIVE SOURCE IN HYPERSONIC FLOW (NO PDC)
TIME .003306 SEC CYCLE 700 PROBLEM 30.000

Figure 32. Mass Distribution—Species B (Oxygen)

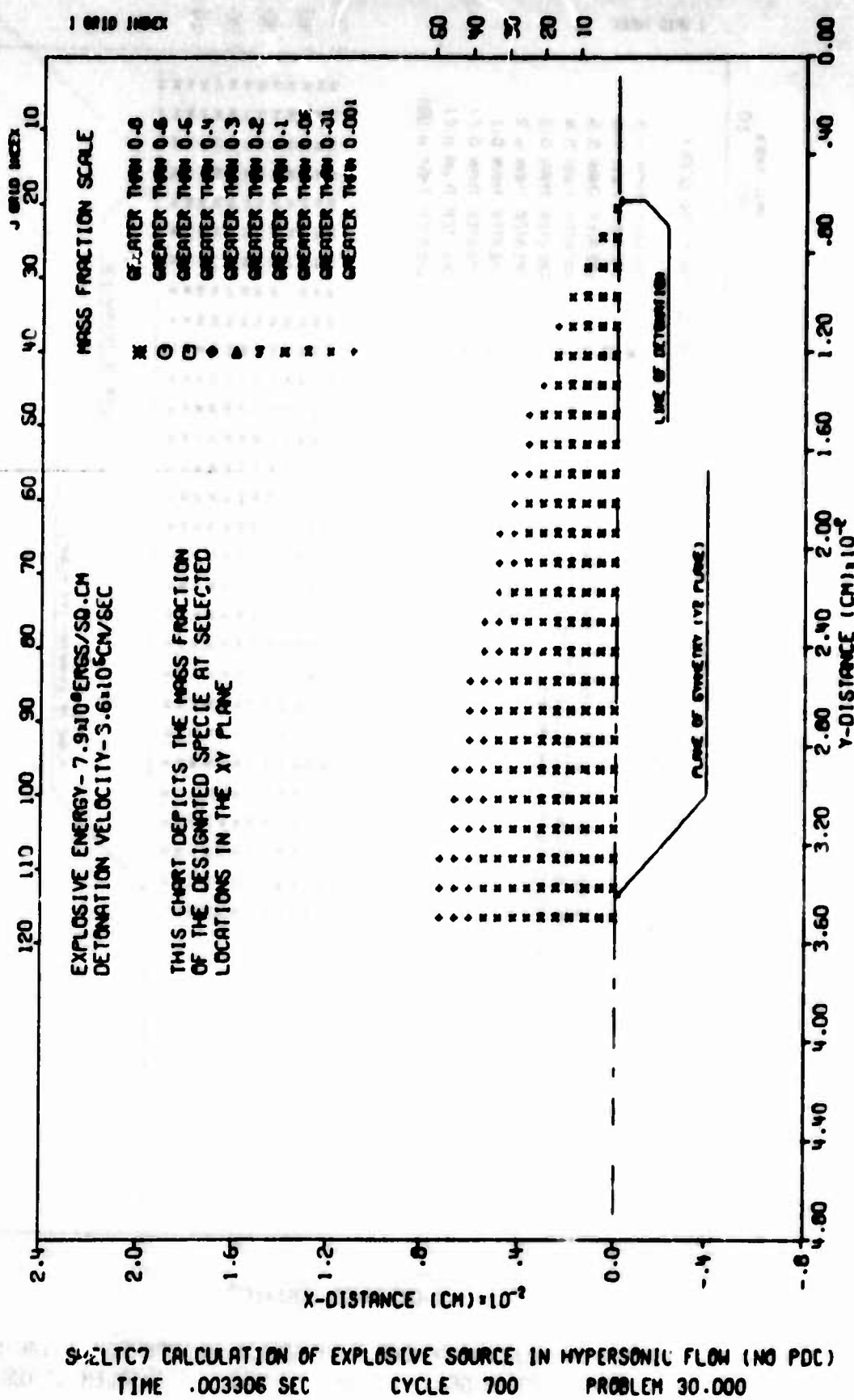
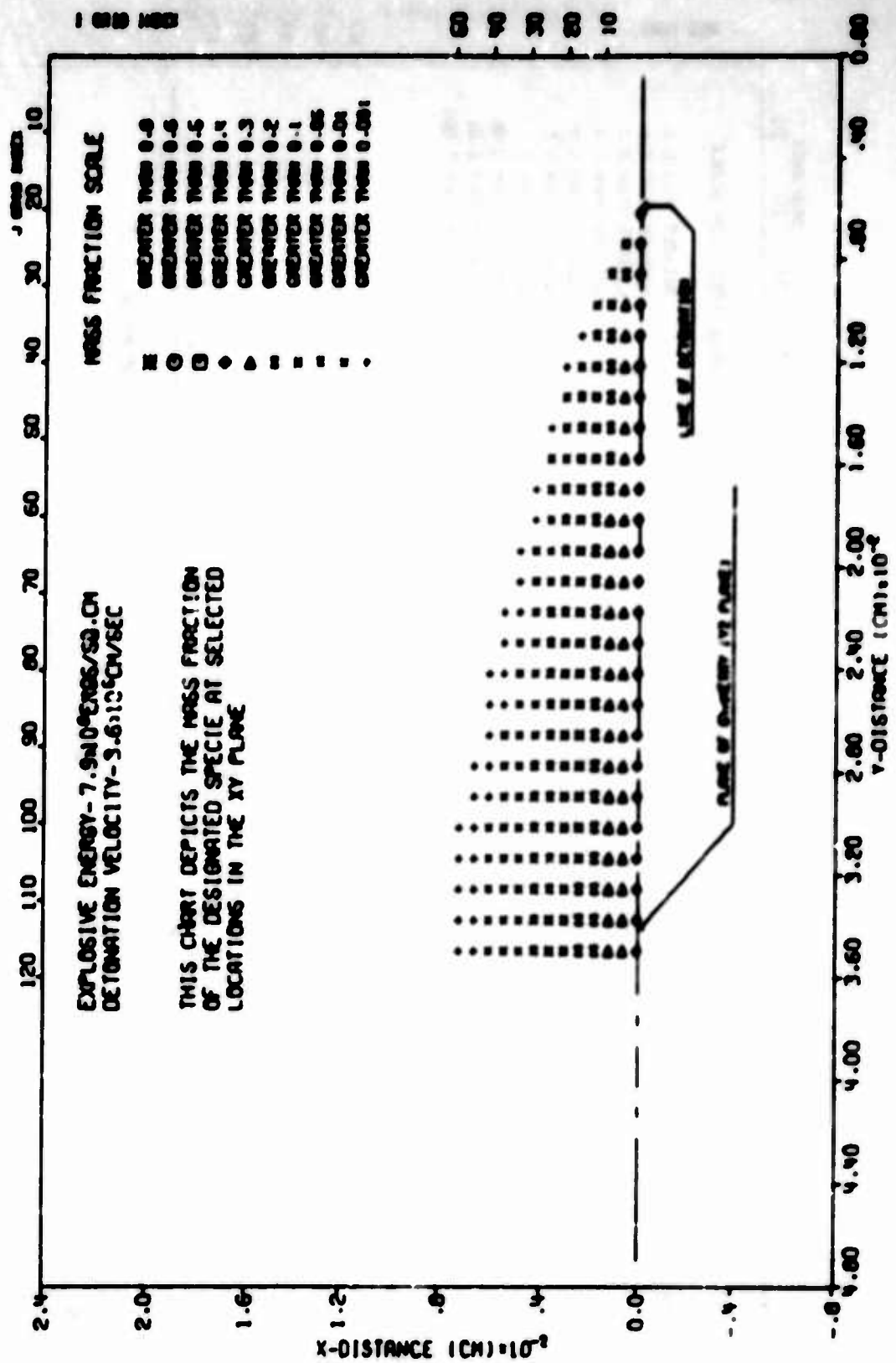
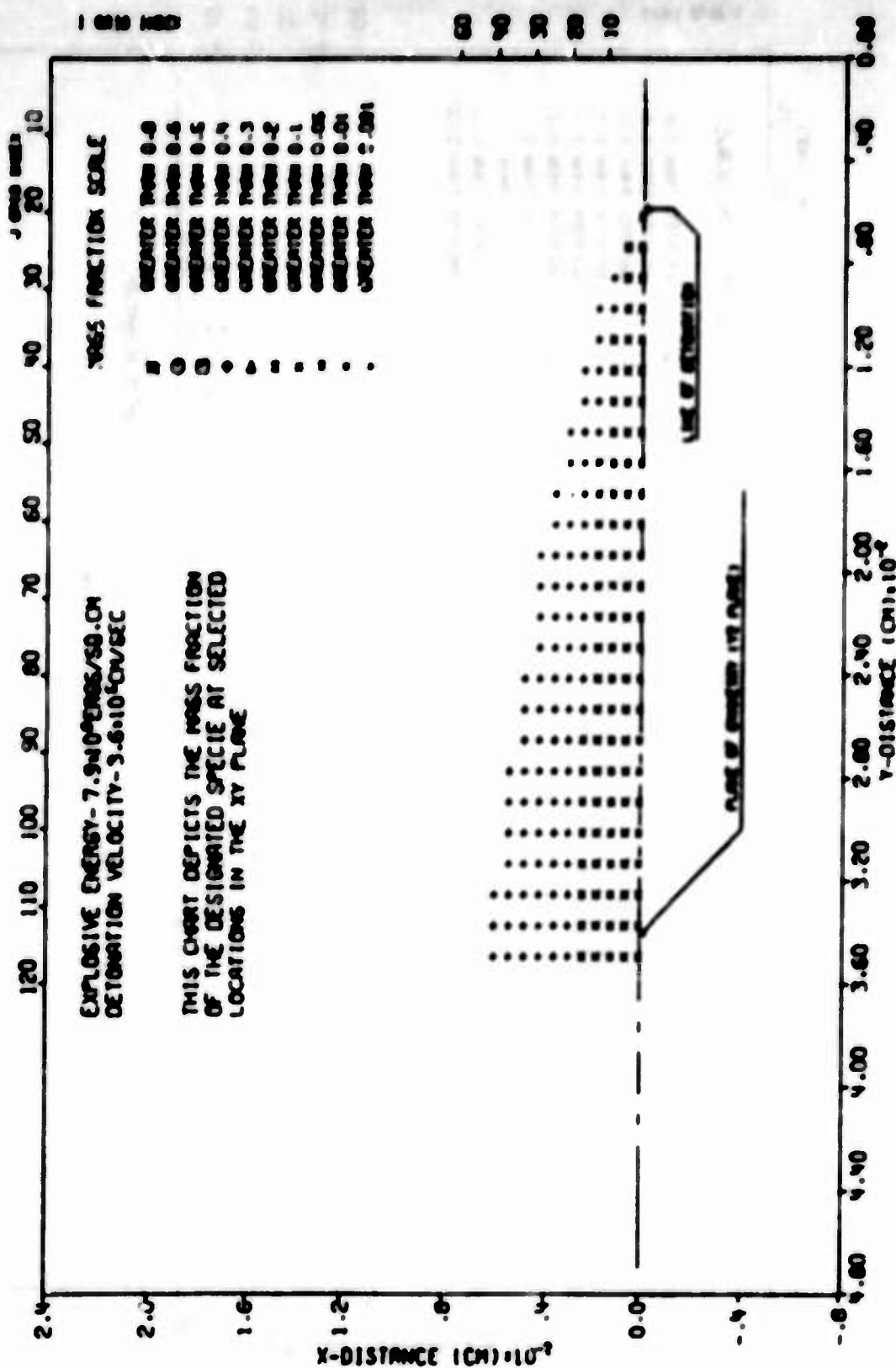


Figure 33. Mass Distribution—Species C (Carbon Monoxide)



SWEETC7 CALCULATION OF EXPLOSIVE SOURCE IN HYPERSONIC FLOW (NO PDC)
TIME .003308 SEC CYCLE 700 PROBLEM 30.000

Figure 36. Mass Distribution—Species D (Carbon Dioxide)



SHELTC7 CALCULATION OF EXPLOSIVE SOURCE IN HYPERSONIC FLOW (NO PDC)
TIME .003308 SEC CYCLE 700 PROBLEM 30.000

Figure 35. Mass Distribution-Species E (Water)

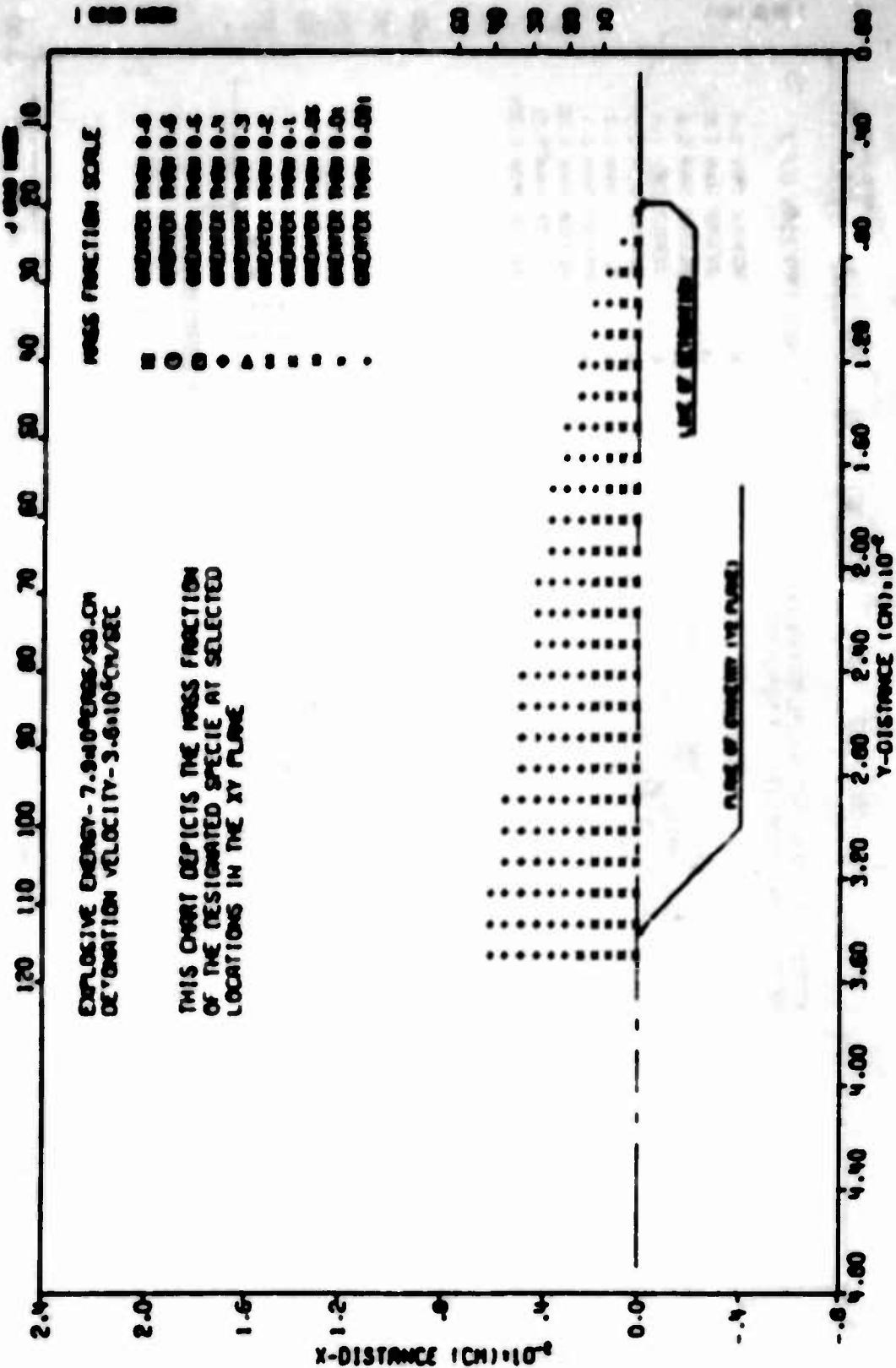
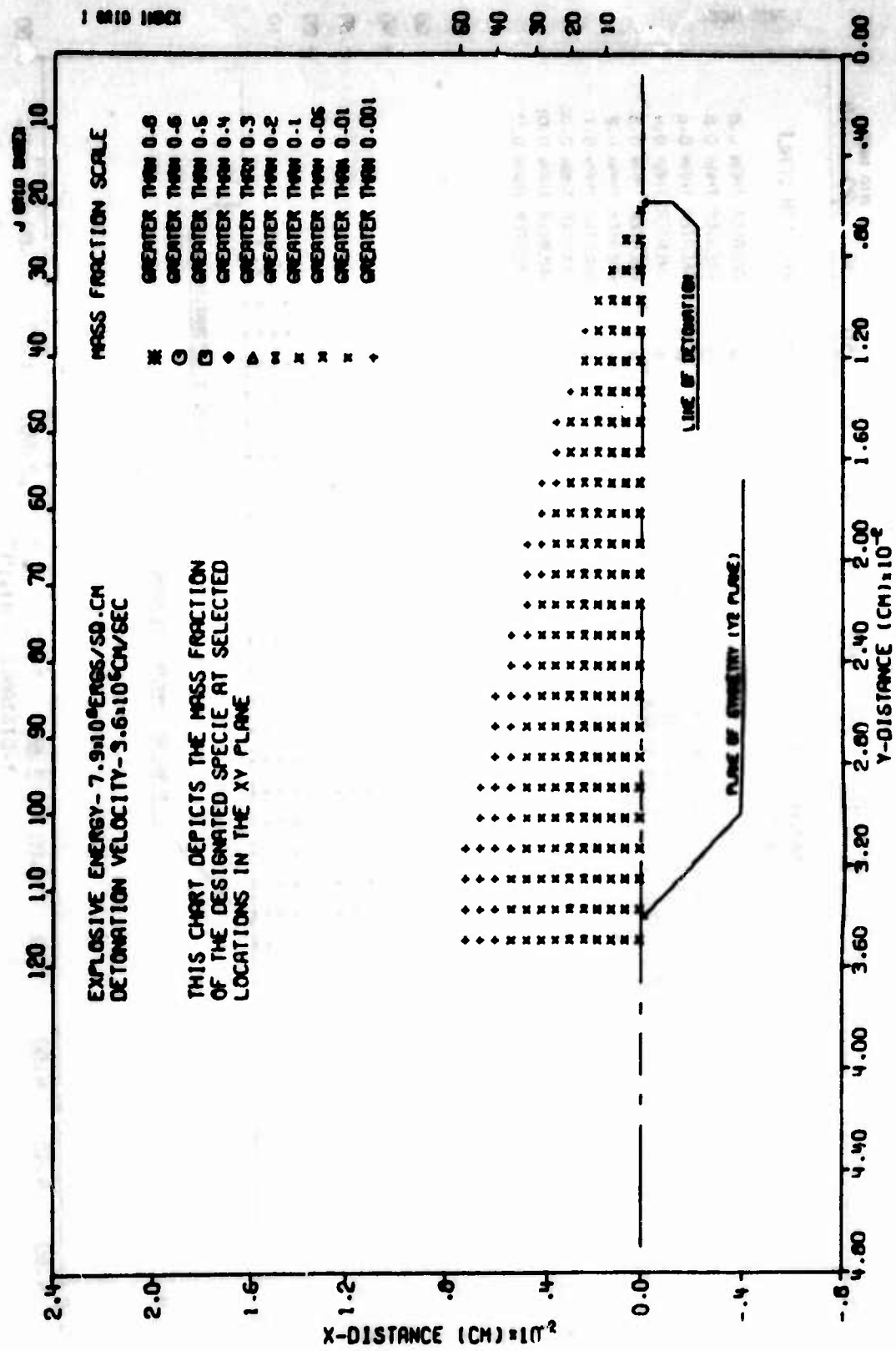


Figure 36. Mass distribution—Species F (Hydrogen)



SHELTC7 CALCULATION OF EXPLOSIVE SOURCE IN HYPERSONIC FLOW (NO PDC)
TIME .003308 SEC CYCLE 700 PROBLEM 30.000

Figure 37. Mass Distribution--Species G (Carbon)

POST-DETONATION COMBUSTION SCHEMES

Several approaches for approximating the PDC were attempted before a successful scheme was finally achieved. First a complete combustion-reaction scheme was tried where all combustion reactions were carried to completion, burning either all the fuel or all the oxygen in a cell once during each time step in an attempt at bounding the problem. Figure 38 shows that the difference between not including PDC and including PDC using the complete combustion scheme is quite drastic in terms of the shock location. However, this resulted in more energy being introduced into the flow from PDC than from the detonation, which is obviously not very representative of the real case. Next, stoichiometric combustion reactions were allowed to proceed to some arbitrarily chosen percent of completion. Here again, to preclude more energy from PDC than from the basic detonation, the percentage had to be set extremely small and there was no way to determine what percentage was correct to use. Next, a crude reaction rate scheme was tried where arbitrary rates were established at which each of the three combustion reactions (C to CO, H₂ to H₂O, and CO to CO₂) were allowed to proceed. These rates were defined as arbitrary functions of the temperature of the cell and the molar concentration of the reactants in the cell. Here again, the arbitrary rate functions led to excessive amounts of energy being deposited during each time step and, in addition, led to the formation of "hot spots." Here the temperature of the cell and the amounts

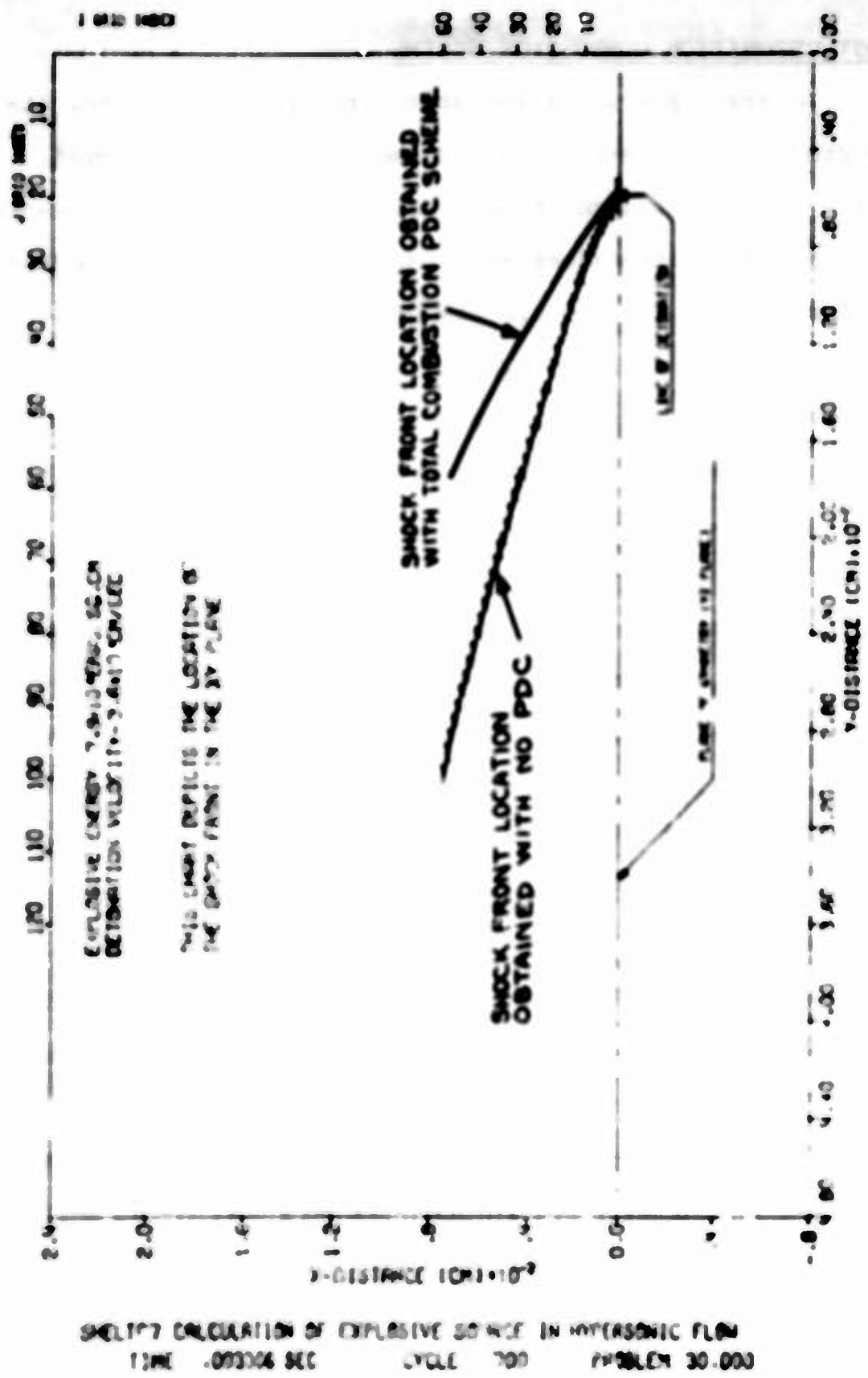


FIGURE 18. Shock front location in the XY plane

of fuel and oxygen in the cell led to large energy deposition in that cell which, in turn, raised the temperature of the cell. This process continued, causing the cell temperature to grow without bounds. It then became apparent that no satisfactory combustion scheme could be devised without somehow incorporating actual reaction kinetics.

A new approach was taken following a study by Cherry (42). The eight reactions listed in Table VIII were considered significant as a starting point.

TABLE VIII
C, H, O, N Reactions with Third Body

Reaction Number	Reaction	Rate Constant*
1	$\text{CO}_2 + M = \text{CO} + \text{O} + M$	$1 \times 10^{16} \exp[-3500/(RT)]$
2	$\text{H}_2\text{O} + M = \text{OH} + \text{H} + M$	$1 \times 10^{19} T^{-1.0}$
3	$\text{CO} + M = \text{C} + \text{O} + M$	$3 \times 10^{16} T^{-0.5}$
4	$\text{H}_2 + M = \text{H} + \text{H} + M$	$7.5 \times 10^{18} T^{-1}$
5	$\text{OH} + M = \text{O} + \text{H} + M$	$2.0 \times 10^{18} T^{-1}$
6	$\text{O}_2 + M = \text{O} + \text{O} + M$	$1.9 \times 10^{16} T^{-0.5}$
7	$\text{N}_2 + M = \text{N} + \text{N} + M$	$1 \times 10^{18} T^{-1}$
8	$\text{NO} + M = \text{N} + \text{O} + M$	$6 \times 10^{16} T^{-0.5}$

*In cm, mole, °K, sec units. Rate is for reverse (exothermic) direction.

No values of the rate constants for the forward (endothermic) reactions were found, so they were approximated by using the Arrhenius rate equation (Ref. 37).

$$R = A e^{\frac{-E}{RT}}$$

(55)

where

A = frequency factor

E = activation energy (ergs)

T = temperature ($^{\circ}$ K)

R = ideal gas constant

Considering, now, the relationship between the forward and the reverse reaction rate constants,

$$\frac{R_f}{R_r} = \frac{A_f e^{\frac{-E_f}{RT}}}{A_r e^{\frac{-E_r}{RT}}}$$

(56)

$$R_f = R_r \cdot \left(\frac{A_f}{A_r} \right) \cdot e^{\frac{E_r - E_f}{RT}}$$

(57)

If the ratio of frequency factors is assumed to be approximately one and the difference in activation energies is taken to be the combustion energy for the reaction, E_c , then

$$R_f = R_r \cdot e^{\frac{-E_c}{RT}}$$

(58)

provides a satisfactory approximation for the forward reaction rate constant. The expressions used to obtain the

forward reaction rate constants for the reactions listed in
Table VIII are

$$R_{f1} = R_{r1} \cdot e^{\frac{-6.26 \times 10^4}{T}}$$

$$R_{f2} = R_{r2} \cdot e^{\frac{-5.92 \times 10^4}{T}}$$

$$R_{f3} = R_{r3} \cdot e^{\frac{-1.29 \times 10^5}{T}}$$

$$R_{f4} = R_{r4} \cdot e^{\frac{-5.22 \times 10^4}{T}}$$

$$R_{f5} = R_{r5} \cdot e^{\frac{-5.10 \times 10^4}{T}}$$

$$R_{f6} = R_{r6} \cdot e^{\frac{-5.92 \times 10^4}{T}}$$

$$R_{f7} = R_{r7} \cdot e^{\frac{-1.13 \times 10^5}{T}}$$

$$R_{f8} = R_{r8} \cdot e^{\frac{-7.54 \times 10^4}{T}}$$

Units of the reaction rate constants are moles/cm³-sec.

In attempting to approximate a reaction rate controlled combustion scheme the rate controlling reaction must be identified. A set of initial conditions was established (arbitrarily taken from a grid cell in a previous computation) containing initial concentrations of each of the species encountered in the reactions listed in Table VIII and a starting temperature. A simplified Euler Time-Centered Predictor-Corrector numerical integration scheme was used in an auxiliary computation to integrate equation 54 for these 16 reactions using the above initial conditions. The results of this computation indicated that the reactions involving nitrogen (reactions 7 and 8, Table VIII) do not progress significantly over any long period of time, hence, they can be ignored. The reaction dissociating molecular oxygen to atomic oxygen (reaction 6 forward, Table VIII) was identified as the rate controlling reaction. The reactions consuming atomic oxygen proceeded at a much greater rate than the reaction producing it. Based on this knowledge a new PDC reaction scheme was devised wherein the actual rate of dissociation of O_2 into O is determined from an adjusted cell temperature. This rate, acting over the period of time of the hydrodynamic time step, determines the amount of atomic oxygen which is formed during a time step and is thus available for reacting with the combustible materials in the cell. To determine how much of this available atomic oxygen goes into the combustion of each of the three fuels (C , CO , H_2), a reaction rate for each is computed. The computation of a rate for the C and

CO combustion presents no problem since the molar concentration of each of these in the cell is known. Determining a rate for combustion of H₂ presents a problem because it depends upon the molar concentration of atomic hydrogen in the cell (which is not a stored variable). A way around this difficulty was obtained by assuming that the atomic and molecular hydrogen have come to dissociative equilibrium at the cell temperature which is not an unreasonable assumption since the time constant for attaining this equilibrium is short compared to the hydrodynamic time step for most cell temperatures. With a concentration of atomic hydrogen defined, a rate for the combustion of hydrogen to water can be computed. Thus, quantities of C, CO, and H₂ are burned proportional to the reaction rates computed above for each until all the atomic oxygen is consumed.

A combustion subroutine, called PDC, was constructed to accomplish these reactions in the above manner. The masses of each of the reactants and products in the cell are adjusted the appropriate amount to account for the reactions and the combustion energy produced by the reactions are added to the cell internal energy. This reaction sequence is accomplished in every cell of the grid once during each time step, the subroutine PDC being accomplished immediately after all mass transport in the code has been performed.

This combustion subroutine has been developed using real reaction rates and good approximations for the unknown molar concentrations. It should, therefore, determine the amount

of combustion in each cell quite well. Nevertheless, experimental verification of this combustion approximation would be very helpful.

COMPUTED RESULTS INCLUDING PDC

The mass and energy addition solution obtained in Section III for the energy values of 7.9×10^8 and 7.9×10^9 ergs/cm² and detonation velocity of 3.6×10^5 cm/sec was recomputed with the combustion subroutine included. For an explosive sheet with an energy density of 7.9×10^8 ergs/cm², the PDC resulted in an approximate total of 4.4×10^3 ergs of energy being deposited in the total grid during a single time step in contrast to approximately 1.4×10^9 ergs being deposited in the grid by the basic detonation during this time. The amount of energy added by the PDC is not sufficient to influence the formation of the blast wave. This fact is borne out by Figure 39 which is a plot of the shock wave shape and location as determined by a SHELTC7 calculation that included the PDC subroutine and is identical with Figure 17, produced by an identical calculation without PDC.

For an energy density of 7.9×10^9 ergs/cm² an approximate total of 2×10^7 ergs was deposited into the grid by PDC reactions compared to 1×10^{10} ergs deposited by the detonation during a time step. Although this is a substantial increase in PDC energy deposited throughout the grid over the amount deposited for the 7.9×10^8 energy density, it is still small compared to the detonation energy deposited and the

shock formation is again essentially uninfluenced by the PDC as can be seen in Figures 40 and 41.

Thus, it appears that the post-detonation combustion of the detonation products in air contributes very little to the initial formation of the blast wave. If one were to continue to sum the PDC effect over the entire history of the blast wave, a small effect would perhaps be observed at late times.

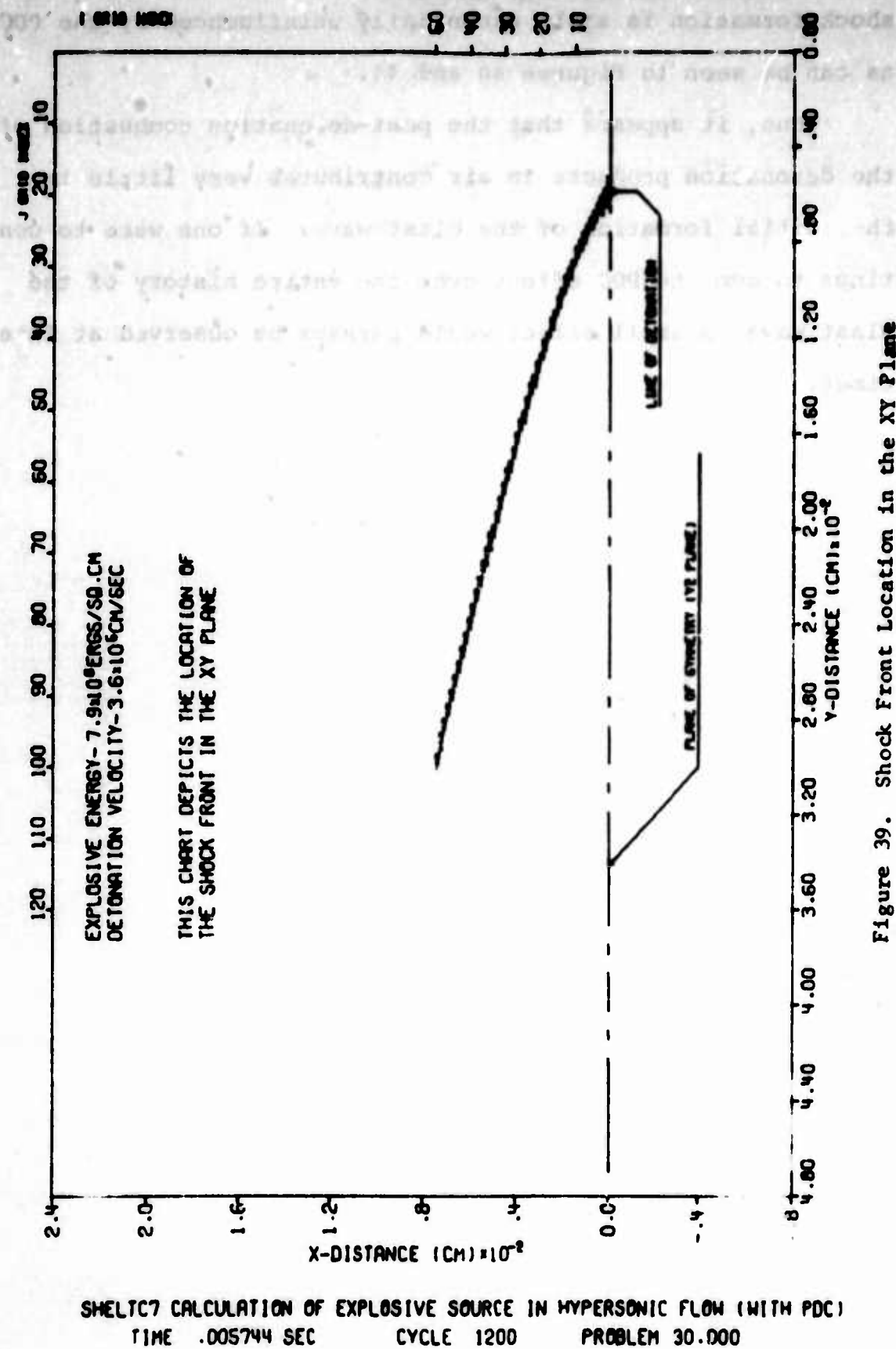


Figure 39. Shock Front Location in the XY Plane

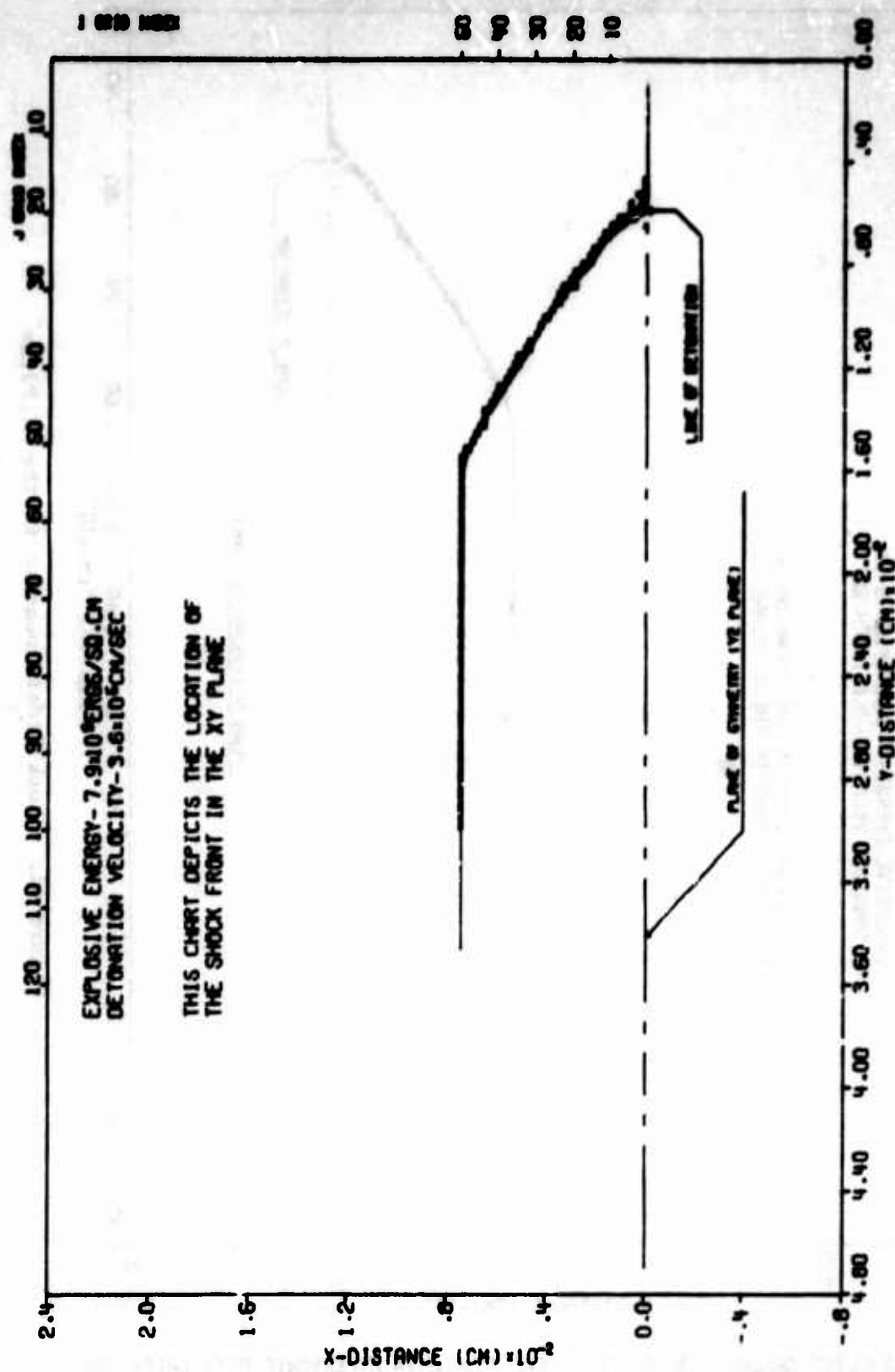
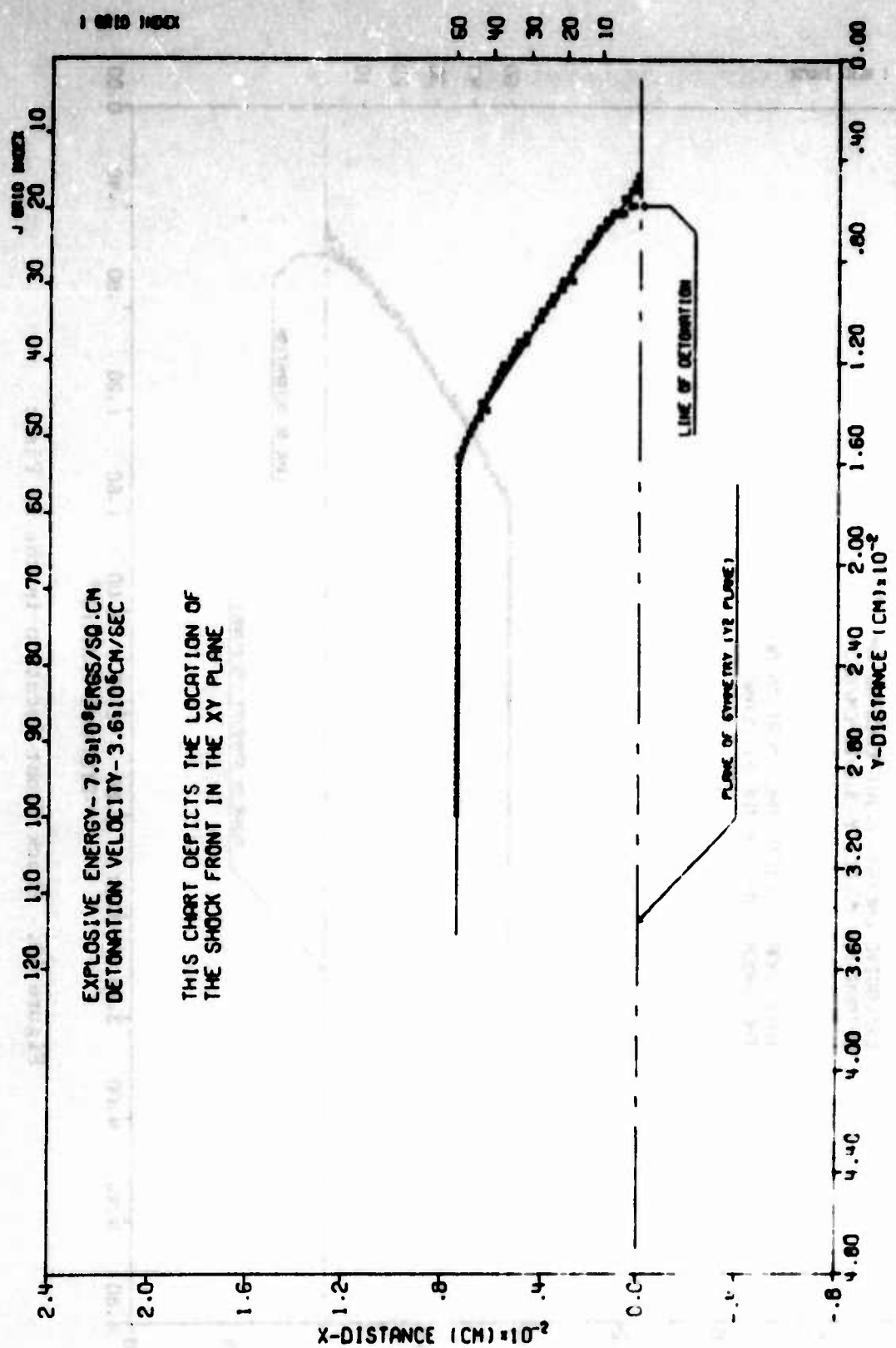


Figure 40. Shock Front Location in the XY Plane



SHELTC7 CALCULATION OF EXPLOSIVE SOURCE IN HYPERSONIC FLOW (WITH PDC)
TIME .005041 SEC CYCLE 1200 PROBLEM 30.000

Figure 41. Shock Front Location in the XY Plane

SECTION V
CONCLUSIONS AND RECOMMENDATIONS

The problem of determining the exact shape, location and properties associated with the blast wave from a constant-velocity detonation of an explosive sheet has been found to be extremely complex. It is unlikely that a closed-form analytical solution for even the most idealized form of the problem can be obtained. Numerical computations using hydrodynamic computer codes offer the greatest hope for obtaining a realistic solution.

A solution for the problem, idealized to consider the explosive sheet as releasing only energy and the surrounding medium to be an ideal gas ($\gamma = 1.4$), has been obtained using the SHELTC computer code. The shape and location of the shock front along with the properties and flow behind the front have been determined for several energies and velocities of detonation.

The shape and location of the shock wave which is formed depend both upon the energy density of the explosive sheet and upon the velocity of detonation. It is clear that the shock forms and remains continually ahead of the line of detonation, the distance in front being determined by the energy density of the explosive sheet and the velocity of detonation. An increase in the energy density causes the shock to move out further in front of the line of detonation while an increase in the velocity of detonation tends to reduce this distance. The shock wave for each energy and velocity

of detonation is near parabolic in shape close to the line of detonation and approaches a fixed angle (the Mach angle) at large distances from the line of detonation. Arguments can be made as to the exact location of the shock front (since in real gases the shock has a finite structure) but these are relatively unimportant so long as a consistent scheme is used for locating the shock in all the computations. However, the spacing between the numerically obtained isobars that form the shock front (see Figure 8) is greater than would be observed in an actual blast wave in air because the "effective viscosity" in SHELLTC spreads the shock over a greater distance than would be observed in the real case.

The pressures behind the blast wave are highest near the line of detonation and are large all along the shock front (see Figure 8). The parameters chosen to determine the "effective viscosity" in SHELLTC (S_1 , S_2 , and S_3 --see Appendix A) tend to show peak pressures slightly lower than an analytical solution for the same problem. However, the values attained here are thought to be accurate within the range of experimental error from any large explosive experiment.

The mass density also is greatest immediately behind the shock where the bulk of the mass behind the blast wave has accumulated. A low pressure, rarefied region forms behind the line of detonation and moves with it as it proceeds along the explosive sheet as can be seen in Figures 42 and 43. Figure 11 shows that in the coordinate system where the

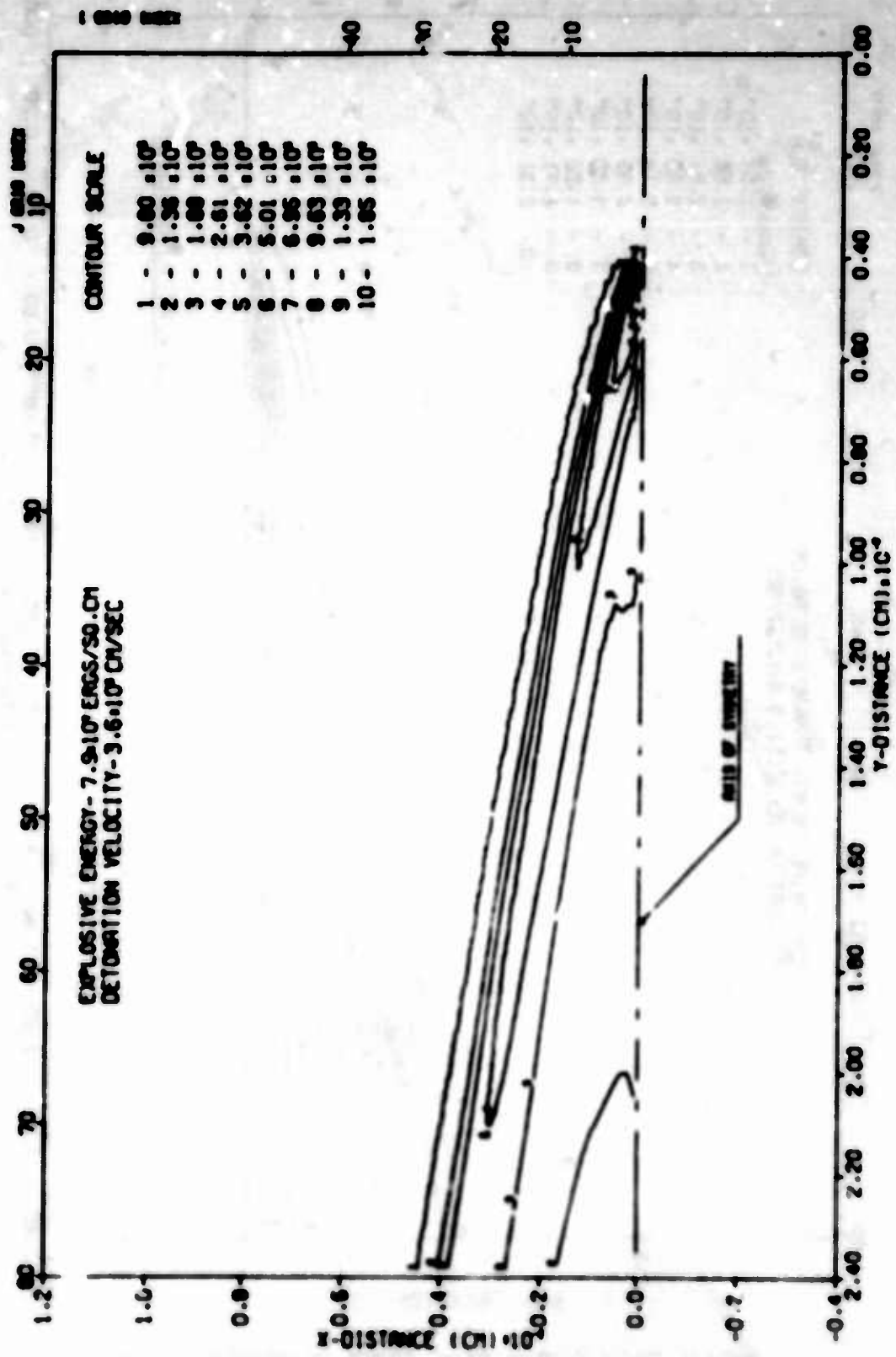
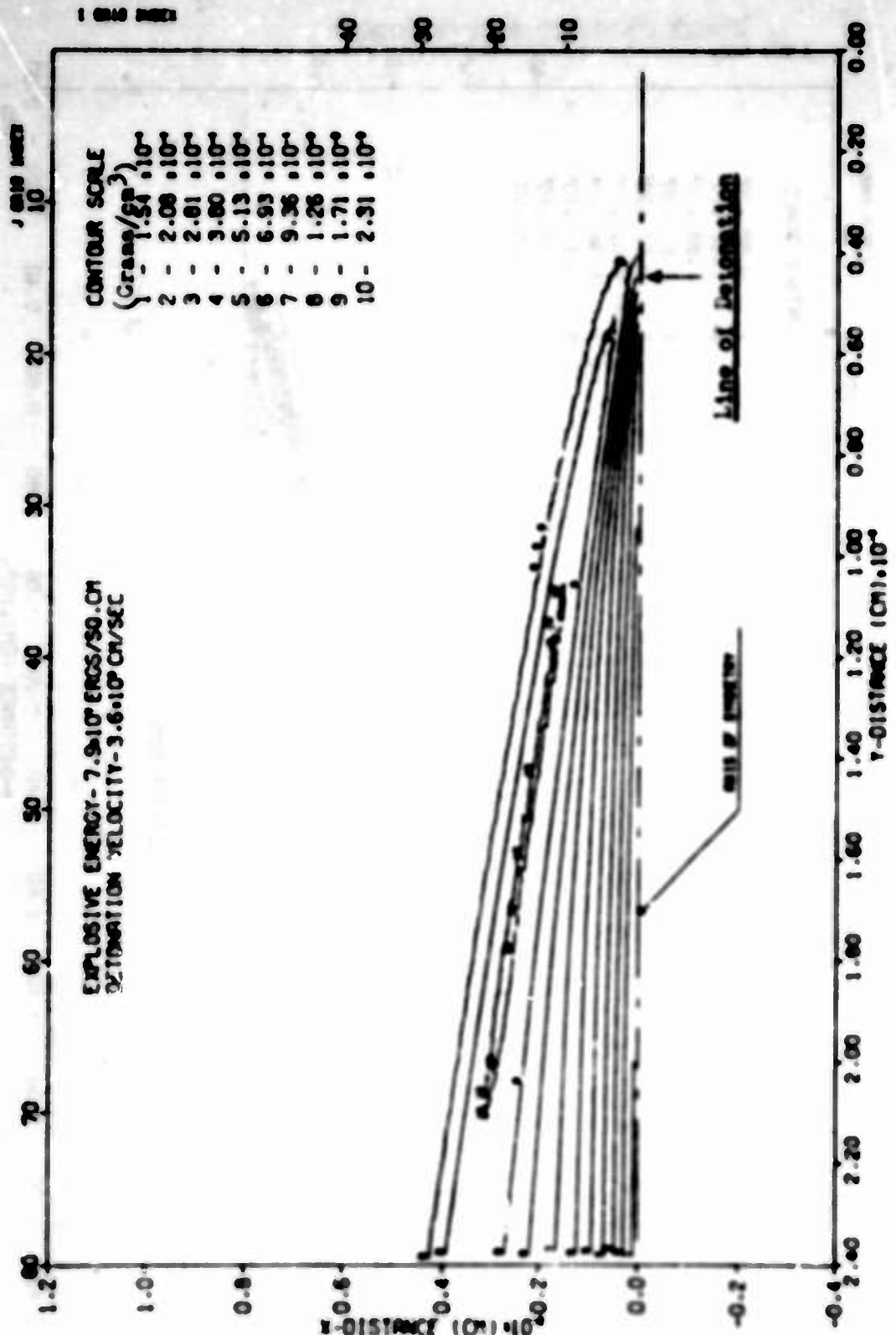


Figure 42. Constant Pressure Contours (Isobars)

SHELL TC CALCULATION OF POINT SOURCE IN HYPERSONIC FLOW
TIME 0.000004 SEC CYCLE 410 PROBLEM 21.000



SHLLIC CALCULATION OF POINT SOURCE IN HYPERSONIC FLOW
 TIME 0.000064 SEC CYCLE 410 PROBLEM 21.000

Figure 43. Constant Density Contours

line of detonation is fixed, all flow is essentially from left to right through the grid. However, in the coordinate system attached to the undisturbed gas (line of detonation moves--see Figure 12), the flow of particles in the region behind the shock and in front of the line of detonation (along the explosive sheet) is forward (toward the shock front), but the particle velocity is less than the velocity of detonation. Hence, the detonation overtakes the mass flow and as the detonation approaches, the particle velocity turns outward, away from the explosive sheet. Finally, downstream from the line of detonation, the particle velocity along the explosive sheet is directly away from the line of detonation. Hence, there is a reversal of flow in the region close to the explosive sheet as the detonation passes.

The sheet explosive problem was more realistically modeled by considering the explosive material to release mass as well as energy. A solution for the blast wave from this model was obtained using the multi-material SHELTC7 hydrodynamic code (which was developed for use in this study) along with a temperature-dependent equation of state. The formation of the blast wave was similar to the idealized case, except that the location and curvature of the shock front were altered. In this mass and energy addition solution the shock front forms farther in front of the line of detonation than for the idealized solution but it curves back more sharply producing a shallower shock profile. This solution is probably more representative of the wave from a real explosion.

A scheme for estimating the contribution to the blast wave of the post-detonation combustion was devised based on an "effective mixing" which is inherent in the SHELTC7 code. A method for approximating the combustion reactions and determining the energy released by these approximate reactions was developed and used to determine the effect of the PDC on the blast wave. The results of this work indicate that post-detonation combustion has little or no effect on the formation of the blast wave. Even though significant amounts of energy may be released by the combustion, the amounts are small compared to the detonation energy released and thus contribute little to the formation of the wave. Even though there is some doubt about the validity of the mixing used in determining the amount of PDC, the above conclusion remains unchanged since a substantial increase in PDC energy would be required before any noticeable change in the blast wave would be obtained. Since the combustion approximation scheme is based on real reaction rates or reasonable approximations thereof, it can be accepted as reasonably valid. Thus, although some error is introduced by the combustion approximation, the major source of uncertainty in determining the PDC energy released is the mixing of mass species which determines the amount of materials available for PDC. Substantial variation in the mixing can occur with only a minimum effect on the formation of the blast wave.

An expression was empirically obtained (Equation 23) which approximates the shape and location of the shock front

as determined by the idealized solution for a given energy density and velocity of detonation. If approximate information on the shock front location is all that is required, then this expression can be used to obtain it directly. A better estimate of the actual shock location can be obtained by adjusting downward the shock profile obtained from Equation 23 an amount comparable to that observed in Figure 22. If additional information about the properties of a particular blast wave is required (such as pressures, particle velocities, etc.), a computer solution following the methods described here is necessary. In view of the negligible contribution of the PDC it need not be included in the computations.

SUGGESTIONS FOR ADDITIONAL RESEARCH

The work accomplished during this study is of sufficient importance and has wide enough application to warrant additional study and expenditure of research effort. Suggestions for further work are described in the following paragraphs.

The empirically obtained expression describing the location and shape of the shock wave (equation 23, Section III) has been developed from limited data. The suitability of this expression for explosive energy densities beyond 7.9×10^9 ergs/cm² has not been verified. In addition, it appears that a similarity in shock-wave profiles exists for different energy densities and for different velocities of detonation. It may be possible to obtain a single nondimensional

expression (nondimensionalized to energy and detonation velocity) which would correctly describe the entire family of shock profiles in the xy plane. An effort to develop such a nondimensional expression or at least to develop an empirical expression for predicting the shock front shape and location from a larger data base is warranted. Some additional computations to obtain a larger data base may be required.

A detailed study and definition of the mass transport, mixing, and diffusion properties of SHELTC7 (or other multi-material Eulerian hydrodynamic codes) would be a significant contribution. Functional relationships should be developed which would describe the mixing of mass species as functions of hydrodynamic flow, species concentrations, grid cell size, etc. Correlation of these relationships with a well designed experiment would be particularly valuable. A meaningful experiment suitable to this goal can be accomplished in a supersonic wind tunnel where a thin flat plate with ports along its leading edge could be used to inject a second mass species directly in opposition (along the same centerline) to the incoming supersonic flow of the first mass species. Boundary layer effects would be minimized in this experiment and a valid calculation of the hydrodynamic flow can be accomplished. Sampling of the concentration of the two species of mass downstream from the point of injection will provide experimental data with which to correlate the mixing predicted by the code. Modifications to the code which would improve its capability to model real-flow mixing would be a valuable contribution.

Some studies of the detonation of explosive materials in confined volumes have been made (25). Additional experiments more carefully designed for correlation of calculations should be performed. A series of cylindrical charges of TNT should be detonated in a large cylindrical detonation chamber and these events calculated both in an idealized manner using SHELTC and then more realistically using SHELTC7. The contribution of PDC can be experimentally determined by purging the chamber with nitrogen prior to one of the detonations. A later experiment in which the chamber is purged with oxygen will provide additional valuable information. Calculation of these experiments with SHELTC7 will determine the capability of the PDC subroutine to predict the contribution of PDC to the blast wave.

Finally, detonation of sheets of explosives (preferably TNT) in open air would provide the most valuable data against which to test the calculational ability of these codes. Here again, the contribution of PDC in the formation of the blast wave can be examined experimentally by enclosing the explosive sheet in a bag made of thin transparent plastic purged with nitrogen or oxygen. Measurement of pressures at selected points corresponding to locations in the computational grid would be required. High-speed color photography of the traveling blast wave would provide data for direct correlation of shock front shape and location. It would be hoped that in a carefully planned experiment some indication of the

**location and extent at which PDC occurs could be detected in
these color photographs.**

After the initial soil samples were taken, photographs were taken to determine the location and extent of PDC. The photographs were taken with a Polaroid camera and Kodachrome film. The camera was held at a height of approximately 10 feet above the ground. The film was processed and developed in a Polaroid processing unit.

The photographs were taken at different times during the investigation. The first photograph was taken on May 20, 1968, at approximately 10:00 A.M. The second photograph was taken on May 21, 1968, at approximately 10:00 A.M.

The third photograph was taken on May 22, 1968, at approximately 10:00 A.M. The fourth photograph was taken on May 23, 1968, at approximately 10:00 A.M.

The fifth photograph was taken on May 24, 1968, at approximately 10:00 A.M. The sixth photograph was taken on May 25, 1968, at approximately 10:00 A.M.

The seventh photograph was taken on May 26, 1968, at approximately 10:00 A.M. The eighth photograph was taken on May 27, 1968, at approximately 10:00 A.M.

The ninth photograph was taken on May 28, 1968, at approximately 10:00 A.M. The tenth photograph was taken on May 29, 1968, at approximately 10:00 A.M.

The eleventh photograph was taken on May 30, 1968, at approximately 10:00 A.M. The twelfth photograph was taken on May 31, 1968, at approximately 10:00 A.M.

The thirteenth photograph was taken on June 1, 1968, at approximately 10:00 A.M. The fourteenth photograph was taken on June 2, 1968, at approximately 10:00 A.M.

The fifteenth photograph was taken on June 3, 1968, at approximately 10:00 A.M. The sixteenth photograph was taken on June 4, 1968, at approximately 10:00 A.M.

The seventeenth photograph was taken on June 5, 1968, at approximately 10:00 A.M. The eighteenth photograph was taken on June 6, 1968, at approximately 10:00 A.M.

The nineteenth photograph was taken on June 7, 1968, at approximately 10:00 A.M. The twentieth photograph was taken on June 8, 1968, at approximately 10:00 A.M.

The twenty-first photograph was taken on June 9, 1968, at approximately 10:00 A.M. The twenty-second photograph was taken on June 10, 1968, at approximately 10:00 A.M.

The twenty-third photograph was taken on June 11, 1968, at approximately 10:00 A.M. The twenty-fourth photograph was taken on June 12, 1968, at approximately 10:00 A.M.

APPENDIX A
THE SHELLTC CODE

The SHELLTC code is a two-coordinate system expansion of SHELL OIL which is the basic code of the SHELL family of hydrodynamic codes. The SHELL family of codes evolved directly from the particle-in-cell (PIC) method of computation developed by F. H. Harlow (15) at Los Alamos in 1955. Development of the SHELL computational scheme, formulation of this scheme into a working code, and conversion from particle to continuum are credited to B. E. Freeman, W. E. Johnson and J. M. Walsh. The most detailed description of the SHELL codes is provided by Whitaker, Nawroki and Needham (16). The following discussion of SHELL follows, in part, that document.

The equations solved in SHELL are the 2-D axisymmetric partial differential equations for nonviscous, nonconducting compressible fluid flow. These equations, including the equation of state, are

Mass

$$\rho \left(\frac{\partial}{\partial t} + \vec{u} \cdot \nabla \right) \rho + \rho \nabla \cdot \vec{u} = 0 \quad (\text{A1})$$

Momentum

$$\rho \left(\frac{\partial}{\partial t} + \vec{u} \cdot \nabla \right) \vec{u} + \nabla p + \rho \nabla \phi = 0 \quad (\text{A2})$$

Energy

$$\rho \left(\frac{\partial}{\partial t} + \vec{u} \cdot \nabla \right) E + \nabla \cdot \vec{p} \vec{u} + \rho u \cdot \nabla \phi = 0 \quad (\text{A3})$$

Equation of State

$$p = p(\rho, I) \quad (A4)$$

where

ρ : density in gms/cm³

u : velocity in cm/sec

p : pressure in dynes/cm³

E : specific total energy in ergs/gm

$$= I + 1/2 u^2$$

I : specific internal energy in ergs/gm

t : time in sec

Φ : potential of external force field in ergs/gm

SHELL-OIL is a one material, pure Eulerian code. It solves the hydrodynamic equations by dividing the region occupied by the fluid into a mesh of fixed cells. The fluid is then described at any instant of time by specifying the velocity, density, and internal energy for each cell. These values are considered to be known at the center of each cell and are constant over it. This forced homogeneity of the cell introduces a false diffusion which poses no problem in this one material code but becomes a major disadvantage in multi-material versions of SHELL.

Other disadvantages of SHELL-OIL are the general inability of Eulerian codes to resolve fine detail moving with the fluid, since the mesh is fixed in space, and the inability to follow material interfaces. However, Eulerian codes enjoy

the major advantage of being able to solve the hydrodynamic equations even in the presence of large fluid distortions.

To begin a SHELL-OIL calculation, the problem must first be generated by CLAM, the generator code for SHELL. CLAM sets up the mesh, giving each cell its dimensions and the following quantities: a radial and an axial velocity component, a mass, and a specific internal energy.

The cell quantities are derived from data entered in groups of packages. These data include the type of material, dimensions, velocity components, density, and specific internal energy of the package. To describe as many geometries and energy, density and velocity distributions as possible, CLAM places N^2 particles into each cell, where $1 \leq N \leq 20$ and is also included in the package data. Each cell is divided into N^2 equal parts, and a particle is placed at the center of each area. Taking this package data, a fit assigns each particle two velocity components--a density and a specific internal energy. Then the mass of each particle is computed: the density times the volume of that part of the cell containing the particle. The mass of the cell is the sum of the masses of all the particles in the cell. Both momentum components are calculated as the sum of the individual momentum components of each particle in the cell. The internal energy of each cell is the sum of the internal energies of all the particles in the cell. Finally, these cell quantities are converted to two velocity components and specific internal energy.

There are five geometries available in CLAM such that mass may be loaded into the grid in zones with the following shapes: rectangle, triangle, ellipse, perturbed ellipse and circle. These zones are in the r-z plane and take their 3-dimensional counterparts upon rotation about the z-axis.

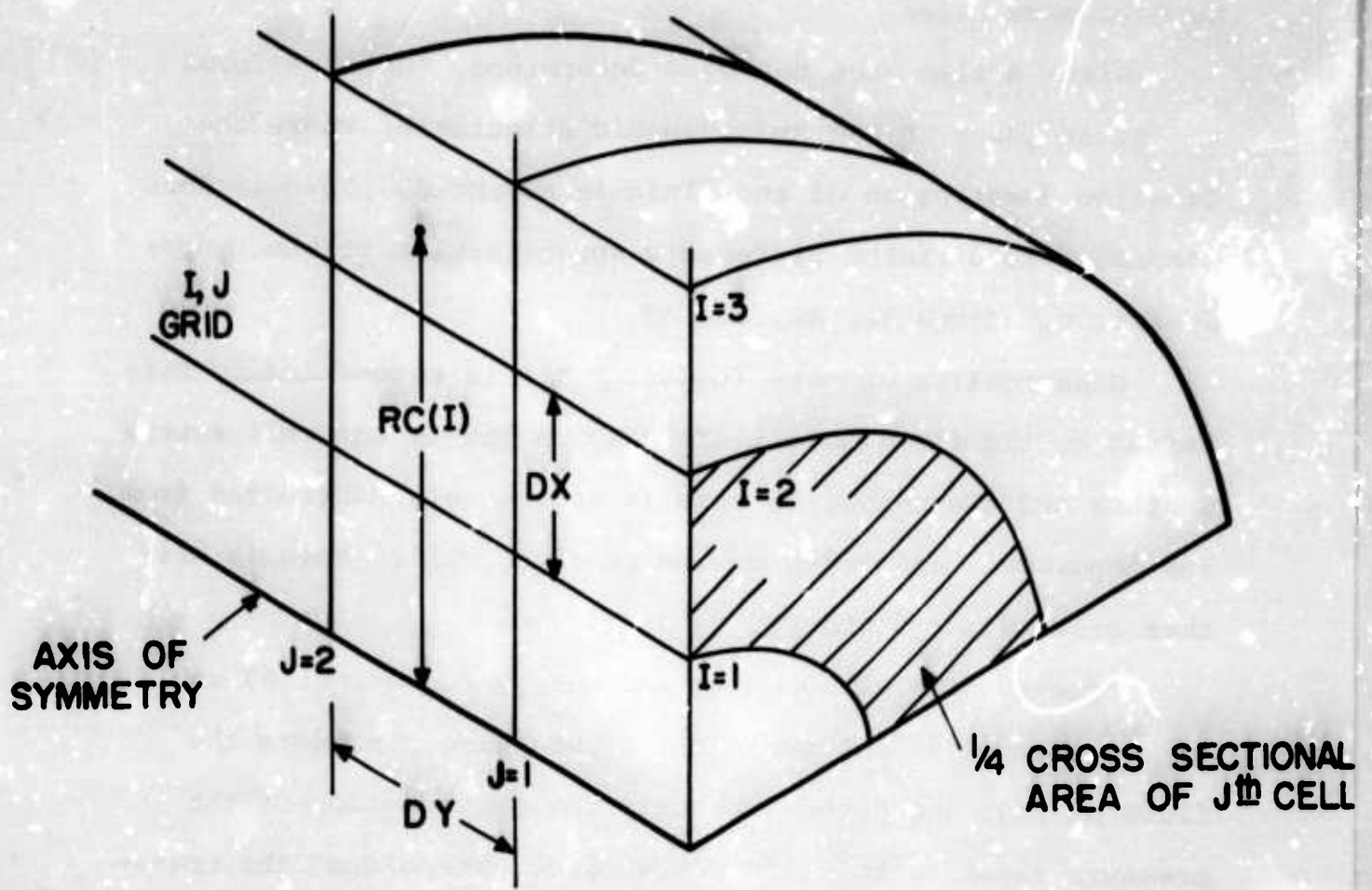
After all packages have been processed, CLAM puts all cell dimensions and quantities on tape.

This output provides the starting conditions for the SHELL calculation. The SHELL calculation advances explicitly in steps or cycles. That is, the cell quantities are calculated for time $t + \Delta t$ in terms of those at time t . The solution of the hydrodynamic equations is divided into two phases. In the first, the Eulerian field functions are updated, considering pressure effects alone while neglecting material transport due to fluid motion. In the second phase, continuous mass flow across cell boundaries, new cell densities, velocities, and specific internal energies are calculated. Mass, momentum, and total energy are conserved.

There are three time-control conditions that govern the time step, Δt . They are

- a. The Courant condition
- b. The maximum of $|\frac{u}{\Delta r}|$ and $|\frac{v}{\Delta z}| < \frac{1}{\Delta t}$
- c. A negative time-step option

The first two conditions prohibit the transmission of a signal or mass across more than one cell in one time interval. This requirement is imposed by considerations of stability



$RC(J)$ is radial distance to center of a cell in the I th column.

Axial dimension of each cell is DY .

Radial dimension of each cell is DX .

Cross-sectional area of each cell is $TAU(I)$ where

$$TAU(I) = 2 \cdot \pi \cdot RC(I) \cdot DX$$

Volume of each cell is

$$VOL(I) = 2 \cdot \pi \cdot RC(I) \cdot DX \cdot DY$$

Figure A1. SHELL ZONING--Two-Dimensional Axisymmetric Case

of the finite difference equations. The third condition will be discussed below.

After a time step has been determined, SHELL performs the first phase of the hydrodynamic calculation where the Eulerian description of the fluid is advanced. This is done according to a finite difference approximation to the hydrodynamic equations A1, A2, and A3.

Conservation of mass (equation A1) is automatically satisfied by the fluid model. Mass which leaves one cell enters another and the change in mass is accordingly subtracted from the donor cell and added to the receiver cell. Mass is neither created nor destroyed.

Conservation of momentum and energy (equations A2 and A3) is treated as follows: the first phase considers the fluid at rest and determines only the contribution of the pressure terms to the time derivative. Therefore, the transport term (second term on the left-hand side) of each equation is dropped. Since the hydrodynamic quantities are defined at the cell centers, the equations in finite difference form become

Momentum

$$\tilde{u}_k^{(n)} = u_k^{(n)} + \frac{1}{\rho_k^{(n)}} \frac{p_L^{(n)} - p_R^{(n)}}{\Delta r} \Delta t \quad (A5)$$

$$\tilde{v}_k^{(n)} = v_k^{(n)} + \frac{1}{\rho_k^{(n)}} \frac{p_B^{(n)} - p_A^{(n)}}{\Delta z} \Delta t \quad (A6)$$

Energy

$$\tilde{I}_k = I_k^{(n)} + \frac{p_k^{(n)}}{\rho_k^{(n)}} \left[\frac{v_B^{(n)} - v_A^{(n)}}{\Delta z} + \frac{v_B - \tilde{v}_A}{\Delta t} \right. \\ \left. + \frac{2}{r_i + r_{i-1}} \frac{u_L^{(n)} - u_R^{(n)}}{\Delta r} + \frac{\tilde{u}_L - \tilde{u}_R}{\Delta t} \right] \frac{\Delta t}{2} \quad (A7)$$

where

$$P_L = \frac{p_k + p_{kL}}{2} \quad P_R = \frac{p_k + p_{kR}}{2}$$

$$P_B = \frac{p_k + p_{kB}}{2} \quad P_A = \frac{p_k + p_{kA}}{2}$$

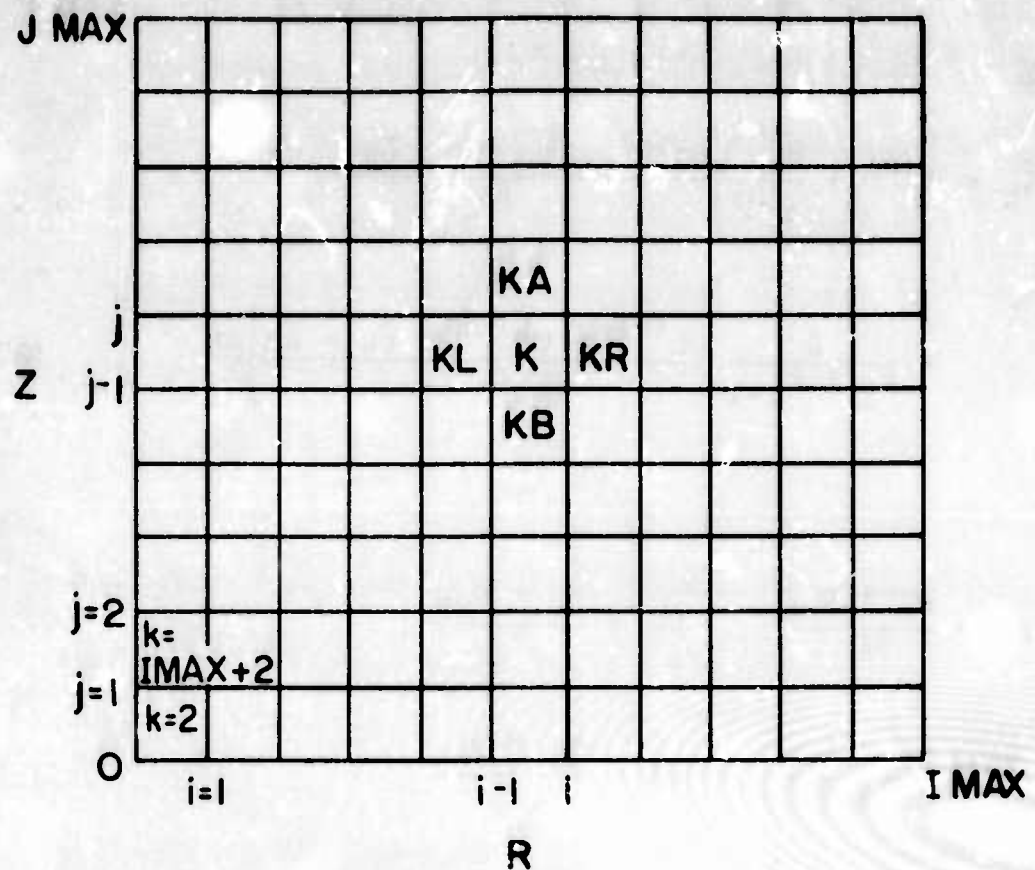
$$V_B = \frac{v_k + v_{kB}}{2} \quad V_A = \frac{v_k + v_{kA}}{2}$$

$$U_L = \frac{u_k(r_i + r_{i-1}) + u_{kL}(r_{i-1} + r_{i-2})}{4}$$

$$U_R = \frac{u_k(r_i + r_{i-1}) + u_{kR}(r_{i+1} + r_i)}{4}$$

and k is the index of the cell center and i is the index of the right-hand boundary of cell k (see Figure A2).

Two passes in succession are made through the first phase of calculation of each cycle. In the first pass, tentative new values of velocity are calculated for a full time step. The internal energy is updated by half a time step, using the old velocities. In the second pass, the internal energy is updated another half-time step, using the tentative



i is the right boundary of cell k

j is the top boundary of cell k

KA is the cell above cell k

etc.

Figure A2. The SHELL Mesh

new velocities calculated in the first pass. The energy equation is treated in this fashion from considerations of stability as well as greatest accuracy in the behavior of fluid entropy. The energy of the system is conserved identically, even in the finite difference approach.

In both passes, the internal energy is checked to see if the updated value has become negative. If it has, an option exists to integrate back to the original configuration of the

fluid at the beginning of the cycle by using the negative Δt . Then the integration goes forward again with a smaller Δt which has been calculated and which will keep the internal energy positive.

In the second phase of the hydrodynamic calculation, continuous mass transport is calculated according to the equation for the conservation of mass, which in finite difference form is

$$\frac{\Delta \rho}{\Delta t} = \left[\frac{r_{i-1}\rho_{i-1}u_{i-1}}{r_{i-1/2}\Delta r} - \frac{r_i\rho_iu_i}{r_{i-1/2}\Delta r} + \frac{\rho_{j-1}v_{j-1} - \rho_jv_j}{\Delta z} \right] \quad (A8)$$

This can be rewritten to the following form, which is used by the code

$$\begin{aligned} m_k^{(n+1)} = m_k^{(n)} &+ \pi \Delta t \left[(r_i^2 - r_{i-1}^2) (\bar{v}_B \rho_B - \bar{v}_T \rho_T) \right. \\ &\left. + 2\Delta z (r_{i-1} \bar{u}_L \rho_L - r_i \bar{u}_R \rho_R) \right] \end{aligned} \quad (A9)$$

where

$\bar{v}_B \rho_B$ ≡ mass flux across bottom face of cell K

$\bar{v}_T \rho_T$ ≡ mass flux across top face of cell K

$\bar{u}_L \rho_L$ ≡ mass flux across left face of cell K

$\bar{u}_R \rho_R$ ≡ mass flux across right face of cell K

and where the densities are those of the donor cells and the velocities are

$$\bar{v} = \frac{1/2(\tilde{v}_M + \tilde{v}_K)}{1 + (\tilde{v}_M - \tilde{v}_K)\frac{\Delta t}{\Delta z}} \quad \text{where } M \text{ is the cell above cell } K$$

$$\bar{u} = \frac{1/2(\tilde{u}_M + \tilde{u}_K)}{1 + (\tilde{u}_M - \tilde{u}_K)\frac{\Delta t}{\Delta r}} \quad \text{where } M \text{ is the cell to right of cell } K$$

The velocity-weighting scheme used above is one that ensures stability in regions behind a shock front.

When mass transport is being calculated for a given cell, the transfer at the left and bottom faces is already available from the previous column sweep and cell below, respectively. Therefore, for a particular cell, the mass transport is calculated for the top and right faces only. After the masses transferred at all faces of a cell have been determined, the momenta and the total specific energy associated with these masses are computed. Then, by conserving both axial and radial momentum, the new velocities are calculated. The total energy carried by the transported masses is subtracted from the donor cell and added to the receiver cell. Then, by conserving both axial and radial momentum the new velocities are calculated. The total energy carried by the transported masses is subtracted from the donor cell and added to the receiver cell. Then, by conserving total energy the new internal energy of each cell is the difference between the new total energy and the new kinetic energy. The new specific internal energy is the new internal energy divided by the new mass.

$$M_k^{(n+1)} = M_k^{(n)} + \Delta M_B + \Delta M_L - \Delta M_T - \Delta M_R \quad (A10)$$

$$v_k^{(n+1)} = \frac{M_k^{(n)} \tilde{v}_k + \Delta M_B \tilde{v}_M + \Delta M_L \tilde{v}_M - \Delta M_T \tilde{v}_M - \Delta M_R \tilde{v}_M}{M_k^{(n+1)}} \quad (A11)$$

$$u_k^{(n+1)} = \frac{M_k^{(n)} \tilde{u}_k + \Delta M_B \tilde{u}_M + \Delta M_L \tilde{u}_M - \Delta M_T \tilde{u}_M - \Delta M_R \tilde{u}_M}{M_k^{(n+1)}} \quad (A12)$$

where M designates the donor cell.

$$\begin{aligned} I_k^{(n+1)} &= \left\{ M_k^{(n)} \left[\tilde{I}_k + \frac{1}{2} (\tilde{u}_k^2 + \tilde{v}_k^2) \right] + \Delta M_B \left[\tilde{I}_M + \frac{1}{2} (\tilde{u}_M^2 + \tilde{v}_M^2) \right] \right. \\ &\quad + \Delta M_L \left[\tilde{I}_M + \frac{1}{2} (\tilde{u}_M^2 + \tilde{v}_M^2) \right] - \Delta M_T \left[\tilde{I}_M + \frac{1}{2} (\tilde{u}_M^2 + \tilde{v}_M^2) \right] \\ &\quad \left. - \Delta M_R \left[\tilde{I}_M + \frac{1}{2} (\tilde{u}_M^2 + \tilde{v}_M^2) \right] \right\} / \\ &\quad \left\{ M_k^{(n+1)} - \frac{\frac{1}{2} [u^{(n+1)}]^2 - \frac{1}{2} [v^{(n+1)}]^2}{M_k^{(n+1)}} \right\} \end{aligned} \quad (A13)$$

where ΔM_B , ΔM_L , ΔM_T , and ΔM_R are the masses, in grams transferred across the bottom, left, top, and right faces of cell K, respectively, and where the quantities enclosed in brackets and subscripted by M are the specific total energies of the donor cells. The above are the final values of velocity, mass, and specific internal energy for the cycle. If any mass leaves the top, right, or bottom boundaries of the grid,

that mass and the associated energy are subtracted from the total mass and energy of the system respectively.

The calculation of mass transport in SHELL-OIL has another feature that removes preferential transfer caused by initial choice of indexing. If the mass out the top and right would remove more than the mass in the cell, the code recalculates new mass transfer by a weighting procedure. The ΔM_R would be its fraction of the total mass out times the mass of the cell and ΔM_T would be its fraction of the total mass out times the mass of the cell. That is,

$$\Delta M_T = \frac{\Delta M_T}{\Delta M_T + \Delta M_R} (M_K^{(n)} + \Delta M_L + \Delta M_B) \quad (A14)$$

$$\Delta M_R = \frac{\Delta M_R}{\Delta M_T + \Delta M_R} (M_K^{(n)} + \Delta M_L + \Delta M_B) \quad (A15)$$

In this calculation ΔM_L and ΔM_B are considered zero if they are flowing into cell K so that the maximum mass that could flow out the top and right is $M_K^{(n)}$. However, if ΔM_L and ΔM_B are flowing out of cell K, the cell is committed to deliver this mass and so the maximum mass that can flow out the top and right is $M_K^{(n)} + \Delta M_L + \Delta M_B$ (where ΔM_L and ΔM_B are negative signifying flow in negative direction).

STABILITY OF SHELL CODES

The Eulerian equations used in the first phase of the calculation are unstable, since they do not contain the dissipative mechanism necessary for a finite difference technique

to calculate shocks. Since shocks appear as mathematical surfaces on which such fluid properties as density, pressure, internal energy, and entropy have discontinuities, suitable boundary conditions (those provided by the Rankine-Hugoniot equations) are needed to connect the values of the above quantities on both sides of the shock. However, Von Neumann and Richtmeyer (6) have shown that the hydrodynamic equations can be straightforwardly solved by numerical methods if an artificial dissipative term is introduced. This term smears the shock so that the surface of discontinuity is replaced by a thin layer in which the above quantities vary rapidly but continuously. Hence, the numerical calculation proceeds as if there were no shock at all and at the same time satisfying the Rankine-Hugoniot conditions.

The instability of the calculations in the first phase introduces the main source of entropy loss in the entire calculation. However, stable calculations can be made by SHELL, since errors introduced in the second phase have the effect of smoothing out the discontinuities.

Harlow (15) has shown that the treatment of mass movement in the second phase of the calculation produces dissipative effects that give stability to the calculation. He demonstrated this by expanding the difference equations in a Taylor series about some central space and time. The result was the original differential equations plus some additional terms that, in lowest order, have the appearance of true

viscous and heat conduction terms. Hence they are called the effective viscosity and effective heat conduction.

Conservation of Mass

$$\frac{\partial \rho}{\partial t} + \frac{\partial(r\rho u)}{\partial r} + \frac{\partial(\rho v)}{\partial z} = 0 \quad (\text{A16})$$

Conservation of Momentum--r direction

$$\rho \left(\frac{\partial u}{\partial t} + u \frac{\partial u}{\partial r} + v \frac{\partial u}{\partial z} \right) + \frac{\partial p}{\partial r} = \frac{\partial}{\partial r} \left(r \lambda_u \frac{\partial u}{\partial r} \right) + \frac{\partial}{\partial z} \left(\lambda_v \frac{\partial u}{\partial z} \right) \quad (\text{A17})$$

Conservation of Momentum--z direction

$$\rho \left(\frac{\partial v}{\partial t} + u \frac{\partial v}{\partial r} + v \frac{\partial v}{\partial z} \right) + \frac{\partial p}{\partial z} = \frac{\partial}{\partial r} \left(r \lambda_u \frac{\partial v}{\partial r} \right) + \frac{\partial}{\partial z} \left(\lambda_v \frac{\partial v}{\partial z} \right) \quad (\text{A18})$$

Conservation of Energy

$$\begin{aligned} \rho \left(\frac{\partial I}{\partial t} + u \frac{\partial I}{\partial r} + v \frac{\partial I}{\partial z} \right) + p \left[\frac{\partial(ru)}{\partial r} + \frac{\partial v}{\partial z} \right] &= \frac{\partial}{\partial r} \left(r \lambda_u \frac{\partial I}{\partial r} \right) \\ &+ \frac{\partial}{\partial z} \left(\lambda_v \frac{\partial I}{\partial z} \right) + \lambda_u \left[\left(\frac{\partial u}{\partial r} \right)^2 + \left(\frac{\partial v}{\partial z} \right)^2 \right] \\ &+ \lambda_v \left[\left(\frac{\partial u}{\partial z} \right)^2 + \left(\frac{\partial v}{\partial r} \right)^2 \right] \end{aligned} \quad (\text{A19})$$

where

$$\lambda_u = 1/2 \rho |u| \Delta r$$

$$\lambda_v = 1/2 \rho |v| \Delta z$$

However, Bjork (40) has shown that any attempt to relate the terms appearing on the right-hand side of the equations above to distinct physical effects leads to many contradictions--the "effective viscosity" terms contain symmetric and

antisymmetric elements; the origin of the symmetric elements is not viscous; the presence of the antisymmetric elements simply adds confusion to any attempted representation; the terms do not leave the flow equations in an invariant form; a heat conduction law is implied where heat flow is proportional to the gradient of specific internal energy rather than of temperature. Moreover, the values of these terms far exceed the magnitude of the analogous physical terms. Therefore, these terms cannot be thought of as anything except errors, but they do make SHELL a practical code.

The form of the effective viscosity suggests another limitation of the SHELL code. Since the viscous effects are proportional to the local mean fluid speed, in regions of low fluid speed the viscosity will become ineffective and the instabilities of the difference equation will cause an exponential growth of any perturbations to the solution. But as the velocities increase and become comparable to the local sound speed, the viscosity again takes effect to limit further growth of instability. Hence, the instability is bounded and calculations can be made. This effective viscosity is the main source of entropy production in the calculation.

A later modification to the SHELL codes, accomplished by Nawrocki, included an artificial viscosity addition scheme. By selecting appropriate values for three parameters, S1, S2 and S3, an energy dissipating effect is obtained associated with the sound speed, the velocity gradient and the magnitude of the velocity, respectively. By proper selection of the

parameters, the effective viscosity inherent in SHELL can be enhanced or diminished.

DEVELOPMENT OF SHELLTC

In developing a version of SHELL for use in cartesian coordinates we return to the basic equations for 2-D inviscid compressible flow in that coordinate system.

Mass

$$\left(\frac{\partial}{\partial t} + \bar{U} \cdot \nabla \right) \rho + \rho \nabla \cdot \bar{U} = 0 \quad (A20)$$

Momentum

$$\rho \left(\frac{\partial}{\partial t} + \bar{U} \cdot \nabla \right) \bar{U} + \nabla p + \rho \nabla \phi = 0 \quad (A21)$$

Energy

$$\rho \left(\frac{\partial}{\partial t} + U \cdot \nabla \right) E + \nabla \cdot p \bar{U} + \rho \bar{U} \cdot \nabla \phi = 0 \quad (A22)$$

State

$$p = p(P, I) \quad (A23)$$

Neglecting $\nabla \phi$ and holding all items constant with respect to z, we have, in cartesian coordinates,

$$\bar{U} \cdot \nabla = U_x \frac{\partial}{\partial x} + U_y \frac{\partial}{\partial y} \quad (A24)$$

$$\nabla \cdot \bar{U} = \frac{\partial U_x}{\partial x} + \frac{\partial U_y}{\partial y} \quad (A25)$$

Using equations A24 and A25; equations A20, A21 and A22 become (letting $U_x = u$, $U_y = v$)

$$\frac{\partial \rho}{\partial t} + \frac{\partial}{\partial x}(\rho u) + \frac{\partial}{\partial y}(\rho v) = 0 \quad (\text{A26})$$

$$\rho \frac{\partial u}{\partial t} + \rho u \frac{\partial u}{\partial x} + \rho v \frac{\partial u}{\partial y} + \frac{\partial p}{\partial x} = 0 \quad (\text{A27})$$

$$\rho \frac{\partial v}{\partial t} + \rho u \frac{\partial v}{\partial x} + \rho v \frac{\partial v}{\partial y} + \frac{\partial p}{\partial y} = 0 \quad (\text{A28})$$

$$\rho \frac{\partial E}{\partial t} + \rho u \frac{\partial E}{\partial x} + \rho v \frac{\partial E}{\partial y} + \frac{\partial}{\partial x}(pu) + \frac{\partial}{\partial y}(pv) = 0 \quad (\text{A29})$$

Dropping the convective terms as was done previously with axisymmetric coordinates we get from equations A27 through A29

$$\frac{\partial u}{\partial t} + \frac{1}{\rho} \frac{\partial p}{\partial x} = 0 \quad (\text{A30})$$

$$\frac{\partial v}{\partial t} + \frac{1}{\rho} \frac{\partial p}{\partial y} = 0 \quad (\text{A31})$$

$$\frac{\partial I}{\partial t} + \frac{P}{\rho} \left[\frac{\partial u}{\partial x} + \frac{\partial v}{\partial y} \right] = 0 \quad (\text{A32})$$

(where E has been replaced by I). In finite difference form equations A30 and A31 are the same as was obtained for the axisymmetric case earlier. They are

$$\tilde{u}_k^{(n)} = u_k^{(n)} + \frac{1}{\rho_k^{(n)}} \left[\frac{p_L^{(n)} - p_R^{(n)}}{\Delta x} \right] \Delta t \quad (\text{A33})$$

$$\tilde{v}_k^{(n)} = v_k^{(n)} + \frac{1}{\rho_k^{(n)}} \left[\frac{p_B^{(n)} - p_A^{(n)}}{\Delta y} \right] \Delta t \quad (\text{A34})$$

where

$$P_L = \frac{P_k + P_{kL}}{2}, \quad P_R = \frac{P_k + P_{kR}}{2}$$

The energy equation A32 takes a somewhat different form in cartesian coordinates than in axisymmetric. In finite difference form it becomes

$$\begin{aligned} \frac{\tilde{I}_k - I_k^{(n)}}{\Delta} &= \frac{-p_k^{(n)}}{\rho_k^{(n)}} \left[\frac{(\tilde{u}_{kR} + \tilde{u}_{kR}^{(n)})}{2} - \frac{(\tilde{u}_{kL} + \tilde{u}_{kL}^{(n)})}{2} \right] \\ &\quad + \frac{(\tilde{v}_{kA} + \tilde{v}_{kA}^{(n)})}{2} - \frac{(\tilde{v}_{kB} + \tilde{v}_{kB}^{(n)})}{2} \end{aligned}$$

Here again the velocity at each point is the average of that at the beginning of the time step and the interim (-) value calculated above in equations A33 and A34. Now let

$$\begin{aligned} V_B &= \frac{v_k + v_{kB}}{2}, \quad V_A = \frac{v_k + v_{kA}}{2} \\ U_L &= \frac{u_k + u_{kL}}{2}, \quad U_R = \frac{u_k + u_{kR}}{2} \end{aligned} \tag{A35}$$

Then

$$\begin{aligned} v_B^{(n)} - v_A^{(n)} + \tilde{v}_B - \tilde{v}_A \\ = \frac{v_k^{(n)} + v_{kB}^{(n)} - v_k^{(n)} - v_{kA}^{(n)} + \tilde{v}_k + \tilde{v}_{kB} - \tilde{v}_k - \tilde{v}_{kA}}{2} \end{aligned}$$

$$= \frac{(v_{kB}^{(n)} + \tilde{v}_{kB}) - (v_{kA}^{(n)} + \tilde{v}_{kA})}{2} \quad (A36)$$

and

$$UL^{(n)} - UR^{(n)} + \tilde{U}_L - \tilde{U}_R = (u_{kL}^{(n)} + \tilde{u}_{kL}) - (u_{kR}^{(n)} + \tilde{u}_{kR}) \quad (A37)$$

With equations A36 and A37, equation A33 can be rewritten

$$\begin{aligned} \tilde{I}_k &= I_k^{(n)} + \frac{p_k^{(n)}}{\rho_k^{(n)}} \left[\frac{v_B^{(n)} - v_A^{(n)}}{\Delta y} + \tilde{v}_B - \tilde{v}_A \right. \\ &\quad \left. + \frac{UL^{(n)} - UR^{(n)} + UL - UR}{\Delta x} \right] \frac{\Delta t}{2} \end{aligned} \quad (A38)$$

This equation is now accomplished by two passes through the code--the first computes the change in energy in time $\Delta t/2$ using the old (n) values of velocities and the second computes the changes in time $\Delta t/2$ using the new velocities (\sim) computed above by equations A33 and A34.

In the phase II calculation mass is permitted to flow governed by the continuity equation. In finite difference form, equation A26 becomes

$$\frac{\Delta \rho}{\Delta t} = \left[\frac{\rho_{i-1} u_{i-1} - \rho_i u_i}{\Delta x} + \frac{\rho_{j-1} v_{j-1} - \rho_j v_j}{\Delta y} \right] \quad (A39)$$

$$\rho_k^{(n+1)} = \rho_k^{(n)} + \left[\frac{\rho_{i-1} u_{i-1} - \rho_i u_i}{\Delta x} + \frac{\rho_{j-1} v_{j-1} - \rho_j v_j}{\Delta y} \right] \Delta t \quad (A40)$$

We again use the same velocity weighting scheme as with axisymmetric coordinates

$$\text{for } v_{j-1} \text{ we use } \bar{v}_B = \frac{1/2 (\tilde{v}_{kB} + \tilde{v}_k)}{1 + (\tilde{v}_{kB} + \tilde{v}_k) \frac{\Delta t}{\Delta y}}$$

$$\text{for } v_j \text{ we use } \bar{v}_T = \frac{1/2 (\tilde{v}_{kT} + \tilde{v}_k)}{1 + (\tilde{v}_{kT} + \tilde{v}_k) \frac{\Delta t}{\Delta y}}$$

(A41)

$$\text{for } u_{i-1} \text{ we use } \bar{u}_L = \frac{1/2 (\tilde{u}_{kL} + \tilde{u}_k)}{1 + (\tilde{u}_{kL} + \tilde{u}_k) \frac{\Delta t}{\Delta x}}$$

$$\text{for } u_i \text{ we use } \bar{u}_R = \frac{1/2 (\tilde{u}_{kR} + \tilde{u}_k)}{1 + (\tilde{u}_{kR} + \tilde{u}_k) \frac{\Delta t}{\Delta x}}$$

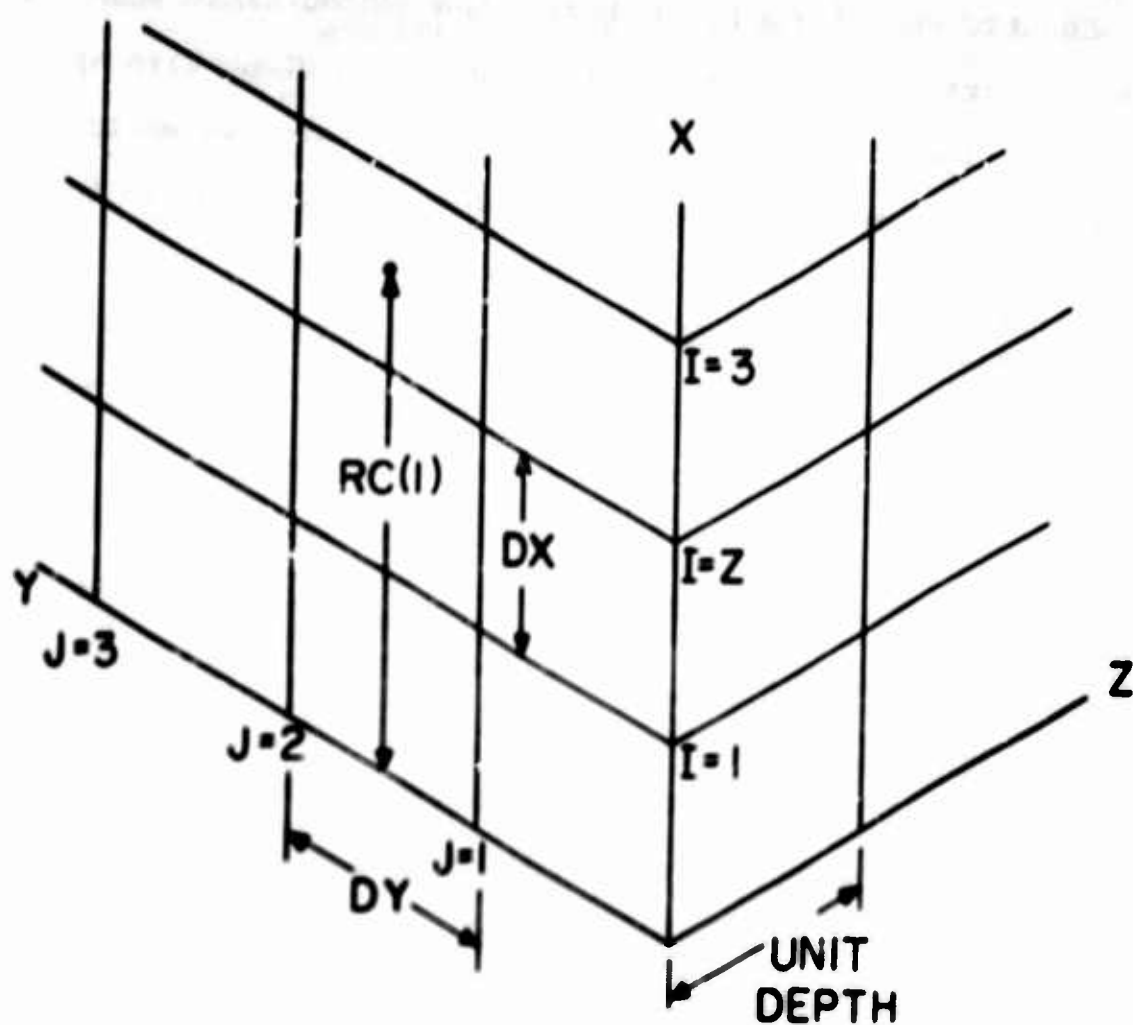
Using these and multiplying by the volume of a cell (where volume = $\Delta x \cdot \Delta y$) equation A40 becomes

$$\rho_k^{(n+1)} \Delta x \Delta y = \rho_k^{(n)} \Delta x \Delta y + [\Delta x (\rho_B \bar{v}_B - \rho_T \bar{v}_T) + \Delta y (\rho_L \bar{u}_L - \rho_R \bar{u}_R)] \Delta t \quad (A42)$$

Finally

$$M_k^{(n+1)} = M_k^{(n)} + \Delta t [\Delta x (\rho_B \bar{v}_B - \rho_T \bar{v}_T) + \Delta y (\rho_L \bar{u}_L - \rho_R \bar{u}_R)] \quad (A43)$$

The computational grid for SHELLTC is constructed in the XY plane and is symmetric about the y axis as depicted in Figure A3. It takes its 3-D form by including a unit depth in the Z direction.



$RC(I)$ is the X distance to the center of a cell in the I th column.

Y dimension of each cell is DY .

X dimension of each cell is DX

Cross-sectional area of each cell is $TAU(I)$ where

$$TAU(I) = DX \cdot \text{Unit Depth} = DX$$

Volume of each cell is

$$VOL(I) = DX \cdot DY$$

Figure A3. SMALL Zonal---Two-Dimensional Planar Case

SHELLTC was formed by including the hydrodynamic equation for cartesian coordinates into SHELL OIL along with appropriate flags for determining which coordinate system is being used. Some modification of CLAM was also required to obtain CLAMTC, the generator code for SHELLTC.

The effective viscosity, inherent in SHELL, is continued in SHELLTC as is the Nawrocki artificial viscosity scheme described above. Consideration was given to reducing the effective viscosity inherent in SHELLTC by a proper selection of the parameters S1, S2 and S3 in hopes of sharpening the shock front produced by a SHELLTC calculation. For this reason a parametric study was performed using a 1-D planar blast wave as a trial problem (similar to Reference 32) to determine the effect of variations in those S parameters. The shape of the shock front obtained for selected values of S1, S2 and S3 are compared with a 1-D similarity solution for the planar blast wave in Figures A4 through A7. The results of this study indicated that the closest reproduction of the analytical solution was obtained with the following values:

$$S_1 = -0.1$$

$$S_2 = 0.1$$

$$S_3 \approx -0.4$$

Although these values worked satisfactorily for problems where the deposited energy was small, difficulty was

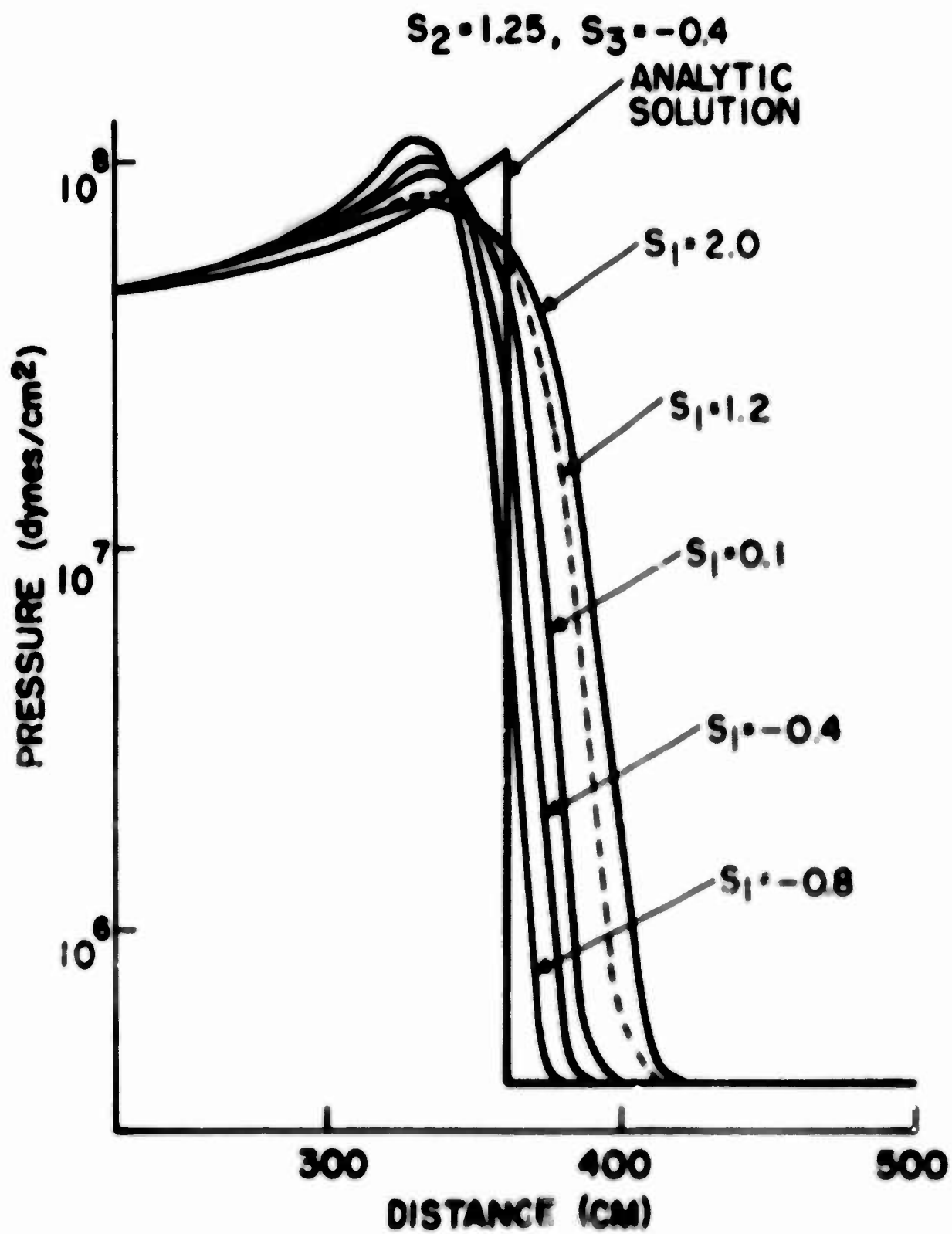


Figure A6. Variation Parameter S_1

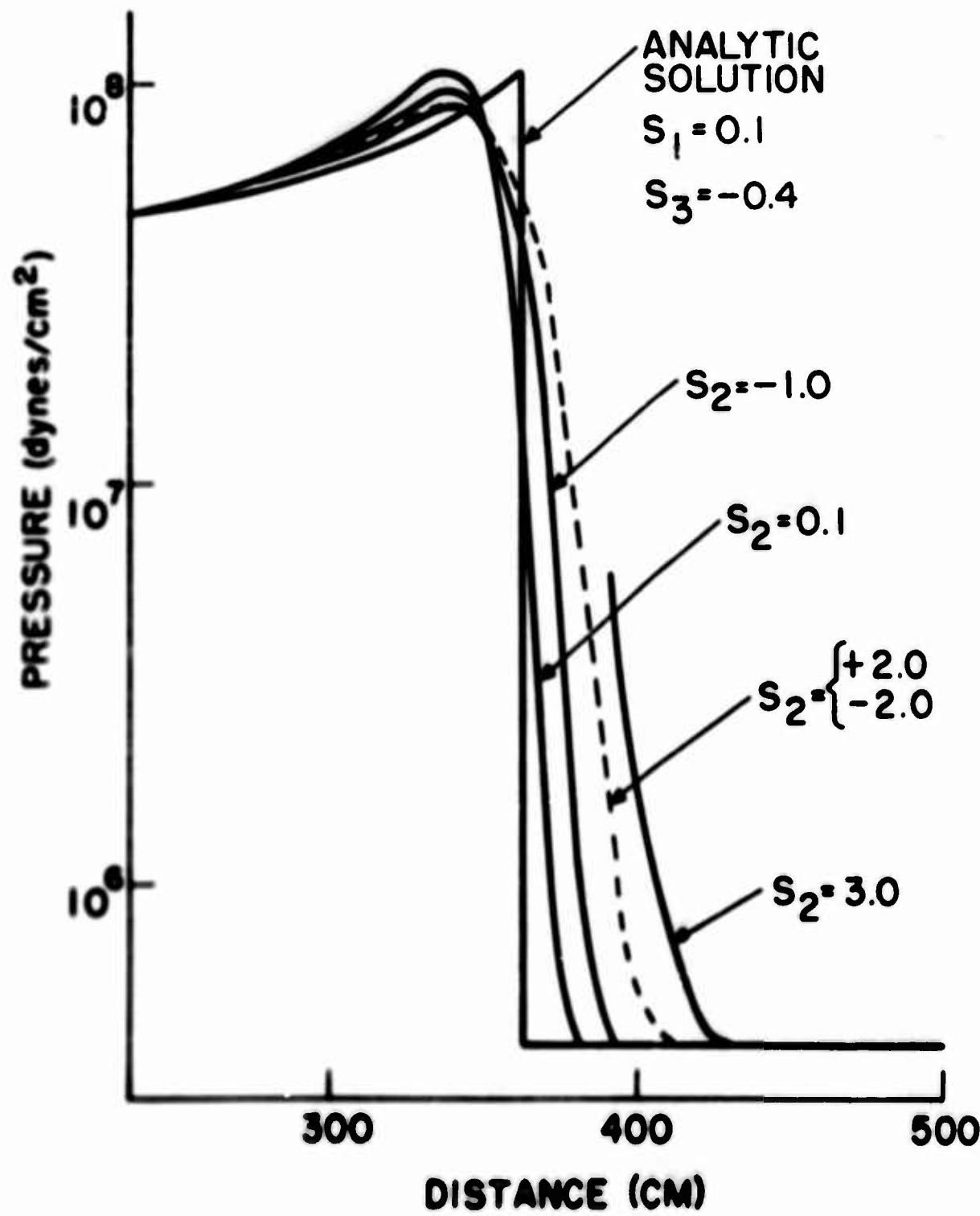


Figure A3. Variation of Parameter S_2 .

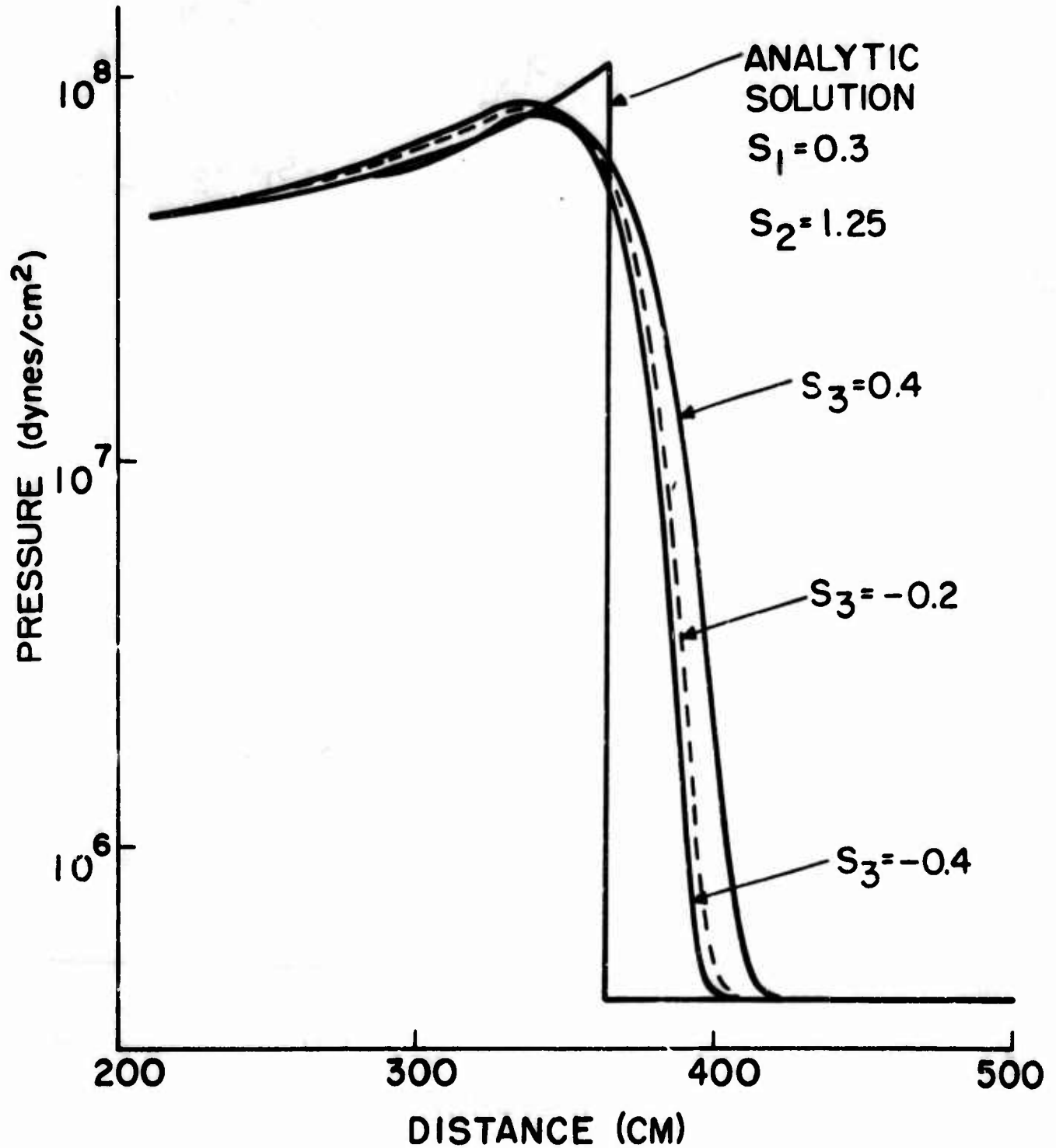


Figure A6. Variation of Parameter S_3

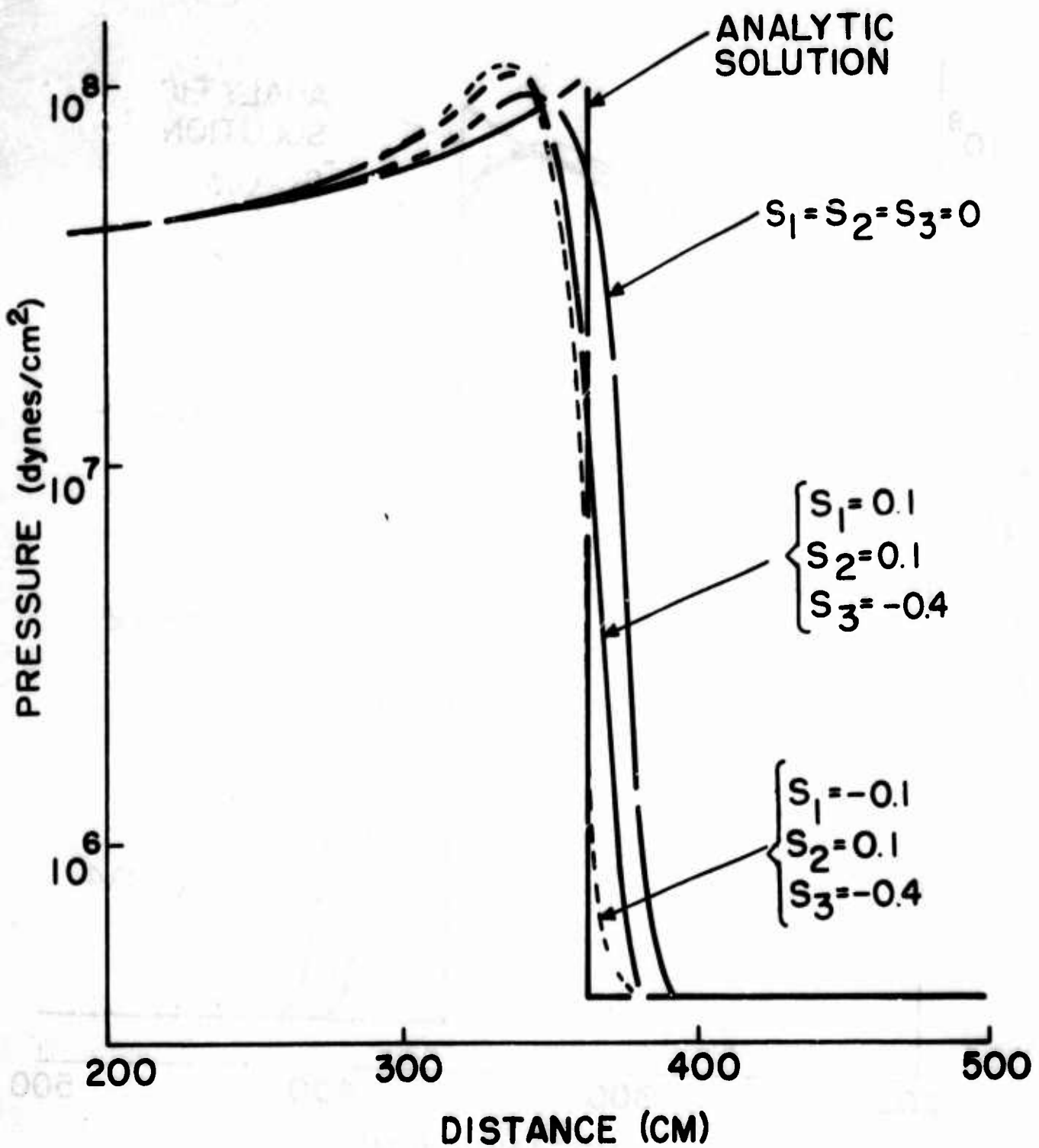


Figure A7. Results of S Parameter Study

encountered during large energy deposition. Excessive computational time was required and in some instance the computation became unstable. For this reason, the three S parameters were set to zero (eliminating, in effect, the Nawrocki artificial viscosity scheme) during all calculations performed for this dissertation. Hence, the shock structure obtained throughout the study is that provided by the effective viscosity inherent in SHELLTC.

An energy deposition scheme, described in the main text, was incorporated into SHELLTC in order to solve the 2-D blast wave problem of interest. The code in its present configuration is suitable for use with the CDC-3400 or CDC-6600 computer. A complete listing of SHELLTC, as used in this work, follows.

LISTING OF SHELLTC CODE

```
PROGRAM SHELLTC(INPUT,OUTPUT,TAPE4,TAPE7,TAPE9,TAPE5=INPUT,
 1 TAPE6=OUTPUT)
C ***** REJECTED FOR CDC-3400 OPERATION
CMAIN
C
C: ***** NOTE 1 MATERIAL ONLY (X) *****

COMMON Z(19000)
CALL INPUT
10 CALL CDT
CALL EDIT
IF(SENSE LIGHT 1)30,20
20 CALL PH1
CALL PH2
GO TO 10
30 CALL EXIT
END
```

SUBROUTINE CARDS

```
DIMENSION TABLE(1),CARD(7),LABLE(1)
COMMON           TABLE
EQUIVALENCE(TABLE(1),LABLE(1))
WRITE (6,10)
1 READ (5,11)IEND,LOC,NUMHPC,(CARD(I),I=1,NUMHPC)
  WRITE (6,12)IEND,LOC,NUMHPC,(CARD(I),I=1,NUMHPC)
  DO 4 I=1,NUMHPC
    J=LOC+I-1
    IF(IEND-2)2,5,2
    5 LABLE(J)=XFIXF(CARD(I))
    GO TO 4
    2 TABLE(J)=CARD(I)
    4 CONTINUE
    IF(IEND-1)1,3,1
    3 RETURN
C           FORMATS
10 FORMAT(20H1SHELL  INPUT CARDS///)
11 FORMAT(I1,I5,I1,0P7E9.4)
12 FORMAT(1H I4,I7,I3,1P7E14.6)
END
```

SUBROUTINE INPUT

	C	O	M	H	J	N
COMMON	Z	,XO	,X	,Y		
COMMON	AIX	,AM	,AMX	,AREA		,E
COMMON	FS	,I	,II	,IR		,IMS
COMMON	J	,K	,KP	,L		,M
COMMON	HZ	,N	,NK	,NO		,NOP
COMMON	NR	,P	,PABOVE	,PALO		,PIDS
COMMON	PQR	,PC	,REZ	,RHO		,RR
COMMON	SIG	,TAU	,TAUDTS	,TTX		,TTY
COMMON	U	,UQR	,UT	,UTEF		,UU
COMMON	UVMAX	,V	,VABOVE	,VBLO		,VEL
COMMON	VTEF	,HS	,HSA	,HSB		,HSC
COMMON	XLF	,XR	,YLW			
COMMON	YU	,UR	,PR			

E	Q	U	I	V	A	L	E	N	C	E
DEQUIVALENCE										
1(Z(4),PRINTS),	(Z,IZ,PP09),	(Z(5),PRINTL),	(Z(6),CYCLE),	(Z(3),DTI),						
2(Z(8),FIDY),	(Z(9),TMZ),	(Z(10),GA4),	(Z(11),DUMPTI),	(Z(7),CSTOP),						
3(Z(12),GAMX),	(Z(13),ETH),	(Z(14),FFA),	(Z(15),GAMD),	(Z(11),GAMD),						
4(Z(16),TH02),	(Z(17),T4XZ),	(Z(18),XMAX),	(Z(19),TXMAX),	(Z(15),FFBI),						
5(Z(20),TYMAX),	(Z(21),AMDM),	(Z(22),AMXM),	(Z(23),UNNI),	(Z(19),TXMAX),						
6(Z(24),OMIN),	(Z(25),FEF),	(Z(26),DTNA),	(Z(27),CVISI),	(Z(23),UNNI),						
7(Z(28),NPRI),	(Z(29),NPRI),	(Z(30),NC),	(Z(31),NPCI),	(Z(27),CVISI),						
8(Z(32),NRC),	(Z(33),IMAX),	(Z(34),IMAXA),	(Z(35),JMAX),	(Z(31),NPCI),						
9(Z(36),JMAXA),	(Z(37),KMAX),	(Z(38),KMAXA),	(Z(39),NMAX),	(Z(35),JMAX),						
DEQUIVALENCE	(Z(40),ND),	(Z(41),KOT),	(Z(42),IXMAX),	(Z(40),ND),						
1(Z(43),NOJ),	(Z(44),NOPP),	(Z(45),NIMAX),	(Z(46),NJMAX),	(Z(43),NOJ),						
2(Z(47),I1),	(Z(48),I2),	(Z(49),I3),	(Z(50),I4),	(Z(47),I1),						
3(Z(51),N1),	(Z(52),N2),	(Z(53),N3),	(Z(54),N4),	(Z(51),N1),						
4(Z(55),N5),	(Z(56),N6),	(Z(57),N7),	(Z(58),N9),	(Z(55),N5),						
5(Z(59),N9),	(Z(60),N10),	(Z(61),N11),	(Z(62),NRM),	(Z(59),N9),						
6(Z(63),TRA),	(Z(64),XNR0),	(Z(65),SN),	(Z(66),DXN),	(Z(63),TRA),						
7(Z(67),RA7ER),	(Z(68),PDET),	(Z(69),RA7ER),	(Z(70),OTRAD),	(Z(67),RA7ER),						
8(Z(71),REZFCI),	(Z(72),PSTOP),	(Z(73),SHELL),	(Z(74),PTOUDI)	(Z(71),REZFCI),						
9(Z(75),TOZONE),	(Z(76),ECK),	(Z(77),SBOUND),	(Z(78),X1),	(Z(75),TOZONE),						
DEQUIVALENCE	(Z(79),X2),	(Z(80),Y1),	(Z(81),Y2),	(Z(79),X2),						
1(Z(82),CARLN),	(Z(83),VISCI),	(Z(84),T1),	(Z(85),GMAXI),	(Z(82),CARLN),						
2(Z(86),WSGN),	(Z(87),WSGX),	(Z(88),GMADR),	(Z(89),GMADRP),	(Z(86),WSGN),						
3(Z(90),S1),	(Z(91),S2),	(Z(92),S3),	(Z(93),S4),	(Z(90),S1),						
4(Z(94),SS),	(Z(95),SS),	(Z(96),ST),	(Z(97),S8),	(Z(94),SS),						
5(Z(98),S9),	(Z(99),S10),	(Z(100),DY),	(Z(101),DT),	(Z(98),S9),						
6(Z(127),DX),	(Z(128),DY),	(Z(129),DY),	(Z(130),DT),	(Z(127),DX),						
7(Z(130),NFTTB),	(Z(131),NFTTI),	(Z(132),NFTTR),	(Z(133),NFTTB),	(Z(130),NFTTB),						
8(Z(133),NPARTB),	(Z(134),NPARTI),	(Z(135),NPARTB),	(Z(136),NPARTB),	(Z(133),NPARTB),						

EQUIVALENCE (P, IMI)

EQUIVALENCE (P(200), GAMC), (P(400), YAMC)

EQUIVALENCE (UO, UL, ELETI), (PB, PL, SIEG)

EQUIVALENCE (Z(120),DETVEL), (Z(122),EXEN)
EQUIVALENCE (Z(123),EXRHO), (Z(124),THICK)
SENSE LIGHT 3
DO 300 I=1,1A999
300 Z(I)=0.

READ (5, A904) IWS
WRITE (6, B904) IWS
6 CALL CARDS

READ TAPE

STOR1 = Z(235)
STOR2 = Z(236)
1000 MZ=150
IWS=0
REWIND 7
1003 REWIND 4
1004 READ(4) PR(1), PR(2), N3
WRITE (6, B900) PR(1), PR(2), N3
A900 FORMAT (10X, 15H FIRST RECORD IS ,2E12.4, I6, /)
NR=N3+5
1006 IF (PR(1)-555.0) 1010, 1016, 1010
1010 IF (PR(1).EQ.666.) 1012, 1013
1012 DO 1014 I=1,5
1014 BACKSPACE 4
IF (GAMD) 1023, 1023, 1015
1015 DO 1017 I = 1,4
1017 BACKSPACE 7
GO TO 1023
1018 IWS=IWS+1
WRITE (6, B901) IWS
B901 FORMAT (10X, 6H IWS = , I2, /)
1019 IF (XHDF(IWS, 3)) 9902, 9902, 1003
1016 WRITE (6, B891) Z(235), Z(236), PR(2), PROB
A891 FORMAT (10X, 9HZ(235) = , E14.6, 12H Z(236) = , E14.6,
1 11H PR(2) = , E14.6, 10H PROB = , E14.6, /)
IF (Z(236)-PR(2)) 1025, 1025, 1019
1019 IF (GAMP) 1020, 1020, 1021
1020 READ(4) DUM
READ(4) DUM
READ(4) DUM
READ(4) DUM
GO TO 1004
1021 WRITE (7) PR(1), PR(2), N3
READ(4) (Z(I), I=1, MZ)
READ(4) (U(I), V(I), AMX(I), AIX(I), P(I), I=1, KMAXA)
READ(4) X(J), (X(I), TAU(I), I=1, IMAX)
READ(4) (Y(I-1), I=1, JMAXA)
WRITE(7) (Z(I), I=1, MZ)
WRITE(7) (U(I), V(I), AMX(I), AIX(I), P(I), I=1, KMAXA)
WRITE(7) X(0), (X(I), TAU(I), I=1, IMAX)
WRITE(7) (Y(I-1), I=1, JMAXA)
WRITE (6, A905) PR(2)
Z(235) = STOR1
Z(236) = STOR2
GO TO 1004

```

1025 IF (GAMD) 1023,1023,1022
1022 WRITE (7) PR(1),PR(2),N3
1023 READ(4)(Z(I),I=1,MZ)
    WRITE (6,3902) (Z(I),I = 1,3)
8802 FORMAT (1JX,25HTHE FIRST 3 Z VALUES ARE ,3E12.6,/1
    IF (ABS(F(PR0B-Z(235))-.01)>0.01) 1024,1024,3901
1024 READ(4)(U(I),V(I),AMX(I),AIX(I),P(I),I=1,KMAXA)
    READ(4)X(0),(X(I),TAU(I),I=1,IIMAX)
    READ(4)(Y(I-1),I=1,JMAXA)
1034 READ(4)FS,RC,RR
    IF (GAMD) 1030,1030,1031
1031 WRITE(7)(Z(I),I=1,MZ)
    WRITE(7)(U(I),V(I),AMX(I),AIX(I),P(I),I=1,KMAXA)
    WRITE(7)X(0),(X(I),TAU(I),I=1,IIMAX)
    WRITE(7)(Y(I-1),I=1,JMAXA)
    WRITE(7)FS,RC,RR
    WRITE (6,48)5) PR(2)
1030 WRITE (6,3903)FS,RC,RR
8803 FORMAT (10X,18HFS, RC AND RR ARE ,3E12.6,/1
501 CONTINUE
1036 IF(FS-555.0)>9904,1040,1038
1038 IF(RC-666.0)>9305,1040,9905
1040 GO TO 10
*
***** END OF READ TAPE ****
*
* READ IN REMAINING INPUT CARDS
*
10 CONTINUE
CALL CARDS
40 DO 45 K=1,KMAXA
45 P(K)=0.0
    T=T-0.1NA
    NC=NC-1
    CYCLE=NC
    NPC=NPC-1
    UVMAX=0.0
    JX=MZ-4
62 DO 80 I=1,JX,4
    K=I+3
    DO 65 J=I,<
    IF(Z(J))70,65,7J
65 CONTINUE
    GO TO 80
70 CONTINUE
    WRITE (6,3111)I,(Z(L),L=I,K)
    WRITE (6,3112) I,(Z(L),L=I,K)
80 CONTINUE
    GO TO 10000
*
            ERROR
9301 NK=1023
    GO TO 9999
9302 NK=1011
    GO TO 9999
*
9304 NK=1036
    GO TO 9999
9305 NK=1038

```

```

GO TO 9999
9906 NK=2000
9999 NR=1
CALL ERRER(NR,NK)

C
10000 RETURN

C
C           FORMATS
3000 FORMAT(7E10.3,I2)
8805 FORMAT (7H0CYCLE ,F5.0,19H COPIED ONTO TAPE 7 //)
40040FORMAT(I1,71H
1
8111 FORMAT (I4,4(4X,1PE16.8))
8112 FORMAT(I4,4025)
END

```

SUBROUTINE COT

	C	O	M	M	J	N
DIMENSION AIX(3500),AMX(3500),P(3500), 1 U(3500),V(3500),X(60),Y(100),Z(150), 2 IZ(150),TAU(60),PL(100),UL(100),PR(100), 3 UR(100),IW1(15),LEFT(100),YAMC(100), 4 SIGC(100),GAMC(100)						
COMMON	Z	XO	X	,Y		
COMMON	AIX	AM	AMX	,AREA	,E	
COMMON	FS	I	II	,IR	,IWS	
COMMON	J	K	KP	,L	,M	
COMMON	MZ	N	NK	,NO	,NOP	
COMMON	NR	P	PABOVE	,PBL0	,PIDS	
COMMON	PRR	RC	REZ	,RHO	,RR	
COMMON	SIG	TAU	TAUDTS	,TTX	,TTY	
COMMON	U	URR	UT	,UTEF	,UU	
COMMON	UVMAX	V	VABOVE	,VBL0	,VEL	
COMMON	VTEF	WS	WSA	,WS3	,WSC	
COMMON	XLF	XR	YLW			
COMMON	YJ	UR	PR			
EQUIVALENCE	(Z,I2,PROB),	(Z(2),CYCLE),	(Z(3),JT),			
1(Z(4),PRINTS),	(Z(5),PRINTL),	(Z(6),DUMPT7),	(Z(7),CSTOP),			
2(Z(8),PIDY),	(Z(9),TMZ),	(Z(10),GAM),	(Z(11),GAMD),			
3(Z(12),GAMX),	(Z(13),ETH),	(Z(14),FFR),	(Z(15),FFB),			
4(Z(16),TMDZ),	(Z(17),TMXZ),	(Z(18),XMAX),	(Z(19),TXMAX),			
5(Z(20),TYMAX),	(Z(21),AMDM),	(Z(22),AMXM),	(Z(23),DNN),			
6(Z(24),DMIN),	(Z(25),FEF),	(Z(26),DTNA),	(Z(27),CVIS),			
7(Z(28),NPR),	(Z(29),NPRI),	(Z(30),NC),	(Z(31),NPC),			
8(Z(32),NRC),	(Z(33),IMAX),	(Z(34),IMAXA),	(Z(35),JMAX),			
9(Z(35),JMAXA),	(Z(37),KMAX),	(Z(38),KMAXA),	(Z(39),NMAX)			
EQUIVALENCE	(Z(40),NO),	(Z(41),KOT),	(Z(42),IXMAX),			
1(Z(43),NOD),	(Z(44),NOPR),	(Z(45),NIMAX),	(Z(46),NJMAX),			
2(Z(47),I1),	(Z(48),I2),	(Z(49),I3),	(Z(50),I4),			

3(Z(92)),N81),	(Z(92)),N21),	(Z(92)),N31),	(Z(92)),N61),
4(Z(93)),N91),	(Z(93)),N61),	(Z(93)),N71),	(Z(93)),N91),
5(Z(94)),N91),	(Z(94)),N111),	(Z(94)),N111),	(Z(94)),N91),
6(Z(95)),T8001),	(Z(95)),T8001),	(Z(95)),S81),	(Z(95)),D81),
7(Z(97)),RADEQ1),	(Z(97)),P8001),	(Z(97)),RADEQ1),	(Z(97)),DT8001),
8(Z(98)),RE2FCG1),	(Z(98)),P8001),	(Z(98)),SMELL1),	(Z(98)),DD00001),
9(Z(99)),TOZONE1),	(Z(99)),LCC1),	(Z(99)),SO00001),	(Z(99)),E11),
DEQUivalence	(Z(79)),Z21),	(Z(99)),Y11),	(Z(99)),Y21),
1(Z(82)),CARLN1),	(Z(82)),V19C1),	(Z(96)),T11),	(Z(99)),G4001),
2(Z(86)),MSG31),	(Z(86)),V928),	(Z(88)),GM0001),	(Z(89)),GM0001),
3(Z(90)),SL1),	(Z(90)),S21),	(Z(92)),S31),	(Z(93)),S41),
4(Z(94)),S51),	(Z(94)),S61),	(Z(96)),S71),	(Z(97)),S81),
5(Z(98)),S91),	(Z(98)),S101),		
6(Z(127)),DX1),	(Z(128)),DY1),	(Z(129)),DY1),	
7(Z(130)),MFITR1),	(Z(131)),MFITR1),	(Z(132)),MFITR1),	
8(Z(133)),MPARR1),	(Z(134)),MPARR1),	(Z(135)),MPARR1)	

C
 EQUIVALENCE (P,IM1)
 EQUIVALENCE(P(1200),GAMC),(P(400),YMC)
 EQUIVALENCE (UR,UL,FLEFT), (PR,PL,SEGC)
 EQUIVALENCE (Z(1101),ENSUM)
 EQUIVALENCE (Z(1121),JCELL)
 EQUIVALENCE (Z(1120),DETVEL), (Z(1122),FDEM)
 EQUIVALENCE (Z(1123),FTH01), (Z(1124),THICK)
 EQUIVALENCE (Z(1125),AJCELL)

C
 C
 C
 DO 300 I = 1,IMAX
 K2 = I + IMAXA
 K3 = K2 + IMAX
 E02 = (AIX(K2) + 0.5*V(K2)*V(K2)) * A4X(K2)
 E03 = (AIX(K3) + 0.5*V(K3)*V(K3)) * A4X(K3)
 AMX(K2) = Z(96)
 AMX(K3) = A4X(K2)
 AIX(K2) = Z(93)
 AIX(K3) = Z(93)
 V(K2) = DETVEL
 V(K3) = DETVEL
 EN2 = (AIX(K2) + 0.5*V(K2)*V(K2)) * A4X(K2)
 EN3 = (AIX(K3) + 0.5*V(K3)*V(K3)) * A4X(K3)
 300 ETH = ETH + EN2 + EN3 - E02 - E03
 IF (INC = 2) 1,2,2
 1 ENSUM = 0.0
 GO TO 3000
 2 DETLEN = DETVEL*DT
 ENDP = DETLEN*THICK*EXEN*EARHO
 ENSUM = ENSUM + ENDP
 WRITE (6,9464) DETLEN,ENDP,ENSIH
 9464 FORMAT (22H00DETONATION LENGTH IS ,1PE12.3,10X,
 1 20HENERGY DEPOSITED IS ,1PE12.3,10X,
 2 26HTOTAL ENERGY DEPOSITED IS ,1PE12.3,10X)
 JCELL = AJCELL
 KCELL = 2 + (JCELL - 1)*IMAX
 AIX(KCELL) = AIX(KCELL) + ENDP/AMX(KCELL)
 ETH = ETH + ENDP
 3000 VEL=1.0
 3005 DO 3050 I=1,IMAX

```

3010 G+801
3015 DD 3250 J+1,3960
3020 IF(3250<11)3251,3250,3279
3025 G+801,J,0
43200,J,0
P101+0,6*840((C)/18018)/01*911110
3030 IF(840*(P101))=1.0E-28)3255,3255,3260
3035 P101+0,0
3040 IF(10150-VEL>3250,3250,3260
3045 VEL+0.5G
3050 C+C+1400
3055 G+701
UV480+1.0
3115 325+00
3120 IF(1015-SIG)>1120,1170,3270
3125 325+00
3130 DD 3255 J+1,3960
3135 C+C+1400
3140 G+701
IF(1015(C))>1120,3255,4000
4010 432001716180*780((1015+C12)/(1015+C13))
3205 432003/516
3210 IF(1015&C=4313210,11,1
3215 N10+1
N11+1
UV480+00
3 IF(60415,0,0
6 432003(U1(C))/1801110*8111/0,5*0100
60 10 3220
6 432003(U1(C))/10
3225 IF(1015&C=4313210,3210,3230
3230 UV480+00
N10+1
N11+1
3235 432003(U1(C))/00
3240 IF(1015&C=4313210,3210,3250
3245 N10+1
N11+1
UV480+00
3250 CONTINUE
3255 C+C+1400
IF(1015&C=3210,3210,3260
3260 DT+.5/VEL/UV480*2(1111)
3295 G+701
3300 T+T+1400

```

THE FOLLOWING SET OF LOOPS DETERMINES A OF SUCH THAT THE NEXT CYCLE
WILL HAVE A STANDARD TIME IF THE CALCULATED DT WILL MAKE THE NEW
TIME GREATER THAN THE STANDARD

```

CALL POWERIT,100,LPI
4000*(10+01)/10.00LP
IF(1000,LE,2,3201,3202
201 DD 210 LX+1,12
C+C1L+0.1/10.
IF(1000,LT,50,400,201,00,00)711,210
210 CONTINUE

```

60 TO 00
 202 IF(NEQ,LE,7,5)203,220
 203 DO 217 L=1,7
 EX+121+29(L-1)/10.
 IF(NEQ,LT,60,843,863,60,61281,212
 212 CONTINUE
 60 TO 00
 224 IF(DEE,LE,7,61283,220
 205 EA=2,3
 IF(NEQ,LT,60,843,863,60,61281,00
 206 IF(DEE,LE,4,61287,220
 207 DO 216 L=1,4
 EX+123,020(L-1)/10.
 IF(NEQ,LT,60,843,863,60,61281,216
 216 CONTINUE
 60 TO 00
 228 IF(NEQ,LE,5,61283,213
 229 DO 218 L=1,2
 EX+122,030(L-1)/10.
 IF(NEQ,LT,60,843,863,60,61281,214
 214 CONTINUE
 60 TO 00
 215 IF(NEQ,LE,5,1217,211
 216 EA=5,
 IF(DEE,LE,5,61283,220
 217 DO 221 L=1,5
 EX+122,030(L-1)/10.
 IF(NEQ,LT,60,843,863,60,61281,221
 221 CONTINUE
 60 TO 00
 222 IF(NEQ,LE,4,1222,206
 223 EA=6,
 IF(NEQ,LT,60,843,863,60,61281,00
 224 DO 231 L=1,6
 EX+120,040(L-1)/10.
 IF(NEQ,LT,60,843,863,60,61281,223
 231 CONTINUE
 60 TO 00
 225 IF(ABS(128-NEQ)+1,0-9100,91,221
 226 0F+128-NEQ+10,00LP
 IF(143 = 101 25,1251,260
 250 PRINT, * 5.0
 PRINTS * 5.0
 OUTPUT * 5.0
 60 TO 00
 260 PRINTL * 200.0
 PRINTS * 200.0
 OUTPUT * 200.0

90 NC=NC+1
 CYCLE=NC
 MPC=MPC+1
 3305 IF(1119909,3329,3310
 3310 IF(10011+910,3315,3320
 3315 WRITE (6,10101),0TH4,01
 3320 DATA=01
 60 TO 3325

— 1 —

1991 00-2320
00 19 0000
0000 00-2320
00 19 0000
0000 00-2320
00 19 0000

3 - 100-21000-92-3, 04 REGISTRATION, 9130

卷之三

Fig. 1. *Streptomyces* sp. 10-1.

— 1 —

200

1998-00000

卷之三

• 44 •

31(4) = 1991 12.3, 13H

5 6 7 8 9 10 11 12

384465108 316115001,400135101,2035101,
1 0123281,711901,211901,
2 1911301,1811501,PL12301,UL11001,2218001,
3 -211001,1811301,FLCF11001,794C11001,
- 316C11001,684C11001
214 45108 311101

C	D	E	F	G	H	I
COMMON	I	.XO	.C	.V		
COMMON	SIG	.A1	.111	.AREA		.L
COMMON	PS	.I	.II	.12		.IMS
COMMON	J	.K	.CP	.L		.M
COMMON	M1	.N	.NC	.NC		.NOD
COMMON	YR	.P	.PAPOVE	.PILO		.PIDIS
COMMON	P22	.RC	.REZ	.RHO		.RR
COMMON	SIG	.TAU	.TAUDTS	.TTX		.TTY
COMMON	U	.URR	.UT	.UTEF		.UU
COMMON	UVH&Z	.V	VABDVF	.VJLJ		.VEL
COMMON	V1CF	.HS	.HSA	.HSJ		.HSC
COMMON	SLF	.XR	.YLH			
COMMON	YJ	.UR	.PR			

C A U I V A T E N S C

EQUIVALENCE	(Z,IZ,PRO3),	(Z(2),CYCLE),	(Z(3),DT),
1(Z(4),PRINTS),	(Z(5),PRINTL),	(Z(6),DUMPT7),	(Z(7),CSTOP),
2(Z(8),PIDV),	(Z(9),TMZ),	(Z(10),GAM),	(Z(11),GAMD),
3(Z(12),GA4X),	(Z(13),ETHI),	(Z(14),FFA),	(Z(15),FFB),
4(Z(16),TMU2),	(Z(17),TMX2),	(Z(18),XMAX),	(Z(19),TXMAX),
5(Z(20),TYMAX),	(Z(21),AMDM),	(Z(22),AMXM),	(Z(23),DNN),
6(Z(24),DMINI),	(Z(25),FEFI),	(Z(26),UTNA),	(Z(27),CVIS),
7(Z(28),NPR),	(Z(29),NPRI),	(Z(30),NC),	(Z(31),NPC),
8(Z(32),NRC),	(Z(33),IMAX),	(Z(34),IMAXA),	(Z(35),JMAX),
9(Z(36),JMAXA),	(Z(37),KMAX),	(Z(38),KMAXA),	(Z(39),NMAX)
EQUIVALENCE	(Z(40),ND),	(Z(41),KDT),	(Z(42),IXMAX),
1(Z(43),NOD),	(Z(44),NOPR),	(Z(45),NIMAX),	(Z(46),NJMAX),

Z(2(47),I1),	(Z(48),I2),	(Z(49),I3),	(Z(50),I4),
3(Z(51),N1),	(Z(52),N2),	(Z(53),N3),	(Z(54),N4),
4(Z(55),N5),	(Z(56),N6),	(Z(57),N7),	(Z(58),N8),
5(Z(59),N9),	(Z(60),N10),	(Z(61),N11),	(Z(62),NRM),
6(Z(63),TRAD),	(Z(64),XNRG),	(Z(65),SN),	(Z(66),DXN),
7(Z(67),RADER),	(Z(68),PADET),	(Z(69),RADEB),	(Z(70),DTRAD),
8(Z(71),REZFCT),	(Z(72),RSTOP),	(Z(73),SHELL),	(Z(74),BBOUND),
9(Z(75),TOZONE),	(Z(76),ECK),	(Z(77),SBOUND),	(Z(78),X1)
DEQUIVALENCE	(Z(79),X2),	(Z(80),Y1),	(Z(81),Y2),
1(Z(82),CABLN),	(Z(83),VISC),	(Z(84),T),	(Z(85),GHAX),
2(Z(86),WSGD),	(Z(87),WSGX),	(Z(88),GMADR),	(Z(89),GMAXP),
3(Z(90),S1),	(Z(91),S2),	(Z(92),S3),	(Z(93),S4),
4(Z(94),S5),	(Z(95),S6),	(Z(96),S7),	(Z(97),S8),
5(Z(98),S9),	(Z(99),S10),		
6(Z(127),DX),	(Z(128),DY1),	(Z(129),DY),	
7(Z(130),NFITB),	(Z(131),NFIIT),	(Z(132),NFIIR),	
8(Z(133),NPARB),	(Z(134),NPART),	(Z(135),NPARR)	

EQUIVALENCE (P,IW1)
EQUIVALENCE (P(200),GAMC),(P(400),YAMC)
EQUIVALENCE (UR,UL,FLEFT), (PR,PL,SIGC)
EQUIVALENCE (Z(120),DETVEL), (Z(122),EXEN)
EQUIVALENCE (Z(123),EXPH0), (Z(124),THICK)

***** NOTE 1 MATERIAL ONLY (X) *****

```

UU=1.E+15
UT=0.0
VEL=1.0
IF(GAM)9000,3301,9000
RC=1.0
RR=RC
GO TO 3304
RC=DX/2.0
RR=(X(1)+X(2))/2.0

```

```

3304 K=2
      DO 3302 J=1,JMAX
      PL(J)=P(K)
      UL(J)=0.0
      QL(J)=0.0
3302 K=K+IMAX
      DO 3360 I=1,IMAX
      K=I+1
      E NOT=IMAX
      S K=I+1+NOT
      IF(CVIF)7002,7003,7003
7003 VBL0=0.0
      PBL0=P(K)
      GO TO 7004
7002 VBL0=V(K)
      PBL0=0.0
7004 TAUDTS=T&U(I)*DT
      Q3=0.0

```

```

3 NO=2
4 DO 3348 J=NO,JMAX
  UQ=U(K)
  VQ=V(K)
  A=0.
  R=0.
  PIOTS=1.0/(PIDY*DT*DY)
  IF(GAM)9002,9004,9002
9002 PIOTS=2.0*PIOTS
9004 N=K+IMAX
3305 IF(AMX(K))9902,3340,3306
3306 IF(IMAX-I)9903,3311,3310
3310 IF(AMX(K+1))9904,3312,3314
3311 PRR=P(K)
  QR=0.0
3307 ETH=ETH-PRR*U(K)/PIOTS*RC
  GO TO 3313
3312 PRR=0.0
  QR=0.0
3313 URR=RC*U(K)
  GO TO 3315
3314 PRR=(P(K)+P(K+1))/2.0
3315 URR=(J(K)*RC+U(K+1)*RR)/2.0
  RHO=0.5*(AMX(K)/TAU(I)+AMX(K+1)/TAU(I+1))/DY
  DUR=U(K)-U(K+1)
  IF(DUR)2003,10001,2005
2003 IF(S3)2004,10001,2004
10001 QR=0.0
  GO TO 3316
2004 UTEF=ABSF(0.5*(U(K)+U(K+1)))
  QR=-S3*RHO*UTEF*DUR
  GO TO 3316
2005 IF(S3)2007,2006,2007
2006 UTEF=0.
  GO TO 2008
2007 UTEF=ABSF(0.5*(U(K)+U(K+1)))
2008 CS=SQRTF(1.4*PRR/RHO)
  QR=RHO*DUR*(S1*CS+S2*S2*DUR+S3*UTEF)
3316 IF(JMAX-J)9305,3318,3320
3318 PABOVE=P(K)
  QT=0.0
  A=1.
3319 ETH=ETH-PABOVE*V(K)/2.0*TAUDTS
  GO TO 3323
3320 IF(AMX(N))9906,3322,3324
3322 PABOVE=0.0
  QT=0.0
3323 VABOVE=V(K)
  GO TO 3328
3324 PABOVE=(P(K)+P(N))/2.0
  RHO=0.5*(AMX(K)+AMX(N))/TAJ(I)/DY
  DVZ=V(K)-V(N)
  IF(DVZ)2009,10003,2011
2009 IF(S3)2010,10003,2010
10003 QT=0.0
  GO TO 7001
2010 VTEF=ABSF(0.5*(V(K)+V(N)))
  QT=-S3*RHO*VTEF*DYZ

```

GO TO 7001
 2011 IF(S3)2016,2012,2016
 2012 VTEF=0.
 GO TO 2014
 2016 VTEF=ABSF(0.5*(V(K)+V(N)))
 2014 CS=SQRRTF(1.4*PABOVE/RHO)
 QT=RHO*DVZ*(S1*CS+S2*S2*DVZ+S3*VTEF)
 7001 IF(NO-J) 3325,7005,9905
 7005 IF(CVIS) 7000,7006,7006
 7000 PBLO=P(K)
 ETH=ETH+PBLO*V(K)/2.0*TAUDTS
 7006 B=1
 3325 VAbove=(V(K)+V(N))/2.0
 3328 IF(VEL) 9907,6016,3400
 3400 G=6.3567E+08
 G=Z(108)*G*G/((G+Y(J)-DY/2.0)**2)
 IF(A+B) 9,3,10
 9 WS=(PBLO-PAbove+QB-QT)*TAUDTS/AMX(K)-G*DT
 GO TO 11
 10 WS=(PBLO-PAbove+QB-QT)*TAUDTS/AMX(K)-0.5*G*DT
 11 V(K)=V(K)+WS
 IF(ABSF(V(K))-1.E-01) 3401,3401,3402
 3401 V(K)=0.0
 3402 U(K)=U(K)+(PL(J)-PRR+QL(J)-QR)/(AMX(K))*RC/PIDTS*2.0
 IF(ABSF(U(K))-1.E-01) 3403,3403,6016
 3403 U(K)=0.0
 6016 CONTINUE
 IF(VEL) 9907,2001,2000
 2000 VQ=(VQ+V(K))/2.0
 UQ=(UQ+U(K))/2.0
 HS=(.5*P(K)*(VBLO-VAbove)+QB*(VBLO-VQ)+QT*(VQ-VAbove))*TAUDTS
 WT=(.5*P(K)*(UL(J)-URR)+QL(J)*(UL(J)-RC*UQ)+QR*(RC*UQ-URR))/PIDTS*
 12.0
 GO TO 2002
 2001 WS=P(K)*(VBLO-VAbove)*TAUDTS/2.0
 WT=P(K)*(UL(J)-URR)/PIDTS
 2002 RHO=HS+WT
 3332 WSX=AIX(K)+RHO/AMX(K)
 1000 IF(WSX) 1011,1001,1001
 1001 AIX(K)=WSX
 GO TO 3342
 1011 UT=1.0
 PRINT 2013
 2013 FORMAT(4X,1H,I,3X,1H,J,5X,3HWSX,10X,3HAIX,10X,3HAMX,10X,3H P,9X,2H
 1T,11X,2HWS,11X,2HDT,11X,3HVEL)
 PRINT 2015,I,J,WSX,AIX(K),AMX(K),P(K),WT,WS,DT,VEL
 2015 FORMAT(X,2I4,X,7(E12.4,X),F4.1,/) /
 WSA=2.0*AIX(K)/3.0*DT/(AIX(K)-WSX)
 1013 IF(WSA-UU) 1014,1001,1001
 1014 UU=WSA
 ISAVE=I
 JSAVE=J
 GO TO 1001
 3340 PRR=0.0
 QR=0.0
 QT=0.0
 URR=U(K+1)*RR
 PAbove=0.0

```

V ABOVE = V(N)
3342 VBL0 = V ABOVE
PL(J) = PRR
UL(J) = URR
QL(J) = QR
QB = QT
K = N
3348 PBLO = ? ABOVE
3355 RC = RR
IF(GAM) 3360,9007,3360
9007 RR = (X(I+1)+X(I+2))/2.0
3360 CONTINUE
3361 IF(VEL) 9911,10000,3363
3363 VEL = 0.0
GO TO 8001
C           ERROR
9902 NK = 3305
GO TO 9999
9903 NK = 3306
GO TO 9999
9904 NK = 3310
GO TO 9999
9905 NK = 3316
GO TO 9999
9906 NK = 3320
GO TO 9999
9907 NK = 3328
GO TO 9999
9911 NK = 3361
9999 NR = 3
CALL ERRER(NR,NK)
10000 IF(SN) 6201,7031,6201
7031 IF(UT) 7020,6201,7010
7010 UT = -1.0
DT = -DT
GO TO 8000
7020 UT = 0.0
PRINT 2060,ISAVE,JSAVE,UU
2060 FORMAT(8H CELL I=,I3,3H J=,I3.25H FINALLY SETS TIME STEP =,E12.4)
DT = UU
DTNA = DT
GO TO 8000
5201 RETURN
END

```

SUBROUTINE EDIT

D I M E N S I O N

```

DIMENSION AIX(3500),AMX(3500),P(3500),
1 U(3500),V(3500),X(60),Y(100),Z(150),
2 IZ(150),TAU(60),PL(100),UL(100),PR(100),
3 UR(100),IW1(15),FLEFT(100),YAMC(100),
4 SIGC(100),GAMC(100)

```

	C	O	M	M	O	N
COMMON	Z	,XO	,X	,Y		
COMMON	AIX	,AM	,AMX	,AREA	,E	
COMMON	FS	,I	,II	,IR	,IWS	
COMMON	J	,K	,KP	,L	,M	
COMMON	MZ	,N	,NK	,NO	,NOP	
COMMON	NR	,P	,PABOVE	,PBLO	,PICTS	
COMMON	PRR	,RC	,REZ	,RHO	,RR	
COMMON	SIG	,TAU	,TAUDTS	,TTX	,TTY	
COMMON	U	,URR	,UT	,UTEF	,UU	
COMMON	UVMAX	,V	,VABOVE	,VBLJ	,VEL	
COMMON	VTEF	,WS	,WSA	,WSB	,WSC	
COMMON	XLF	,XR	,YLW			
COMMON	YU	,UR	,PR			

	E	2	U	I	V	A	L	E	N	C	E
UEQUIVALENCE	(Z,IZ,PRO3),						(Z(2),CYCLE1),				(Z(3),DT1),
1(Z(4),PRINTS),	(Z(5),PPINTL),						(Z(6),DUMPT7),				(Z(7),CSTOP),
2(Z(8),PIDY),	(Z(9),TMZ),						(Z(10),GAM),				(Z(11),GAM0),
3(Z(12),GAMX),	(Z(13),ETH),						(Z(14),FFA),				(Z(15),FF8),
4(Z(16),TM0Z),	(Z(17),TMXZ),						(Z(18),XMAX),				(Z(19),TXMAX),
5(Z(20),TYMAX),	(Z(21),AM0M),						(Z(22),AMXM),				(Z(23),DMN),
6(Z(24),DMIN),	(Z(25),FEF),						(Z(26),DTNA),				(Z(27),CVIS),
7(Z(28),NPR),	(Z(29),NPRI),						(Z(30),NC),				(Z(31),NPC),
8(Z(32),NRC),	(Z(33),IMAX),						(Z(34),IMAXA),				(Z(35),JMAX),
9(Z(36),JMAXA),	(Z(37),KMAX),						(Z(38),KMAXA),				(Z(39),NMAX)
DEQUIVALENCE	(Z(40),ND),						(Z(41),KN1),				(Z(42),IXMAX),
1(Z(43),NOD),	(Z(44),NOPH),						(Z(45),NIMAX),				(Z(46),NJMAX),
2(Z(47),I1),	(Z(48),I2),						(Z(49),I3),				(Z(50),I4),
3(Z(51),N1),	(Z(52),N2),						(Z(53),N3),				(Z(54),N4),
4(Z(55),N5),	(Z(56),N6),						(Z(57),N7),				(Z(58),N8),
5(Z(59),N9),	(Z(60),N10),						(Z(61),N11),				(Z(62),NRM),
6(Z(63),TRAD),	(Z(64),XNRG),						(Z(65),SN),				(Z(66),DXN),
7(Z(67),RADEP),	(Z(68),RADET),						(Z(69),RADEB),				(Z(70),DTRAD),
8(Z(71),REZFCT),	(Z(72),PSTOP),						(Z(73),SMELL),				(Z(74),B9OUND),
9(Z(75),TOZONE),	(Z(76),ECX),						(Z(77),SBOUND),				(Z(78),X1)
DEQUIVALENCE	(Z(79),X2),						(Z(80),Y1),				(Z(81),Y2),
1(Z(82),CA3LN),	(Z(83),VISCI),						(Z(84),T),				(Z(85),GMAX),
2(Z(86),WSGD),	(Z(87),WSGX),						(Z(88),GMADR),				(Z(89),GMAXR),
3(Z(90),S1),	(Z(91),S2),						(Z(92),S3),				(Z(93),S4),
4(Z(94),S5),	(Z(95),S6),						(Z(96),S7),				(Z(97),S8),
5(Z(98),S9),	(Z(99),S10),										
6(Z(127),DX),	(Z(128),DY),						(Z(129),DY),				
7(Z(130),NFITB),	(Z(131),NFITT),						(Z(132),NFITR),				
8(Z(133),NPARR),	(Z(134),NPART),						(Z(135),NPARR)				

EQUIVALENCE (P,IW1)

EQUIVALENCE(P(200),GAMC),(P(400),YAMC)

EQUIVALENCE (UR,UL,FLEFT), (PR,PL,SIGC)

EQUIVALENCE (Z(120),DETVEL), (Z(122),EXEN)

EQUIVALENCE (Z(123),EXRHO), (Z(124),THICK)

C
C

102 IF(SENSE SWITCH 4) 122,104
104 IF(SENSE LIGHT 3) 106,108
108 IF(CYCLE - CSTOP) 112,122,122
112 IF(MODF(CYCLE,DUMPT7)) 114,1,114
114 IF(MODF(CYCLE,PRINTL)) 120,126,120
120 IF(MODF(CYCLE,PRINTS)) 140,6000,140
140 IF(SENSE LIGHT 1) 142,144
142 REWINJ 4
 IF(GAM0) 9,9,10
10 REWINJ 7
 9 SENSE LIGHT 1
 IF(GAMX) 144,144,143
143 CALL STEADY
144 GO TO 10000

C
C

DUMP ON TAPE 7

C

122 SENSE LIGHT 1
PRINTL=CYCLE
1 IF(DJMP7) 30,2,2
2 IF(GAM0) 3,3,203
203 BACKSPACE 7
204 WS = 555.0
 WRITE(7) WS,CYCLE,N3
220 WRITE(7) (Z(L),L=1,MZ)
206 WRITE(7)(U(K),V(K),AMX(K),AIX(K),P(K),K=1,KMAXA)
207 WRITE(7)(X(0),(X(K),TAU(K),K=1,IMAX)
221 WRITE(7)(Y(K-1),K=1,JMAXA)
222 WS = 666.0
 WRITE(7) WS,WS,WS
GO TO 8
3 BACKSPACE 4

C
C
NOTE, ADDITIONAL DATA ON TAPE 7

4 WS=555.0
 WRITE(4) WS,CYCLE,N3
20 WRITE(4)(Z(L),L=1,MZ)
6 WRITE(4)(U(K),V(K),AMX(K),AIX(K),P(K),K=1,KMAXA)
7 WRITE(4)(X(0),(X(K),TAU(K),K=1,IMAX)
21 WRITE(4)(Y(K-1),K=1,JMAXA)
22 WS=666.
 WRITE(4) WS,WS,WS
8 IF(SENSE SWITCH 2) 5,24
5 REWINJ 4
 PRINT 8121,CYCLE
8121 FORMAT(7H CYCLE ,F5.0,18H BEGINS NEW TAPE 4)
PAUSE 10
GO TO 4
24 WRITE(6,8120)NC
30 GO TO 114

C
C

106 SENSE LIGHT 3
126 SENSE LIGHT 4
 IF(SENSE SWITCH 1) 11,6000

```

11 CALL )DISPLA (7HCYCLE = ,NC)
6000 DO 6012 I=1,12
6012 PR(I)=0.0
DO 6020 K=2,KMAX
WSB=(J(K)**2+V(K)**2)/2.0
6017 PR(1)=0.0
PR(2)=0.0
PR(4)=0.0
6019 IF(AMX(K))9917,6028,6020
6020 PR(5)=PR(5)+AIX(K)*AMX(K)
PR(6)=PR(6)+WSB*AMX(K)
PR(8)=PR(8)+AMX(K)
6028 CONTINUE
PR(3)=PR(1)+PR(2)
PR(7)=PR(5)+PR(6)
XNRG=PR(7)
PR(9)=PR(1)+PR(5)
PR(10)=PR(2)+PR(6)
PR(11)=PR(3)+PR(7)
PR(12)=PR(4)+PR(8)
WSA=(ETH-PR(11))/ETH
PR(18)=(WSA-0NN)/FLOATF(NPC)
ECK=PR(18)
0NN=WSA
NPC=0
WRITE (6,8116)PROB,NC,T,DTNA,TRAD,DTRAD,NR,N1,N2,N3,N4
WRITE (6,8117)(PR(I),I=1,8)
WRITE (6,8118)(PR(I),I=9,12)
WRITE (6,8119)UVMAX,ETH,ECK
WRITE (6,9040)N10,N11,I1,I2,I3,I4
6090 IF(SENSE LIGHT 4)5000,136
***** END OF S P SUBROUTINE ****
C
C
***** SUBROUTINE L P ****
5000 CONTINUE
5001 WRITE (6,8116)PROB,NC,T,DTNA,TRAD,DTRAD,NR,N1,N2,N3,N4
5004 DO 5050 I=1,IMAX
SENSE LIGHT 4
J=JMAX+1
K=JMAX*IMAX+I+1
DO 5046 L=1,JMAX
J=J-1
K=K-IMAX
5012 IF(AMX(K))9917,5046,5014
5014 IF(SENSE LIGHT 4)5016,5019
5016 WRITE (6,8135)I,X(I),DX
5019 WS=AMX(K)/(TAU(I)**DY)
5018 WRITE(6,8109)J,U(K),V(K),P(K),AMX(K),WS,AIX(K),Y(J)
5046 CONTINUE
IF (CYCLE - CSTOP) 136,5050,136
5050 CONTINUE
136 IF (ABSF(ECK)-0MIN)140,140,9905
***** END OF L P SUBROUTINE ****
C
C
C
         ERROR
9901 NK=110

```

```

GO TO 9999
C           ENERGY CHECK
9905 NK=136
         GO TO 9999
C           NEGATIVE MASS
9917 NK=6015
         GO TO 9999
9920 NK=904
         GO TO 9999
9921 NK=912
         GO TO 9999
9922 NK=918
         GO TO 9999
9923 NK=922
         GO TO 9999
9924 NK=926
9999 NR=6
         CALL ERROR(NR,NK)
10000 RETURN
C
C           FORMATS
8108 FORMAT(I4,1X,1P7E16.6)
81160FORMAT(8H1PROBLEM6X,5HCYCLE9X,4HTIME13X,2HDT13X,4HTRAJ11X,5HDTRO1
   12X,2HNR6X,2HN14X,2HN24X,2HN34X,2HN4/(F9.3,I10,1X,1P4E16.7,I10,2X,4
   2I6))
81170FORMAT(1H//17X2HA16X,2HAK14X,5HAI+AK15X,2HAM/4H DOT3X,1P4E18.7/3
   1H X4X,4E18.7)
81180FORMAT(12X,13H-----5X,13H-----5X,13H-----5
   1X,13H-----/7H TOTALS1P4E18.7)
81190FORMAT(2H0 //16X,7HMAX VEL13X,3HTHE12X,9HREL ERROR/6X,1P6E19.7///)
8120 FORMAT(1H0//21H TAPE 7 DUMP ON CYCLE15///)
81350FORMAT(1H //4H I =I3,6X,6HX(I) =F12.3,3X,6H DX =F12.3//3H J10X,
   11HX15X,1HY14X,3HF/A13X,3HAMX13X,3HRHO13X,3HAIX14X,1HY/)
9040 FORMAT(1H / 6I6)
         END

```

```

SUBROUTINE POWER(X,XX,N)
XX=LOGF(ABSF(X))/2.302585093
N=XX
IF(XX)1,2,2
1 N=N-1
2 XX=X/10.**N
RETURN
END

```

SUBROUTINE PH2

```

C           D I M E N S I O N
C
DIMENSION AIX(3500),AMX(3500),P(3500),
1 U(3500),V(3500),X(60),Y(100),Z(150),

```

2 IZ(130), TAU(60), PL(100), UL(100), PR(100),
 3 UR(100), TH1(15), FLEFT(100), YAMC(100),
 4 SIGC(100), SAVC(100)

	C	D	H	I	S	N
COMMON	Z	,X0	,I1	,T	,Y	
COMMON	AIX	,AH	,AHK	,AREA	,E	
COMMON	FS	,I	,II	,IR	,INS	
COMMON	J	,K	,KP	,L	,M	
COMMON	M2	,N	,NC	,NO	,NOP	
COMMON	M2	,P	,PABOVE	,PAHO	,PIOTS	
COMMON	P22	,RC	,REZ	,RHO	,RR	
COMMON	SIG	,TAU	,TAUDTS	,TIX	,TTT	
COMMON	U	,U22	,UT	,UTEF	,UU	
COMMON	UVMAX	,V	,VABOVE	,VALO	,VLL	
COMMON	VTEF	,WS	,WSD	,WSD	,WSC	
COMMON	XLF	,X4	,YLM			
COMMON	YU	,U2	,P2			

	C	D	H	I	S	N
DEQUIVALENCE	(Z,IZ,PR01),	(Z,I1,CYLE1),	(Z,I1,311),			
1(Z(4),PRINTS),	(Z,I1,PRINTL),	(Z,I1,DUMP17),	(Z,I1,CSTOP),			
2(Z(8),PIDY),	(Z,I1,TH21),	(Z,I1,GA11),	(Z,I1,GA01),			
3(Z(12),GAMC),	(Z,I1,TH4),	(Z,I1,FF4),	(Z,I1,FFH1),			
4(Z(16),TH02),	(Z,I1,TH62),	(Z,I1,TH82),	(Z,I1,TH83),			
5(Z(20),YMAX),	(Z,I1,AH21),	(Z,I1,AMEM1),	(Z,I1,DVNT),			
6(Z(24),DMIN),	(Z,I1,FEF),	(Z,I1,DT41),	(Z,I1,CVIS1),			
7(Z(28),NP21),	(Z,I1,NPRI),	(Z,I1,NG1),	(Z,I1,NPC1),			
8(Z(32),NRC),	(Z,I1,IA22),	(Z,I1,IM821),	(Z,I1,J488),			
9(Z(35),JMAX),	(Z,I1,KMAX),	(Z,I1,KM821),	(Z,I1,KM83)			
DEQUIVALENCE	(Z,I1,N1),	(Z,I1,KD1),	(Z,I1,KM83),			
1(Z(43),N07),	(Z,I1,NOPR1),	(Z,I1,NI482),	(Z,I1,NJ883),			
2(Z(47),I1),	(Z,I1,I2),	(Z,I1,I3),	(Z,I1,I4),			
3(Z(51),N1),	(Z,I1,N2),	(Z,I1,N3),	(Z,I1,N63),			
4(Z(55),N5),	(Z,I1,N5),	(Z,I1,N7),	(Z,I1,N9),			
5(Z(59),N9),	(Z,I1,N11),	(Z,I1,N11),	(Z,I1,N21),			
6(Z(63),TRAJ1),	(Z,I1,XHRC1),	(Z,I1,SNI),	(Z,I1,DEH1),			
7(Z(67),RADCL1),	(Z,I1,RADLT1),	(Z,I1,RADE1),	(Z,I1,DTRAD1),			
8(Z(71),PFZFC1),	(Z,I1,PSTOP),	(Z,I1,SHELL),	(Z,I1,HROUND),			
9(Z(75),TOZONE1),	(Z,I1,TG1),	(Z,I1,SDOUN1),	(Z,I1,Z1),			
DEQUIVALENCE	(Z,I1,X21),	(Z,I1,Y11),	(Z,I1,Y21),			
1(Z(82),GABL1),	(Z,I1,VISCI),	(Z,I1,T1),	(Z,I1,G488),			
2(Z(85),WSD1),	(Z,I1,WSD2),	(Z,I1,GM001),	(Z,I1,G488),			
3(Z(90),S1),	(Z,I1,S2),	(Z,I1,S3),	(Z,I1,S61),			
4(Z(96),S5),	(Z,I1,S6),	(Z,I1,S7),	(Z,I1,S97),			
5(Z(99),S9),	(Z,I1,S10),					
6(Z(127),CX),	(Z,I1,YY1),	(Z,I1,DT1),				
7(Z(130),NFTT1),	(Z,I1,NFTT1),	(Z,I1,NFTT2),				
8(Z(133),NPAPR1),	(Z,I1,NPAPR1),	(Z,I1,NPAPR2),				

EQUIVALENCE	(P,IN1)
EQUIVALENCE(P(2)0),GAHC1,(P(4)0),YAMC1)	
EQUIVALENCE (UR,UL,FLEFT), (PR,PL,SIGC1)	
EQUIVALENCE (Z(120),DETVEL), (Z(122),EXLH1)	
EQUIVALENCE (Z(123),EXPHO1), (Z(124),THICK1)	

J307=2(146)
 2(141)=0.
 2(142)=0.
 2(143)=0.
 RZ=3.0
 SENSE LIGHT 0
 P101S=1.0/P101T=0.0
 101 DO 103 J=1,JMAX
 102 GANCI(J)=0.0
 LEFT(J)=0.0
 VAGC(J)=0.0
 103 S1CC(J)=0.0
 104 DO 567 I=1,IMAX
 J=2
 105 C(J-1)=1480.0+1
 00 IF(LAHC(C))1000,17,41
 01 IF(LV(C))42,47,47
 07 ANHVC=0.0
 ANHVR=0.
 DELE9=0.
 GO TO 107
 42 ANHVT=ANH(U(C))**V(C)**/21
 NSPAHC(C)
 IF(GAHC(J))700,43,43
 7000 NS=ANH(U(C))+GANC(J)
 43 IF(LAH97+NS)16,43,45
 46 ANHVT=NS
 45 IF(CVIS)116,107,107
 106 ANHVI=ANHVT*U(C)
 ANHVC=ANHVT*V(C)
 DELE9=A72(C)+U(C)**2+V(C)**2/2.0
 NS=1.0*(1002+V(C)**2)/2.0
 ET4=C10+ANH70*(A72(C)+NS)
 IF(-ANHVT/(TAU(U))**2)-TO204C)107,107,47
 99 RCZ=1.
 2(143)=1.
 2 MASS HAS LEFT THE BOTTOM
 GO TO 107
 100 ANHVC=0.0
 ANHVR=0.0
 ANHVT=0.0
 DELE9=0.0
 107 DO 565 J=2,JMAX
 104 L=C+1487
 VEL=0.0
 FS=0.0
 210 IF(JMAX-J)211,211,217
 211 VEL=1.0
 GO TO 204
 217 IF(LANL(L))213,213,216
 214 IF(LANL(K))214,216,216
 216 VABOVE=VEL

GO TO 212
 215 IF(AMX(K)) 205,235,205
 205 VAROVE=0.0
 GO TO 212
 208 VAROVE=V(<)
 GO TO 212
 209 VAROVE=(V(K)+V(L))/2.0
 212 CONTINUE
 FS=0.0
 404 IF(IMAX-I) 412,412,435
 405 IF(AMX(K+1)) 411,411,409
 409 IF(AMX(K)) 410,410,407
 410 URR=U(K+1)
 GO TO 409
 411 IF(AMX(K)) 403,403,406
 403 URR=0.0
 GO TO 409
 412 FS=1.0
 406 URR=U(K)
 GO TO 409
 407 URR=(J(K)+U(K+1))/2.0
 408 CONTINUE
 301 IF(VABOVE) 300,334,302
 302 IF(AMX(K)) 3703,334,4000
 1900 IF(J-1) 9901,303,1901
 1901 KP=K-IMAX
 IF(AMX(KP)) 3900,303,303
 303 M=K
 JJ=J
 GO TO 307
 304 AMPY=0.0
 304 AMUT=0.0
 AMVT=0.0
 DELET=0.0
 GO TO 501
 300 IF(VEL) 9901,305,304
 305 IF(AMX(L)) 7903,304,306
 306 M=L
 JJ=J+1
 307 IF(VEL) 6130,6130,6140
 6130 HSA=(V(K)+V(L))/2.0
 HSB=1.0+(V(L)-V(K))/(DY*5.0000)*DT
 VAROVE=HSA/HSB
 6140 AMPY=AMX(M)*VAROVE/DY*DT
 501 IF(URR) 500,504,502
 502 IF(AMX(K)) 3700,504,503
 503 M=K
 N=I
 GO TO 509
 504 AMMP=0.0
 AMUR=0.0
 AMVR=0.0
 DELET=0.0
 GO TO 1
 500 IF(FS) 9905,506,506
 506 IF(AMX(K+1)) 3406,506,507
 507 M=K+1

N=I+1
 500 IF(FS)6100,6130,6110
 6100 WSA=(J(K)+U(K+1))/2.0
 WSB=1.0+(U(K+1)-U(K))/(DX*SBOUND)*DT
 URR=WSA/WSB
 6110 DEN=AMX(M)/TAU(N)
 IF(GAM)9990,9949,9930
 9989 CART=X(I)*2.0
 GO TO 9991
 9990 CART=1.0
 9991 AMMP=DEN/PI]TS*CART*URR
 1 IF(AMMP)16,74,3820
 8820 IF(GAMC(J))74,74,9921
 8821 IF(FS)6120,6120,74
 6120 IF(AMX(K+1))9903,74,74
 74 JT4G=0
 2 IF(AMPY)3,4,4
 3 ITAG=1
 WSB=AMPY
 AMPY=0.0
 GO TO 64
 4 ITAG=0
 64 IF(AMMY)9,5,5
 5 IF(GAMC(J))7,6,0
 6 WS=AMX(K)
 GO TO 11
 7 WS=AMX(K)+GAMC(J)
 GO TO 11
 9 IF(GAMC(J))10,8,8
 8 WS=AMX(K)+AMMY
 GO TO 11
 10 WS=AMX(K)+GAMC(J)+AMMY
 11 WSA=A4PY+AMM2
 12 IF(WSA-WS)75,75,13
 13 AMPY=A4PY*WS/WSA
 AMMP=AMMP*WS/WSA
 75 IF(JTAG)14,73,14
 73 WSC=A4MP
 14 IF(ITAG)15,7000,15
 15 AMPY=WSB
 ITAG=0
 GO TO 40
 16 IF(FS)76,17,76
 76 WSC=A4MP
 GO TO 40
 17 IF(I+1-IMAX)19,19,9908
 18 URRR=J(K+1)/2.0
 GO TO 20
 19 URRR=(U(K+1)+U(K+2))/2.0
 20 IF(URRR)39,39,21
 21 IF(GAM)9993,9992,9993
 9992 CART=X(I+1)*2.0
 GO TO 9994
 9993 CART=1.0
 9994 URRR=JRRR/TAU(I+1)*AMX(K+1)/PI]TS*CART
 22 IF(J-1)9903,23,24
 23 VBL0=V(K+1)/2.0

```

      GO TO 26
24 KP=K+1-IMAX
      VBL0=(V(K+1)+V(KP))/2.0
26 IF(VBL0)25,35,38
25 VBL0=AMX(K+1)/DY*VBL0*DT
27 IF(VEL)28,29,28
28 VAB=V(K+1)/2.0
      GO TO 31
29 KP=K+IMAX+1
      VAB=(V(K+1)+V(KP))/2.0
31 IF(VAB)36,36,30
30 VAB=AMX(K+1)/DY*VAB*DT
32 HS=AMX(K+1)
33 WSA=URRR-AMMP-VBL0+VAB
34 IF(WSA-HS)77,77,35
35 AMMP=AMMP*HS/WSA
77 JTAG=1
      WSC=AMMP
      AMMP=0.0
      GO TO 2
36 HS=AMX(K+1)
37 WSA=URRR-AMMP-VBL0
      GO TO 34
38 VBL0=0.0
      GO TO 27
39 URRR=0.0
      GO TO 22
40 IF(VE-)7000,41,7000
41 IF(FS)42,43,42
42 KP=K+IMAX
      URT=U(KP)/2.0
      GO TO 45
43 KP=K+IMAX
      URT=(U(KP)+U(KP+1))/2.0
45 IF(URT)46,46,70
46 URT=0.0
      GO TO 47
70 KP=K+IMAX
      IF(GAM)9997,9996,9997
9996 CART=X(I)*2.0
      GO TO 9998
9997 CART=1.0
9998 URT=URT/TAU(I)*AMX(KP)/PIOTS*CART
47 IF(J+1-JMAX)48,43,9910
48 KP=K+IMAX
      KL=KP+IMAX
      VABT=(V(KP)+V(KL))/2.0
      GO TO 51
49 KP=K+IMAX
      KL=KP+IMAX
      VABT=V(KP)/2.0
51 IF(VABT)8810,71,72
8810 IF(AMX(K))9903,71,71
71 VABT=0.0
      GO TO 60
72 VABT=VABT*AMX(KP)/DY*DT
52 IF(GAMC(J+1)154,53,53

```

```

53 WS=AMX(KP)
  GO TO 55
54 WS=AMX(KP)+GAMC(J+1)
55 WSA=VART-AMPY+URT
  GO TO 57
60 IF(GAMC(J+1))61,61,59
61 WS=AMX(KP)+GAMC(J+1)
  GO TO 58
59 WS=AMX(KP)
58 WSA=-AMPY+URT
57 IF(WSA-WS)7000,7000,56
56 AMPY=AMPY*WS/WSA
  GO TO 7000
7000 AMMP=WSC
309 IF(AMPY)8834,8831,8833
8833 IF(JMAX-J)9911,318,8835
8835 KP=K+IMAX
8836 IF(AMX(KP))9900,8837,318
8837 IF(AMPY/(TAU(I)*DY)-TOZONE)8838,318,318
8838 AMPY=0.
  GO TO 8831
8834 IF(J-1)9911,8831,8839
8839 IF(AMX(K))9900,8840,8831
8840 IF(-AMPY/(TAU(I)*DY)-TOZONE)8841,8831,8831
8841 AMPY=0.
  GO TO 8831
318 DELM=GAMC(J)+AMMY-AMPY
322 IF(VEL)9901,324,323
323 WS=U(K)**2+V(K)**2
  ETH=ETH-AMPY*(AIX(K)+WS/2.0)
  IF(AMPY/(TAU(I)*DY)-TOZONE)324,324,6900
6900 REZ=1.0
Z(141)=1.
? MASS HAS LEFT THE TOP
324 AMUT=AMPY*U(K)
  AMVT=AMPY*V(K)
  GO TO 326
4831 AMUT=AMPY*U(L)
  AMVT=AMPY*V(L)
  DELM=GAMC(J)-AMPY+AMMY
326 IF(AMPY)327,328,328
327 DELET=AIX(L)+(U(L)**2+V(L)**2)/2.0
  GO TO 333
328 IF(AMMY)329,330,330
329 DELET=DELET
  GO TO 333
330 IF(GAMC(J))331,332,332
331 DELET=SIGC(J)
  GO TO 333
332 DELET=AIX(K)+(U(K)**2+V(K)**2)/2.0
333 SIGMU=FLEFT(J)+AMMU-AMUT
  SIGMV=YAMC(J)+AMMV-AMVT
  DELEK=GAMC(J)*SIGC(J)+AMMY*DELET-AMPY*DELET
509 IF(AMMP)8843,518,8844
8844 IF(IMAX-I)9911,518,8845
J845 IF(AMX(K+1))9900,8846,518
8846 IF(AMMP/(TAU(I+1)*DY)-TOZONE)8847,518,518

```

8847 AMMP=0.
 GO TO 518
 8843 IF(I-1)9911,512,8848
 8848 IF(AMX(K))9900,8849,512
 8849 IF(-AMMP/ (TAU(I)*DY) -TOZONE)8850,512,512
 8850 AMMP=0.
 GO TO 518
 512 DELM=DELM-AMMP+AMX(K)
 8828 AMUR=AMMP*U(K+1)
 AMVR=AMMP*V(K+1)
 GO TO 525
 518 DELM=DELM-AMMP+AMX(K)
 522 IF(FS)9905,524,523
 523 WS=U(K)**2+V(K)**2
 ETH=ETH-AMMP*(AIX(K)+WS/2.0)
 IF(AMMP/ (TAU(I)*DY) -TOZONE)524,524,6901
 6901 REZ=1.
 Z(142)=1.
 MASS HAS LEFT THE RIGHT SIDE
 524 AMUR=AMMP*U(K)
 AMVR=AMMP*V(K)
 525 SIGMU=SIGMU-AMUR
 SIGMV=SIGMV-AMVR
 526 TIC=0.0
 527 IF(AMMY)529,529,529
 528 DELER=AIX(K+1)+(U(K+1)**2+V(K+1)**2)/2.0
 GO TO 537
 529 IF(AMPY)530,531,531
 530 DELER=DELE3
 GO TO 536
 531 IF(GAMC(J))532,533,533
 532 DELER=SIGC(J)
 GO TO 536
 533 IF(AMPY)535,535,534
 534 DELER=DELET
 GO TO 536
 535 DELER=AIX(<)+(U(K)**2+V(K)**2)/2.0
 536 TIC=1.0
 537 DELEK=DELEK-AMMP*DELER
 538 IF(TIC)9907,539,550
 550 WS=DELER
 GO TO 999
 539 WS=AIX(K)+(U(K)**2+V(K)**2)/2.0
 999 IF(DELM)999,543,540
 998 IF(AMX(K)*1.E-6+DELM)9906,997,997
 997 DELM=0.0
 GO TO 543
 540 ENK=AMX(K)*WS+DELEK
 541 U(K)=(SIGMU+AMX(K)*U(K))/DELM
 601 V(K)=(SIGMV+AMX(K)*V(K))/DELM
 603 WS=U(<)**2+V(K)**2
 542 AIX(K)=ENK/DELM-WS/2.0
 543 AMX(K)=DELM
 IF(AMX(K))3900,2007,544
 2007 AIX(K)=0.0
 U(K)=0.0
 V(K)=0.0

```

544 GAMC(J)=AMMP
      FLEFT(J)=AMUR
      YAMC(J)=AMVR
      SIGC(J)=DELER
545 AMMY=AMPY
      AMMU=AMUT
      AMMV=AMVT
      DELER=DELET
C     DELET=SPECIFIC TOTAL ENERGY OUT OF THE TOP
C     OF CELL IN QUESTION
C     AMPY=MASS(IN GRAMS)OUT OF THE TOP
C     OF CELL IN QUESTION
546 K=K+IMAX
547 CONTINUE
6802 GO TO 548
9901 NK=300
      GO TO 9999
9900 NK=302
      GO TO 9999
9903 NK=303
      GO TO 9999
9904 NK=505
      GO TO 9999
9905 NK=500
      GO TO 9999
9906 NK=513
      GO TO 9999
9911 NK=8833
      GO TO 9999
9908 NK= 17
      GO TO 9999
9909 NK= 22
      GO TO 9999
9910 NK= 47
      GO TO 9999
9907 NK=538
9939 NR=4
      CALL ERROR(NR,NK)
548 SUM=0.0
2005 DO 2001 I=1,IMAX
      K=I+1
      DO 2000 J=1,JMAX
2008 IF(AIX(K))2J04,2000,200J
2004 SUM=SJM+AIX(K)*AMX(K)
      AIX(K)=0.0
2000 K=K+IMAX
2001 CONTINUE
2003 ETH=ETH-SUM
      Z(104)=Z(104)+SUM
8002 IF(REZ)8001,8001,8003
8003 GO TO 8001
8001 RETURN
END

```

SUBROUTINE REZONE
RETURN
END

SUBROUTINE FIT 1
HS = 1.2E-3
HSA=1.E9
HSB=0.0
HSC=0.0
RETURN
END

SUBROUTINE STEADY

D I M E N S I O N

DIMENSION AIX(3500),AMX(3500),P(3500),
1 U(3500),V(3500),X(60),Y(100),Z(150),
2 IZ(150),TAU(60),PL(100),UL(100),PR(100),
3 UR(100),IW1(15),LEFT(100),YAMC(100),
4 SIGC(100),GAMC(100)

C	O	M	N	O	N
COMMON	Z	XO	X	,Y	
COMMON	AIX	,A	,AMX	,AREA	,E
COMMON	FS	,I	,II	,IR	,IWS
COMMON	J	,K	,KP	,L	,M
COMMON	MZ	,N	,NK	,NO	,NOP
COMMON	NR	,P	,PAROVE	,PBLD	,PIOTS
COMMON	PRR	,PC	,REZ	,RHO	,RR
COMMON	SIG	,TAU	,TAUDTS	,TTX	,TTY
COMMON	U	,URR	,UT	,UTEF	,UU
COMMON	UVMAX	,V	,VABOVE	,VBLD	,VEL
COMMON	VTEF	,HS	,HSA	,HSB	,HSC
COMMON	XLF	,XR	,YLW		
COMMON	YU	,UR	,PR		

E Q U I V A L E N C E

DEQUIVALENCE	(Z,IZ,PRO9),	(Z(2),CYCLE),	(Z(3),DT),
1(Z(4),PRINTS),	(Z(5),PRINTL),	(Z(6),DUMPT7),	(Z(7),CSTOP),
2(Z(8),PIDY),	(Z(9),TMZ),	(Z(10),GAM),	(Z(11),GAMD),
3(Z(12),GAMX),	(Z(13),FT4),	(Z(14),FFA),	(Z(15),FFB),
4(Z(16),TMDZ),	(Z(17),TMXZ),	(Z(18),XMAX),	(Z(19),TXMAX),
5(Z(20),TYMAX),	(Z(21),AMDM),	(Z(22),AMXM),	(Z(23),DNN),
6(Z(24),DMINI),	(Z(25),FEF),	(Z(26),DTNA),	(Z(27),CVIS),
7(Z(28),NPR),	(Z(29),NPRI),	(Z(30),NC),	(Z(31),NPC),
8(Z(32),NRC),	(Z(33),IMAX),	(Z(34),IMAXA),	(Z(35),JMAX),
9(Z(36),JMAXA),	(Z(37),KMAX),	(Z(38),KMAXA),	(Z(39),NMAX)
DEQUIVALENCE	(Z(40),N7),	(Z(41),KOT),	(Z(42),IXMAX),
1(Z(43),NOD),	(Z(44),NOPR),	(Z(45),NIMAX),	(Z(46),NJMAX),

2(Z(47),I1),	(Z(48),I2),	(Z(49),I3),	(Z(50),I4),
3(Z(51),N1),	(Z(52),N2),	(Z(53),N3),	(Z(54),N4),
4(Z(55),N5),	(Z(56),N6),	(Z(57),N7),	(Z(58),N8),
5(Z(59),N9),	(Z(60),N10),	(Z(61),N11),	(Z(62),NRM),
6(Z(63),TRAD),	(Z(64),XNRG),	(Z(65),SN),	(Z(66),DXN),
7(Z(67),RADER),	(Z(68),PADET),	(Z(69),RADE8),	(Z(70),DTRAD),
8(Z(71),REZFCT),	(Z(72),RSTOP),	(Z(73),SHELL),	(Z(74),BBOUND),
9(Z(75),TOZONE),	(Z(76),ECK),	(Z(77),SBOUND),	(Z(78),X1)
DEQUIVALENCE	(Z(79),X2),	(Z(80),Y1),	(Z(81),Y2),
1(Z(82),CABLN),	(Z(83),VISC),	(Z(84),T),	(Z(85),GMAX),
2(Z(86),MSG0),	(Z(87),MSGX),	(Z(88),GMADR),	(Z(89),GMAXR),
3(Z(90),S1),	(Z(91),S2),	(Z(92),S3),	(Z(93),S4),
4(Z(94),S5),	(Z(95),S6),	(Z(96),S7),	(Z(97),S8),
5(Z(98),S9),	(Z(99),S10),		
6(Z(127),DX),	(Z(128),DY1),	(Z(129),DY),	
7(Z(130),NFITB),	(Z(131),NFITT),	(Z(132),NFITR),	
8(Z(133),NPARB),	(Z(134),NPART),	(Z(135),NPARR)	

EQUIVALENCE (P,IW1)

EQUIVALENCE(P(200),GAMC),(P(400),YAMC)

EQUIVALENCE (UR,UL,FLEFT), (PR,PL,SIGC)

```

VEL = 0.0
FLAG2 = 12.0
20 FLAG1 = 0.0
30 READ (4) PR(1), PR(2), N3
      WRITE (6,8006) PR(1),PR(2),N3
      IF (PR(1).EQ.555.0) 40,31
31 IF (PR(1).EQ.666.0) 32,35
32 WRITE (6,8008)
      GO TO 1000
35 FLAG1 = FLAG1 + 1.0
      IF (FLAG1 - FLAG2) 34,34,3901
34 WRITE (6,8100) FLAG1
      GO TO 30
40 READ (4) (Z(I),I=1,3)
      WRITE (6,8104) (Z(I),I=1,3)
      READ (4) (DUM,DUM,DUM,DUM,P(I),I = 1,KMAXA)
      WRITE (6,8106) (P(I),I=1,3)
      READ (4) DUM
      READ (4) DUM
      IF (VEL) 50,50,60
50 DO 55 I = 1,KMAX
55 AMX(I) = P(I)
      VEL = 1.0
      WRITE (6,8102)
      GO TO 30
60 SUM = 0.0
      I = 3
70 DO 75 J = 2,JMAX
      K = I + 1 + (J - 1)*IMAX
      DIFF = ABS(P(K)) - ABS(AMX(K))
75 SUM = SUM + ABS(DIFF)
80 WRITE (6,8002) PR(2), SUM
      IF (CSTOP - PR(2)) 1000,1000,90
90 DO 95 I = 1,KMAX
95 AMX(I) = P(I)

```

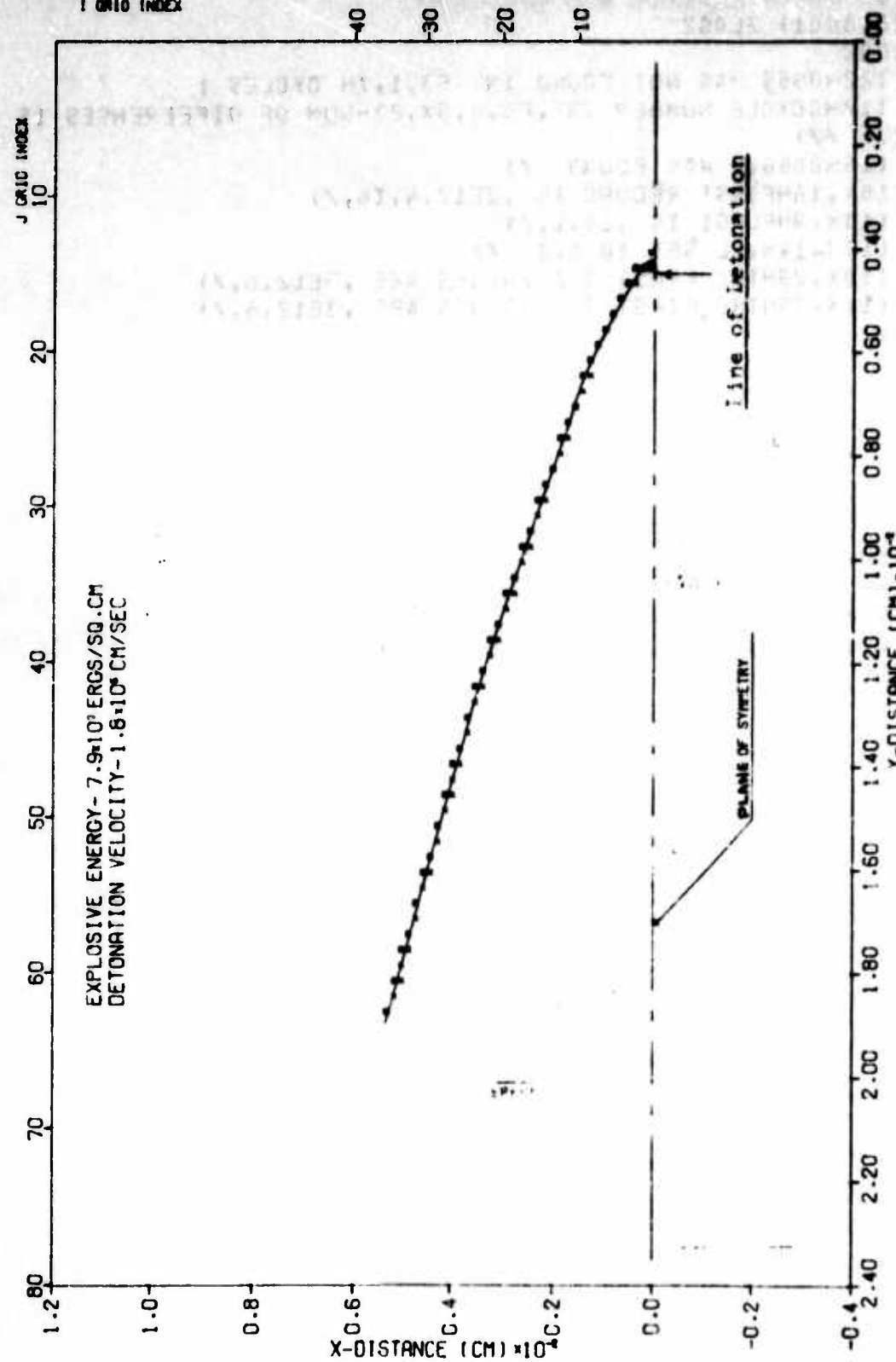
```
GO TO 20
9901 WRITE (6,8001) FLAG2
GO TO 1000
8001 FORMAT (22H0555 WAS NOT FOUND IN ,F5.1,7H CYCLES )
8002 FORMAT (1740CYCLE NUMBER IS ,F5.0,5X,22HSUM OF DIFFERENCES IS ,
1    0PE12.6 //)
8008 FORMAT (16H0666.0 WAS FOUND  /)
8006 FORMAT(10X,16HFIRST RECORD IS ,2E12.4,I6,/)
8100 FORMAT (10X,9HFLAG1 IS ,F5.1,/)
8102 FORMAT (10X,14HVEL SET TO 1.0  /)
8104 FORMAT (10X,25HTHE FIRST 3 Z VALUES ARE ,3E12.6,/)
8106 FORMAT (1UX,25HTHE FIRST 3 P VALUES ARE ,3E12.6,/)
1000 REWIND 4
RETURN
END
```

```
SUBROUTINE LRRER(NR,NK)
CALL TIME
WRITE (6,1380) NR,NK
8880 FORMAT (10X,5H NR= ,I2,5X,5H NK= ,I4,/)
CALL EXIT
END
```

APPENDIX B

ADDITIONAL PLOTS FOR THE IDEALIZED PROBLEM

I ORIC INDEX



SHELLTC CALCULATION OF POINT SOURCE IN HYPERSONIC FLOW
TIME 0.001672 SEC CYCLE 310 PROBLEM 22.000

Figure B1. Shock Front Location in the XY Plane

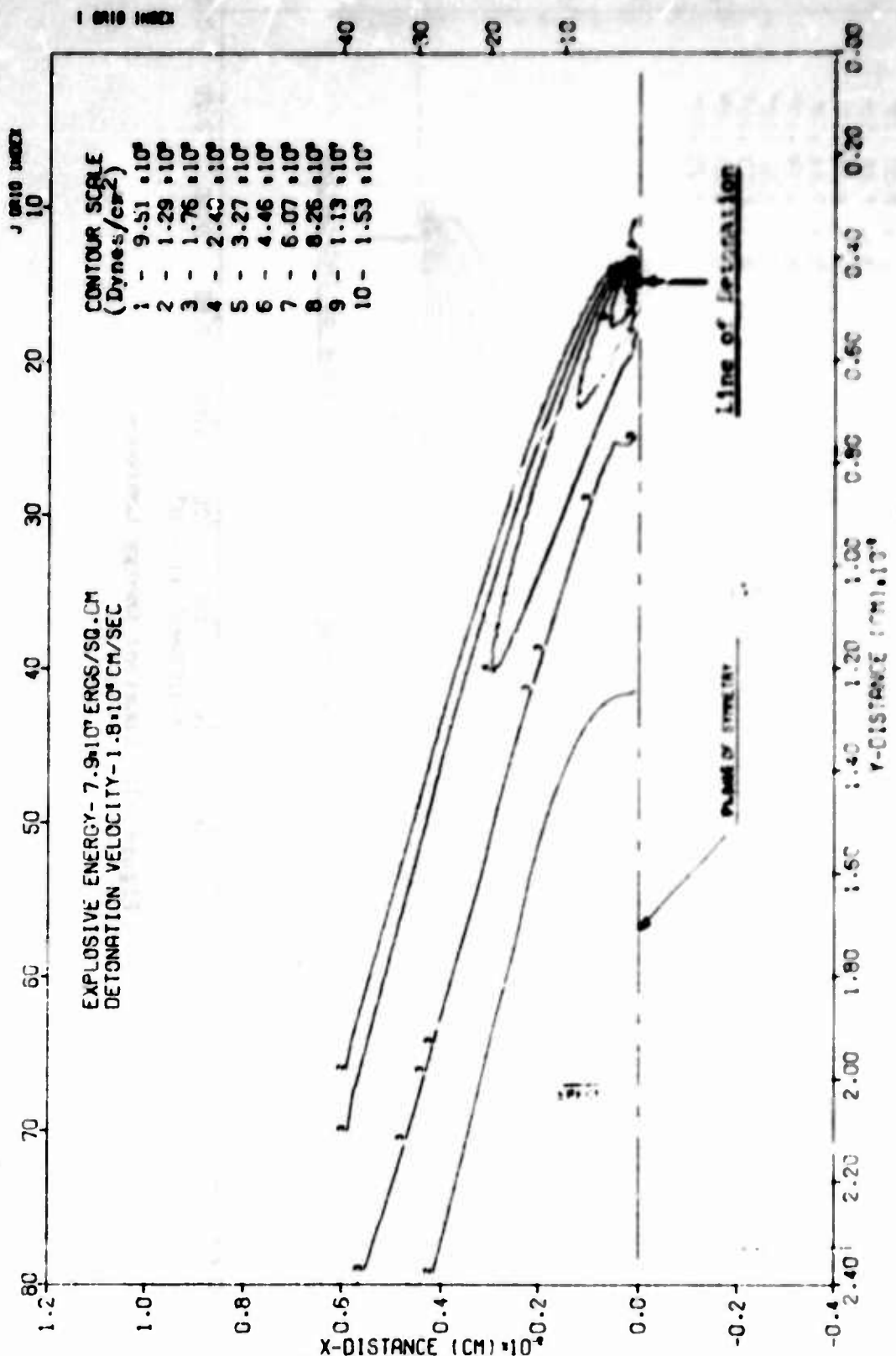


Figure E2. Constant Pressure Contours (Inches)

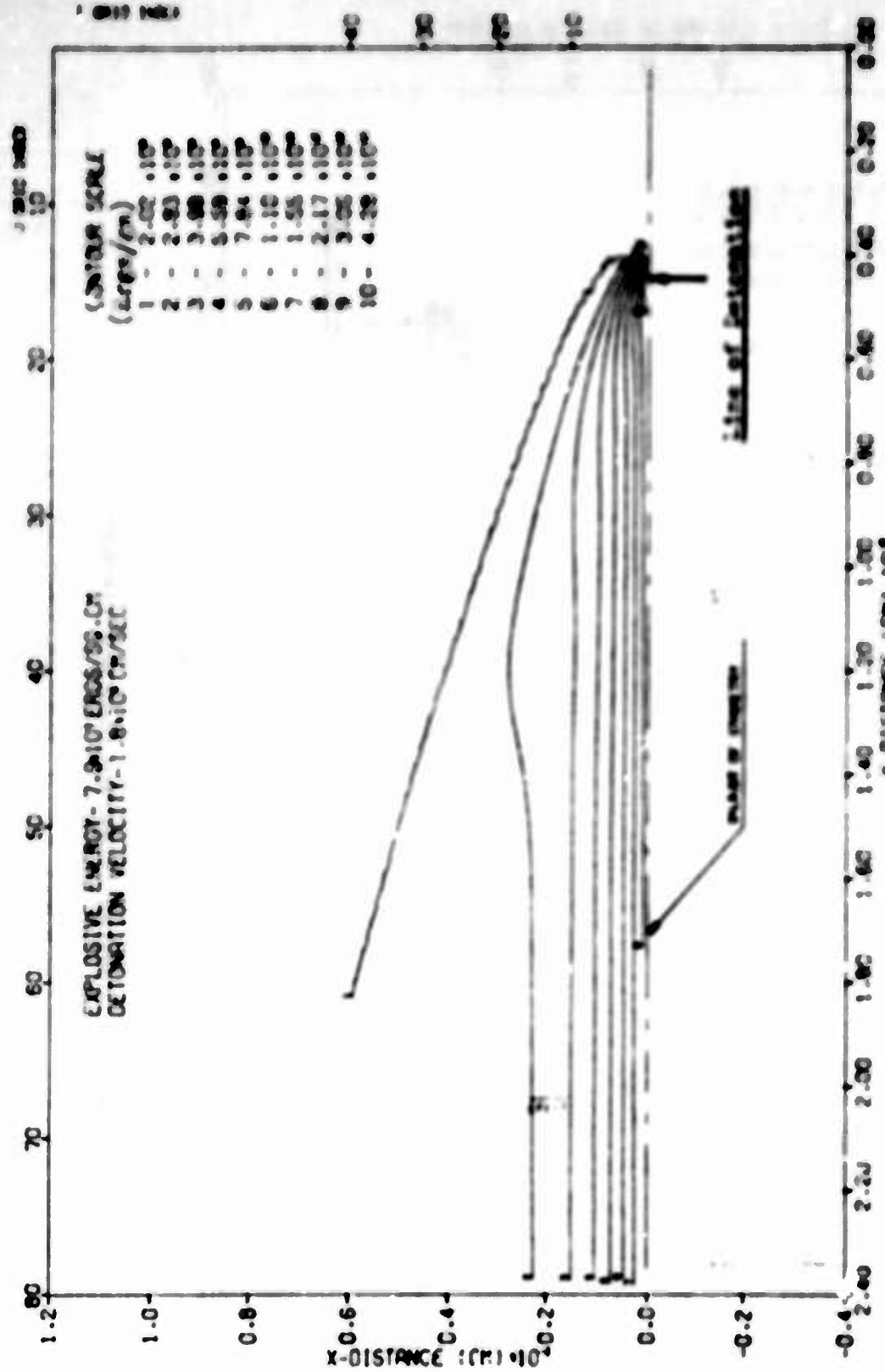
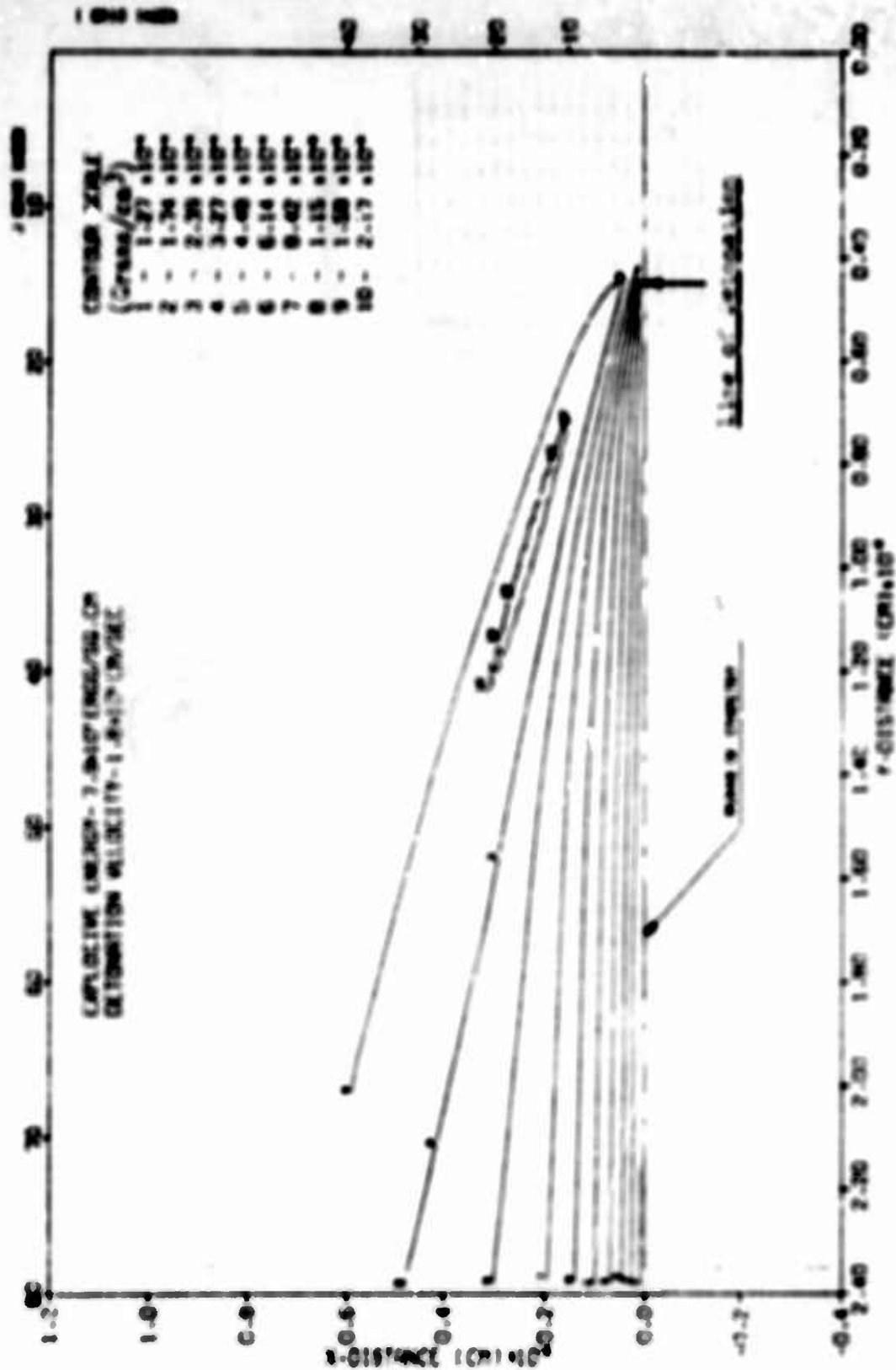
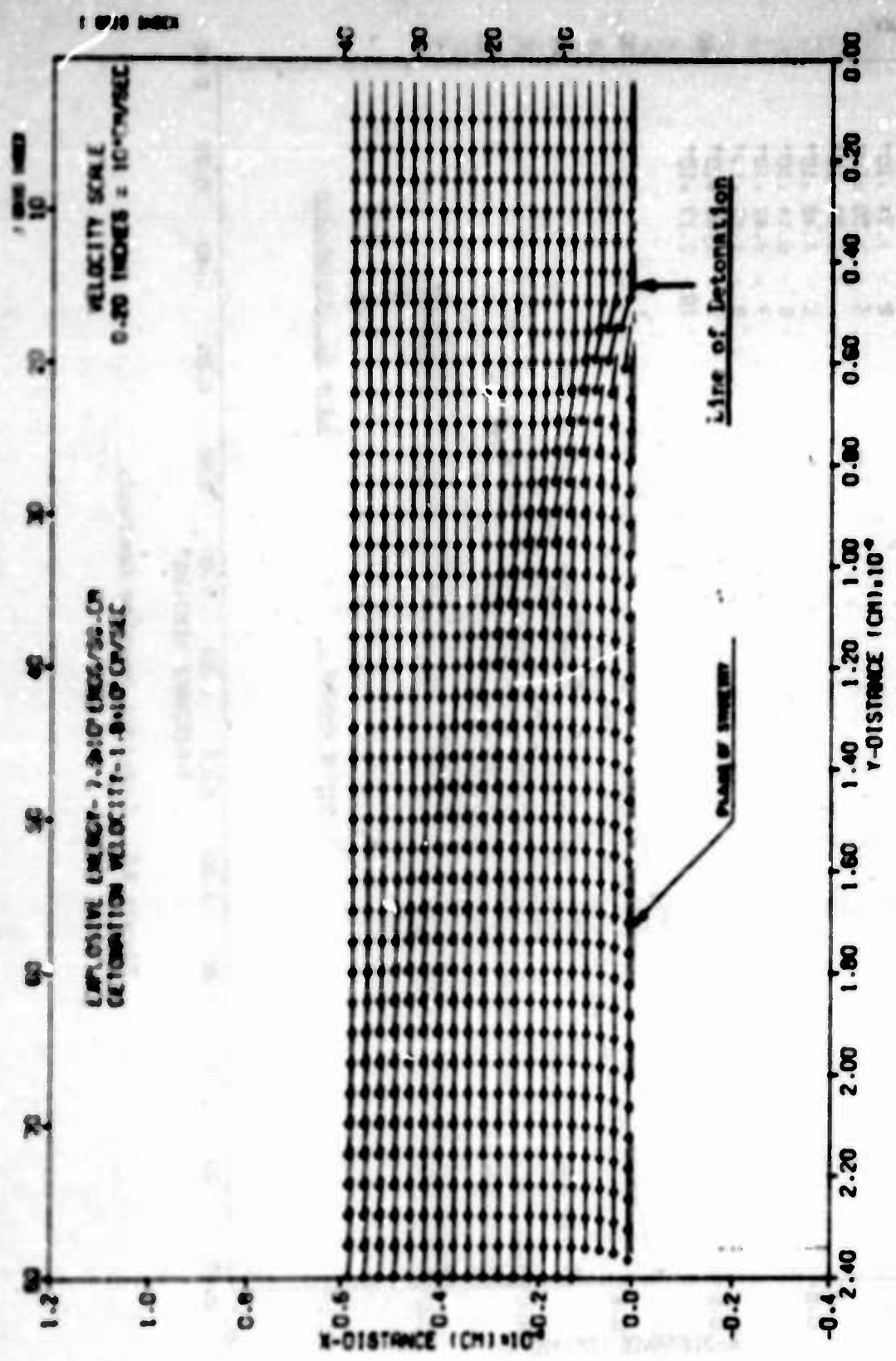


Figure 33. Constant Energy Contours



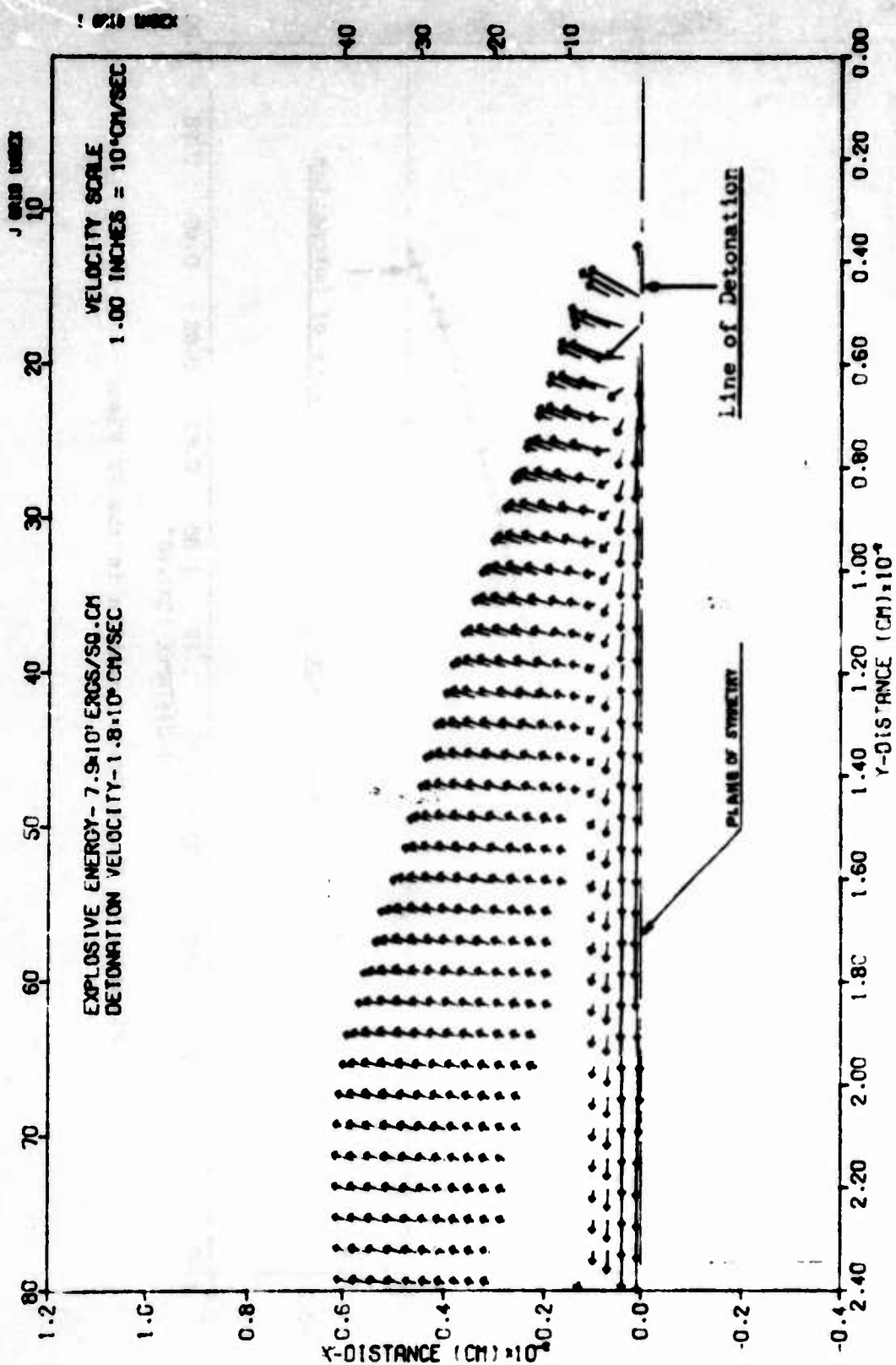
SHELLIG CALCULATION OF POINT SOURCE IN SUPERSONIC FLOW
 TIME 0.001672 SEC CYCLE 310 PESSEL 22.000

Figure 34. Constant Density Contours



SHLLTC CALCULATION OF POINT SOURCE IN HYPERSONIC FLOW
TIME 0.001672 SEC CYCLE 310 PROBLEM 22.000

Figure E5. Velocity Vector Plot



SMELLTC CALCULATION OF POINT SOURCE IN HYPERSONIC FLOW
TIME 0.001672 SEC CYCLE 310 PROBLEM 22.000

Figure B6. Plot of Velocity Vector with Background Velocity Subtracted

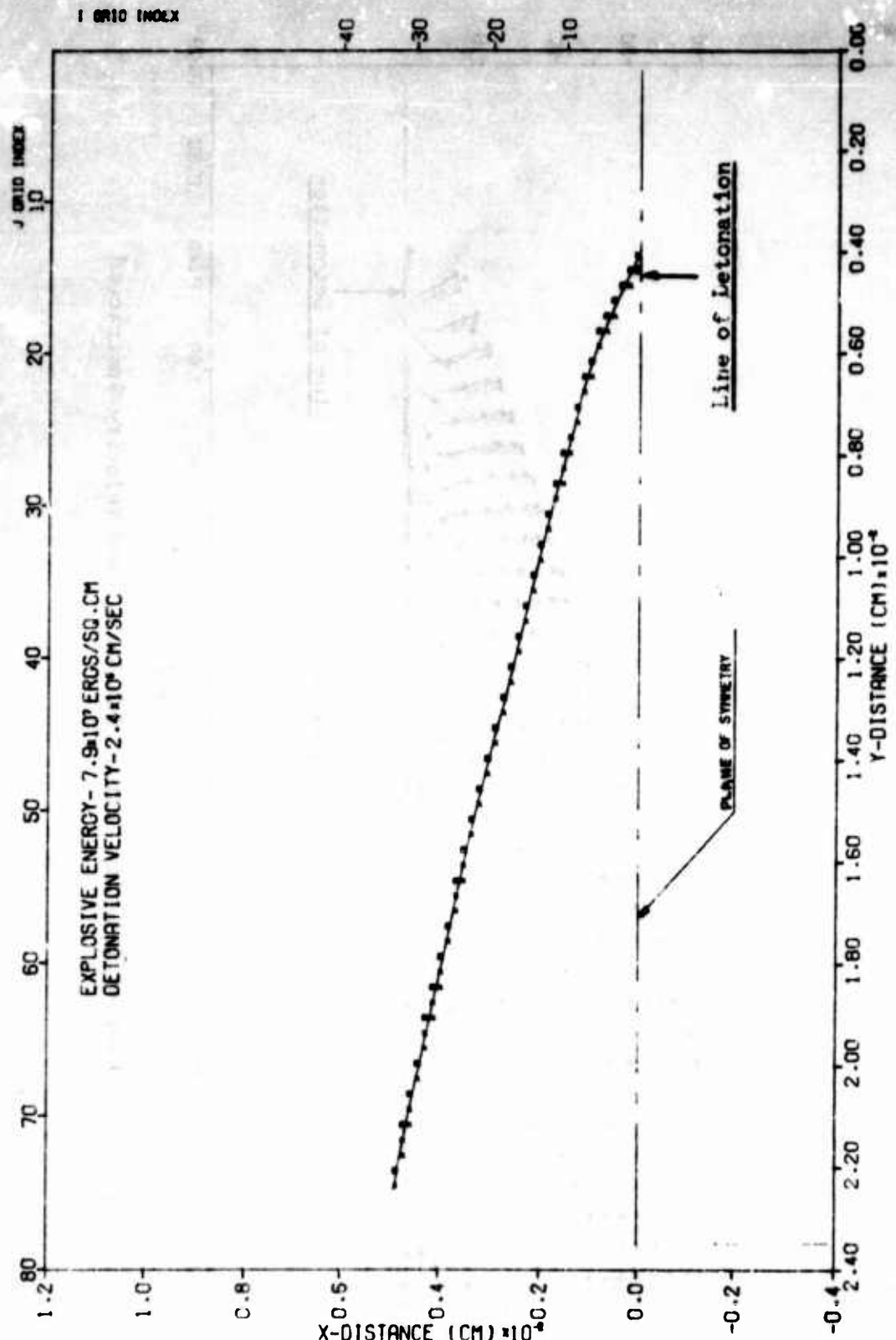
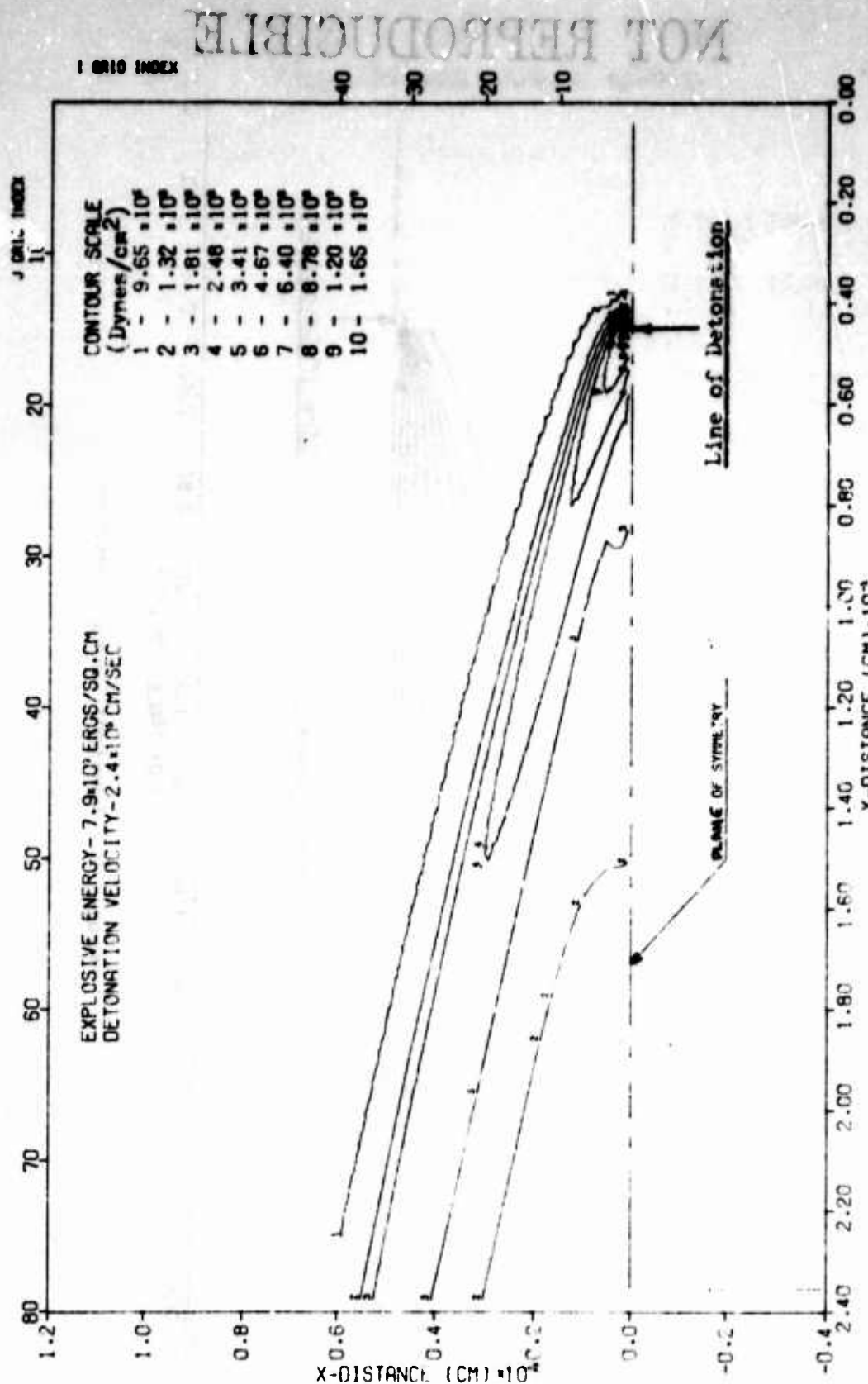


Figure B7. Shock Front Location in the XY Plane



SHELL TC CALCULATION OF POINT SOURCE IN HYPERSONIC FLOW
TIME 0.001199 SEC CYCLE 430 PROBLEM 22.000

Figure B8. Constant Pressure Contours (Isobars)

NOT REPRODUCIBLE

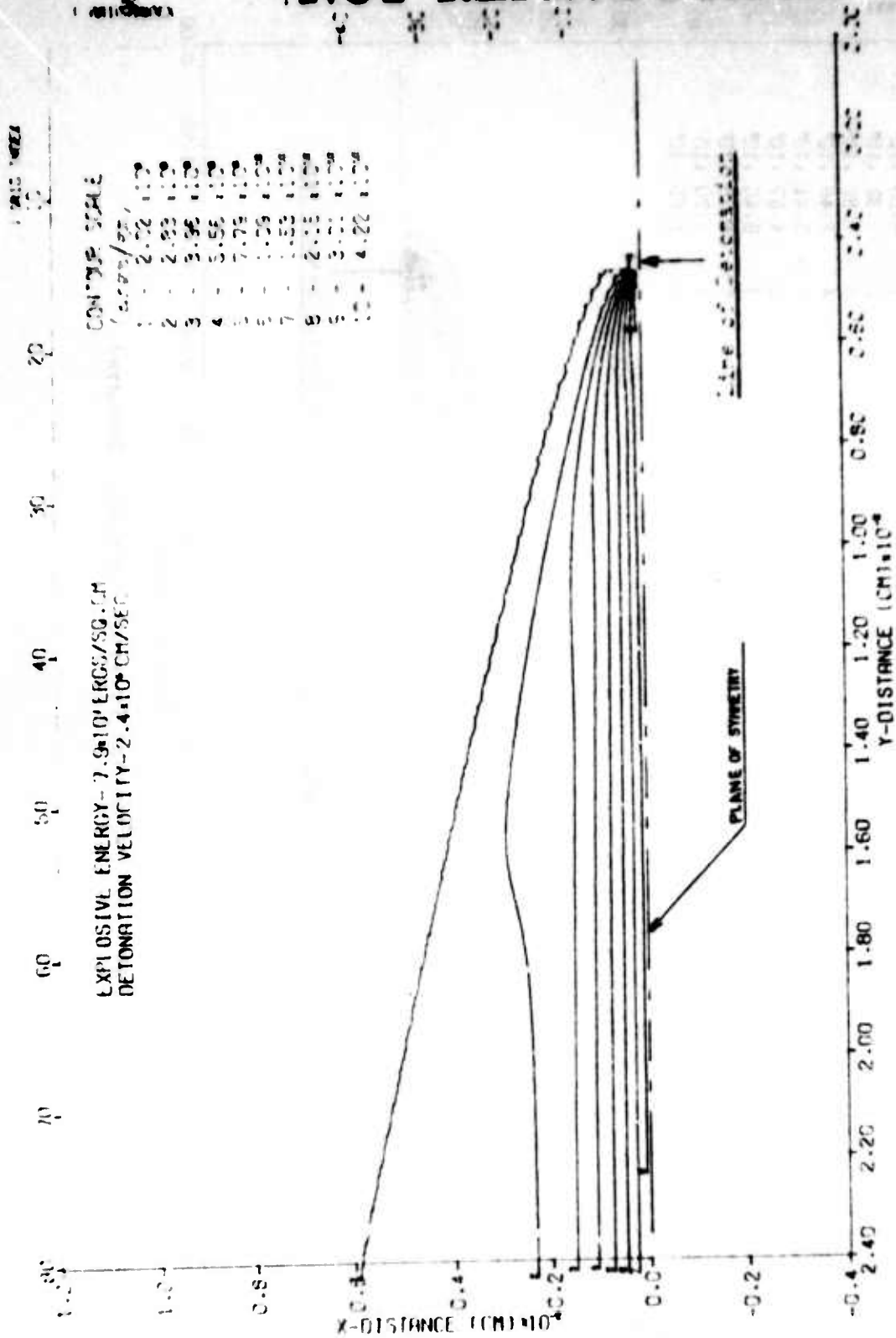


Figure 10. Constant energy contours

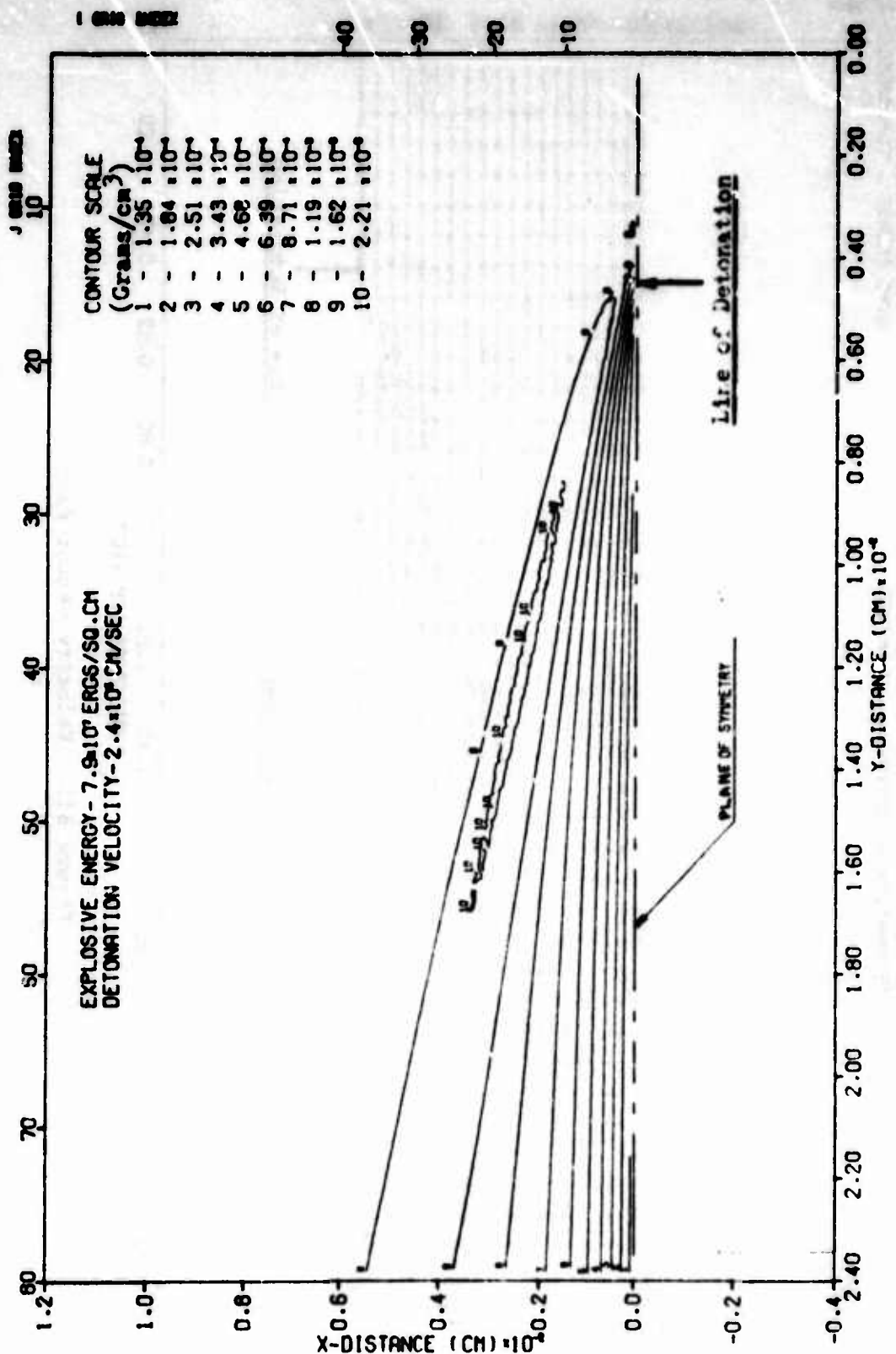


Figure B10. Constant Density Contours

SHELL TC CALCULATION OF POINT SOURCE IN HYPERSONIC FLOW
TIME 0.001199 SEC CYCLE 430 PROBLEM 22.000

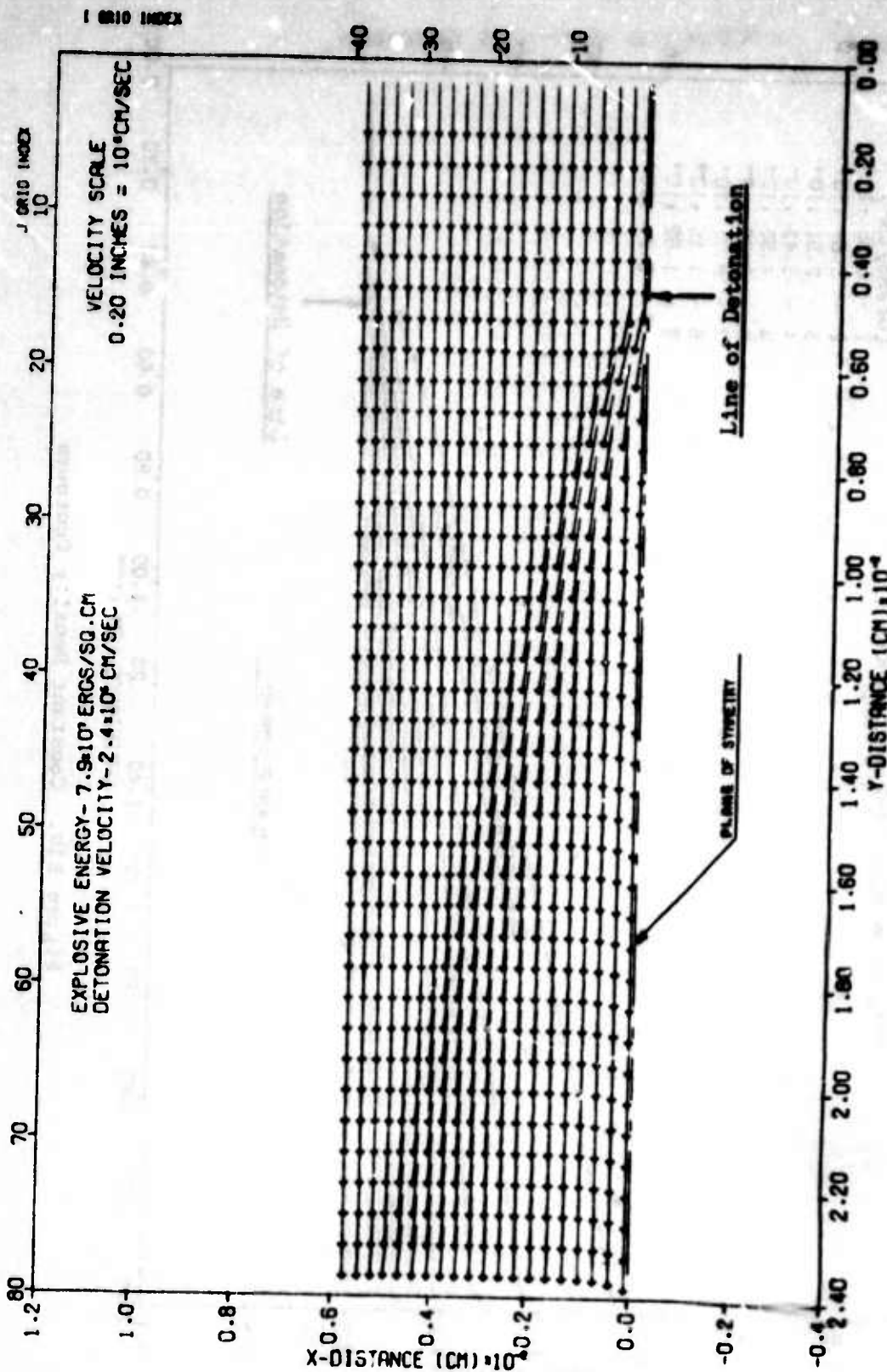
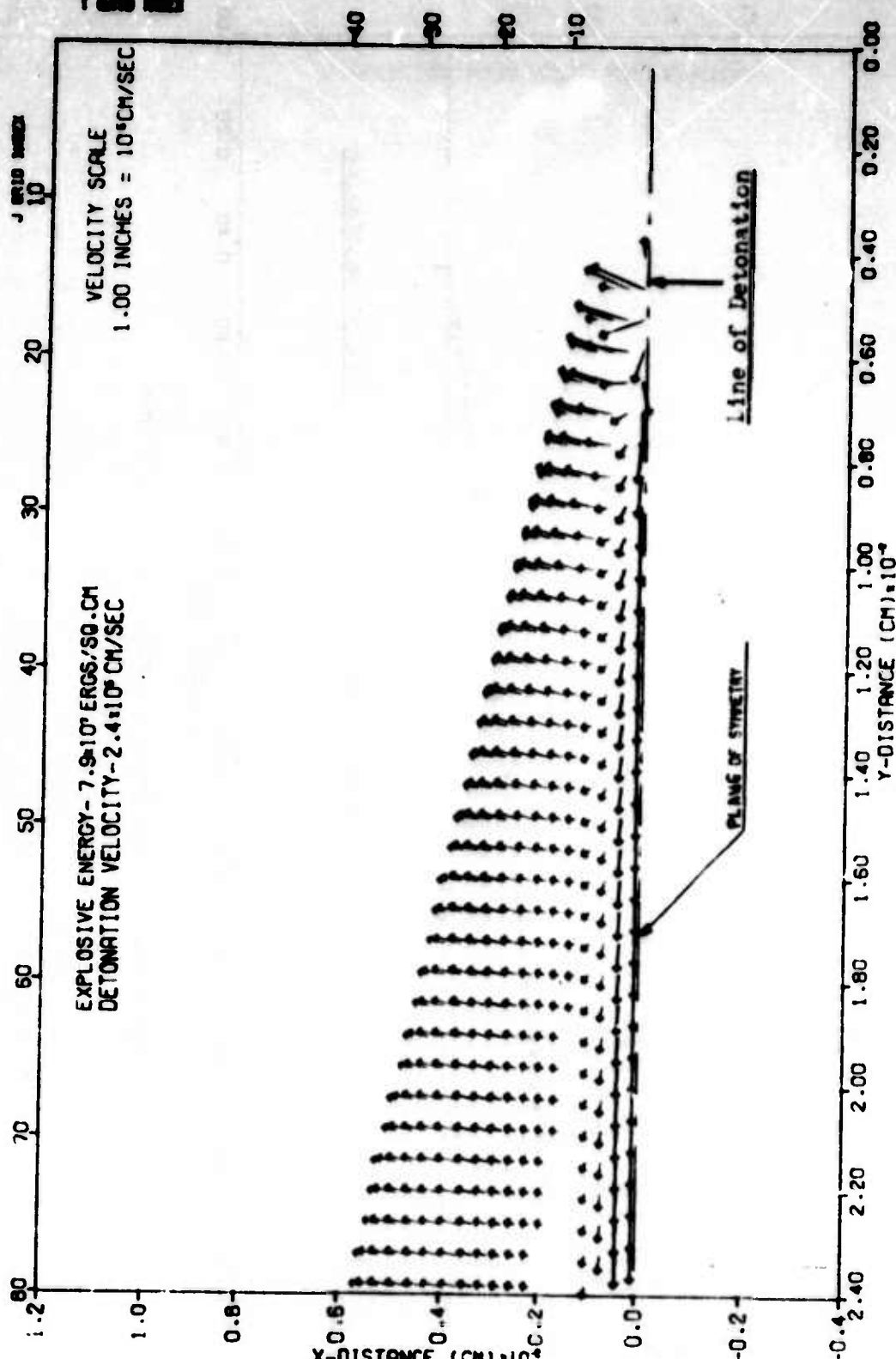


Figure BII. Velocity Vector Plot



SHELLTC CALCULATION OF POINT SOURCE IN HYPERSONIC FLOW
TIME 0.001198 SEC CYCLE 430 PROBLEM 22.000

Figure 312. Plot of Velocity Vector with Background Velocity Subtracted

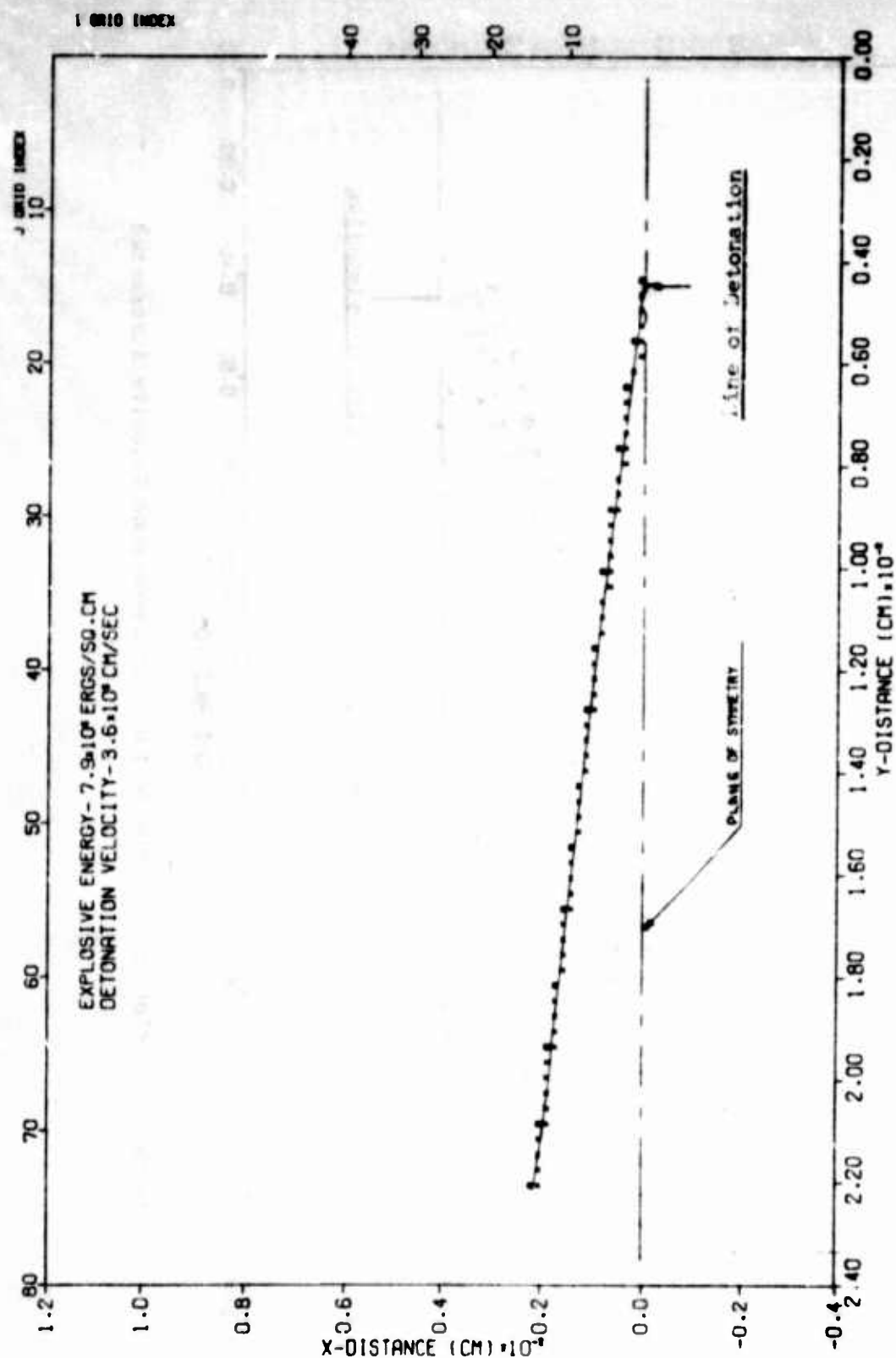
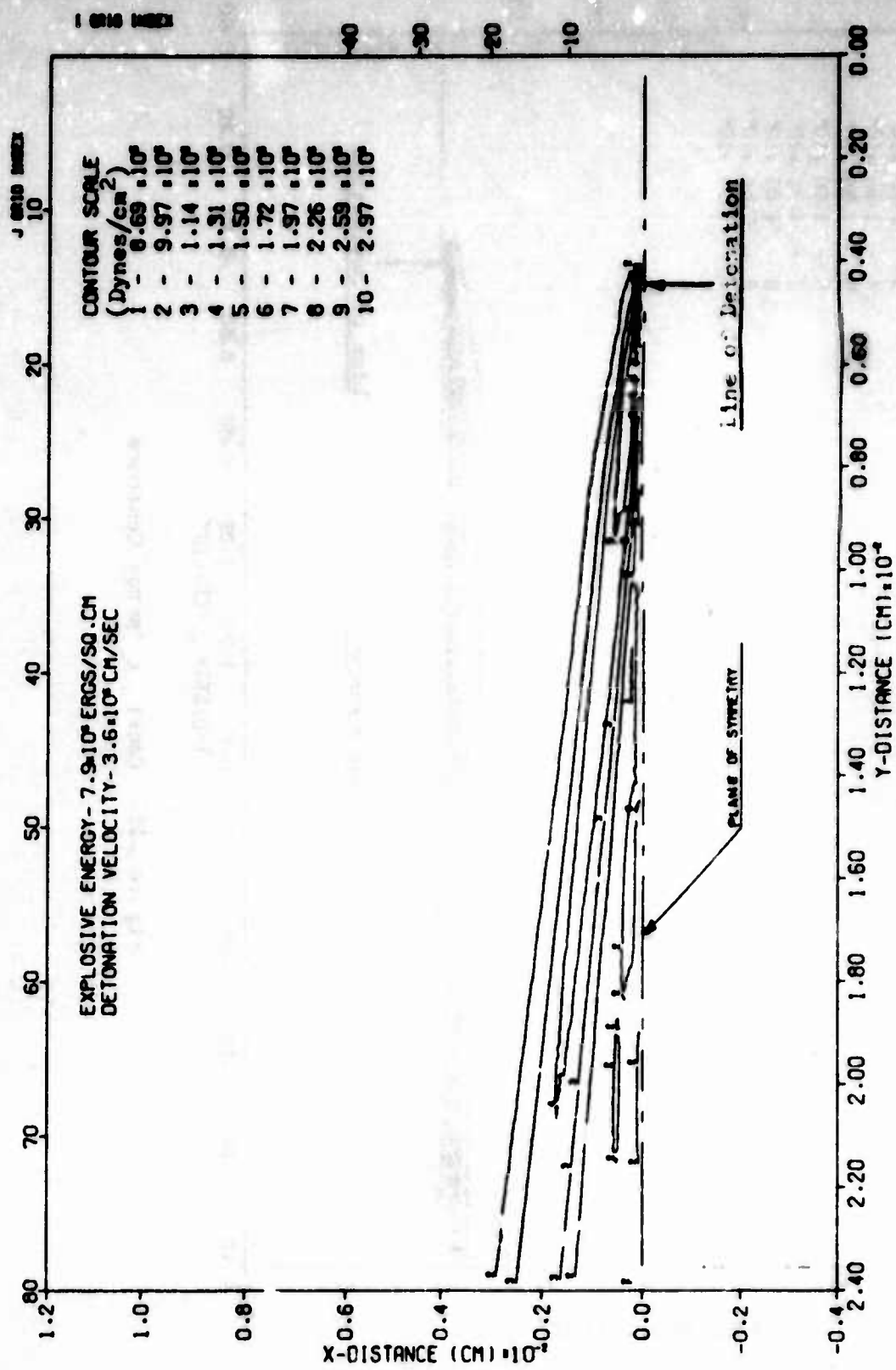
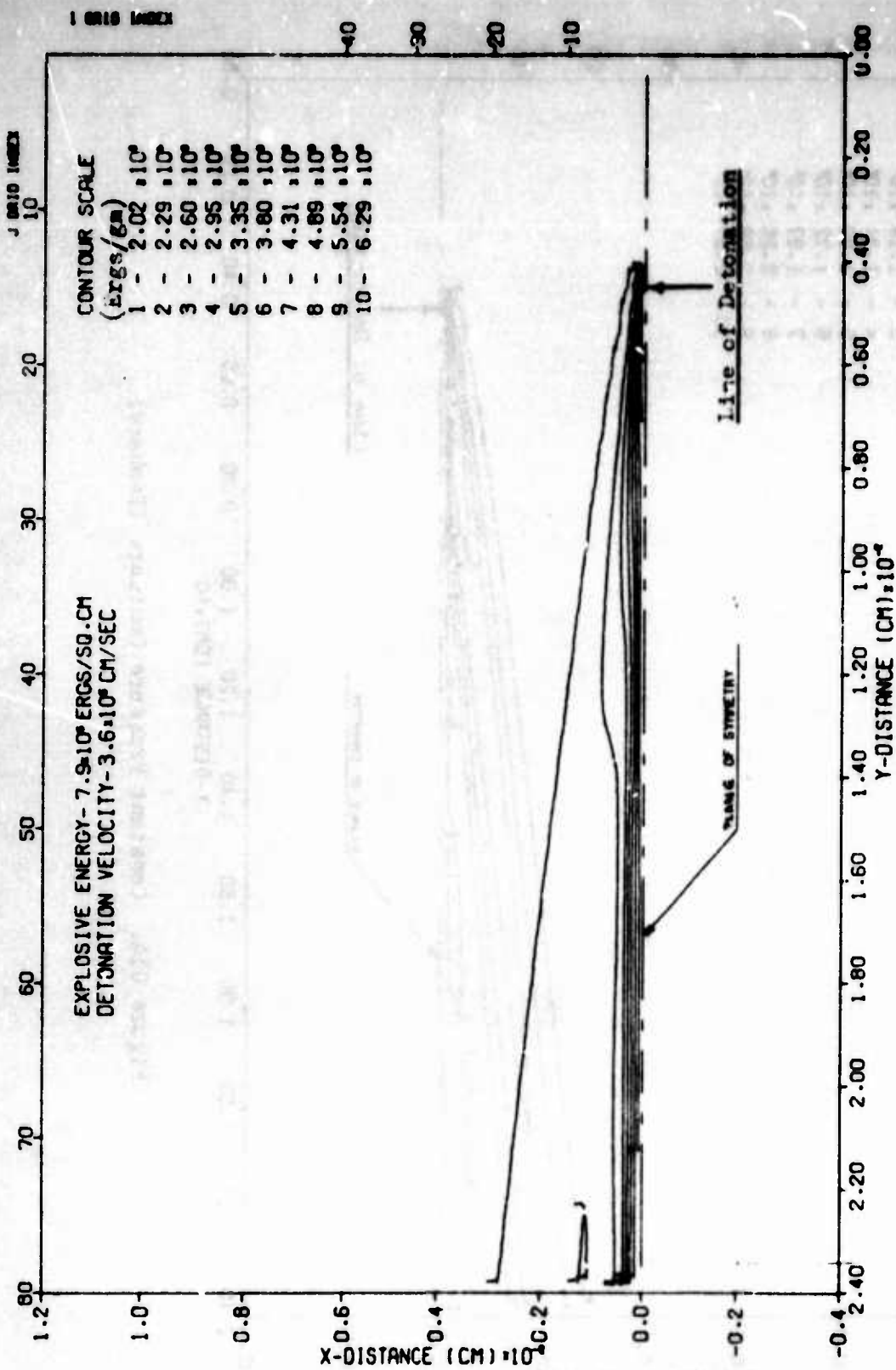


Figure 313. Shock Front Location in the XY Plane



SHELL TC CALCULATION OF POINT SOURCE IN HYPERSONIC FLOW
TIME 0.000913 SEC CYCLE 380 PROBLEM 21.000

Figure 314. Constant Pressure Contours (Isobars)



SMELLTC CALCULATION OF POINT SOURCE IN HYPERSONIC FLOW
TIME 0.000913 SEC CYCLE 380 PROBLEM 21.000

Figure 315. Constant Energy Contours

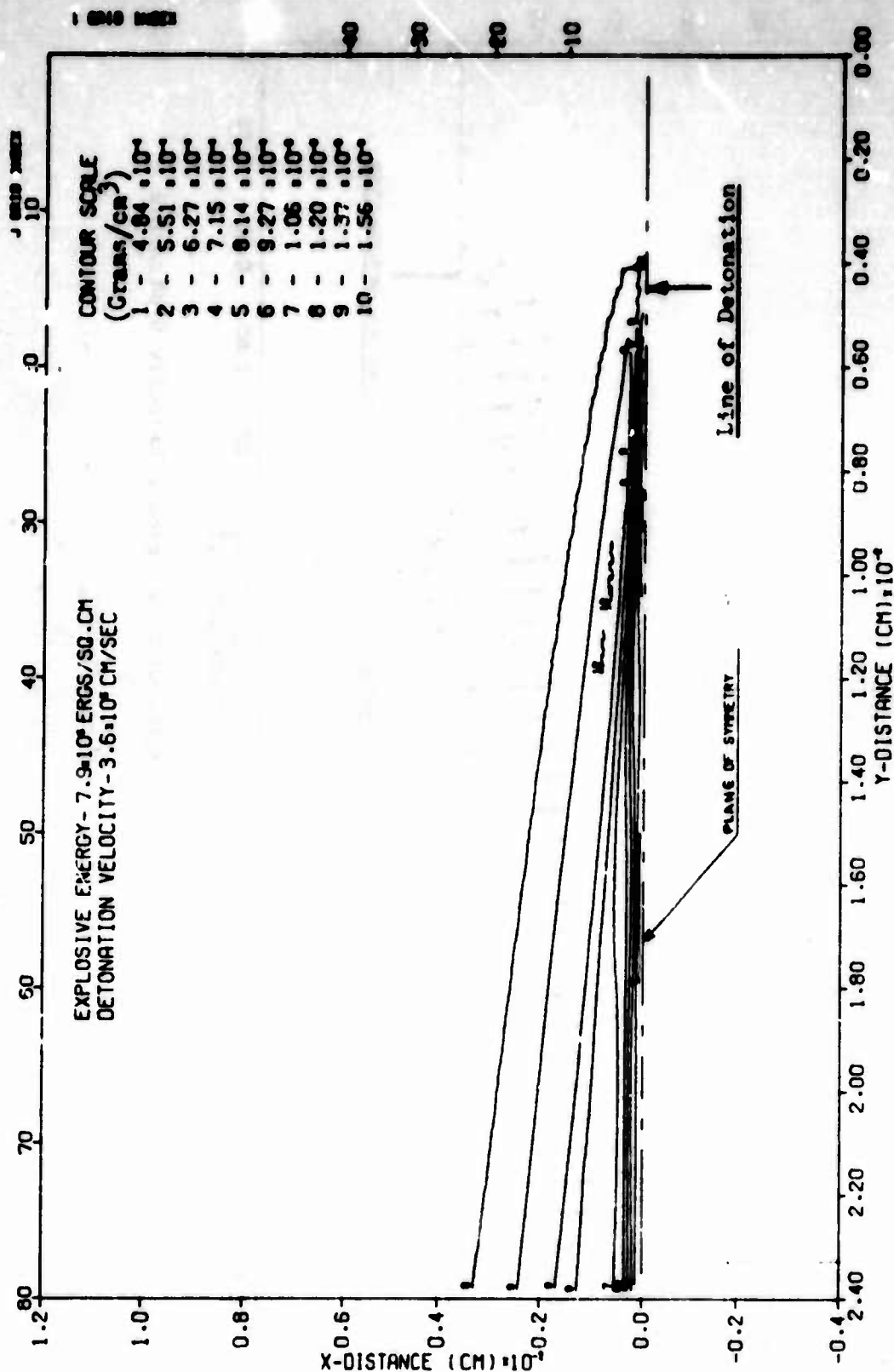


Figure 316. Constant Density Contours

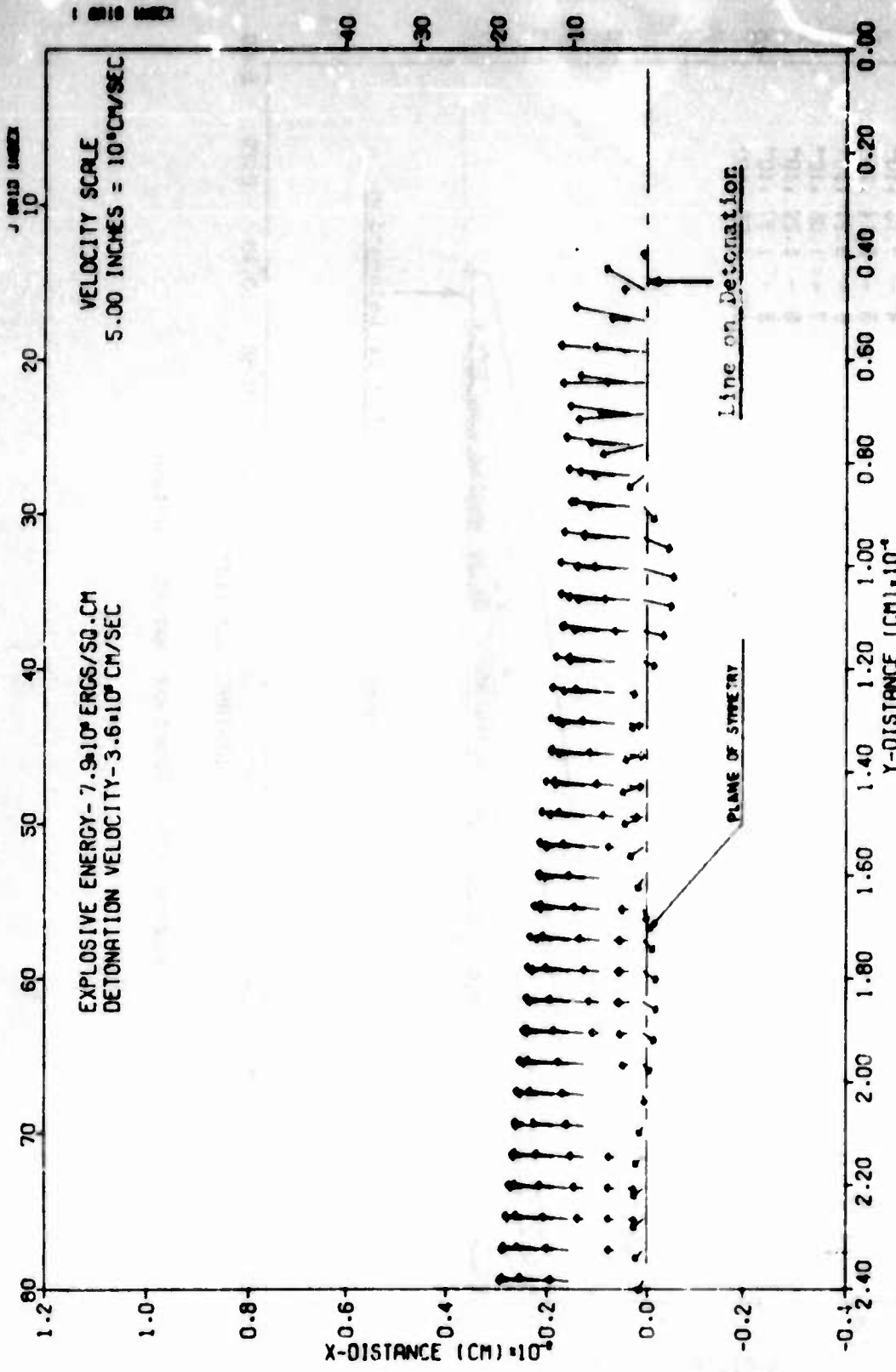


Figure S17. Plot of Velocity Vector with Background Velocity Subtracted

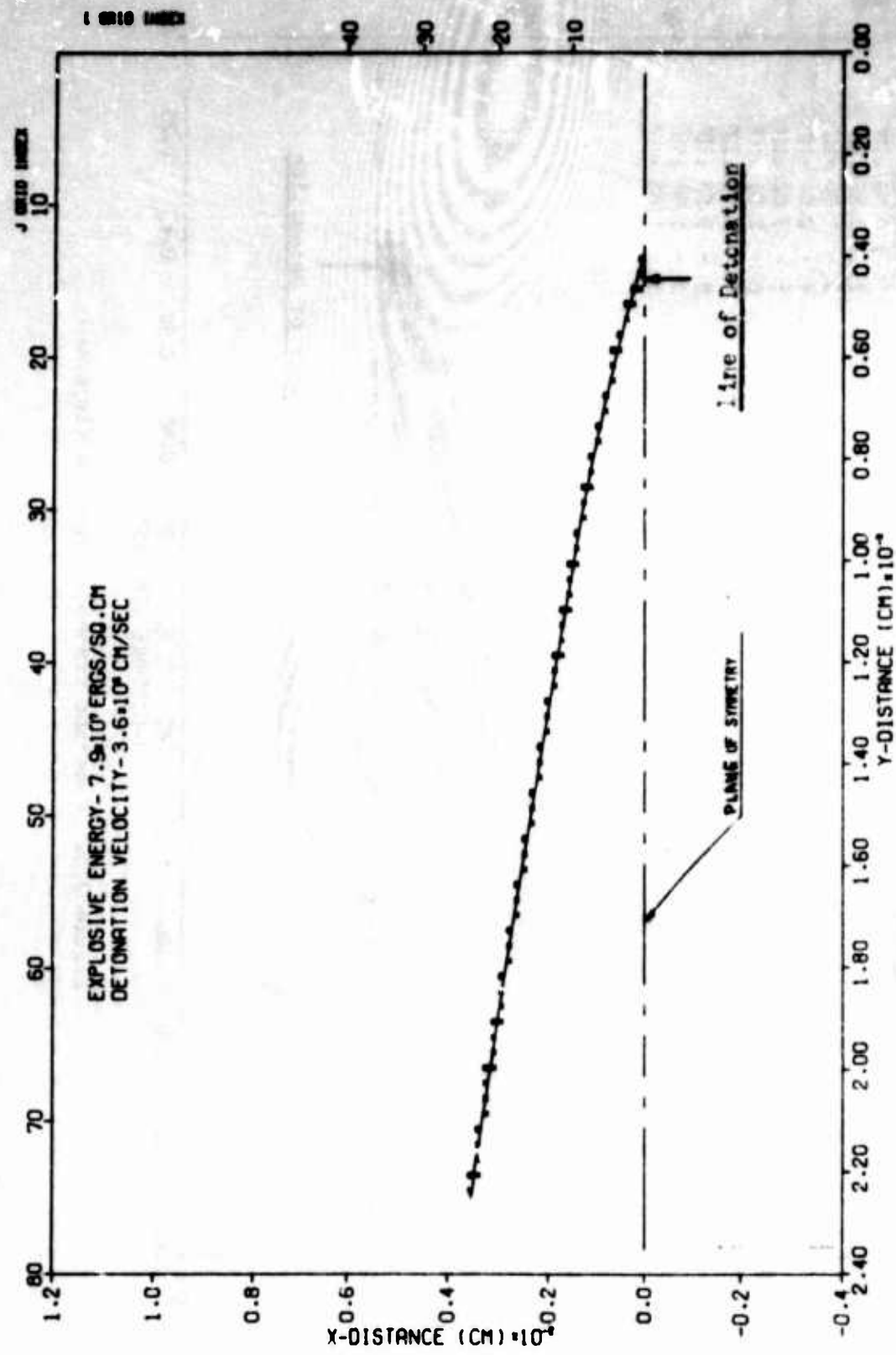
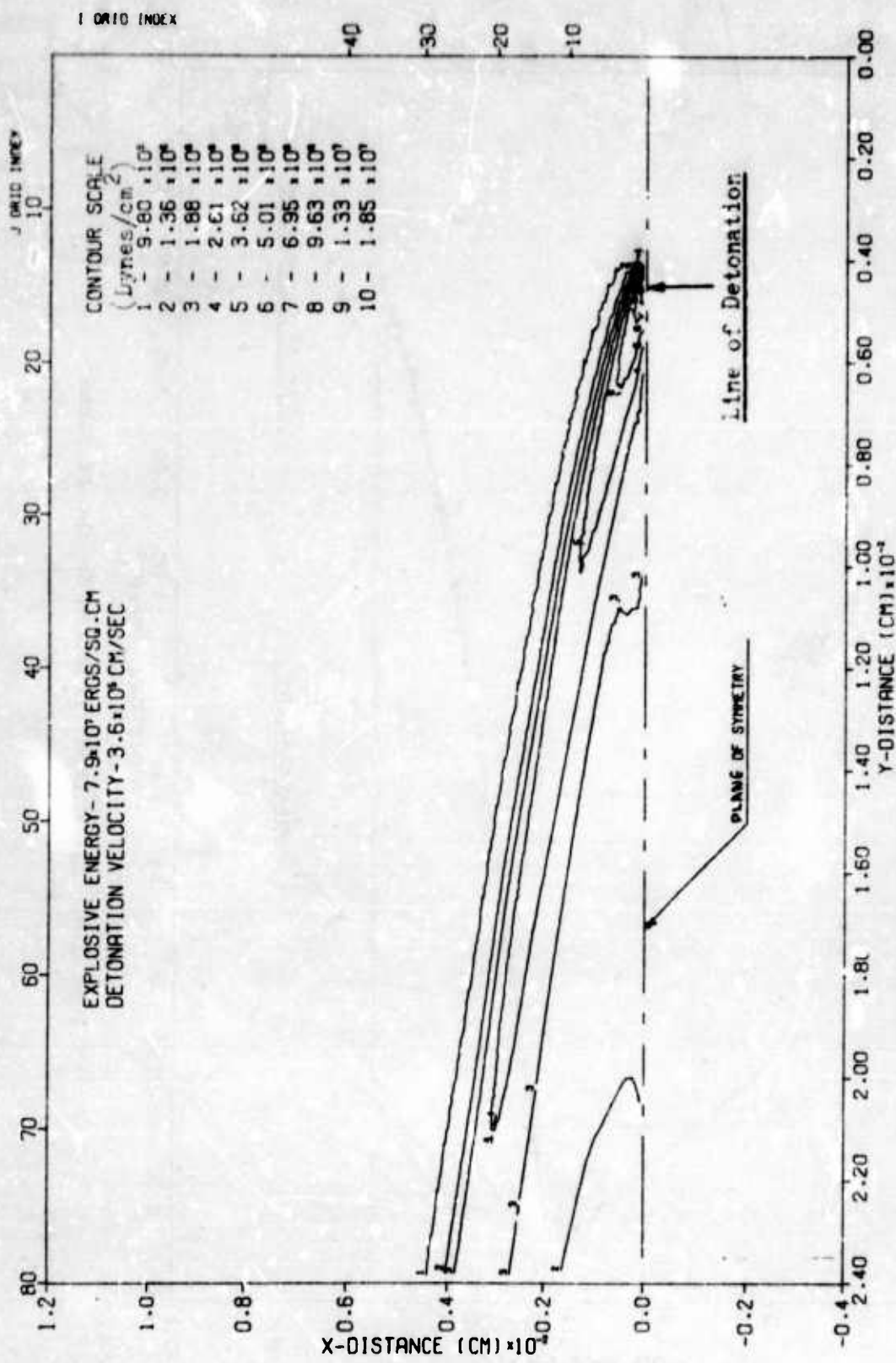


Figure B18. Shock Front Location in the XY Plane



SHELLTC CALCULATION OF POINT SOURCE IN HYPERSONIC FLOW
TIME 0.000864 SEC CYCLE 410 PROBLEM 21.000

Figure B19. Constant Pressure Contours (Isobars)

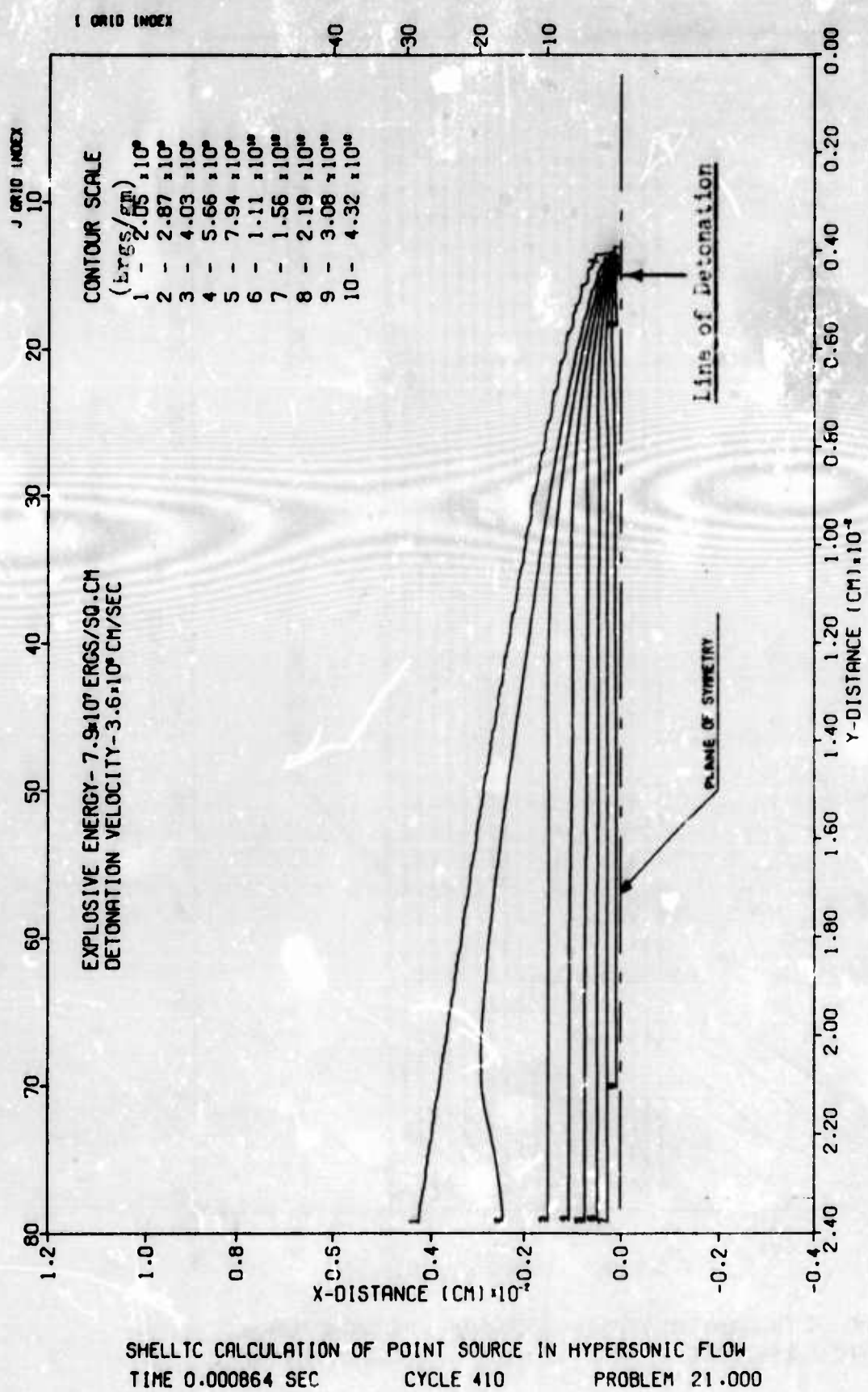


Figure 320. Constant Energy Contours

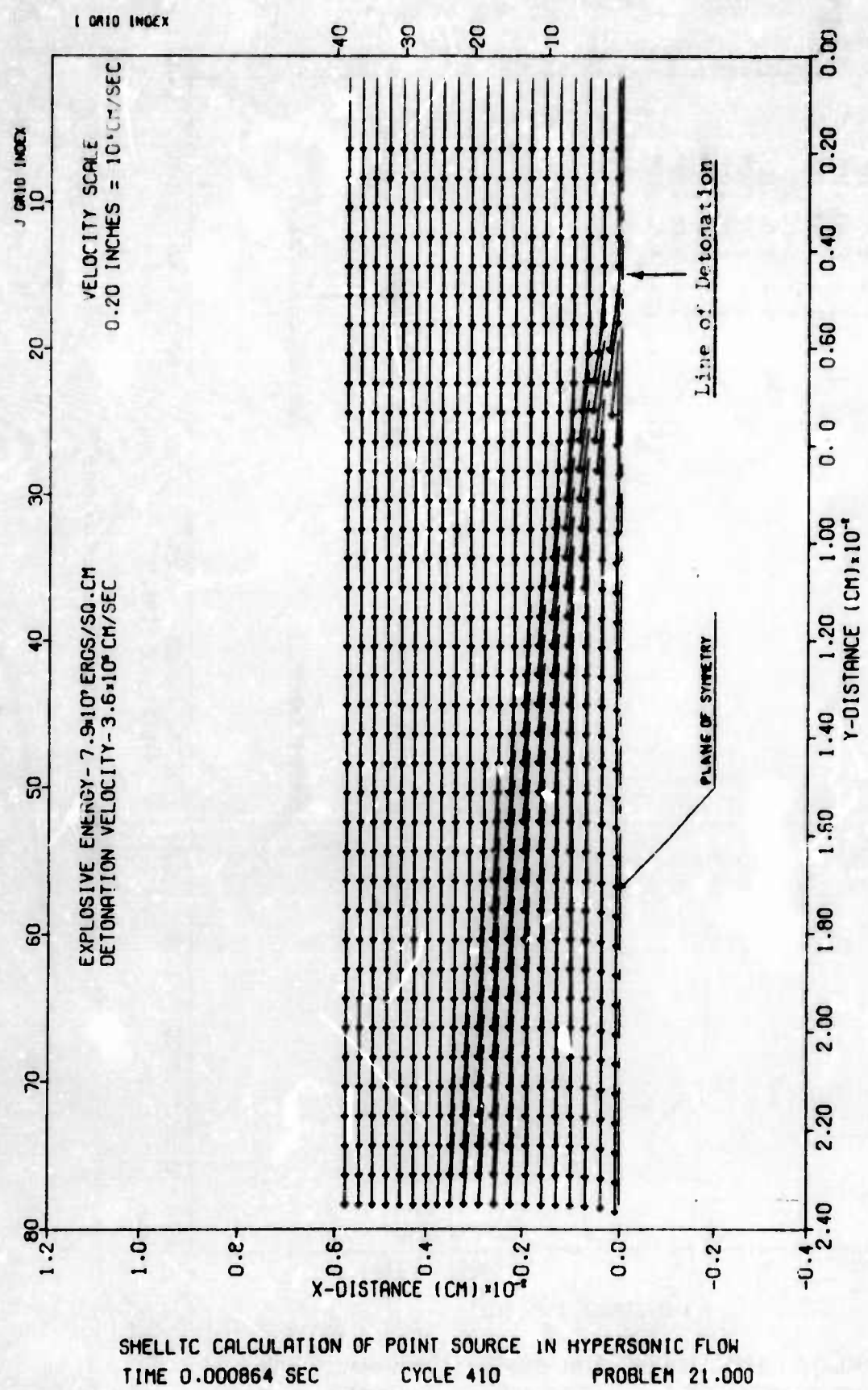


Figure 321. Velocity Vector Plot

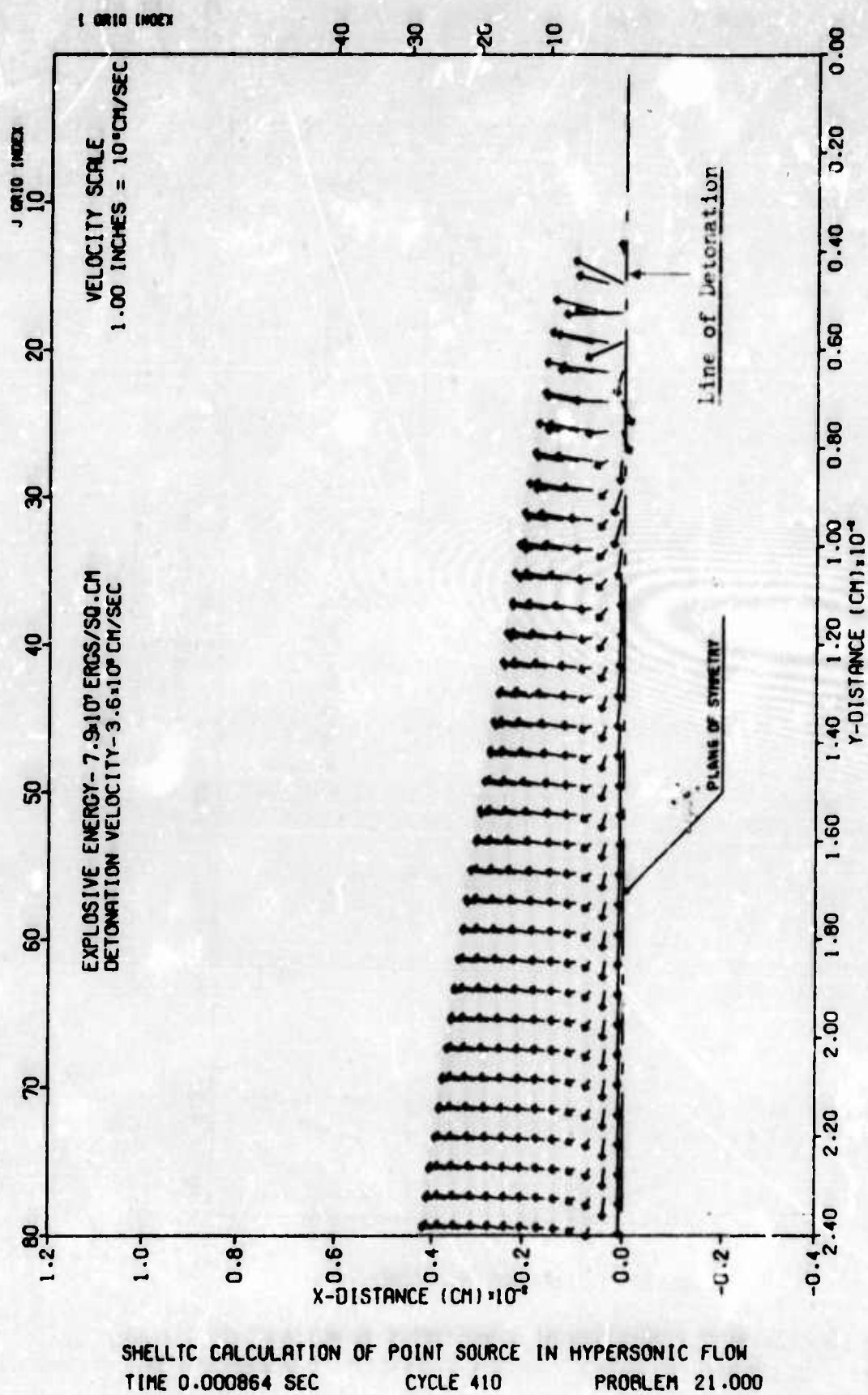


Figure E22. Plot of Velocity Vector with Background Velocity Subtracted

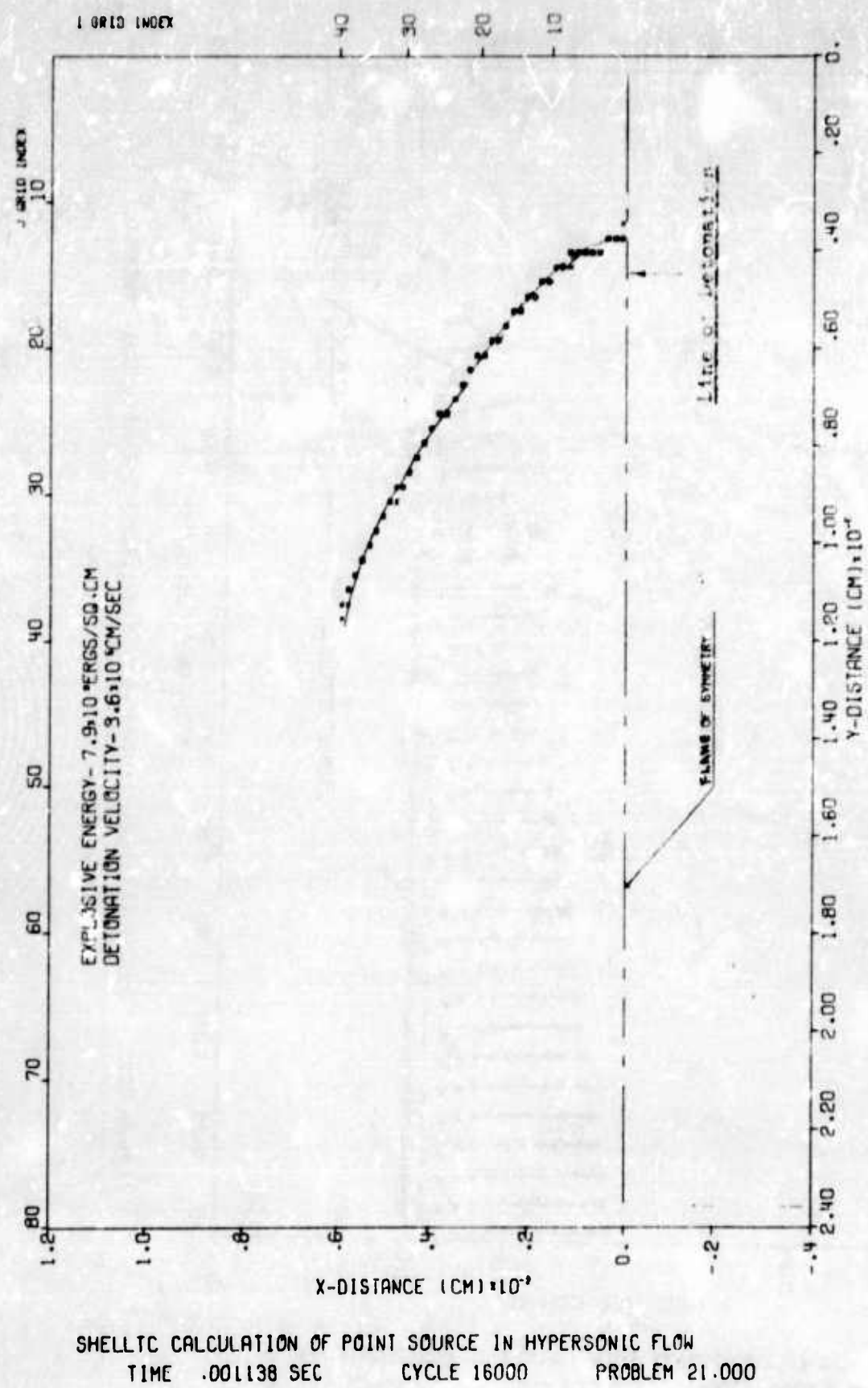


Figure 323. Shock Front Location in the XY Plane

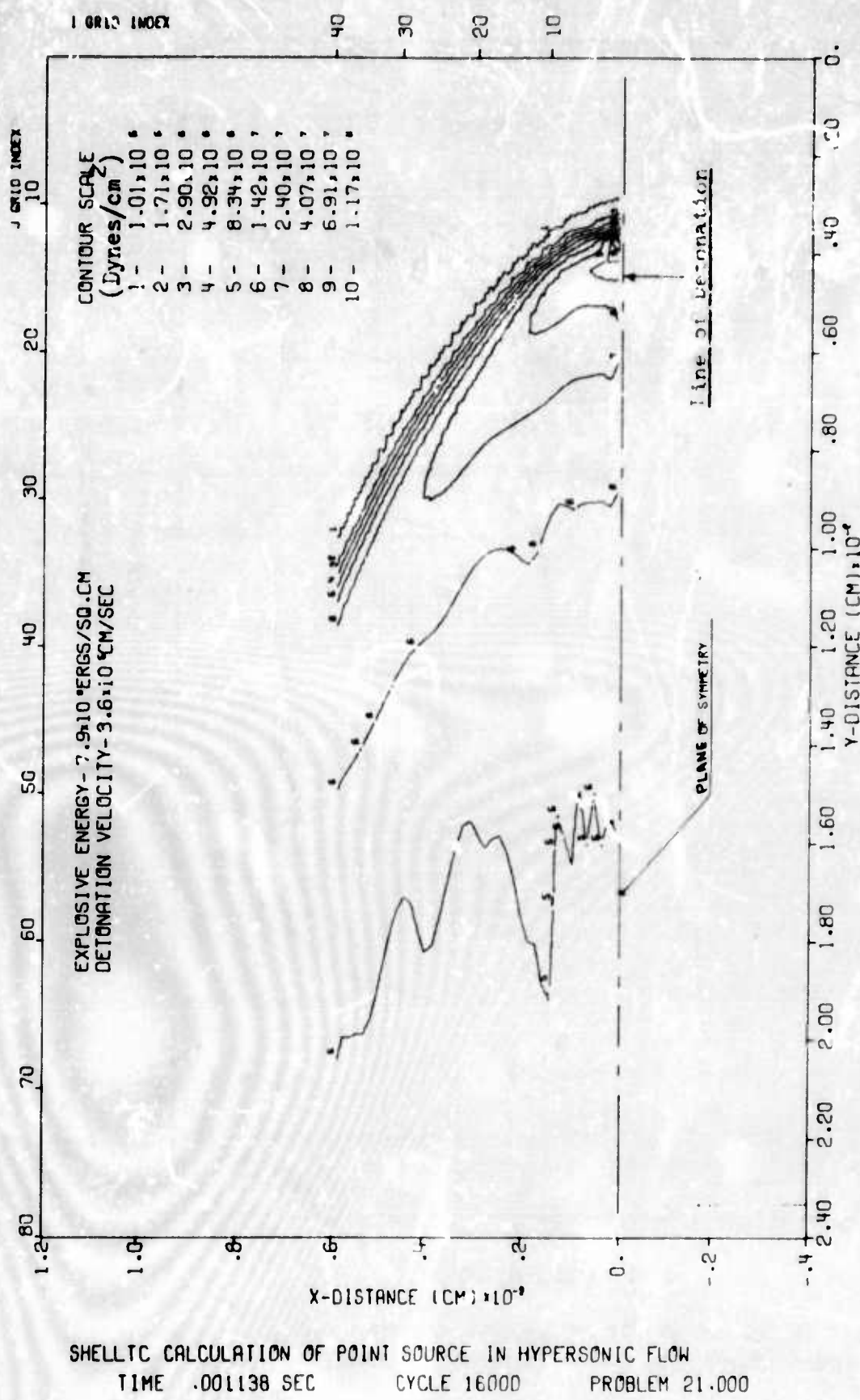
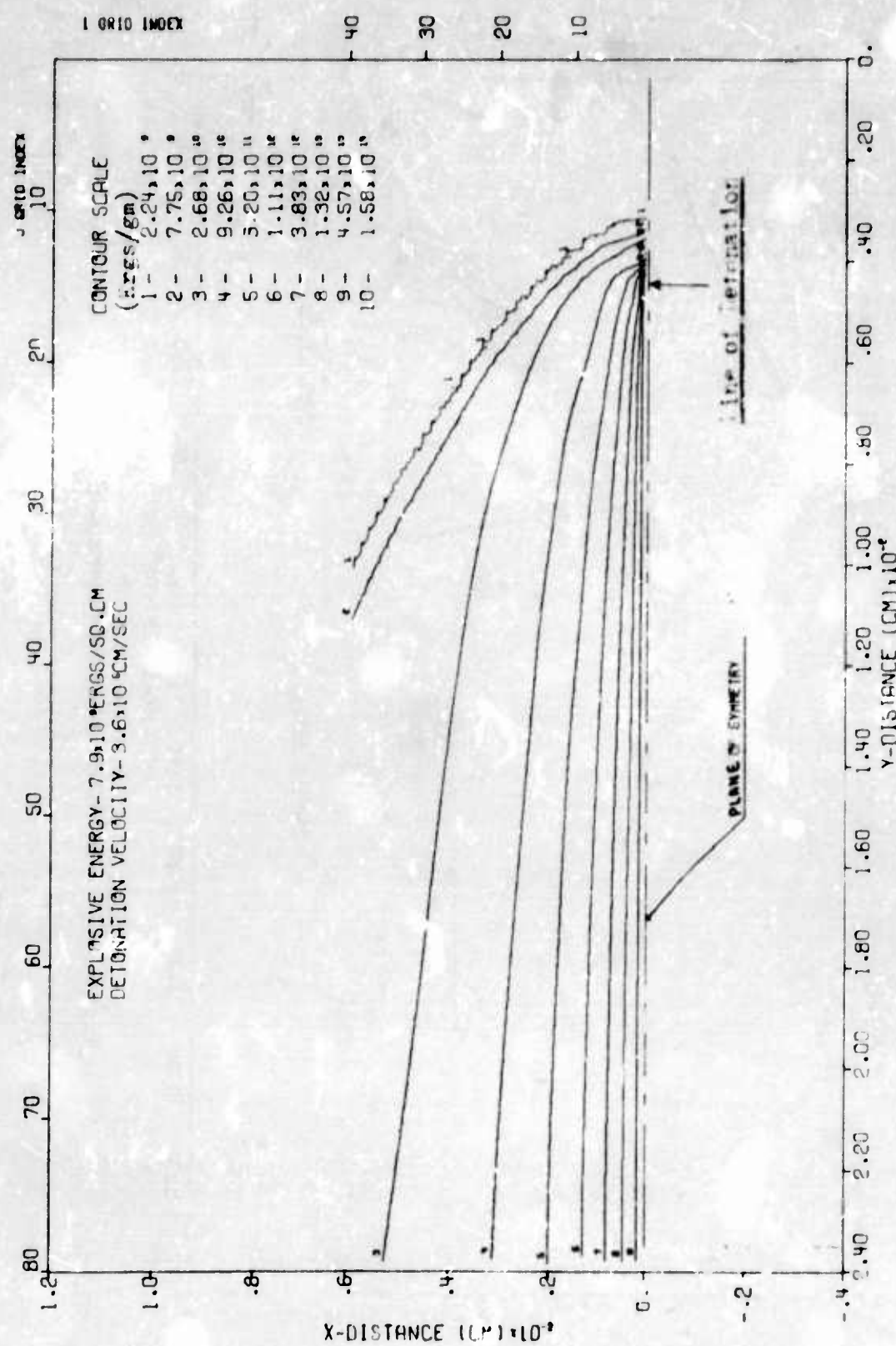
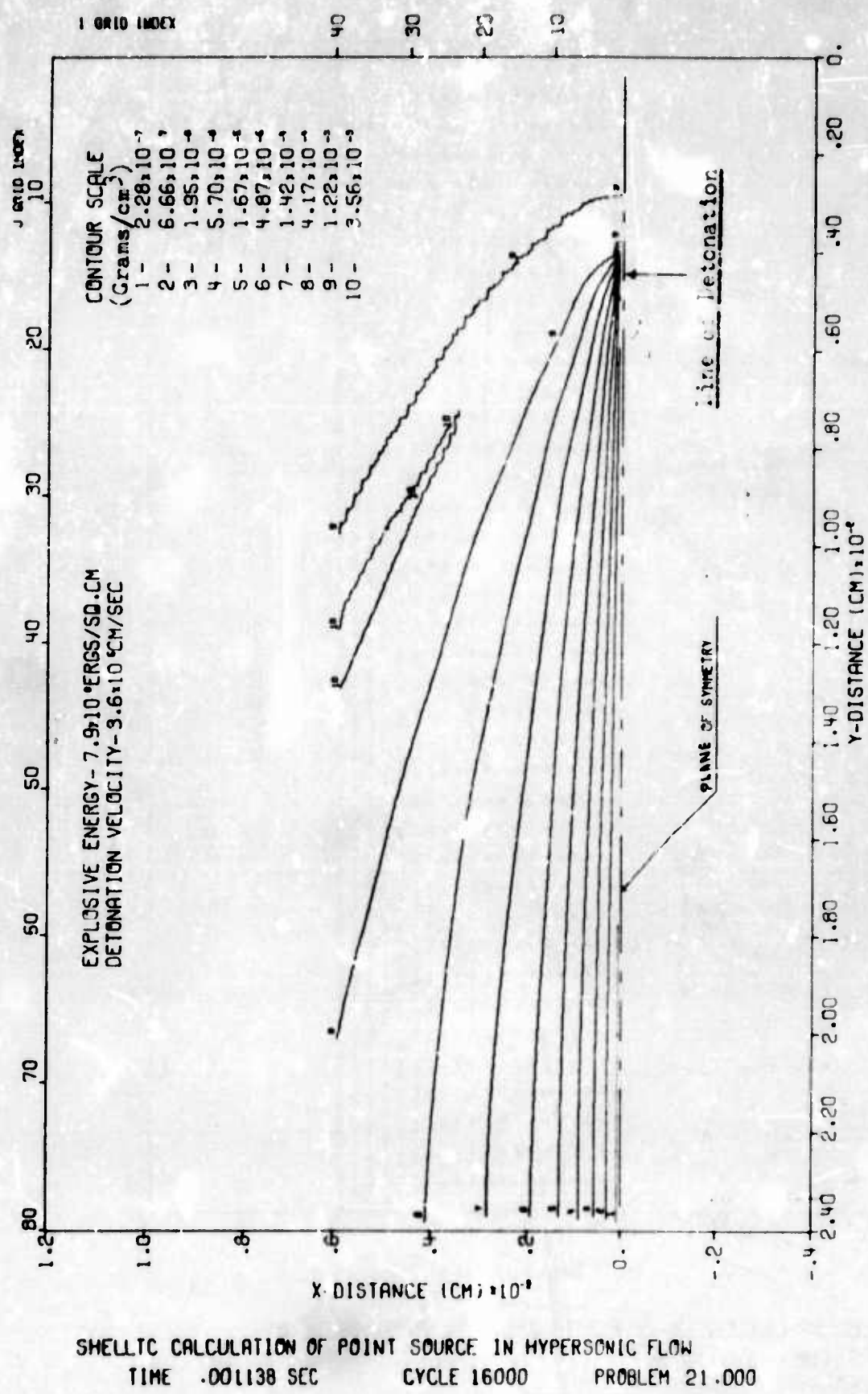


Figure B24. Constant pressure Contours (Isobars)



SHELLTC CALCULATION OF POINT SOURCE IN HYPERSONIC FLOW
TIME .000138 SEC CYCLE :6000 PROBLEM 21.000

Figure 325. Constant Energy Contours



SHELLTC CALCULATION OF POINT SOURCE IN HYPERSONIC FLOW
TIME .001138 SEC CYCLE 16000 PROBLEM 21.000

Figure 326. Constant Density Contours

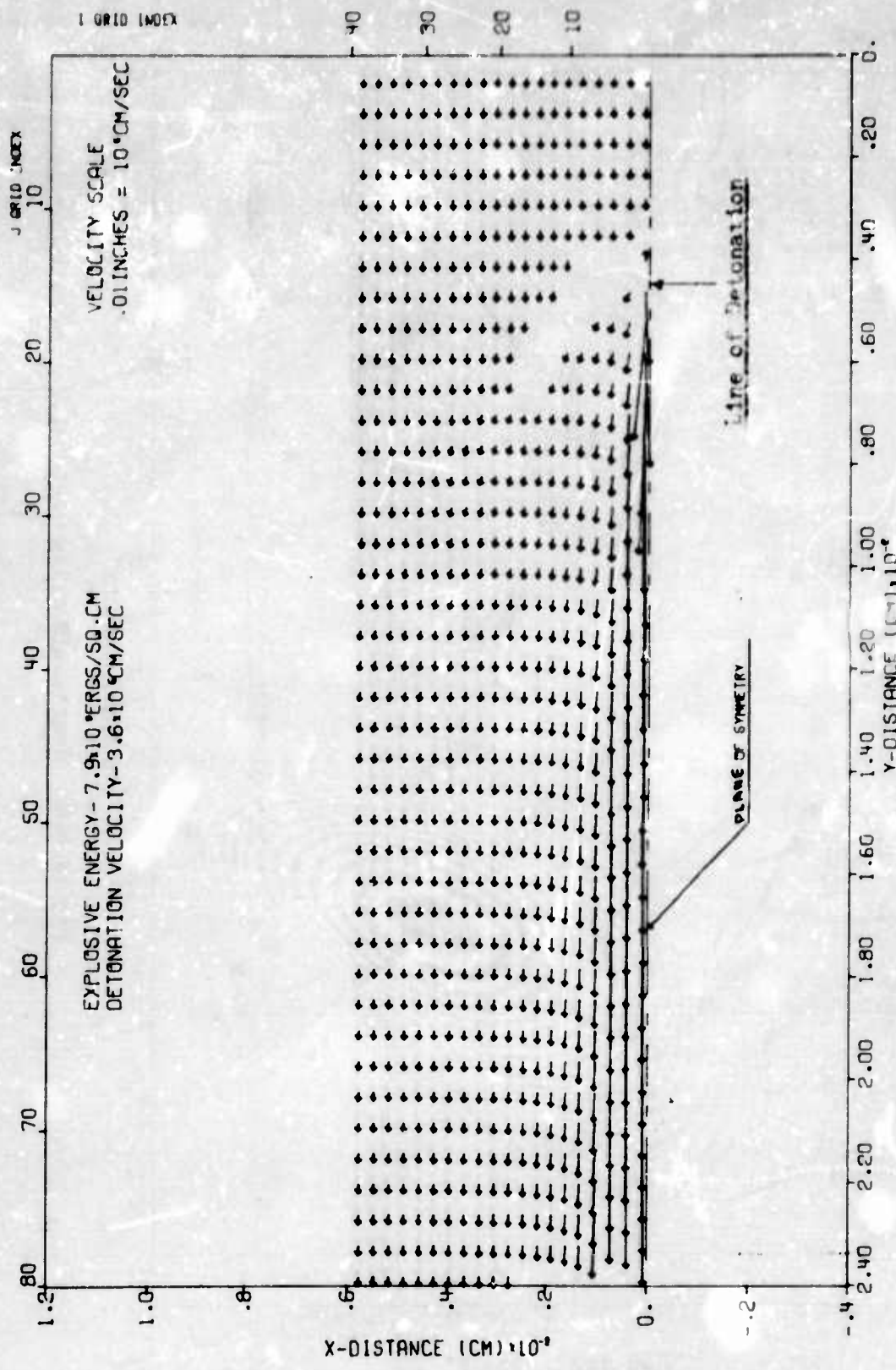


Figure B27. Velocity Vector Plot

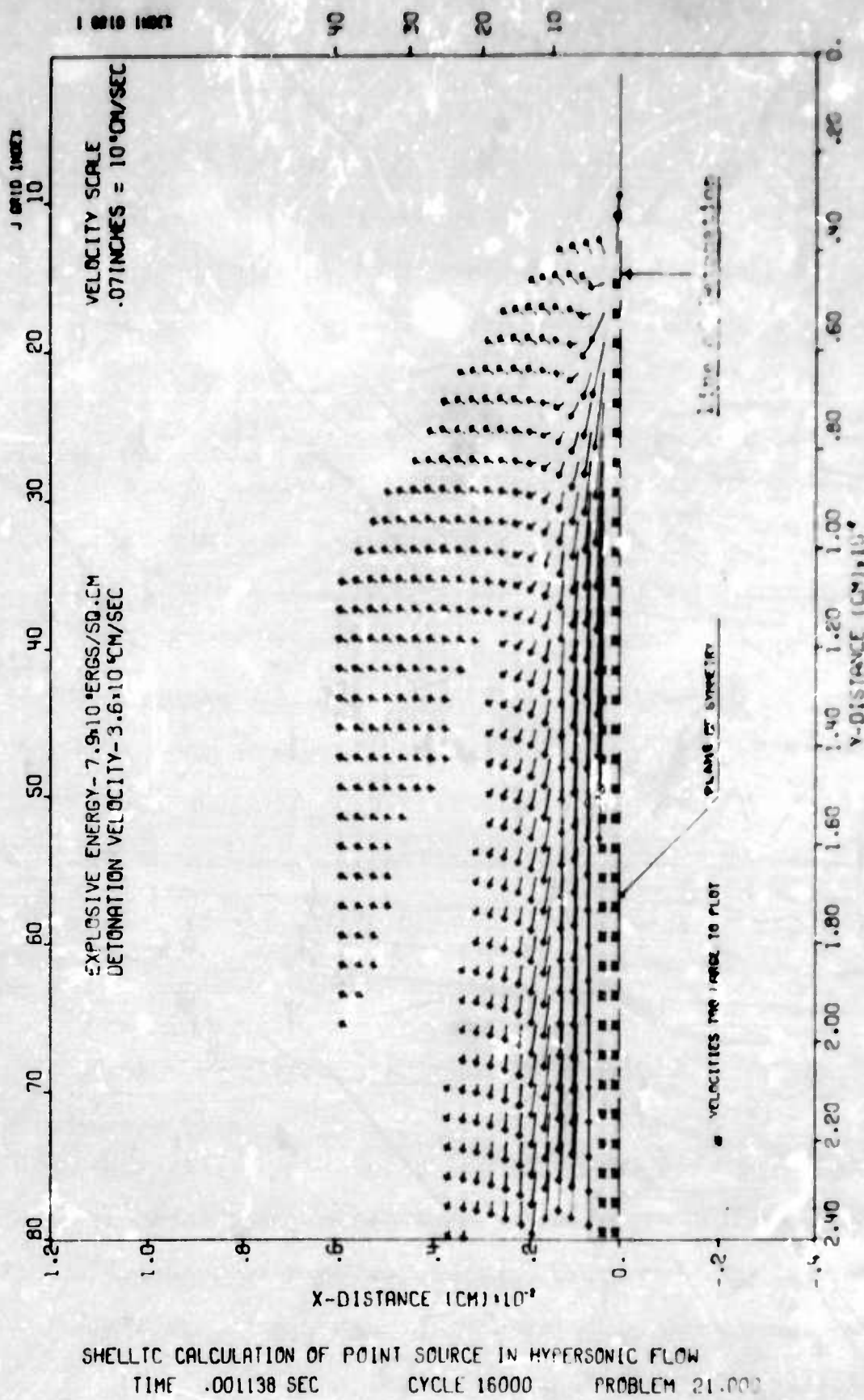


Figure 23. Plot of velocity versus time based on model calculations.

SHELLTC CALCULATION OF POINT SOURCE IN HYPERSONIC FLOW
TIME .001138 SEC CYCLE 16000 PROBLEM 21.00

APPENDIX C
THE SHELTC7 CODE

The SHELTC7 code is a seven-material member of the SHELL family of hydrodynamic codes. It was developed for use in determining the flow of seven distinct mass species through an Eulerian grid and can be used with either cylindrical or cartesian coordinates.

SHELTC7 was developed from the RADISH5 code which is a five-material member of the SHELL family. The basic operation of RADISH5 is described in Reference 35. The same basic equations that govern SHELL-OIL (see Appendix A) apply to SHELTC7. In this case, however, the equation of conservation of mass described in Appendix A (Equation A1) is a global continuity equation and refers to the total mass in the problem. In expanding from single material to multi-material, an individual species continuity equation is incorporated for each specie carried by the multi-material code. In a cartesian coordinate system

$$\frac{\partial \rho_i}{\partial t} + \frac{\partial}{\partial x}(\rho_i u) + \frac{\partial}{\partial y}(\rho_i v) = 0 \quad (i = 1, 2, \dots, 7) \quad (C1)$$

It is assumed here that the total quantity of each individual specie is preserved during the mass transport phase (none is produced or destroyed--no reactions are allowed to occur). The momentum and energy associated with each specie are also conserved during the mass transport phase.

The same basic computational scheme which was used in SHELLTC is employed in SHELTC7. A computational grid is established by an auxiliary generator code (CLAMTC7) and loaded with an initial distribution of seven materials. Initial values of velocity, energy, and temperature are assigned to the total mass in each cell. This information is established as the zero cycle on the problem tape by this generator code. The equation of state subroutine (STATE7) is called from CDT to determine a cell temperature and pressure. The multi-material equation of state is discussed in Section III of the main body of the text. A time increment for the cycle is determined by CDT based on the particle velocity criteria, the same as for SHELLTC (see Appendix A).

The PHASE I computations are also the same in SHELTC7 as in SHELLTC. Only the negative integration option is deleted. In this case, if an unstable situation is encountered (such as negative internal energy), the computation is immediately terminated with an appropriate error message. In Phase I, the mass in each cell is considered to be a single uniform material because multiple materials in the cell do not affect the Phase I calculations.

It is in the Phase II computations that all mass transport occurs and multi-material effects are seen in SHELTC7. First the total mass transport in and out of a particular cell is accomplished much as in the single-material case. Then the individual mass species are transported across the cell boundaries by a weighting scheme which assigns the same

proportions amongst the species in the transported mass as existed in the donor cell just before the mass transport. Conservation of energy is used to determine new cell energies and conservation of momentum is used to compute new velocities. Conservation of momentum and energy is also accomplished for each individual mass specie, and this information is also used in obtaining the new velocities. Once mass transport into and out of any cell is completed, the mass in that cell is considered to be uniformly mixed. This leads to an artificial mixing and diffusion of one mass specie through the others which is discussed in some detail in the main body of the text (Section IV).

The code then accomplishes subroutines INTFACE and PDC (both discussed in Section III, main body of text) before returning to CDT. The INPUT and EDIT subroutines are essentially the same as for SHELLTC except provisions for recording and printing out the quantities of all seven species in each cell are provided.

In SHELLTC7 a total of 13 variables must be stored for each cell in the computational grid. Hence, it can only be run on computers with large memory capacities. Further, the time required for execution is substantial (3 to 5 cycles per second) making it imperative to run this code on a fast computer. SHELLTC7 is currently structured for running on the CDC 6600 computer. A listing of SHELLTC7 as used in this work follows.

LISTING OF SHELT C7 CODE

PROGRAM SHELT C7(TAPE4,INPUT,OUTPUT,TAPE5=INPUT,TAPE6=OUTPUT)

***** NOTE-THIS PROGRAM CHANGED TO ACCOMMODATE SEVEN *****
MATERIALS AND TWO COORDINATE SYSTEMS

MATERIAL DESIGNATORS ARE

A - NITROGEN
B - OXYGEN
C - CARBON MONOXIDE
D - CARBON DIOXIDE
E - WATER
F - HYDROGEN
G - CARBON(SOLID)

COMMON Z(8300)
CALL INPUT
10 CALL C)T
CALL E)T
IF(SENSE LIGHT 1) 50,20
20 CALL P41
CALL P42
CALL INTERFACE
CALL P)C
GO TO 10
50 CALL PRINTZ
STOP
END

SUBROUTINE INPUT

DIMENSION AIX(6200),AHY(6200),P(6200),J(6200),V(6200),
1AMA(6200),1M1(6200),AMF(6200),A1D(6200),AMc(6200),AMF(6200),
2AMG(6200),THETA(6200),DY(200),KK(100),YY(200)
DIMENSION X(100), Y(200), Z(100), IP(150), FLEFT(200)
DIMENSION TAU(100), PL(200), JL(200), PR(200), JR(200)
DIMENSION IN1(15), YAMG(200), SIGG(200), GAMG(200), DX(100)

COMMON	Z	,XX	,UR	,PR	,YY	
COMMON	AID	,AIX	,AM	,THETA	,AMX	,AREA
COMMON	BIG	,BOUNCE	,DOXN	,DOVK	,KE	,DVK
COMMON	DX	,DY	,E	,FJ	,FS	,FK
COMMON	OUT	,P	,PABOVE	,PBLO	,PIDTS	,PPABOV
COMMON	PRR	,PUL	,QDT	,RC	,REZ	,RHO
COMMON	RL,RR,SIG,QDQFL,SWITCH		TABL			
COMMON	TAU	,TAUDTS	,TAUDTX	,U	,UK	,URR
COMMON	UT	,UU	,UUU	,UTEF	,UVMAX	,V
COMMON	VABOVE	,VBLO	,VEL	,VK	,VT	,VTEF
COMMON	VV	,VVABOV	,VVRLO	,W2	,W3	,WPS
COMMON	WS	,WSA	,WSB	,WSC	,XL	,XLF
COMMON	XN	,XR	,Y-	,Y-W	,VN	,YU
COMMON	ZMAX	,I	,II	,IV	,IR	,IWS
COMMON	IWSA	,IWSB	,IWSC	,IW1	,J	,JN
COMMON	JP	,JP	,K	,KV	,KP	,KR
COMMON	KRM	,L	,M	,MA	,MB	,MC
COMMON	MJ	,ME	,MZ	,N	,NK	,NKMAX
COMMON	NK1	,NO	,NR	,IW2		
COMMON	ANA,AM1,AMC,AMD,AME,AMF,AMG					

E Q U I V A L E N C E

DEQUIVALENCE	(Z,I2,PRO3),	(Z(2),CYCLE),	(Z(?) ,DT),
1(Z(4),PRINTS),	(Z(5),PRINTL),	(Z(6),DUMPT7),	(Z(7),CSTOP),
2(Z(8),PIDY),	(Z(9),TM7),	(Z(10),GAM),	(Z(11),GAMD),
3(Z(12),GAMX),	(Z(13),ETH),	(Z(14),FFA),	(Z(15),FFB),
4(Z(16),TMDZ),	(Z(17),TMXZ),	(Z(18),KMAX),	(Z(19),TXMAX),
5(Z(20),TYMAX),	(Z(21),AMDY),	(Z(22),AMX1),	(Z(23),DNN),
6(Z(24),DMIN),	(Z(25),FCF),	(Z(26),DTNA),	(Z(27),CVIS),
7(Z(28),NPRI),	(Z(29),NPRI),	(Z(30),NC),	(Z(31),NPC),
8(Z(32),NRC),	(Z(33),IMAX),	(Z(34),IMA(A),	(Z(35),JMAX),
9(Z(36),JMAXA),	(Z(37),KHAX),	(Z(38),KMAXA),	(Z(39),NMAX)
DEQUIVALENCE	(Z(40),ND),	(Z(41),KD1),	(Z(42),IXMAX),
1(Z(43),NOD),	(Z(44),NOPR),	(Z(45),NIMAX),	(Z(46),NJMAX),
2(Z(47),I1),	(Z(48),I2),	(Z(49),I3),	(Z(50),I4),
3(Z(51),N1),	(Z(52),N2),	(Z(53),N3),	(Z(54),N4),
4(Z(55),N5),	(Z(56),N6),	(Z(57),N7),	(Z(58),N8),
5(Z(59),N9),	(Z(60),N10),	(Z(61),N11),	(Z(62),NRM),
6(Z(63),TRA1),	(Z(64),XNRG),	(Z(65),SN),	(Z(66),DXN),
7(Z(67),RADEI),	(Z(68),RADET),	(Z(69),RADEB),	(Z(70),UTRAD),
8(Z(71),REZFT),	(Z(72),RSTOP),	(Z(73),SHELL),	(Z(74),BROUND),
9(Z(75),TOZJN),	(Z(76),ECK),	(Z(77),S30JN),	(Z(78),X1)
DEQUIVALENCE	(Z(79),X2),	(Z(80),Y1),	(Z(81),Y2),
1(Z(82),CABL),	(Z(83),VISCO),	(Z(84),T),	(Z(85),GMAX),
2(Z(86),WSG),	(Z(87),WSGX),	(Z(88),GMADR),	(Z(89),GMAXP),
3(Z(90),S1),	(Z(91),S2),	(Z(92),S3),	(Z(93),S4),
4(Z(94),S5),	(Z(95),S6),	(Z(96),S7),	(Z(97),S8),
5(Z(98),S9),	(Z(99),S10),		
7(Z(130),NFITR),	(Z(131),NFITT),	(Z(132),NFITR),	
8(Z(133),NPART),	(Z(134),NPART),	(Z(135),NPARR),	

```

C
C EQUIVALENCE(P(2,1),GAM1),(P(4,3)),(AMC)
C EQUIVALENCE      (UR,UL,FLEFT),    (PR,PL,SIGC)
C EQUIVALENCE      (XX(2),X(1)),    (YY(2),Y(1))
C
C
C SENSE LIGHT ?
C PRINT 3E13
3013 FORMAT(*1*)
C
C READ  (5,9)04)IWS
C WRITE (6,9)04)TWS
C CALL CARDS
C
C          READ TAPE
C
C
C
C
C
1001 NZ=150
1002 IWS=0
1003 REWIND 4
1004 READ(4)P(1),P(2),NR
NR=NZ+5
1005 IF(PR(1)-5>5.0)1010,1016,1017
1010 IF(PR(1).E).566.)1012,1013
1011 DO 1014 I=1,6
1014 BACKSPACE +
GO TO 1023
1015 IWS=IWS+1
1016 IF(XMDF(IWS,3))1022,4002,1003
1017 IF(Z(235)-PR(2))1023,1025,1020
1021 READ(4) DU1
READ(4) DU1
READ(4) DU1
READ(4) DU1
GO TO 1004
1023 READ(4)(Z(I),I=1,12)
IF(ABSF(PR)B-Z(235))=. 1)1024,1024,3001
1024 READ(4)(U(I),V(I),AM1X(I),AM1X(I),P(I),THETAC(I),I=1,<MAX(A)
READ(4)(AM1(I),AM1(I),AMC(I),A44)(I),A45(I),A46(I),A47(I),A48(I),
I=1,KMAXA)
READ(4)X(0),(X(I),TAU(I)),I=1,[MAX]
A(0) = L.0
READ(4)(V(I),T=0,JMAX)
1034 READ(4)FS,RG,R2
1035 IF(F<-5E5.)10314,1041,1039
1033 IF(RG-6E6.)10315,1041,9906
C
C ***** END OF READ TAPE *****
C
C          READ IN REMAINING INPUT CARDS
C

```

```

1043 CALL CARDS
  IF (NC) 40,41,4
  40 DO 45 K=1,NMAX
  45 R(K)=0.0
  T=T-0.1
  NC=NC-1
  CYCLE=NPC
  NPC=NPC-1
  UVMAX=J..0
  46 DO 50 I=1,I'MAX
  50 X(I)=X(I)-X(I-1)
  DO 55 J=1,JMAX
  55 Y(J)=Y(J)-Y(J-1)
  JX=17-4
  57 TO 58 I=1,JX,4
  K=I+?
  DO 59 J=I,<
  IF (Z(J)) 70,60,70
  60 GO TT11
  GO TO 48
  7 CONTINUE
  WRITE (*,8111) I,(Z(L),L=1,K)
  WRITE (*,8112) I,(Z(L),L=1,K)
  8 CONTINUE
  CALL PRINT2
  Z(1+4)=2.13337E7
  GO TO 1000

```

C READ IN REMAINING INPUT CARDS

C ERROR

```

3901 NK=1023
  GO TO 3939
3902 NK=1011
  GO TO 3939
3903 NK=1030
  GO TO 3939
3904 NK=1031
  GO TO 3939
3905 NK=2030
  GO TO 3939
3906 NK=2012
  GO TO 3939
3999 NR=1
  CALL ERROR(11,1K)

```

C 10001 RETURN

C FORMATS

```

4001 FORMAT(7E11.3,I2)
4002 FORMAT(I1,'1'
           1)
8111 FORMAT (I4,4(4X,1D10.0))
8112 FORMAT(I4,-025)

```

C END

NOT REPRODUCIBLE

SUBROUTINE CARDS

```

DIMENSION TABLE(1),CARD(7),LABLE(1)
COMMON           TABLE
EQUIVALENCE(TABLE(1),LABLE(1))
WRITE (6,17)
1 READ (5,11) IEND,LOC,NJMWPC,(CARD(I),I=1,NUMAPC)
  WRITE (6,12) IEND,LOC,NUMWPC,(CARD(I),I=1,NUMWPC)
  DO 4 I=1,NJMWPC
    J=LOC+I-1
    IF(IEND-2)2,5,?
  3 LABLE(J)=IFIX(CARD(I))
    GO TO 4
  2 TABLE(J)=CARD(I)
  4 CONTINUE
    IF(IEND-1)1,3,1
  3 RETURN
C          FORMATS
10 FORMAT(20H1SH LL  INPUT CARDS///)
11 FORMAT(I1,I5,I1,0P7E3,L)
12 FORMAT(1H I4,I7,I3,1P7E14.5)
  END

```

SUBROUTINE PPIITZ

```

COMMON Z(150)
PRINT 3112,(Z(I),I=1,63)
PRINT 3113,(Z(I),I=67,104)
PRINT 3114,(Z(I),I=105,150)
  3112 FORMAT(4H1 1,3X,6HPP?0. F10.3,5X,6HCVCL E16.9,5X,6HDT   E16.8,5
AX,6HPRINTS[16.3/4H 5,3X,6HPRINTLE10.9,5X,6HJUMPTZ[16.8,5X,6HCSTO
BP E16.8,5X,6HPTD/ E16.9/4H 9,3X,6HT47  E16.8,5X,6HGMAM E16.8,
C5X,6HGMAM] ,E16.8,5X,6HGMK E16.8/4H 17,3X,6HETH E16.8,5X,6HFF
DA E16.8,5X,6HFF] E16.8,5X,6HTM7Z [16.8/4H 17,3X,6HTMKZ E16.
E9,5X,6HXMAX E16.8,5X,6HTYMAX E16.9,5X,6HTYMAX E16.8/4H 21,3X,6HA
FMDM E16.8,5X,6HAI1XM [16.8,5X,617NII E16.8,5X,6HMIN E16.8/4H
G25,3X,6HFEF E16.8,5X,6HDT1A E16.8,5X,6HCVIS E16.8,5X,6HNPR 1
HK,I15/4H 29,3X,7HNP?I I15,5X,7HNC I15,5X,7HPC I15,5X,7H
INRC I15/4H 35,3X,7HIMAX I15,5X,7HIMAXA I15,5X,7HJMAX I15,
J5X,7HJMAXA I15/4H 37,3X,7H

```

```

IMZ(1U0)E16.9/4H 101,9X,E16.8,3(11X,E16.8)
811+ FORMAT(* 175*3XE16.8,3(11XE16.8)/* 109*9XE16.8,3(11XE15.8)/* 117*9
AXE16.8,3(11XE16.8)/* 117*9XE16.8,3(11XE16.8)/* 121*9XE16.8,3(11XE1
86.8)/* 125*9XE16.8,3(11XE16.8)/* 129*9XE16.8,3(12XI15)/* 133*10XI1
CJ,? (12XI15),11XE16.8/* 137*9XE16.8,3(11XE16.8)/* 141*9XE16.8,3(11X
UL15.8)/* 145*9XE16.8,3(11XE16.8)/* 149*9XE16.8,11XE16.8)

      RETURN
      END

```

SUBROUTINE COT

```

C
C
C
      DIMENSION AIX(6200),AMX(6200),P(6200),U(6200),V(6200),
1AMA(5200),AM3(6200),AMC(6200),AMD(6200),AME(6200),AMF(6200),
2AMG(6200),THETA(6200),DY(200),XX(101),YY(201)
      DIMENSION X(100),    Y(200),    Z(150),    IZ(150),    FLEFT(200)
      DIMENSION TAU(100),  PL(200),  UL(200),  PR(200),  UR(200)
      DIMENSION IW1(15),   YAMC(200), SIGC(200), GAMC(200), DX(100)
```

```

COMMON      Z      ,XX      ,UR      ,PR      ,FF
COMMON      AIX      ,AM      ,THETA      ,AMX      ,AREA
COMMON      BIG      ,BOUNCE      ,DXN      ,DVK      ,DKE      ,DVK
COMMON      IX      ,UV      ,E      ,FD      ,FS      ,FX
COMMON      OUT      ,P      ,PAROVE      ,PBLO      ,PIOTS      ,PPABOV
COMMON      PRR      ,PUL      ,DT      ,PC      ,REZ      ,RHO
COMMON      RL,RR,SIG,2000FL,SWITCH,TAUBL
COMMON      TAU      ,TAUDTS      ,TAUDTX      ,U      ,UK      ,URR
COMMON      UT      ,UU      ,UUU      ,UTEF      ,UVMAX      ,V
COMMON      VABOVE      ,VBLO      ,VEL      ,VK      ,VT      ,VTEF
COMMON      VV      ,VV430V      ,VVBLO      ,W2      ,W3      ,WPS
COMMON      HS      ,WSA      ,WSB      ,WSC      ,XL      ,XLF
COMMON      XN      ,XR      ,YL      ,YLW      ,YN      ,YU
COMMON      ZMAX      ,I      ,II      ,IV      ,IR      ,IWS
COMMON      IWSA      ,IWSB      ,IWSC      ,IW1      ,J      ,JN
COMMON      JP      ,JP      ,K      ,KN      ,KP      ,KR
COMMON      KRM      ,L      ,M      ,MA      ,MB      ,MC
COMMON      MD      ,ME      ,IZ      ,N      ,NK      ,NKMAX
COMMON      JK1      ,NO      ,NR      ,IN2
COMMON      AMA,AM3,AMC,AMD,AME,AMF,AMG
```

```

C
C
C
      EQUIVALENCE   (Z,IZ,PROB),     (Z(2),CYCLE),     (Z(3),DT),
1(Z(4),PRINTS),     (Z(5),PRINTL),     (Z(6),DUMPT7),     (Z(7),CSTOP),
2(Z(8),PIDY),     (Z(9),TMZ),     (Z(10),GAM),     (Z(11),GAMD),
3(Z(12),GAMX),     (Z(13),ETH),     (Z(14),FFA),     (Z(15),FFB),
4(Z(16),TMDZ),     (Z(17),TMXZ),     (Z(18),XMAX),     (Z(19),TXMAX),
5(Z(20),TMAX),     (Z(21),AMDM),     (Z(22),AMX4),     (Z(23),DNN),
6(Z(24),DMIN),     (Z(25),FEF),     (Z(26),DTNA),     (Z(27),CVIS),
7(Z(28),NPR),     (Z(29),NPRI),     (Z(30),NC),     (Z(31),NPC),
8(Z(32),NRC),     (Z(33),IMAX),     (Z(34),IMAXA),     (Z(35),JMAX),
9(Z(36),JMAXA),     (Z(37),KMAX),     (Z(38),KMAXA),     (Z(39),NMAX)
```

EQUIVALENCE	(Z(40),NU),	(Z(41),KDT),	(Z(42),IXMAX),
1(Z(43),NOD),	(Z(44),NOPR),	(Z(45),VIMAX),	(Z(46),NJMAX),
2(Z(47),I1),	(Z(49),I2),	(Z(49),I3),	(Z(50),I4),
3(Z(51),N1),	(Z(52),N2),	(Z(53),N3),	(Z(54),N4),
4(Z(55),N5),	(Z(56),N6),	(Z(57),N7),	(Z(58),N8),
5(Z(59),N9),	(Z(60),N10),	(Z(61),N11),	(Z(62),NRM),
6(Z(63),TRAJ),	(Z(64),XNRG),	(Z(65),SN),	(Z(66),DXN),
7(Z(67),PADER),	(Z(69),RADET),	(Z(69),RADES),	(Z(70),DTRAD),
8(Z(71),REZFCT),	(Z(72),RSTOP),	(Z(73),SHELL),	(Z(74),BBOUND),
9(Z(75),TOZONE),	(Z(76),ECK),	(Z(77),SBOUN),	(Z(78),X1),
EQUIVALENCE	(Z(79),X2),	(Z(80),T1),	(Z(81),T2),
1(Z(92),FABLH),	(Z(93),VISG),	(Z(84),T),	(Z(85),GMAX),
2(Z(96),HSG7),	(Z(97),HSGA),	(Z(89),SHAR),	(Z(99),GMAXR),
3(Z(96),S1),	(Z(91),S2),	(Z(92),S3),	(Z(93),S4),
4(Z(94),S5),	(Z(95),S6),	(Z(96),S7),	(Z(97),S8),
5(Z(98),S9),	(Z(99),S10),		
7(Z(130),NFITB),	(Z(131),NFITT),	(Z(132),NFITR),	
8(Z(133),NPART),	(Z(134),NPART),	(Z(135),NPART)	

C

EQUIVALENCE (P(20)), GAMC, (P(40)), YAMC
 EQUIVALENCE (UR,UL,FLIFT), (PR,PL,SIGC)
 EQUIVALENCE (XX(2),X(1)), (// (2),/(1))
 EQUIVALENCE (Z(175),RATA), (Z(176),RATB), (Z(177),RATC)
 EQUIVALENCE (Z(113),RATO), (Z(107),PATE), (Z(110),RATF)
 EQUIVALENCE (Z(111),PATG), (Z(112),ENIA), (Z(113),ENIB)
 EQUIVALENCE (Z(114),ENIC), (Z(115),EVID), (Z(116),ENIE)
 EQUIVALENCE (Z(117),ENIF), (Z(118),EVIS)
 EQUIVALENCE (Z(120),DEIVEL), (Z(121),EVISUM), (Z(122),EXEN)
 EQUIVALENCE (Z(123),EXPNO), (Z(124),THICK), (Z(125),AJCEL)
 EQUIVALENCE (Z(126),TOTLEN)

CCCC

IF (SENSE LIGHT 3) 230,210
 200 SENSE LIGHT 3
 IF (NC) 211,235,235
 205 GO TO 3225
 21. JBOT = Z(144)
 JSTART=Z(1+7)
 IF (NC) 7,8,4
? Z(93) = AIX(10)
 Z(94) = AMX(10)
 Z(95) = AMA(10)
 Z(96) = AMB(10)
 3 DO 300 I=1,IMAX
 K2 = I + IMAX1
 K3 = K2 + IMAX
 E02 = AIX(K2)+0.5*V(K2)*V(K2)*AMX(K2)
 E03 = AIX(K3)+0.5*V(K3)*V(K3)*AMX(K3)
 AMX(K2) = Z(94)
 AMX(K3) = Z(94)
 AMA(K2) = Z(95)
 AMA(K3) = Z(95)
 AMB(K2) = Z(96)
 AMB(K3) = Z(96)
 AIX(K2) = Z(93)
 AIX(K3) = Z(93)

```

U(K2) = 0.0
U(K3) = 0.0
V(K2) = DETVEL
V(K3) = DETVEL
EN2 = AIX(K2)+J.5*V(K2)*V(K2)*AMX(K2)
EN3 = AIX(K3)+J.5*V(K3)*V(K3)*AMX(K3)
300 ETH = ETH + EN2 + EN3 - F02 - E03
IF (NC=2) 1,2,?
1 ENSUM = J.0
TOTLEN = 0.0
GO TO 3000
2 DETLEN = DETVEL*DT
DETMAS = DETLEN*THICK*EXPHO

EKENVD = 0.5*DETMAS*(DETVEL**2)
EKENUD = 0.0
JCCELL = AJCELL
KCELL = 2 + (JCCELL - 1)*IMAX
EKENUD = 0.5*AMX(KCELL)*(U(KCELL)**2)
EKENVD = 0.5*AIX(KCELL)*(V(KCELL)**2)
U(KCELL) = (U(KCELL)*AMX(KCELL))/(AMX(KCELL)+DETMAS)
V(KCELL) = (AMX(KCELL)*V(KCELL)+DETMAS*DETVEL)/(AMX(KCELL)+DETMAS)
AMX(KCELL) = AIX(KCELL) + DETMAS
EKENUN = 0.5*AMX(KCELL)*(U(KCELL)**2)
EKENVN = 0.5*AMX(KCELL)*(V(KCELL)**2)
DEKEN = EKENUD+EKENVD+EKENUD+EKENVD-EKENUN-EKENVN
IF (DEKEN.LT.0.1) GO TO 9904
AIX(KCELL) = AIX(KCELL) + DEKEN
UMASA = PATA*DETMAS
DMASB = RATB*DETMAS
DMASC = RATC*DETMAS
DMASD = RATO*DETMAS
DMASE = RATE*DETMAS
DMASF = RATF*DETMAS
DMASG = RATG*DETMAS
AMA(KCELL) = AIA(KCELL) + DMASA
AMB(KCELL) = AIB(KCELL) + DMASB
AMC(KCELL) = AMC(KCELL) + DMASC
AMD(KCELL) = AID(KCELL) + DMASD
AME(KCELL) = AIE(KCELL) + DMASE
AMF(KCELL) = AMF(KCELL) + DMASF
ANG(KCELL) = AMG(KCELL) + DMASG
ENA = ENIA*D1A5A
ENB = ENIB*D1A5B
ENC = ENIC*D1A5C
END = ENID*D1A5D
ENE = ENIE*D1A5E
ENF = ENIF*D1A5F
ENG = ENIG*D1A5G
ENI = ENA+ENB+ENC+END+ENE+ENF+ENG
AIX(KCELL) = AIX(KCELL) + ENI
ENDEP = DETLEN*THICK*EXRHO*EXEN
AIX(KCELL) = AIX(KCELL) + ENDEP
ENSUM = ENSUM+ENDEP
TOTLEN = TOTLEN+DETLEN
WRITE (6,8444) DETLEN,TOTLEN
WRITE (6,8445) ENDEP, ENSUM

```

```

8444 FORMAT(22H)DETONATION LENGTH IS,1PE12.3,5X,
   1 27HTOTAL DETONATION LENGTH IS ,1PE12.3)
8445 FORMAT (21H0ENERGY DEPOSITED IS ,1PE12.3,5X,
   1 26HTOTAL ENERGY DEPOSITED IS ,1PE12.3,/)
   EKN = EKENUD + EKENVD
   ETH = ETH + E1)EP + EKN + ENI
3003 VEL=0.0
   IF (SENSE LIGHT 3) 215,220
215 SENSE LIGHT 3
   ININ = IMAX
   JNIN = JMAX
   GO TO 3055
223 INI4 = I1
   JN14 = I2
3005 DO 3059 I=1,ININ

3010 K=I+1
3015 DO 3050 J=1,JNIN
3021 IF (AMX(K).EQ.0.0..0-.AIX(K).EQ.0.0) 3021,3025
3021 THETA(K)=0.
   P(K)=0.
   GO TO 3050
C
3025 IF (THETA(K).EQ.0.) THETA(K)=90.
   CALL STATE7
C
3030 IF (ABS(P(K))-1.0E-20) 3035,3035,3040
3035 P(K)=0.0
3040 IF (WSGX-VEL) 3050,3050,7045
3045 VEL=WSGX
3050 K=K+IMAX
220 T=T+DTNA
3055 KOT=1
   UVMAX=-1.0
3070 DO 3255 I=1,I1
   K=I+1+IMAX*J37T
3095 DO 3255 J=JSTART,I2
3100 KP=K+I*IMAX
   IF (AIX(K)) 3901,3255,4
      4 IF (AMX(K)/(TAU(I)*DY(J))-2(139)) 3255,3255,3115
3115 SIG=DX(I)
3120 IF (DY(J)-SIG) 3125,4000,4000
3125 SIG=UY(J)
4000 WS=SQRT(GMAX*TAU(I)*UY(J)*ABS(P(K))/(AMX(K)))
3205 WS=WS/SIG
3210 IF (UVMAX-WS) 3215,3,3
3215 N10=I
   N11=J
   UVMAX=WS
3  IF (GAM) 5,6,5
6  WS=ABS(U(K))/TAU(I)*X(I)/.5*PI)Y
   GO TO 3225
5  WS = ABSF(U(K))/JX
3225 IF (UVMAX-WS) 3230,3235,3235
3230 UVMAX=WS
   N10=I
   N11=J

```

```

323, WS-AWS(V(K)) / DT(J)
324, IF (UVMAX-W5) 3245,3250,3250
325, W10=1
      W11=.J
      UVMAX=WS
3251 CONTINUE
3252 K=K+1MAX
      IF (UVMAX) 9312,3312,91
      9 DT=.5/VEL/UVMAX*Z(13)
3253 K1T=0
21, CONTINUE
  A, NC=NC+1
  C/CLE=NC
  NPC=NPC+1
330, IF (T) 9304,3320,3310
331, IF (K1T) 9913,3315,3320
331, WRITE (E,3303) T,DTNA,DT
332, DTNA=DT
      GO TO 3325
C      NEGATIVE MASS
9901 NK=3020
      GO TO 9999
9902 NK = ?
      GO TO 9999
9903 NK=3305
      GO TO 9999
9904 NK=3310
      GO TO 9999
C      THE DT WILL BE 0. OR NEGATIVE , STOP
9912 NK=1
      GO TO 9999
9911 NK=85
9999 NR=2
      CALL ERER(NP,NK)
332, RETURN
80000FORMAT (17HCHANGE DT ... T=1PE12.3,11H      DT(N)=1PE12.3,
  1 13H      DT(N+1)=1PE12.3)
      END

```

SUBROUTINE PHI

D	I	M	E	N	S	I	O	N
---	---	---	---	---	---	---	---	---

```

C
DIMENSION AIX(6200),AMX(6200),P(6200),U(6200),V(6200),
1AMA(6200),AM3(6200),AMC(6200),AMD(6200),AME(6200),AMF(6200),
2AMG(6200),THETA(6200),YY(200),XX(101),YY(201)
DIMENSION X(101), Y(200), Z(150), IZ(150), FLEFT(200)
DIMENSION TAU(100), PL(200), UL(200), PR(200), UR(200)
DIMENSION IH1(15), YANC(200), SIGC(200), GAMC(200), DX(100)

```

DIMENSION QL(200)
 COMMON Z ,XX ,UR ,PR ,//
 COMMON AIO ,AIX ,AM ,THETA ,AMX ,AREA
 COMMON SIG ,BOUNCE ,DDXN ,DDVK ,DKE ,DKV
 COMMON DX ,DY ,E ,FD ,FS ,FX
 COMMON OUT ,P ,PABOVE ,PBLO ,PIOTS ,PPABOV
 COMMON PRR ,PUL ,QDT ,PC ,REZ ,RHO
 COMMON RL,RR,SIG,Q000FL,SWITCH ,TABLM
 COMMON TAU ,TAUDTS ,TAUDTX ,U ,UK ,URR
 COMMON UT ,UU ,JUU ,UTEF ,UVMAX ,V
 COMMON VAbove ,Velo ,VEL ,VK ,VT ,VTEF
 COMMON VV ,VVABOV ,VVBL0 ,W2 ,W3 ,WPS
 COMMON WS ,WSA ,WSB ,WSC ,XL ,XLF
 COMMON XN ,XR ,YL ,YLW ,YN ,YU
 COMMON ZMAX ,I ,II ,IN ,IR ,IHS
 COMMON IHSA ,IWSH ,IWSC ,IH1 ,J ,JN
 COMMON JP ,JR ,K ,KV ,KP ,KR
 COMMON KRM ,L ,M ,MA ,MB ,MC
 COMMON MD ,ME ,MZ ,N ,NK ,NKMAX
 COMMON NK1 ,NO ,NR ,IW2
 COMMON AMA,AMB,AMC,AMD,AME,AMF,AMG

C
C
C
C

E Q U I V A L E N C E

0EQUIVALENCE	(Z,I2,PP03),	(Z(2),CYCLE),	(Z(3),DT),
1(Z(4),PRINTS),	(Z(5),PPINTL),	(Z(6),DUMPT7),	(Z(7),CSTOP),
2(Z(8),PIDY),	(Z(9),TMZ),	(Z(10),GAM),	(Z(11),GAMD),
3(Z(12),GAMX),	(Z(13),ETH),	(Z(14),FFA),	(Z(15),FFB),
4(Z(16),TMDZ),	(Z(17),TMXZ),	(Z(18),XMAX),	(Z(19),TXMAX),
5(Z(20),TYMAX),	(Z(21),AMDM),	(Z(22),AMX1),	(Z(23),DNN),
6(Z(24),DMIN),	(Z(25),FEF),	(Z(26),DTNA),	(Z(27),CVIS),
7(Z(28),NPR),	(Z(29),NPRI),	(Z(30),VC),	(Z(31),NPC),
8(Z(32),NRC),	(Z(33),IMAX),	(Z(34),JMAXA),	(Z(35),JMAX),
9(Z(36),JMAXA),	(Z(37),KMAX),	(Z(38),KMAXA),	(Z(39),NMAX)
0EQUIVALENCE	(Z(40),ND),	(Z(41),KDT),	(Z(42),IXMAX),
1(Z(43),NOD),	(Z(44),NOPR),	(Z(45),NIMAX),	(Z(46),NJMAX),
2(Z(47),I1),	(Z(48),I2),	(Z(49),I3),	(Z(50),I4),
3(Z(51),N1),	(Z(52),N2),	(Z(53),N3),	(Z(54),N4),
4(Z(55),N5),	(Z(56),N6),	(Z(57),V7),	(Z(58),N8),
5(Z(59),N9),	(Z(60),N10),	(Z(61),N11),	(Z(62),NRM),
6(Z(63),TRAD),	(Z(64),XNRG),	(Z(65),SN),	(Z(66),DXN),
7(Z(67),RADER),	(Z(68),RADET),	(Z(69),RADEB),	(Z(70),DTRAD),
8(Z(71),REZFCT),	(Z(72),RSTOP),	(Z(73),SHELL),	(Z(74),BBOUNCE),
9(Z(75),TOZONE),	(Z(76),ECK),	(Z(77),SBOUND),	(Z(78),X1)
0EQUIVALENCE	(Z(79),X2),	(Z(80),(1),	(Z(81),(2),
1(Z(82),CABL),	(Z(83),VISCO),	(Z(84),T),	(Z(85),GMAX),
2(Z(86),WSG),	(Z(87),WSGX),	(Z(88),GMADR),	(Z(89),GMAXP),
3(Z(90),S1),	(Z(91),S2),	(Z(92),S3),	(Z(93),S4),
4(Z(94),S5),	(Z(95),S6),	(Z(96),S7),	(Z(97),S8),
5(Z(98),S9),	(Z(99),S10),		
7(Z(130),NFITD),	(Z(131),NFITT),	(Z(132),NFITR),	
8(Z(133),NPART),	(Z(134),NPART),	(Z(135),NPARP),	

EQUIVALENCE(P(200),GAMC), (P(400),YAMC)

EQUIVALENCE (UR,UL,FLEFT), (PR,PL,SIGC)

EQUIVALENCE (XX(2),X(1)), (/(2),/(1))

C
C
C

C
C
C

MIN = -2
LOK = -2
NRT=0
NRC=0
JSTART=Z(147)
JBOT=Z(144)
UU=1.E+15
UT=0.0
80L VEL=1.0
8001 IF (GAM) 9000,3301,9000
9000 RC = 1.0
RR = RC
GO TO 3304
3301 RC=DX(1)/2.0
RR=(X(1)+X(2))/2.0
3304 K=2
DO 3302 J=1,JMAX
PL(J)=P(K)
UL(J)=0.0
QL(J)=0.0
3302 K=K+IMAX
DO 3360 I=1,I1
K=I+1+JBOT*IMAX
IF (CVIS) 7002,7103,7003
7002 VBL0=V(K)
PBL0=0.0
GO TO 7004
7003 VBL0=0.0
PBL0=P(K)
7004 TAUOTS=TAU(I)
QB=1.0
DO 3349 J=JSTART,I2
A=0.
B=0.
UQ=U(K)
VQ=V(K)
PIOTS=1.0/(PIDT*DT*D(J))
IF (GAM) 9002,9004,9002
9002 PIDTS = 2.0*PIOTS
9004 N = K+IMAX
3305 IF (AMX(K)) 9902,3301,3306
3306 IF (IMAX-I) 9903,3311,3310
3310 IF (AMX(K+1)) 9904,3312,3314
3311 PRR=P(K)
QR=0.0

3307 ETH=ETH-PRR*U(K)/PIOTS*RC
GO TO 3313
3312 PRR=0.0
QR=0.0
3313 URR=RC*U(K)
GO TO 3316
3314 PRR=(P(K)+P(K+1))/2.0
3315 URR=(U(K)+RC+U(K+1)+QR)/2.0
RHO=0.5*(AMX(K)/TAU(I)+AMX(K+1)/TAU(I+1))/DY(J)
DUR=U(K)-U(K+1)

IF(OUR)2003,10001,2005
 2003 IF(S3)2004,10011,2004
 10001 QR=0.0
 GO TO 3316
 2004 UTEF=A3SF(1.5*(U(K)+U(K+1)))
 QR=-S3*RHO*UTEF*DUR?
 GO TO 3316
 2005 IF(S3)2007,2000,2007
 2005 UTEF=0.
 GO TO 2008
 2007 UTEF=A3SF(1.5*(U(K)+U(K+1)))
 2008 CS=SQRTF(1.4*PRR/RHO)
 QR=RHO*DUR*(S1*C3+S2*S2*DUR+S3*UTEF)
 3310 IF(JMAX-J)9905,3313,3320
 3318 PABOVE=P(K)
 A=1.
 QT=0.0
 3319 ETH=ETH-PABOVE*V(K)/2. *TAUDTS
 GO TO 3323
 3320 IF(A1X(N))9906,3322,3324
 3322 PABOVE=0.0
 QT=0.0
 3323 VABOVE=V(K)
 GO TO 3328
 3324 PABOVE=(P(K)+P(N))/2.0
 RHO=1.5*(A1X(K)+A1X(N))/TAU(T)/D(J)
 DVZ=V(K)-V(N)
 IF(DVZ)2003,10003,2011
 2009 IF(S3)2010,10003,2010
 10003 QT=0.0
 GO TO 7001
 2010 VTEF=A3SF(1.5*(V(K)+V(N)))
 QT=-S3*RHO*VTEF*DYZ
 GO TO 7001
 2011 IF(S3)2016,2012,2016
 2012 VTEF=0.
 GO TO 2014
 2016 VTEF=A3SF(1.5*(V(K)+V(N)))
 2017 CS=SQRTF(1.4*PABOVE/RHO)
 QT=RHO*DYZ*(S1*C3+S2*S2*DYZ+S3*VTEF)
 7001 IF(JSTART-J)3325,7005,9905
 7005 IF(CVIS)700,7006,7006
 7007 PBL0=P(K)
 ETH=FT4+PBL0*V(K)/2.0*TAUDTS
 7006 B=1
 3325 VABOVE=(V(K)+V(N))/2.0
 3326 IF(VEL)9907,3404,3400
 3400 G=6.3567E+18

G=Z(198)*G*G/((G+Y(J)-Y(J)/2.0)**2)
 IF(A+B)9,9,10
 9 WS=(PBL0-PABOVE+QB-QT)*TAUDTS/A1X(K)-G*DT
 GO TO 11
 10 WS=(PBL0-PABOVE+QB-QT)*TAUDTS/A4X(K)-C.5*G*DT
 11 V(K)=V(K)+WS

```

IF (AHSF(V(K))-1.E-01) 3401,3401,3402
3401 V(K)=0.0
3402 U(K)=U(K)+(PL(J)-PRR+QL(J)-QR)/(QMX(K))*RC/PIOTS*2.0
    IF (AHSF(U(K))-1.E-01) 3403,3403,3404
3403 U(K)=0.0
3404 IF (I=I1) 6016,6105,6005
6005 IF (U(K)) 6605,6600,6605
6605 NRC=1
6606 IF (V(K)-Z(120)) 6607,6004,6607
6607 NRC=1
6008 IF (AIX(K) - Z(1+9)) 6015,6016,6015
6015 NRC=1
6016 CONTINUE
    IF (VEL) 9907,2001,2000
2000 VQ=(VQ+V(K))/2.0
    UQ=(UQ+U(K))/2.0
    WS=(P(K)/2.* (VBLO-VABOVE)+QB*(VBLO-VQ)+QT*(VQ-VABOVE))*TAUDTS
    WT=(P(K)/2.* (UL(J)-URR)+QL(J)*(UL(J)-RC+UQ)+QR*(RC+UQ-URR))/PIOTS*
1 2.0
    GO TO 2002
2001 WS=(VBLO-VABOVE)+.5*TAUDTS*P(K)
    WT=P(K)*(UL(J)-URR)/PIOTS
2002 RHO=WS+WT
    WSX=AIX(K) + RHO
    NIT = 1
    IF (NC.EQ.1IM.AND.K.EQ.LOK) PRINT 9901,NC,K,NIT,AIX(K),WSX,RHO,
1   WS,WT,VBLO,VABOVE,UL(J),URR
8861 FORMAT (2X,I4,1X,I5,1X,I2,9(1X,E12.4),/)
1000 IF (WSX) 9903,1001,1101
1001 AIX(K) = WSX
    GO TO 3342
3342 PRR=0.0
    QR=0.0
    QT=0.0
    URR=U(K+1)*RR
    PABOVE=0.0
    VABOVE=V(N)
3342 VBLO=VABOVE
    PL(J)=PPR
    UL(J)=URR
    QL(J)=QR
    QB=QT
    K=N
3343 PBLO=PABOVE
    LL=K-IMAX
    IF (U(LL)) 6003,6001,6000
6000 NRT=1
6001 IF (V(LL) - Z(120)) 6012,6103,6102
6002 NRT=1
6003 IF (AIX(LL) - Z(149)) 6017,6019,6017
6017 NRT=1
6018 CONTINUE

```

```

3355 RC=QQ
    IF (6A4) 3360,3007,3360
3007 RR=(X(I+1)+X(I+2))/2.0
3360 CONTINUE
3361 IF(VEL)9911,7030,3363
3363 VEL=0.0
    GO TO 9001
C          ERROR
9902 NK=3305
    GO TO 9999
9903 NK=3306
    GO TO 9999
9904 NK=3310
    GO TO 9999
9905 NK=3316
    GO TO 9999
9906 NK=3320
    GO TO 9999
9907 NK=3323
    GO TO 9999
9908 NK=1000
    PRINT 4800,I,J,AIX(K),HS,HT,DT
880J FORMAT(30H ****NEGATIVE ENERGY FOUND**** ,2I5,5E12.4)
    GO TO 9999
9911 NK=3361
9999 NR=3
    CALL IPRER(NP,IK)
7030 I1=I1+NRC
6203 I2=I2+NPT
    IF(I1-IMAX)610J,2100,620C
610J I1=IMAX
610C IF(I2-JMAX)6201,6211,6202
6202 I2=JMAX
6201 CONTINUE
    RETURN
    END

```

SUBROUTINE PH2

D I M E N S I O N

```

DIMENSION LIX(6200), AMX(6200), P(6200), U(6200), V(6200),
1AMA(6200), AMB(6200), AMC(6200), AMD(6200), AME(6200), AMF(6200),
2AMG(6200), THETA(6200), DI(200), XX(101), YY(201), GAMMA(200),
3GAM(200), GAMC(200), GAMDD(200), GAMF(200), GAMG(200)
DIMENSION X(100), Y(200), Z(150), IZ(150), FLEFT(200)
DIMENSION TAU(100), PL(200), U_(200), PR(200), JR(200)
DIMENSION IH1(15), YM(200), SIGC(200), GAMC(200), DX(100)
COMMON      Z      ,XX      ,UR      ,PR      ,YY
COMMON      AID     ,AIX     ,AM      ,THETA   ,AMX    ,AREA
COMMON      BIG     ,BOUNCE  ,DXN    ,DVK     ,DKE    ,DK
COMMON      JX     ,DI     ,E      ,D     ,FS     ,FX
COMMON      OUT    ,P      ,PABOVE  ,PBLO   ,PIOTS  ,PPABOV
COMMON      ORR    ,PUL    ,QDT    ,RC     ,REZ    ,RHO
COMMON      RL,RR,SIG,QDCDFL,SWITCH1,TABLM
COMMON      TAU    ,TAUDTS ,TAUDTX ,U      ,UK     ,URR
COMMON      UT     ,UU     ,UUC    ,UTEF   ,UVMAX ,V
COMMON      VABOVE ,VALO   ,VEL    ,VK     ,VT     ,VTEF
COMMON      VV     ,VVABOV ,VVVALO ,W2     ,W3     ,WPS
COMMON      WS     ,WSA    ,WSB    ,WSC    ,XL     ,XLF
COMMON      XN     ,XR     ,YL    ,YLN   ,YN     ,YLI
COMMON      ZMAX   ,I      ,II    ,IV     ,IR     ,IWS
COMMON      IHSA   ,IWSB   ,IWSC   ,IWI   ,J      ,JN
COMMON      JP     ,JR     ,K      ,KN     ,KP     ,KR
COMMON      KRN    ,L      ,M      ,MA     ,MB     ,MC
COMMON      ID     ,ME     ,NZ     ,N      ,NK     ,NKMAX
COMMON      NK1   ,NO     ,NR     ,NIH2
COMMON      AMA,AMB,AMC,AMD,AME,AMF,AMG

```

E Q U I V A L E N C E

DEQUIVALENCE	(Z,IZ,PRO3),	(Z(2),CYCLE),	(Z(3),DT),
1(Z(4),PRINTS),	(Z(5),PRINTL),	(Z(6),DUMPT7),	(Z(7),CSTOP),
2(Z(9),PINY),	(Z(7),TMZ),	(Z(10),GAM),	(Z(11),GAMD),
3(Z(12),GAMY),	(Z(13),ETH),	(Z(14),FFA),	(Z(15),FFB),
4(Z(16),TMDZ),	(Z(17),TMXZ),	(Z(18),XMAX),	(Z(19),TXMAX),
5(Z(20),TYMAX),	(Z(21),AMD),	(Z(22),AMX1),	(Z(23),JNN),
6(Z(24),DMI),	(Z(25),FEF),	(Z(26),JTN),	(Z(27),CVIS),
7(Z(29),NPR),	(Z(29),NPRI),	(Z(30),VC),	(Z(31),NPC),
8(Z(32),NRC),	(Z(33),IMAX),	(Z(34),IMAXA),	(Z(35),JMAX),
9(Z(36),JMAXA),	(Z(37),KMAX),	(Z(38),KMAXA),	(Z(39),NMAX)
DEQUIVALENCE	(Z(40),ND),	(Z(41),KOT),	(Z(42),IXMAX),
1(Z(43),NOD),	(Z(44),NOPR),	(Z(45),NIMAX),	(Z(46),NJMAX),
2(Z(47),I1),	(Z(49),I2),	(Z(49),I3),	(Z(50),I4),
3(Z(51),H1),	(Z(52),N2),	(Z(53),N3),	(Z(54),N4),
4(Z(55),NS),	(Z(56),N6),	(Z(57),N7),	(Z(58),N8),
5(Z(59),H9),	(Z(60),N10),	(Z(61),V11),	(Z(62),NRM),
6(Z(63),TRAD),	(Z(64),XNRG),	(Z(65),SN),	(Z(66),DXN),
7(Z(67),PADER),	(Z(68),RADET),	(Z(69),RADEBI),	(Z(70),DTRAD),
8(Z(71),REZFCT),	(Z(72),RSTOP),	(Z(73),SHELL),	(Z(74),BBOUND),
9(Z(75),TOZONE),	(Z(76),ECK),	(Z(77),SBOUND),	(Z(78),X1)
DEQUIVALENCE	(Z(79),X?),	(Z(80),Y1),	(Z(81),Y2),
1(Z(82),CABL),	(Z(83),VISG),	(Z(84),T),	(Z(85),GMAX),
2(Z(86),HSGD),	(Z(87),HSGX),	(Z(88),GHAD),	(Z(89),GMAXR),
3(Z(90),S1),	(Z(91),S2),	(Z(92),S3),	(Z(93),S4),

4(Z(94),S5), (Z(95),S6), (Z(95),S7), (Z(97),S8),
5(Z(98),S9), (Z(99),S10), (Z(130),NFI79), (Z(131),NFI7T), (Z(132),NFI7R),
8(Z(133),NPARR), (Z(134),NPART), (Z(135),NPARR)

C

EQUIVALENCE(P(20)),GAMC),(P(400),VAMC)
1,(P(600),GAMA),(P(800),GAM3),(P(1000),GAMDD),(P(1200),GAME),
2(P(1400),GAMCC),(P(1600),GAMF),(P(1800),GAMG)
EQUIVALENCE (UR,UL,FLEFT), (PR,PL,SIGC)
EQUIVALENCE (XX(2),X(1)), (YY(2),Y(1))

C

C

C

C

C

MIN = -2
LOK = -2
J87T=Z(144)
JSTART=Z(147)
Z(141)=0.
Z(142)=0.
Z(143)=0.
NRT=0
NRC=0
PE Z=0.
SENSE LIGHT 0
PIOTS=1.0/(PI)*JT
101 DO 103 J=1,JMAX
102 GAMC(J)=0.
FLEFT(J)=0.0
GAMA(J)=0.
GAM3(J)=0.
GAMCC(J)=0.
GAMDD(J)=0.
GAME(J)=0.
GAMF(J)=0.0
GAMG(J)=0.0
VAMC(J)=0.0
SIGC(J)=0.1
103 CONTINUE
104 DO 547 I=1,I1
J=JSTART
K=I+1+J80T*IIMAX
81 IF(AMX(K)) 3900,37,31
82 IF(V(K)) 32,97,97
97 AMMV=0.0
GO TO 38
82 AMHY=AMX(K)*V(K)*DT/V(J)
HS=AMX(K)
IF(GAMC(J)) 7900,53,53
790 HS=HS+GAMC(J)
83 IF(AMHY+HS) 84,35,35
84 AMHY=-HS
85 IF(CVIS) 105,79,79
106 AMMU=AMHY*U(K)
AMMV=AMHY*V(K)
PAT=AMHY/AMX(K)
DMAT=AMX(K)*PAT

```

DMBB=A1P(K)*PAT
DMCH=A1G(K)*PAT
DMDB=A1H(K)*PAT
DMEB=AL(K)*PAT
DMFR=AMF(K)*PAT
DMGR=AMG(K)*PAT
DELEB=AIX(K)/AIX(K)+(U(K)**2+V(K)**2)/2.
HS=(U(K)**2+V(K)**2)/2.
ETH=ETH+AM1Y*(AIX(K)/AMX(K)+HS)

```

C **** PASS HAS LEFT THE BOTTOM****

```

94 SEZ=1.
Z(143)=1.
GO TO 107
99 AMMV=0.
98 AM1Y=0.
DMAJ=0.
DMRJ=0.
DMCJ=0.
DMIJ=0
DMEJ=0
DMFJ=0.0
DMGJ=0.0
AM1U=0.0
DELCJ=0.0
107 DO 546 J=JSTART,12
108 L=K+I:MAX
AREA=0.0
IF (K.EQ. 752) LOK=K
VEL=.0
FS=0.)
217 IF (JMAX-J) 211,211,207
211 VEL=1.J
GO TO 203
207 IF (AMX(L)) 215,215,214
214 IF (AMX(K)) 216,216,201
215 VABOVE=V(L)
GO TO 212
216 IF (AMX(K)) 205,205,203
205 VABOVE=0.0
GO TO 212
213 VABOVE=V(K)
GO TO 212
203 VABOVE=(OY(J+1)*V(K)+OY(J)*V(L))/((OY(J)+OY(J+1))
212 CONTINUE
FS=1.0
404 IF (IMAX-I) +12,+12,403
405 IF (AMX(K+1)) +11,+11,403
409 IF (AMX(K)) +10,+10,+07
410 UR2=U(K+1)
GO TO 408
411 IF (AMX(K)) +03,+03,+06
403 UR2=0.0
GO TO 408
412 FS=1.0
400 UR2=U(K)
GO TO 408
407 UR2=(OY(I+1)*U(K)+OY(I)*U(K+1))/(OY(I)+OY(I+1))
404 CONTINUE

```

```

109 IF( AREA ) 9901, 301, 547
301 IF( V ABOVE ) 300, 304, 302
302 IF( AMX( K ) ) 9903, 304, 303
303 M=K
MM=L
JJ=J
GO TO 307
304 AMPY=0.0
DMAT=0
DMBT=0
DMCT=0
DMDT=0
DMET=0
DMFT=0.0
DMGT=0.0
305 AMUT=0.0
AMVT=0.0
DELET=0.0
GO TO 501
306 IF( VEL ) 9901, 305, 304
305 IF( AMX( L ) ) 9903, 304, 306
306 M=L
MM=K
JJ=J+1
307 IF( VEL ) 6130, 6130, 6140
6130 WSA=0.5*(V(L)+V(K))
WSB=(V(L)-V(K))*DT/DY(J)
IF( ABS(V(M))+DT.GT.0.5*DY(JJ))4S3=0.
V ABOVE = WSA/(1.+4S3)
6140 AMPY=A1X(M)*VA ABOVE/DY(JJ)*DT
6141 RAT = AMPY/AMX(M)
DMAT=AMA(M)*RAT
DMBT=AMR(M)*RAT
DMCT=AMC(M)*RAT
DMDT=A1D(M)*RAT
DMET=A1E(M)*RAT
DMFT=A1F(M)*RAT
DMGT=A1G(M)*RAT
IF( VEL .GT. 1.) GO TO 501
IF( AMA(M)/AMX(1).LT..01 AND A1E(MM).LE.0.) D1AT=0.
IF( AM )(M)/AMX(1).LT..01 AND A1E(MM).LE.0.) D1BT=0.
IF( AMG(M)/AMX(1).LT..01 AND A1G(MM).LE.0.) D1CT=0.
IF( AMH(M)/AMX(1).LT..01 AND A1H(MM).LE.0.) D1DT=0.
IF( AME(M)/AMX(1).LT..01 AND A1E(MM).LE.0.) D1ET=0.
IF( AMF(M)/AMX(1).LT..01 AND A1F(MM).LE.0.) D1FT=0.
IF( AMG(M)/AMX(1).LT..01 AND A1G(MM).LE.0.) D1GT=0.
ADELM=DMAT+DMBT+DMCT+DMDT+DMET+DMFT+DMGT
ADELM=AMPY/ADELM
DMAT=D1AT*ADELM
DMBT=D1BT*ADELM
DMCT=D1CT*ADELM
DMDT=D1DT*ADELM
DMET=D1ET*ADELM
DMFT=D1FT*ADELM
DMGT=D1GT*ADELM
501 IF( URR ) 500, 504, 512
502 IF( AMX( K ) ) 9903, 504, 503
503 M=K

```

```

MM=K+1
N=I
GO TO 508
504 AHMP=0.0
DMAR=0
DMBR=0
DMCR=0
DMDR=0
DMER=0
DMFR=0.0
DMGR=0.0
AMUR=0.0
AMVR=0.0
AELER=0.0
GO TO 1
505 IF (FS) 9005,506,504
506 IF (AMX(K+1)) 9904,504,507
507 M=K+1
MM=K
N=I+1
508 IF (FS) 6100,6101,6110
610J WSA=0.5*(U(K)+U(K+1))
WSI=(U(K+1)-U(K))*DT/DX(I)
IF (ABS(U(M))>DT,GT,DX(M)*0.5) WSRI=0.
UR?=WSA/(1.+WSI)
6110 DEM=A14(M)/TAU(M)
IF (GAM) 9397,1933,939
9983 CAPT = Y(2)*2.0
GO TO 9991
9990 CAPT = 1.0
9991 AHMP = UEN/PIOTS*CAPT*URP
6111 PAT=AHM IF/A IX(M)
DMAR=A1A(M)*PAT
DMBR=A1B(M)*PAT
DMCR=A1C(M)*PAT
DMDR=A1D(M)*PAT
DMER=A1E(M)*PAT
DMFR=A1F(M)*PAT
DMGR=A1G(M)*PAT
IF (FS,GT,0.0) GO TO 1
IF (AM4(M)/AMX(1).LT..0.1,A1D,A1A(14),LE,0.) D14R=1,
IF (AM3(M)/AMX(1).LT..0.1,A1D,A1B(14),LE,0.) D1BR=1,
IF (AMC(M)/AMX(1).LT..0.1,A1D,A1C(14),LE,0.) D1CR=1,
IF (AMD(M)/AMX(1).LT..0.1,A1D,A1D(M4),LE,0.) D1DR=1,
IF (AME(M)/AMX(1).LT..0.1,A1D,A1E(M4),LE,0.) D1ER=1,
IF (AMF(M)/AMX(1).LT..0.1,A1D,A1F(M4),LE,0.) D1FR=1,
IF (AMG(M)/AMX(1).LT..0.1,A1D,A1G(M4),LE,0.) D1GR=1,
ADELM=DMAR+DMR+DMC+DMD+DMF+DMG+H5R
ADELM=AHMP/ADELM
DMAR=DMAR*ADELM
DMBR=DMBR*ADELM
DMCR=DMCR*ADELM
DMDR=DMDR*ADELM
DMER=DMER*ADELM
DMFR=DMFR*ADELM
DMGR=DMGR*ADELM
1 IF (AMMPI) 16,74,3920
9825 IF (GAMC(J)) 74,74,9821

```

6821 IF (FS) 6121, 6170, 74
 6123 IF (AMX(K+1)) 9903, 74, 74
 74 JTAG=0
 2 IF (AMD(I)) 3, 4, 4
 3 ITAG=1
 WS=AMX(K)
 AMPY=0.0
 GO TO 64
 4 ITAG=0
 64 IF (AMM(Y)) 9, 5, 5
 5 IF (GAMC(J)) 17, 6, 5
 6 WS=AMX(K)
 GO TO 11
 7 WS=AMX(K)+GAMC(J)
 GO TO 11
 8 IF (GAMC(J)) 10, 3, 3
 9 WS=AMX(K)+AMM(Y)
 GO TO 11
 10 WS=AMX(K)+GAMC(J)+AMM(Y)
 11 WSA=A17Y+AMMP
 12 IF (WSA-WS) 75, 75, 13
 13 RAT=WS/WSA
 IF (ITAG.EQ.1) GO TO 551
 AMPY=AMPY*RAT
 DMAT=D1AT*RAT
 DM3T=D1AT*RAT
 DMCT=D1CT*RAT
 DMOT=D1DT*RAT
 UMET=D1ET*RAT
 UMF1T=D1FT*RAT
 DMGT=D1GT*RAT
 551 IF (JTAG.EQ.1) GO TO 75
 AM1P=A1MP*RAT
 DMAR=D1AP*RAT
 DMAR=D1EP*RAT
 DMCR=D1CP*RAT
 DMCR=DMUR*RAT
 DMER=D1ER*RAT
 UMFR=DMFR*RAT
 DMGR=D1GR*RAT
 75 IF (JTAG) 14, 73, 14
 73 WSG=AMM(Y)
 14 IF (ITAG) 15, 7011, 15
 15 AMPY=WSB
 ITAG=0
 GO TO 40
 16 IF (FS) 76, 17, 75
 76 WSG=AMMP
 GO TO 40
 17 IF (I+1-I'MAX) 19, 19, 9929
 18 UP2R=U(K+1)/2.0
 GO TO 20
 19 UP2R=(J(K+1)+J(K+2))/2.0
 20 IF (UP2R) 39, 39, 21
 21 IF (WSA) 9992, 1992, 9992
 9992 CLRT = X(I+1)*2.0
 GO TO 3994
 9993 CLRT = 1.0

9994 URRR = URRR/TAU(I+1)*AMX(K+1)/PIOTS*CART
 22 IF(J-JSTART) 9999,23,24
 23 VBL0=V(K+1)/2.0
 GO TO 26
 24 KP=K+1-IMAX
 VBL0=(V(K+1)+V(KP))/2.0
 26 IF(VBL0) 25,38,38
 25 VBL0=AMX(K+1)/DY(J)*VBL0*DT
 27 IF(VEL) 28,29,28
 28 VAB=V(K+1)/2.0
 GO TO 31
 29 KP=K+IMAX+1
 VAB=(V(K+1)+V(KP))/2.0
 31 IF(VAB) 36,36,36
 33 VAB=AMX(K+1)/DY(J)*VAB*DT
 32 HS=AMX(K+1)
 33 WSA=URRR-AMMP-VBL0+VAB
 34 IF(HSA-HS) 77,77,35
 35 AMMP=AMMP*HS/WSA
 RAT=HS/WSA
 DMAR=DMAR*RAT
 DMBR=DMBR*RAT
 DMCR=DMCR*RAT
 DMDR=DMDR*RAT
 DMER=DMER*RAT
 DMFR=DMFR*RAT
 DMGR=DMGR*RAT
 77 JTAG=1
 WSC=AMMP
 AMMP=0.0
 GO TO 2
 36 WS=AMX(K+1)
 37 WSA=URRR-AMMP-VBL0
 GO TO 34
 38 VBL0=0.0
 GO TO 27
 39 URRR=0.0
 GO TO 22
 40 IF(VEL) 7000,41,7000
 41 IF(FS) 42,43,42
 42 KP=K+IMAX
 URT=U(KP)/2.0
 GO TO 45
 43 KP=K+IMAX
 URT=(U(KP)+U(KP+1))/2.0
 45 IF(URT) 46,46,7
 46 URT=0.0
 GO TO 47
 70 KI=K+IMAX
 IF(GAM) 9997,3996,9997
 9996 CART=X(I)*2.0
 GO TO 9998
 9997 CART=1.0
 9998 URT=URT/TAU(I)*AMX(KP)/PIOTS*CART
 47 IF(J+1-JMAX) 48,49,9910
 48 KP=K+IMAX
 KL=KP+IMAX
 VABT=(V(KP)+V(KL))/2.0

GO TO 51
 49 KP=K+1 MAX
 KL=KP+IMAX
 VABT=V(KP)/2.0
 51 IF (VABT) 8810,71,72
 8810 IF (AMX(K)) 9713,71,71
 71 VABT=0.0
 GO TO 60
 72 VABT=VABT*AMX(KP)/UY(J+1)*DT
 52 IF(GAMC(J+1)) 54,53,53
 53 WS=AMX(KP)
 GO TO 55
 54 WS=AMX(KP)+GAMC(J+1)
 55 WSA=VABT-A1PY+URT
 GO TO 57
 60 IF(GAMC(J+1)) 61,61,53
 61 WS=AMX(KP)+GAMC(J+1)
 GO TO 58
 58 WS=AMX(KP)
 59 WSA=-AMPY+URT
 57 IF(WSA-WS) 7010,7000,56
 56 AMPY=A1PY*WS/WSA
 PMAT=WS/WSA
 DMAT=DMAT+RAT
 DMAT=DMAT+RAT
 DMCT=DMCT+RAT
 DMAT=DMAT+RAT
 CMET=CMET+RAT
 DMFT=DMFT+RAT
 DMGT=DMGT+RAT
 7000 AMMP=WSC
 304 IF(AMPY) 8834,4831,4837
 8833 IF(JMAX-J) 3911,313,8837
 8835 KP=K+IMAX
 8833 IF(AMX(KP)) 9901,3137,314
 8837 IF(AMPY/(TAU(I)*Y(J+1))-TOZONE) 9833,714,310
 8834 AMPY=0.0
 DMAT=0
 DMAT=0
 DMCT=0
 DMAT=0
 DMCT=0
 DMFT=0.
 DMGT=0.
 GO TO 4831
 8834 CONTINUE
 8837 IF(AMX(K)) 9911,9941,325
 8840 IF(-AMPY/(TAU(I)*Y(J))-TOZONE) 4941,325,325
 8841 AMPY=0.0
 DMAT=0
 DMAT=0
 DMCT=0
 DMCT=0
 CMET=0
 DMFT=0.
 DMGT=0.
 GO TO 4831
 314 DELH=GAMC(J)+A1HY-AMPY

322 IF(VEL) 9901,324,323
 323 WS=U(K)**2+V(K)**2

$$\text{ETH}=\text{ETH}-\text{AMPY}*(\text{AIX}(K)/\text{AMX}(K)+\text{WS}/2.)$$

$$\text{AMUT}=\text{AMPY}*\text{U}(K)$$

$$\text{AMVT}=\text{AMPY}*\text{V}(K)$$

 C ****MASS HAS LEFT THE TOP
 6900 REZ=1.0

$$Z(141)=1.0$$

 GO TO 32E
 324 AMUT=AMPY*J(K)

$$\text{AMVT}=\text{AMPY}*\text{V}(K)$$

 GO TO 32E
 325 CONTINUE
 8831 AMUT=AMPY*J(L)

$$\text{AMVT}=\text{AMPY}*\text{V}(L)$$

$$\text{DELM}=\text{GAMC}(J)-\text{AMPY}+\text{AMM1}$$

 326 IF(AMPY) 327,328,329
 327 DELET=AIX(L)/AIX(L)+(U(L)**2+V(L)**2)/2.
 GO TO 333
 328 IF(AMM1) 329,330,331
 329 DELET=DELET
 GO TO 333
 331 IF(GAMC(J)) 331,332,332
 331 DELET=SIGC(J)
 GO TO 333
 332 IF(AMX(K).EQ.0.) GO TO 333

$$\text{DELET}=\text{AIX}(K)/\text{AMX}(K)+(\text{U}(K)**2+\text{V}(K)**2)/2.$$

 333 SIGMU=LEFT(J)+AMMU-AMUT

$$\text{SIGMV}=\text{YAMC}(J)+\text{AMMV}-\text{AMVT}$$

$$\text{DELEK}=\text{GAMC}(J)*\text{SIGC}(J)+\text{AMMY}*\text{DELER}-\text{AMPY}*\text{DELET}$$

 503 IF(AMMP) 5843,518,8844
 8841 IF(I MAX-I) 9911,518,8845
 8845 IF(AMX(K+1)) 9900,8846,518
 8846 IF(AMMP/(TAU(I+1)*DY(J))-TOZONE) 3847,519,518
 8847 AMMP=0.0

$$\text{DMAR}=J$$

$$\text{DMBR}=J$$

$$\text{DMCR}=J$$

$$\text{DMDR}=J$$

$$\text{DMER}=J$$

$$\text{DMFR}=J$$

$$\text{DMGR}=J.$$

 GO TO 518
 8848 IF(I-1) 9911,512,8848
 8849 IF(AMX(K)) 9900,8849,512
 8849 IF(-AMMP/(TAU(I)*DY(J))-TOZONE) 8850,512,512..
 8851 AMMP=0.0

$$\text{DMAR}=J$$

$$\text{DMBR}=0$$

$$\text{DMCR}=0$$

$$\text{DMDR}=0$$

$$\text{DMER}=0$$

$$\text{DMFR}=0.$$

$$\text{DMGR}=J.$$

 GO TO 518
 512 DELM=DELM-AMMP+AMX(K)
 8828 AMUR=AMMP*U(K+1)
 AMVR=AMMP*V(K+1)

GO TO 525
 518 DELM=DEL M-AMMP+AMX(K)
 521 CONTINUE
 522 IF (FS) 9905,524,523
 523 WS=U(K)**2+V(K)**2
 IF (AIX(K).EQ.0.) GO TO 524
 ETH=ETH-AMMP*(AIX(K)/AMX(K)+WS/2.)
 AMUR=AMMP*U(K)
 AMVR=AMMP*V(K)
 6401 PEZ=1.0
 C ****MASS HAS LEFT THE RIGHT****
 Z(1+2)=1.0
 GO TO 525
 524 AMUR=AMMP*U(K)
 AMVR=AMMP*V(K)
 525 SIGMU=SIGMU-AMUR
 SIGMV=SIGMV-AMVR
 526 TIC=0.0
 527 IF (AMMP) 528,529,529
 528 DELER=AIX(K+1)/AMX(K+1)+(U(K+1)**2+V(K+1)**2)/2.
 GO TO 527
 529 IF (AMMY) 530,531,531
 530 DELEP=DELE3
 GO TO 536
 531 IF (GAMC(J)) 532,533,533
 532 DELER=SIGC(J)
 GO TO 536
 533 IF (AMPY) 535,535,534
 534 DELER=DELET
 GO TO 536
 535 IF (AMX(K).EQ.0.) GO TO 536
 DELER=AIX(K)/AMX(K)+(U(K)**2+V(K)**2)/2.
 536 TIC=1.0
 537 DELEK=DELEK-AMMP*DELER
 NIT = 2
 IF (NC.EQ.MIN.AND.K.EQ.LOK) PRINT 8005, NC,K,NIT,AMMP,DELER,
 1 GAMC(J),SIGC(J),AMMY,DELEB,AMP/,DELET
 8005 FORMAT (2X,I4,1X,I5,1X,I2,9(1X,E12.4),/)
 538 IF (TIC) 9907,539,550
 550 WS=DELER
 GO TO 999
 539 WS=0.
 IF (AIX(K).GT.0.) WS=AIX(K)/AMX(K)+0.5*(U(K)**2+V(K)**2)
 990 IF (DELM) 991,543,540
 991 IF (AMX(K)*1.E-6+DELM) 9906,997,997
 997 DELM=0.0
 GO TO 543
 541 ENK=AMX(K)*WS+DELEK
 542 U(K)=(SIGMU+AMX(K)*U(K))/DELM
 IF (ABS(U(K))-1.E-2) 1601,601,601
 1601 U(K)=0.
 601 V(K)=(SIGMV+AMX(K)*V(K))/DELM
 IF (ABS(V(K))-1.E-2) 1701,1702,1702
 1701 V(K)=0.
 1702 CONTINUE
 IF (I-I1) 603,6604,6604
 6604 IF (U(K)+V(K)-Z(120)+AIX(K)-Z(149)) 6605,6606,6605
 6605 NRC=1

```

6606 CONTINUE
603 WS=U(K)**2+V(K)**2
542 AIX(K)=ENK-DEL 1*WS/2.
    NIT = 3
    IF (NC.EQ.MIN.AND.K.EQ.LOK) PRINT 6005, NC,K,NIT,AIX(K),ENK,DELH,
1   WS,DELEK
543 AMX(K)=DEL 1
    AMA(K)=AMA(K)+DMA9-DMAT-DMAR+GAMA(J)
    AMB(K)=AMB(K)+DMB9-DMBT-DMBR+GAM9(J)
    AMC(K)=AMC(K)+DMC9-DMCT-DMCR+GAMCC(J)
    AMD(K)=AMD(K)+DMDB-DMDT-DMDR+GAMDD(J)
    AME(K)=AME(K)+DME9-DMET-DMER+GAME(J)
    AMF(K)=AMF(K)+DMFB-DMFT-DMFR+GAMF(J)
    AMG(K)=AMG(K)+DMGB-DMGT-DMGR+GAMG(J)
    IF(AMX(K)) 9900,2007,544
2007 AIX(K)=0.0
    AMA(K)=0
    AMP(K)=0
    AMC(K)=0
    AMD(K)=0
    AME(K)=0
    AMF(K)=0.
    AMG(K)=0.
    U(K)=0.0
    V(K)=0.0
544 GAMC(J)=AM 1P
    GAMA(J)=DMAR
    GAMB(J)=DMBR
    GAMCC(J)=DMCR
    GAMDD(J)=DMDR
    GAME(J)=DMER
    GAMF(J)=DMFR
    GAMG(J)=DMGR
    FLEFT(J)=AMUR
    YAMC(J)=AMVR
    SIGC(J)=DELER
545 AMMY=AMPY
    UMAB=DMAT
    DM3B=DMBT
    DMCB=DMCT
    DMDB=DMDT
    DMEB=DMET
    DMFB=DMFT
    DMGB=DMGT
    AMMU=AMUT
    AMMV=AMVT
    DELEB=DELET
546 K=K+IMAX
    LL=K-IMAX
    IF(U(LL)+V(LL)-Z(120)+AIX(LL)-Z(149)) 6500,547,6500
6500 NRT=1
547 CONTINUE
    I1=I1+NRC
    I2=I2+NRT
    IF(IMAX-I1) 6700,5701,6702
6703 I1=IMAX
6701 CONTINUE
6702 IF(JMAX-I2) 6800,6801,6802

```

```

6803 I2=JMAX
6801 CONT INJE
6802 GO TO 548
9901 NK=300
    GO TO 9999
9902 NK = 2000
    GO TO 9999
9903 NK=302
    GO TO 9999
9904 NK=305
    GO TO 9999
9905 NK=506
    GO TO 9999
9906 NK=500
    GO TO 9999
9907 NK=513
    GO TO 9999
9911 NK=8833
    GO TO 9999
9912 NK=105
    PRINT 906,I,J,A4X(K),A4A(K),A4B(<),AMC(K),A4D(K),A4E(K)
8006 FORMAT(2I5,6E17.9)
    GO TO 9999
9904 NK = 17
    GO TO 9999
9909 NK = 22
    GO TO 9999
9910 NK = 47
    GO TO 9999
9907 NK = 539
9999 NR=4
    CALL ERPER(NR,NK)
544 SU 1=6.J
2005 LA=1MA
    LB=1MB
    LC=1MC
    LD=1MD
    LE=1ME
    LF=1MF
    LG=1MG
DO 2001 I=1,I1
K=I+1+JBOT*I4MAX
DO 2000 J=JSTART,I2
IF (AMA(K).LT.0..4ND.AMA(K).GT.-1.E-15) AMA(K)=0.
IF (AMB(K).LT.J..4N).AMB(K).GT.-1.E-15) AMB(K)=J.
IF (AMC(K).LT.0..4N).AMC(K).GT.-1.E-15) AMC(K)=0. --
IF (AMD(K).LT.J..4N).AMD(K).GT.-1.E-15) AMD(K)=J.
IF (AME(K).LT.0..4N).AME(K).GT.-1.E-15) AME(K)=0.
IF (AMF(K).LT.J..4N).AMF(K).GT.-1.E-15) AMF(K)=0.
IF (AMG(K).LT.0..4N).AMG(K).GT.-1.E-15) AMG(K)=0.
IF (AMA(K).LT.0) PRINT 9201,I,J,LA,AMA(K)
IF (AMB(K).LT.0) PRINT 9201,I,J,LD,AMB(K)
IF (AMC(K).LT.0) PRINT 9201,I,J,LC,AMC(K)
IF (AMD(K).LT.0) PRINT 9201,I,J,LB,AMD(K)
IF (AME(K).LT.0) PRINT 9201,I,J,LE,AME(K)
IF (AMF(K).LT.0) PRINT 9201,I,J,LF,AMF(K)
IF (AMG(K).LT.0) PRINT 9201,I,J,LG,AMG(K)
9201 FORMAT(26H NEGATIVE MASS FOUND AT I=,I5,2HJ=,I5,4I,15H MATERIAL MA

```

```

1SS=,E19.4
TOT=AHA(K)+AHB(K)+AMC(K)+AMD(K)+AME(K)+AMF(K)+AMG(K)
IF(TOT.EQ.0) GO TO 150
ERR=TOT-AMX(K)
F=1.0-ERR/TOT
AMX(K)=AHA(K)*F
AMT(K)=AHB(K)*F
AMC(K)=AMC(K)*F
AMD(K)=AMD(K)*F
AME(K)=AME(K)*F
AMF(K)=AMF(K)*F
AMG(K)=AMG(K)*F
151 IF(AMX(K).GT.0.0,2001,20 9
2004 IF(AMX(K)/(TAU(I)**0.7*(J))-1.0E-5) 2010,2008,2006
2001 HS=(U(K)**2+V(K)**2)/2.0
Z(100)=Z(100)+AMX(K)*HS
HS=ATX(K)+AMX(K)*HS
Z(111)=Z(111)+HS
ETH=ETH-HS
Z(102)=Z(102)+AMX(K)*U(K)
Z(103)=Z(103)+AMX(K)*V(K)
AMX(K)=0.0
AIX(K)=0.0
P(K)=0.0
AMA(K)=0.0
AMB(K)=0.0
AMC(K)=0.0
AMD(K)=0.0
AME(K)=0.0
AMF(K)=0.0
AMG(K)=0.0
THE TAU(K)=0.0
U(K)=0.0
V(K)=0.0
GO TO 2000
2004 IF(AIX(K).GT.0.0,2004,2000,20 0
2004 SUM1=SUM1+AIX(K)
AIX(K)=0.0
PRINT 9200,I,J
9200 FORMAT(2I8,Z12.0) ENERGY AT I,J=,?15)
GO TO 4002
2005 K=K+IMAX
2001 CONTINUE
2003 ETH=ETH-SUM1
Z(104)=Z(104)+SUM1
8001 RETURN
END

```

SUBROUTINE EDIT

D I M E N S I O N

C
C

DIMENSION MSG(6)
 DIMENSION AIK(6200), AMK(6200), P(6200), U(6200), V(6200),
 1AMA(6200), AMB(6200), AMC(6200), AMD(6200), AME(6200), AMF(6200),
 2AMG(6200), THETA(6200), DY(200), XX(101), YY(201)
 DIMENSION X(100), Y(200), Z(150), IZ(150), FLEFT(200)
 DIMENSION TAU(100), PL(200), UL(200), PR(200), UR(200)
 DIMENSION IH1(15), YAMC(200), SIGC(200), GAMC(200), DX(100)

COMMON L , XX , UR , PR , YY
 COMMON AID , AIK , AM , THETA , AMK , AREA
 COMMON BIG , BOUNCE , DDXN , DVK , DKE , DVK
 COMMON IX , DY , E , F , FS , FX
 COMMON OUT , P , PABOVE , PBLO , PIDTS , PPABOV
 COMMON PRR , PUL , QNT , QC , REZ , RHO
 COMMON RL , RR , SIG , T0 , CFL , SWITCH , TABLM
 COMMON TAU , TAUJTS , TAUDTX , U , UK , URR
 COMMON JT , UU , UUU , UTEF , UVMAX , V
 COMMON VABOVE , VB_0 , VEL , VK , VT , VTEF
 COMMON VV , VVABOVE , VVBL0 , V2 , V3 , VPS
 COMMON WS , WSA , WSB , WSC , XL , XLF
 COMMON XN , XP , VL , VLN , YN , YU
 COMMON ZMAX , I , II , IN , IR , IHS
 COMMON IWSA , IWS3 , IWSC , IH1 , J , JN
 COMMON JP , JR , K , KN , KP , KR
 COMMON KRM , L , M , MA , MR , MC
 COMMON ND , ME , NZ , NH , NK
 COMMON NK1 , NO , NR , IH2 , NKMAX
 COMMON AMA , AM3 , AMC , AM1 , AME , AMF , AMG

C
C
C
C

E Q U I V A L E N C E

DEQUIVALENCE	(Z,I2,PROB),	(Z(2),CYCLE),	(Z(3),DT),
1(Z(4),PPINTS),	(Z(5),PRINTL),	(Z(6),NUMPT7),	(Z(7),CSTOP),
2(Z(3),PIDY),	(Z(9),TMZ),	(Z(10),GAM),	(Z(11),GAMD),
3(Z(12),GAMX),	(Z(13),ETH),	(Z(14),FA),	(Z(15),FF9),
4(Z(16),TMDZ),	(Z(17),THXZ),	(Z(18),XMAX),	(Z(19),TXMAX),
5(Z(20),TYMA/),	(Z(21),AMDH),	(Z(22),AMX1),	(Z(23),DNN),
6(Z(24),DMIN),	(Z(25),FEF),	(Z(26),DTN4),	(Z(27),CVIS),
7(Z(28),NPRI),	(Z(29),NPRI),	(Z(30),NC),	(Z(31),NPC),
8(Z(32),NRC),	(Z(33),IMAX),	(Z(34),IMAXA),	(Z(35),JMAX),
9(Z(36),JMA(A),	(Z(37),KMAX),	(Z(38),KMAXA),	(Z(39),NMAX)
DEQUIVALENCE	(Z(43),NDI),	(Z(41),KDT),	(Z(42),IXMAX),
1(Z(43),NOD),	(Z(44),NODP),	(Z(45),NIMAX),	(Z(46),NJMAX),
2(Z(47),I1),	(Z(48),I2),	(Z(49),I3),	(Z(50),I4),
3(Z(51),N1),	(Z(52),N2),	(Z(53),N3),	(Z(54),N4),
4(Z(55),N5),	(Z(56),N6),	(Z(57),N7),	(Z(58),N8),
5(Z(59),N9),	(Z(60),N10),	(Z(61),N11),	(Z(62),NRM),
6(Z(63),TRA)),	(Z(64),XNRG),	(Z(65),SN),	(Z(66),DXN),
7(Z(67),RADER),	(Z(68),RADET),	(Z(69),RADE3),	(Z(70),DTRAD),
8(Z(71),REZFCT),	(Z(72),RSTOP),	(Z(77),SHELL),	(Z(74),BBOUND),
9(Z(75),TOZONE),	(Z(76),ECK),	(Z(77),SBJND),	(Z(78),X1),
DEQUIVALENCE	(Z(79),X2),	(Z(80),Y1),	(Z(91),Y2),
1(Z(92),GABL),	(Z(93),VISG),	(Z(84),T),	(Z(95),GMAX),
2(Z(96),WSG)),	(Z(97),WSGX),	(Z(85),GMAXR),	(Z(89),GMAXR),

3(Z(90),S1), (Z(91),S2), (Z(92),S3), (Z(93),S4),
 4(Z(94),S5), (Z(95),S6), (Z(96),S7), (Z(97),S8),
 5(Z(98),S9), (Z(99),S10),
 7(Z(130),NFI7B), (Z(131),NFI7T), (Z(132),NFI7R),
 8(Z(133),NPARI), (Z(134),NPAPT), (Z(135),NPARR)

EQUIVALENCE (P(201),GAMC), (P(403),/AMC)
 EQUIVALENCE (UP,UL,FLEFT), (PL,PL,SIGC).
 EQUIVALENCE (XX(2),A111), (YY(2),Y(1))

103 IF(SENSE SHITCH .->122,104
 104 IF(SENSE LIGHT 3)106,1,8
 105 IF(CYCLE = CSTOP)112,122,122
 112 IF(MODF(CYCLE, PRINT7))114,1,114
 114 IF(MODF(CYCLE, PRINT8))120,121,120
 121 IF(MODF(CYCLE, PRINT9))114,0,0,0,1+0
 147 IF(SENSE LTIGHT 1)142,1-4
 148 PRINT1
 SENSE LIGHT 1
 IF(GAMC)144,144,1+1
 149 CALL STADY
 14+ GO TO 105()

JUMP ON TAPE+

121 SENSE LTIGHT 1
 PRINTL=CYCLE
 1 IF(JUMP17)30,3,3
 3 BACKSPACE 4
 HS=555.0
 WRITE(4)IS,CYCLE,N?
 20 WRITE(4)(Z(L),L=1,92)
 21 WRITE(4)(JK),V(K),A1*(K),A1<(K),P(K),TA(TACK),K=1,<14XA)
 WRITE(4)(A1A(I),A1T(I),AHC(I),A1D(I),AHE(I),
 1AMF(I),ANG(I),I=1,KMAXA)
 22 WRITE(4)X(C),((K),TAU(K),K=1,IMAX)
 WRITE(4)(Y(K),K=1,IMAX)
 HS=555.0
 WRITE(4)HS,WS,15
 IF(SENSE SHITCH 2)5,24
 PRINT1 8121,CYCLE
 8121 FORMAT(*1*//////////10(1EN******)// CYCLE*FS.0* BEGINS NEW T
 APE 6//10(104******)/*/*)
 PAUS 1.
 GO TO 4
 24 WRITE(4,8121)10
 31 GO TO 114

100 SENS- LIGHT 3
 120 SENS- LIGHT 4
 500 10 1012 I=1,12
 5-12 PR(I)=J.
 GO 6124 K=2,K'1AY

NOT REPRODUCIBLE

```

WS8=(U(K)**2+V(K)**2)/2.0
6019 IF(AMX(K)) 9917,6028,6029
6020 PR(5)=PR(5)+AIX(K)
PR(6)=PR(6)+WS3*AMX(K)
PR(8)=PR(8)+AYX(K)
6028 CONTINUE
PR(3)=PR(1)+PR(2)
PR(7)=PR(5)+PR(6)
AN*G=PR(7)
PR(3)=PR(1)+PR(5)
PR(10)=PR(2)+PR(6)
PR(11)=PR(3)+PR(7)
PR(12)=PR(4)+PR(3)
WSA=(ETH-PR(11))/ETH
PR(18)=(WSA-DNN)/FLOAT(NPC)
ECK=PR(18)
DNV=WSA
NPC=0
WRITE (6,8116) PROB,NC,T,DTNA,TRAD,DTRAD,NR,N1,N2,N3,N4
WRITE (6,8117)(PR(I),I=1,8)
WRITE (6,8118)(PR(I),I=9,12)
WRITE (6,8119) RADER,RADER,RADET,IJMAX,ETH,ECK
II=S8
IX=S10
WRITE (6,9040) N10,N11,I1,I2,II,IX
6090 IF(SENSE LIGHT 4)5050,136
C**** END OF S P SUBROUTINE ****
C
C
5000 CONTINUE
5001 WRITE (6,8116) PROB,NC,T,DTNA,TRAD,DTRAD,NR,N1,N2,N3,N4
5004 DO 5050 I=1,I1
SENSE LIGHT 4
J=I2+1
K=I2*IIMAX+I+1
DO 5046 L=1,I2
J=J-1
K=K-IIMAX
5012 IF(AMX(K)) 3917,5146,5014
5014 IF(SENSE LIGHT +)5015,5019
5015 WRITE (6,8135) I,X(I),DX(I)
5017 WS=AMX(K)/(TAJ(I)*DY(J))
WSA=THETA(K)
5018 WRITE (6,8108) J,U(K),V(K),P(K),WSA,AMX(K),AIX(K),WS,Y(J)
5040 CONTINUE
WRITE (6,8404)
J = I2+1
K = I2*IIMAX+I+1
DO 5044 L=1,I2
J = J-1
K = K-IIMAX
IF (AMX(K)) 9917,5044,5022
5022 WRITE (6,8400) J,AIA(K),AMR(K),AYC(K),AMD(K),AIE(K),AYF(K),AYG(K)
5044 CONTINUE
IF (C/CLE - CSTOP) 136,5050,136
5050 CONTINUE
136 IF (ABSF(ECK)-JMIN)140,140,9905
C**** END OF L P SUBROUTINE ****

```

```

C
C
C           ERROR
9901 NK=110
      GO TO 9999
C           ENERGY CHECK
9905 NK=136
      GO TO 9999
C           NEGATIVE MASS
9917 NK=6015
      GO TO 9999
9920 NK=904
      GO TO 9999
9921 NK=912
      GO TO 9999
9922 NK=913
      GO TO 9999
9923 NK=922
      GO TO 9999
9924 NK=926
9999 NR=6
      CALL ERPER(NR,NK)
10000 RETURN
C
C           FORMATS
81(3 FORMAT(I4,2E14.6,3E15.6,E14.6,E15.6,E14.6)
8110 FORMAT(841 PROBLEM6X,5HFCYCLE9X,4HTIME13X,4HTRAD11X,5H)TRAD1
     12X,2HNREX,2HN14X,2HN24X,2HN34X,24N4/(F7.1,I11,2X,1P4E15.7,I10,2X,4
     2I6))
81170 FORMAT(1H//17X2HA I16X,2HAK14X,5HAI+AK15X,2HAM/4H DOT3X,1P4E18.7/3
     1H X4X,4E18.7)
81180 FORMAT(12X,13H-----5X,13H-----5X,13H-----5
     1X,13H-----/7H TOTALS1P4E18.7)
8119 FORMAT(2H0 //1DX*RADE8*13X*RADE2*13X*RADET*12X*MAX VEL*13X*ETH*12X
     1*REL ERROR*/7X5E18.7///)
8120 FORMAT(1H)//* TAPE4 DUMP ON CYCLE*I5///)
81240 FORMAT(3H K12X,5HAM(K)11X,9HSUM AM(K)11X,6HP(K),2X,4H)(K)/(I3,4X,
     11P4E18.7))
8131 FORMAT(1H //1H DY(J) J=1,I2//(10F12.3))
8133 FORMAT(1H //1H Y(J) J=0,I2//(10F12.3))
81350 FORMAT(1H //44 I =I3,FX,6HX(I) =F12.3,6X,7H)X(I) =F12.3//3H JFX,
     1*X*13X*Y*14X*P*13X*THETA*10X*AMX*11X*ATY*12X*RHO*11X*Y*)
8201 FORMAT(I10,2H I54A2)
8202 FORMAT(10X,2H I54A2)
8211 FORMAT(F7.1,I3,2H I54A2)
8222 FORMAT(F7.1,3X,2H I54A2)
8302 FORMAT(I12,10IL)
83070 FORMAT(5H X1 =1P12.0,3X,4HX2 =E12.6,3X,6HXMAX =E12.5,5X,6HX1 =E12
     1.6,3X,4H/2 =E12.0,3X,6H/MAX =E12.6)
8308 FORMAT(1H /)
8401 FORMAT(I4,7E15.6)
8404 FORMAT(1H /,2X,*J*,3X,*A*,14X,*3*,14X,*0*,14X,*0*,14X,*E*,14X,
     1 *F*,14X,*G*,/)
9040 FORMAT(1H / 6I6)
8999 FORMAT(I5,1X,1P5E12.6)
      END

```

```

SUBROUTINE TYPE(.I)
CALL TIME (26H4OUNT NEW TAPE IN PLACE OF 1)
CALL DISPLAY(5HTAPE ,N)
PAUSE
RETURN
END

```

```

SUBROUTINE POWER(X,XX,N)
XX=LOGF(ABSF(X))/2.30258993
N=XX
IF(XX)1,2,2
1 N=N-1
2 XX=X/10.**N
RETURN
END

```

SUBROUTINE STATE7

	D	I	M	E	N	S	I	O	N
DIMENSION	AIX(6200), AMY(6200), P(6200), U(6200), V(6200), 1AMA(6200), AMB(6200), AMC(6200), AMI(6200), AME(6200), AMF(6200), 2AMG(6200), THETA(6200), Y(200), XX(101), YY(201)								
DIMENSION	X(100), Y(200), Z(150), IZ(150), FLEFT(200)								
DIMENSION	TAU(100), PL(200), UL(200), PR(200), UR(200)								
DIMENSION	IW1(15), YANG(200), SIGC(200), GAMC(200), DX(100)								
COMMON	Z, XX, UR, PR, YY								
COMMON	AI, AIX, AM, THETA, AMX, AREA								
COMMON	BIG, BOUNCE, DDZN, DDVK, JKE, DVK								
COMMON	JX, CY, E, FD, FS, FX								
COMMON	JUT, P, PABOVE, PBL, PIDTS, PABOV								
COMMON	PBL, PUL, PBT, PC, PEZ, RHO								
COMMON	PL, RR, SIG, QFL, SWITCH, TABLM								
COMMON	TAU, TAUOTS, TAUOTX, U, UK, URR								
COMMON	JT, UU, UUU, UTEF, UVMAX, V								
COMMON	VABOVE, VBL, VEL, VK, VT, VTEF								
COMMON	VV, VVA-BOV, VVBL, W2, W3, WPS								
COMMON	WS, WSA, WSR, WSC, XL, XLF								
COMMON	XN, XR, YL, YLA, YN, YU								
COMMON	ZMAX, I, II, IV, IR, IWS								
COMMON	IWSA, IWSB, IWSC, IW1, J, JN								
COMMON	JP, JR, K, KV, KP, KR								
COMMON	KR1, L, M, MA, MB, MC								
COMMON	M1, ME, MZ, N, NK, NKMAX								
COMMON	NK1, NO, NR, TW2								
COMMON	AMA, AMB, AMC, AMI, AME, AMF, AMG								

C
C
C
C

E Q U I V A L E N C E

DEQUIVALENCE	(Z,IZ,PROB),	(Z(2),CYCLE),	(Z(3),DT),
1(Z(4),PRINTS),	(Z(5),PPINTL),	(Z(6),DUMPT7),	(Z(7),CSTOP),
2(Z(8),PIDY),	(Z(9),THZ),	(Z(10),GAM),	(Z(11),GAMD),
3(Z(12),GAMX),	(Z(13),ETH),	(Z(14),FFA),	(Z(15),FFB),
4(Z(16),TM0Z),	(Z(17),THXZ),	(Z(18),XMAX),	(Z(19),TMAX),
5(Z(20),TYMAX),	(Z(21),A47Y),	(Z(22),KMXH),	(Z(23),DNN),
6(Z(24),DMIN),	(Z(25),FEF),	(Z(26),DTNA),	(Z(27),CVIS),
7(Z(28),NPR),	(Z(29),NPRI),	(Z(30),NC),	(Z(31),NPC),
8(Z(32),NRC),	(Z(33),IMAX),	(Z(34),IMAXA),	(Z(35),JMAX),
9(Z(36),JMAXA),	(Z(37),KMAX),	(Z(38),KMAXA),	(Z(39),NMAX)
DEQUIVALENCE	(Z(40),ND),	(Z(41),KOT),	(Z(42),IXMAX),
1(Z(43),NODI),	(Z(44),NOPR),	(Z(45),NIMAX),	(Z(46),NJMAX),
2(Z(47),I1),	(Z(48),I2),	(Z(49),I3),	(Z(50),I4),
3(Z(51),N1),	(Z(52),N2),	(Z(53),N3),	(Z(54),V4),
4(Z(55),N5),	(Z(56),N6),	(Z(57),V7),	(Z(58),N8),
5(Z(59),N9),	(Z(60),N10),	(Z(61),N11),	(Z(62),NRM),
6(Z(63),TRAD),	(Z(64),XNRG),	(Z(65),SN),	(Z(66),DXN),
7(Z(67),RADET),	(Z(68),RADET),	(Z(69),RADEB),	(Z(70),DTRAD),
8(Z(71),REZFCT),	(Z(72),PST0D),	(Z(73),SHELL),	(Z(74),BBOUND),
9(Z(75),TOZONE),	(Z(76),ECK),	(Z(77),SBOUN),	(Z(78),X1)
DEQUIVALENCE	(Z(79),X2),	(Z(80),Y1),	(Z(81),Y2),
1(Z(92),CABLN),	(Z(93),VISCI),	(Z(94),T),	(Z(95),GMAX),
2(Z(96),WSGD),	(Z(97),WSGX),	(Z(98),GMAXR),	(Z(99),GMAXR),
3(Z(98),S1),	(Z(99),S2),	(Z(100),S3),	(Z(101),S4),
4(Z(94),S5),	(Z(95),S6),	(Z(96),S7),	(Z(97),S8),
5(Z(29),S9),	(Z(99),S10),		
7(Z(130),NFITR),	(Z(131),NFITT),	(Z(132),NFITR),	
A(Z(133),NPART),	(Z(134),NPART),	(Z(135),NPARR)	

EQUIVALENCE(P(?)J),GAMC),(P(400),FAHC)
 EQUIVALENCE(IJL,UL,FLEFT), (PL,PL,SIGC)
 EQUIVALENCE(XX(2),X(1)), (YY(2),Y(1))

C

C
C
C
C

```
M = -2
LOK = -2
IF (NC.GE.960.J.AN).NC.LT.962.J) M = NC
IF (K.EQ. 752) LOK=K
IF (K.EQ. 753) LOK=K
IF (K.EQ. 754) LOK=K
IF (K.EQ. 902) LOK=K
IF (I.EQ. 903) LOK=K
IF (K.EQ. 904) LOK=K
IF (K.EQ. 352) LOK=K
IF (K.EQ. 453) LOK=K
IF (K.EQ. 354) LOK=K
IF (K.EQ. 302) LOK=K
IF (K.EQ. 903) LOK=K
IF (K.EQ. 904) LOK=K
IF (K.EQ. 952) LOK=K
IF (K.EQ. 953) LOK=K
IF (K.EQ. 954) LOK=K
```

```

IF (K.EQ.1002) LOK=K
IF (K.EQ.1003) LOK=K
IF (K.EQ.1004) LOK=K
IF (K.EQ.1052) LOK=K
IF (K.EQ.1053) LOK=K
IF (K.EQ.1054) LOK=K
IF (AIX(K).LT.0.0) GO TO 300
C COMPUTE VOLUME OF SOLID CARBON IN CELL
  VEL = 0.0
  VOL=TAU(I)*DV
  RHOG=2.3
  VOLG = AMG(K)/RHOG
  IF (NC.EQ.M.AND.K.EQ.LOK) PRINT 8001,VOL,VOLG,NC,K
8001 FORMAT (1H ,/,2X,*VOL = *,E14.4,2X,*VOLG = *,E14.4,
1 2X,*NC = *,I4,2X,*K = *,I4)
  IF (VOLG.GT.0.01*VOL) 10,20
10 VOL=VOL-VOLG
C COMPUTE VALUES FOR GAMMA AT CELL TEMPERATURE
20 IF (THETA(K).GT.200.0) 30,28
28 GMA = 1.4
  GMB = 1.4
  GMC = 1.4
  GMJ = 1.33
  GME = 1.33
  GMF = 1.4
  GO TO 31
30 CALL GAMGAM (THETA(K),GMA,GMB,GMC,GMJ,GME,GMF)
C FIND MAX VALUE OF GAMMA
31 GMAX = 0.0
  IF (NC.EQ.M.AND.K.EQ.LOK) PRINT 8002,THETA(K),GMA,GMB,GMC,GMJ,
1 GME,GMF
8002 FORMAT (2X,*THETA(K) = *,E14.4,2X,*GAMMAS ARE *,6(E12.3,2X))
  IF (GMA.GT.GMAX) GMAX=GMA
  IF (GMB.GT.GMAX) GMAX=GMB
  IF (GMC.GT.GMAX) GMAX=GMC
  IF (GMJ.GT.GMAX) GMAX=GMJ
  IF (GME.GT.GMAX) GMAX=GME
  IF (GMF.GT.GMAX) GMAX=GMF
  WSGX = GMAX-1.0
C COMPUTE NEW CELL TEMPERATURE
  IF (AMG(K).LT.0.01*AMX(K)) GO TO 86
  IF (THETA(K).GT.1500.) 80,85
80 CVGB = (4.2+4.19E-4*THETA(K))*4.184E7/12.0
  GO TO 84
84 CVGB = (0.9+2.555E-3*THETA(K))*4.184E7/12.0
  GO TO 86
86 CVG9 = 0.0
88 AIG=AIX(K)-AMG(K)*CVGB*(THETA(K)-292.)
  IF (NC.EQ.M.AND.K.EQ.LOK) PRINT 8003,AIG,AIX(K),AMG(K),CVGB,THETA(K)
8003 FORMAT (2X,*AIG = *,E14.4,2X,*AIX(K) = *,E14.4,2X,*AMG(K) = *,
1 E14.4,2X,*CVGB = *,E12.3,2X,*THETA(K) = *,E12.3)
  AMOLA=(AMA(K))/(28.0*(GMA-1.0))
  AMOLB=(AMB(K))/(32.0*(GMB-1.0))
  AMOLC=(AMC(K))/(28.0*(GMC-1.0))
  AMOLD=(AMD(K))/(44.0*(GMJ-1.0))
  AMOLE=(AME(K))/(15.0*(GME-1.0))
  AMOLF=(AMF(K))/(2.0*(GMF-1.0))
  AMOL=AMOLA+AMOLB+AMOLC+AMOLD+AMOLE+AMOLF
  IF (NC.EQ.M.AND.K.EQ.LOK) PRINT 8004,AMOLA,AMOLB,AMOLC,AMOLD,

```

```

2 AMOLE,AMOLF,AMOL
8004 FORMAT (2X,*THE A10LS ARE *,6(E14.4,2X),*AMOL = *,E14.4)
IF (AMO_) 89, 93, 90
89 TEMP = 0.0
GO TO 92
90 R = 8.317E7
TEMP=AIG/(R*AMOL)
92 CONTINUE
C BRING GASES AND SOLID CARBON TO TEMPERATURE EQUILIBRIUM
NTIME = 0
MTIME = 0
IF (AMG(K).LT.J.01*AMX(K)) GO TO 290
IF(ABSF(THETA(K)-TEMP).LE.10.0) GO TO 250
TEMPG=THETA(K)
IF(TEMP.LT.TEMPG) GO TO 150
100 DTEMP = ABSF(TEMP-TEMPG)/6.0
110 FLAG = 1.0
TEM=TEMP-0.5*DTEMP
IF(NC.EQ.M.AND.K.EQ.LOK)PRINT 4000,TEM,TEMP,DTEMP
8000 FORMAT (2X,*TEM = *,E14.4,2X,*TEMP = *,E14.4,2X,*DTEMP = *,E14.4)
IF(NC.EQ.M.AND.K.EQ.LOK)PRINT 3010,TEMPG,DTEMPG,K,NTIME,FLAG
8010 FORMAT(2X,*TEMPG = *,E14.4,2X,*DTEMPG = *,E14.4,2X,2I6,F6.2)
CALL CVGAM (TE1,CVA,CVB,CVC,CVD,CVE,CVF)
DQA=AMA(K)*CVA*DTEMP
DQB=AMB(K)*CVB*DTEMP
DQC=AMC(K)*CVC*DTEMP
DQD=AMD(K)*CVD*DTEMP
DQE=AME(K)*CVE*DTEMP
DQF=AMF(K)*CVF*DTEMP
Q=DQA+DQB+DQC+DQD+DQE+DQF
IF(NC.EQ.M.AND.K.EQ.LOK)PRINT 8015,DQA,DQB,DQC,DQD,DQE,DQF,0
8005 FORMAT(2X,6(E14.4,2X),*Q = *,E14.4)
IF (AMG(K).LE.J.0.R.CVGR.LE.0.0) GO TO 200
UTEMPQ=Q/(AMG(K)*CVG3)
IF (DTEMPG.GT.1.9SF(TEMP-TEMPG)) 130,140
130 RAT = (0.9*ABSF(TEMP-TEMPG))/UTEMPQ
DTEMP = DTEMP*RAT
GO TO 110
140 TE1P = TEMP-DTEMP
TEMPG = TE1P+DTEMPG
IF(NC.EQ.M.AND.K.EQ.LOK)PRINT 8006,AMG(K),CVG3,DTEMPG,TEMP,TEMPG
8006 FORMAT (2X,*AMG(K) = *,E14.4,2X,*CVG3 = *,E14.4,2X,*DTEMPG = *,
1 E14.4,2X,*TEMP = *,E14.4,2X,*TEMPG = *,E14.4)
NTIME = NTIME + 1
IF (ABSF(TEMP-DTEMPG).LE.10.0) GO TO 200
IF (TEMP.LT.TE1P) 150,160
150 DTEMP = ABSF(TE1P-TEMP)/6.0
155 FLAG = 2.0
TEM=TEMP+0.5*DTEMP
IF(NC.EQ.M.AND.K.EQ.LOK)POINT 4000,TEM,TEMP,DTEMP,
1 TEMP,DTEMPG,<,1TIME,FLAG
CALL CVGAM (TEM,CVA,CVB,CVC,CVD,CVE,CVF)
DQA=AMA(K)*CVA*DTEMP
DQB=AMB(K)*CVB*DTEMP
DQC=AMC(K)*CVC*DTEMP
DQD=AMD(K)*CVD*DTEMP
DQE=AME(K)*CVE*DTEMP
DQF=AMF(K)*CVF*DTEMP

```

```

Q=0QA+DQB+DQC+DQD+DQE+DQF
IF (NC.EQ.4.AND.K.EQ.LOK)PRINT 8005,DQA,DQB,DQC,DQD,DQE,DQF,Q
IF (AMG(K).LE.0.J.OR.CVGB.LE.0.0) GO TO 200
UTEMPG=Q/(AMG(K)+CVGB)
IF (DTEMPG.GT.4BSF(TEMP-TEMPG)) 160,170
160 RAT = (0.9*ABSF(TEMP-TEMPG))/DTEMPG
UTEMF = DTEMP*RAT
GO TO 155
170 TEMP = TEMP + DTEMP
TEMPG = TEMP - DTEMPG
IF (NC.EQ.M.AND.K.EQ.LOK)PRINT 8006,AMG(K),CVS,J,DTEMPG,TEMP,TEMPG
MTIMJ = MTIME + 1
IF (ABSF(TEMP-TEMPG).LT.1E.0) GO TO 200
IF (TEMP.LT.TEMP) 150,160
200 IF (AMG(K).LT.).01*AMX(K)) GO TO 205
TEMP = (TE1P + TEMPG)*1.5
TEMPG = TEMP
205 IF (ABSF(THETA(K)-TE1P).LE.10.0) GO TO 250
210 THETA(K) = THETA(K) + 0.9*(TEMP - THETA(K))
VEL = VFL + 1.0
IF (NC.EQ.M.AND.K.EQ.LOK)PRINT 8007,THETA(K),TEMP,VEL
8007 FORMAT (2X,*THETA(K) = *,E14.4,2X,*TEMP = *,E14.4,2X,*VEL = *,1 F6.2)
GO TO 20
300 P(K) = L.0
THETA(K) = 50.0
PRINT 8009,K
8009 FORMAT (2X,*NEGATIVE AIX IN CELL*,I6,*PRESSURE SET TO ZERO*)
GO TO 10000
250 THETA(K) = 0.5*(THETA(K) + TEMP)
RTV = (R*THETA(K))/VOL
PA = (AMA(K)*RTV)/28.0
PB = (AMB(K)*RTV)/32.0
PC = (AMC(K)*RTV)/28.0
PD = (AMD(K)*RTV)/44.0
PE = (AME(K)*RTV)/18.0
PF = (AMF(K)*RTV)/2.0
P(K) = PA+PB+PC+PD+PE+PF
IF (NC.EQ.M.AND.K.EQ.LOK)PRINT 8008,THETA(K),P(K),PA,PB,PC,PD,PE,PF
8008 FORMAT (1X,*THETA = *,E14.4,1X,*P = *,E14.4,1X,*PRESS. ARE *,1 6(E12.3,1X))
10000 RETURN
END

```

SUBROUTINE CVGAM (TMP,CA,CB,CC,CD,CE,CF)

T = TMP

CALERG=4.194E7

IF (T.LT.50.0) T = 50.0

IF (T.GT.6000.) T = 6000.0

TT=T*T

TTT = T*TT

CA=(4.4163+1.7675E-3*T-4.0340E-7*TT+3.0933E-11*TTT)*CALERG/28.0

CB=(4.6089+1.9774E-3*T-3.6968E-7*TT+2.6853E-11*TTT)*CALERG/32.0

CC=(4.4239+1.8033E-3*T-4.4233E-7*TT+3.4856E-11*TTT)*CALERG/28.0

CD=(5.8423+5.4368E-3*T-1.5217E-6*TT+1.2629E-10*TTT)*CALERG/44.0

CE=(4.7832+3.9433E-3*T-7.9342E-7*TT+5.4627E-11*TTT)*CALERG/18.0

CF=(4.5507+9.0593E-4*T-4.9424E-8*TT-3.1041E-12*TTT)*CALERG/2.0

105 RETURN

END

SUBROUTINE GAMGAM (T4P,GA,GB,GC,GD,GE,GF)

T = TMP

IF (T.LT.50.0) T = 50.0

IF (T.GT.6000.0) T = 6000.0

TT=T*T

TTT = T*TT

CALERG = 4.184E7

CPA=(5.3931+1.7739E-3*T-4.1020E-7*TT+3.1975E-11*TTT)*CALERG/28.0

CPB=(6.6745+1.3603E-3*T-3.6215E-7*TT+2.5902E-11*TTT)*CALERG/32.0

CPC=(6.4114+1.3637E-3*T-4.4326E-7*TT+3.5674E-11*TTT)*CALERG/28.0

CPD=(7.8263+5.3673E-3*T-1.5678E-6*TT+1.3213E-10*TTT)*CALERG/44.0

CPE=(6.7246+3.9907E-3*T-7.4975E-7*TT+4.9546E-11*TTT)*CALERG/18.0

CPF=(6.5543+8.6152E-4*T-2.7312E-3*TT-3.1196E-12*TTT)*CALERG/2.0

CALL CVGAM (T,CVA,CV3,CVC,CVD,CVE,CVF)

GA = CPA/CVA

GB = CPB/CVB

GC = CPC/CVC

GD = CPD/CVD

GE = CPE/CVE

GF = CPF/CVF

RETURN

END

SUBROUTINE INTERFACE

C
C
C

D I N E N S I) V

```

DIMENSION AIX(6200), AMX(6200), P(6200), U(6200), V(6200),
1AMX(6200), AMB(6200), AMF(6200), AMT(6200), AME(6200), AMF(6200),
2AMG(6200), THETA(6200), D/(200), XX(101), Y(201)
DIMENSION X(100), Y(200), Z(150), IZ(150), FLEFT(200)
DIMENSION TAU(100), PL(200), UL(200), PR(200), UR(200)
DIMENSION IW1(15), YAMC(200), SIGC(200), GAMC(200), DX(100)

```

C

COMMON	Z	,XX	,UR	,ZR	,YY
COMMON	AID	,AIX	,AM	,THETA	,AMX
COMMON	BIG	,BOUNCE	,DOXN	,DDVK	,DKE
COMMON	UX	,D/	,E	,FD	,FS
COMMON	OUT	,P	,DAGOVE	,PBLO	,PIOTS
COMMON	PRR	,PUL	,IDT	,RC	,REZ
COMMON	RL,RR,SIG,Q000FL,SWITCH,TABLM				
COMMON	TAU	,TAUDTS	,TAUDTX	,U	,UK
COMMON	UT	,UU	,UUU	,UTEF	,UVMAX
COMMON	V430VE	,V3.0	,VE.	,VK	,VT
COMMON	VV	,VV430V	,VV6L0	,W2	,W3
COMMON	WS	,WSA	,WSB	,WSC	,XL
COMMON	XN	,XR	,YL	,Y_N	,YN
COMMON	ZMAX	,I	,II	,IN	,IR
COMMON	IWSA	,IWSB	,IWSC	,IW1	,J
COMMON	JP	,JR	,K	,KN	,KP
COMMON	KRY	,L	,M	,MA	,MB
COMMON	TD	,ME	,MZ	,N	,NK
COMMON	NK1	,NO	,NR	,IN2	
COMMON	AMA,AM3,AMC,AMD,AME,AMF,AMG				

C
C
C

E 2 U I V A L E N C E

DEQUIVALENCE	(Z,IZ,PROB),	(Z(2),CYCLE),	(Z(3),DT),
1(Z(4),PPINTS),	(Z(5),PRINTL),	(Z(6),DUMPT?),	(Z(7),CSTD?),
2(Z(9),PIDV),	(Z(9),TMZ),	(Z(10),GAM),	(Z(11),GA40),
3(Z(12),GAMX),	(Z(13),ETH),	(Z(14),FFA),	(Z(15),FFB),
4(Z(16),THDZ),	(Z(17),THXZ),	(Z(18),XMAX),	(Z(19),TXMAX),
5(Z(20),TYMAX),	(Z(21),AMDN),	(Z(22),AMX?),	(Z(23),DMN),
6(Z(24),DMIN),	(Z(25),FEF),	(Z(26),DTNA),	(Z(27),CVIS),
7(Z(28),NPRI),	(Z(29),NPRI),	(Z(30),NC),	(Z(31),NPC),
8(Z(32),NRC),	(Z(33),IMAX),	(Z(34),IMAKA),	(Z(35),JMAX),
9(Z(36),JMAXA),	(Z(37),KMAX),	(Z(39),KMAXA),	(Z(39),NMAX)
DEQUIVALENCE	(Z(40),ND),	(Z(41),KDT),	(Z(42),IXMAX),
1(Z(43),NOD),	(Z(44),NOPR),	(Z(45),NIMAX),	(Z(46),NJMAX),
2(Z(47),I1),	(Z(48),I2),	(Z(49),I3),	(Z(50),I4),
3(Z(51),N1),	(Z(52),N2),	(Z(53),V3),	(Z(54),N4),
4(Z(55),N5),	(Z(56),N6),	(Z(57),V7),	(Z(58),N8),
5(Z(59),N9),	(Z(60),N10),	(Z(61),V11),	(Z(62),NRM),
6(Z(63),TRA?),	(Z(64),XNRG),	(Z(65),SN),	(Z(66),DXN),
7(Z(67),PADEU),	(Z(68),PADETI),	(Z(69),RADE?),	(Z(70),DTRAD?),
9(Z(71),REZFT),	(Z(72),RSTOP),	(Z(73),SHEL-),	(Z(74),330JN),
9(Z(75),TOZONE),	(Z(76),ECK),	(Z(77),S80JN),	(Z(78),X1)
DEQUIVALENCE	(Z(79),X2),	(Z(80),Y1),	(Z(81),Y2),
1(Z(82),CARLN),	(Z(83),VISCI),	(Z(84),T),	(Z(85),G44X),
2(Z(86),HSGD),	(Z(87),WSGX),	(Z(88),GMAZ?),	(Z(89),GMAXR),

3(Z(90),S1), (Z(91),S2), (Z(92),S3), (Z(93),S4),
 4(Z(94),S5), (Z(95),S6), (Z(96),S7), (Z(97),S8),
 5(Z(98),S9), (Z(99),S10),
 7(Z(130),NFIITB), (Z(131),NFIITT), (Z(132),NFIITR),
 8(Z(133),NPARB), (Z(134),NPART), (Z(135),NPARR)

EQUIVALENCE(P(200),GAMC), (P(400),YAMC)
 EQUIVALENCE (UR,UL,FLEFT), (PR,PL,SIGC)
 EQUIVALENCE (XX(2),X(1)), (YY(2),Y(1))
 EQUIVALENCE (Z(105),RATA), (Z(106),RATB), (Z(107),RATC)
 EQUIVALENCE (Z(119),RATO), (Z(103),RATE), (Z(110),RATF)
 EQUIVALENCE (Z(111),RATG), (Z(112),EVIA), (Z(113),EVIG)
 EQUIVALENCE (Z(114),ENIC), (Z(115),ENID), (Z(116),ENIE)
 EQUIVALENCE (Z(117),ENIF), (Z(118),ENIS)
 EQUIVALENCE (Z(120),DETVEL), (Z(121),EVSUM), (Z(122),EXEN)
 EQUIVALENCE (Z(123),EXPHO), (Z(124),THICK), (Z(125),AJCEL)
 EQUIVALENCE (Z(126),TOTLEN)

KNIT = 14
 NIT = 0
 JCELL = AJCEL
 JCELL = JCELL - 4
 KCELL = 2 + (JCELL - 1)*IMAX

17 KKCEL = KCELL + 1
 IF (AMC(KKCEL).GT.0.0001*AMX(KKCEL)) GO TO 20
 IF (AM)(KKCEL).GT.0.0001*A1X(KKCEL)) GO TO 20
 IF (AME(KKCEL).GT.0.0001*AMX(KKCEL)) GO TO 20
 IF (AMF(KKCEL).GT.0.0001*AMX(KKCEL)) GO TO 20
 IF (AMG(KKCEL)).LE.0.0001*A1X(KKCEL)) GO TO 100

C ***** THE QUANTITY OF AIR IN A CELL IS TAKEN TO BE 4.083 TIMES
 C ***** THE MASS OF OXYGEN IN THE CELL

20 AIRMAS = A18(KCELL)*4.083
 PRODMAS = AMX(KKCEL) - 4.083*AM3(KKCEL)
 IF (AIRMAS.LE.PRODMAS) GO TO 30
 BBTRAN = PRODMAS/4.083
 ATRAN = 3.093*BBTRAN
 CTRAN = AMC(KKCEL)
 DTRAN = AMD(KKCEL)
 ETRAN = AME(KKCEL)
 FTRAN = AMF(KKCEL)
 GTRAN = AMG(KKCEL)
 ATRAN = AMA(KKCEL) - 3.083*AM3(KKCEL)
 GO TO 40

30 BBTRAN = A19(KCELL)
 ATRAN = 3.083*BBTRAN
 FACTR = AIRMAS/PRODMAS
 CTRAN = FACTR*AMC(KKCEL)
 DTRAN = FACTR*AMD(KKCEL)
 ETRAN = FACTR*AME(KKCEL)
 FTRAN = FACTR*AMF(KKCEL)
 GTRAN = FACTR*AMG(KKCEL)
 ATRAN = FACTR*(A18(KKCEL) - 3.083*AM3(KKCEL))

40 AMA(KKCEL) = AMA(KKCEL) + ATRAN - ATRAN
 AM3(KKCEL) = A18(KKCEL) + BBTRAN
 AMA(KCELL) = AMA(KCELL) - ATRAN + ATRAN
 AM3(KCELL) = A18(KCELL) - BBTRAN
 AMG(KCELL) = A1C(KCELL) + CTRAN

```

AMC(KKCEL) = AMC(KCELL) - CTRAN
AMD(KCELL) = AMD(KCELL) + DTRAN
AMD(KKCEL) = AMD(KKCEL) - DTRAN
AME(KCELL) = AME(KCELL) + ETRAN
AME(KKCEL) = AME(KKCEL) - ETRAN
AMF(KCELL) = AMF(KCELL) + FTRAN
AMF(KKCEL) = AMF(KKCEL) - FTRAN
AMG(KCELL) = AMG(KCELL) + GTRAN
AMG(KKCEL) = AMG(KKCEL) - GTRAN
TMASK = AMA(KCELL) + AMB(KCELL) + AMC(KCELL) + AMD(KCELL) + AME(KCELL)
1   + AMF(KCELL) + AMG(KCELL)
TMASKK = AMA(KKCEL) + AMB(KKCEL) + AMC(KKCEL) + AMD(KKCEL) + AME(KKCEL)
1   + AMF(KKCEL) + AMG(KKCEL)
IF (ABS(TMASK-AMX(KCELL)).GT.1.0E-6) GO TO 200
IF (ABS(TMASKK-AMX(KKCEL)).GT.1.0E-6) GO TO 200
KCELL = KCELL + 1
GO TO 10
100 NIT = NIT + 1
IF (NIT.GE.KNIT) GO TO 150
KCELL = KCELL + IMAX
GO TO 10
150 PRINT 8800
8800 FORMAT (10X,* SUBROUTINE INTERFACE COMPLETED *)
GO TO 300
200 PRINT 8801
8801 FORMAT (10X,* MASS BALANCE NOT CORRECT *)
300 RETURN
END

```

SUBROUTINE POC

D I M E N S I O N

```

DIMENSION AIX(6200), AMX(6200), P(6200), U(6200), V(6200),
1AMA(6200), AMH(6200), AMC(6200), AMD(6200), AME(6200), AMF(6200),
2AMG(6200), THETA(6200), DY(200), XX(101), YY(201)
DIMENSION X(101), I(200), Z(150), IZ(150), FLEFT(200)
DIMENSION TAU(100), PL(200), UL(200), PR(200), UR(200)
DIMENSION IW1(15), YAMC(200), SIGC(200), GAMC(200), IX(100)
COMMON      Z     ,XX   ,UR   ,PR   ,YY
COMMON      AID   ,AIX  ,AM   ,THETA ,AMX  ,AREA
COMMON      BIG   ,BOUNCE ,DDKN  ,DDVK  ,DKE  ,DVK
COMMON      DX    ,DY   ,E    ,F    ,FS   ,FX
COMMON      OUT   ,P    ,VAbove ,VBL0  ,PIDTS ,PPABOV
COMMON      PRR   ,PUL  ,QDT  ,P2  ,REZ   ,RHJ
COMMON      RL,RR,SIG,Q000FL,SWITCH ,TAHLM
COMMON      TAU   ,TAUDTS ,TAUDTX ,U    ,UK   ,URR
COMMON      UT    ,UU   ,UUU  ,UTEF  ,UVMAX ,V
COMMON      VAbove ,VBL0  ,VEL   ,VK   ,VT   ,VTEF
COMMON      VV    ,VVABOV ,VVRLO ,W2   ,W3   ,WPS
COMMON      WS    ,WSA  ,WSA  ,WSC  ,XL   ,XLF
COMMON      XN    ,XR   ,YL   ,YLN  ,VN   ,YU
COMMON      ZMAX  ,I    ,II   ,IV   ,IR   ,INS
COMMON      IWSA  ,IWS3  ,IWSC  ,IW1  ,J    ,JN
COMMON      JP    ,JR   ,K    ,KV   ,KP   ,KR
COMMON      CRM   ,L    ,Y    ,YA   ,IB   ,MC
COMMON      ND    ,ME   ,YZ   ,N    ,NK   ,NKMAX
COMMON      NK1   ,NO   ,NR   ,IH2
COMMON      AMA,AMH,AMC,AMD,AME,AMF,AMG

```

E Q U I V A L E N C E

EQUIVALENCE	(Z,IZ,PRO3),	(Z(2),CYCLE),	(Z(3),DT),
1(Z(4),PRINTS),	(Z(5),PRINTL),	(Z(6),DUMPT7),	(Z(7),CSTOP),
2(Z(8),PID),	(Z(9),TMZ),	(Z(10),GAM),	(Z(11),GAMD),
3(Z(12),GAMX),	(Z(13),ETH),	(Z(14),FFA),	(Z(15),FFB),
4(Z(16),TMDZ),	(Z(17),TIXZ),	(Z(18),XMAX),	(Z(19),TXMAX),
5(Z(20),TYMAX),	(Z(21),ADM),	(Z(22),AMX4),	(Z(23),DNN),
6(Z(24),DMIN),	(Z(25),FEF),	(Z(26),DTNA),	(Z(27),CVIS),
7(Z(28),NPR),	(Z(29),NPRI),	(Z(30),NC),	(Z(31),NPC),
8(Z(32),NPC),	(Z(33),IMAX),	(Z(34),IMAXA),	(Z(35),JMAX),
9(Z(36),JMAXA),	(Z(37),KMAX),	(Z(38),KMAXA),	(Z(39),NMAX)
EQUIVALENCE	(Z(40),ND),	(Z(41),KDT),	(Z(42),IXMAX),
1(Z(43),NOD),	(Z(44),NOPR),	(Z(45),NIMAX),	(Z(46),NJMAX),
2(Z(47),I1),	(Z(48),I2),	(Z(49),I3),	(Z(50),I4),
3(Z(51),N1),	(Z(52),N2),	(Z(53),N3),	(Z(54),N4),
4(Z(55),N5),	(Z(56),N6),	(Z(57),V7),	(Z(58),V8),
5(Z(59),N9),	(Z(60),N10),	(Z(61),N11),	(Z(62),NRM),
6(Z(63),TRAD),	(Z(64),XNRG),	(Z(65),SN),	(Z(66),DXN),
7(Z(67),RADER),	(Z(68),RADET),	(Z(69),RADEB),	(Z(70),DTRAD),
8(Z(71),REZFCT),	(Z(72),RSTOP),	(Z(73),SHELL),	(Z(74),BBOUND),
9(Z(75),TOZONE),	(Z(76),ECK),	(Z(77),SBOUND),	(Z(78),X1)
EQUIVALENCE	(Z(79),X2),	(Z(80),Y1),	(Z(81),Y2),
1(Z(82),CABL),	(Z(83),VISCO),	(Z(84),T),	(Z(85),GMAX),
2(Z(86),WSGD),	(Z(87),WSGX),	(Z(88),GMAJR),	(Z(89),GMAXR),
3(Z(90),S1),	(Z(91),S2),	(Z(92),S3),	(Z(93),S4),

4(Z(94),S5), (Z(95),S6), (Z(95),S7), (Z(97),S8),
5(Z(98),S9), (Z(99),S10),
7(Z(130),NFI1), (Z(131),NFI1T), (Z(132),NFI1R),
8(Z(133),NPART), (Z(134),NPART), (Z(135),NPART)

C

EQUIVALENCE (P(200),GAMC), (P(400),YAMC)
EQUIVALENCE (UR,U-,LEFT), (PR,PL,SIGC)
EQUIVALENCE (XX(2),X(1)), (YY(2),Y(1))
EQUIVALENCE (Z(1)0), P0>SUM1

C

C

C

C

LOK = -2
M = -2
IF (NC.GE.700.) AND (NC.LE.750.0) M = NC
POCSUM = 0.0
VOLM = 4.5
DO 1200 K=?,<14X
NIT = 1
TEMPEN = 0.0
TG = TH; TA(K)
TB = TG
IF (TG.GT.2000.0) TB=31.0+0.95*TG-5.0E-05*TG*TG
KOXC = ?
KOXC0 = ?
KOXM = ?
IF (K.EQ. 751) LOK=K
IF (K.EQ. 752) LOK=K
IF (K.EQ. 753) LOK=K
IF (K.EQ. 754) LOK=K
IF (K.EQ. 402) LOK=K
IF (K.EQ. 403) LOK=K
IF (K.EQ. 404) LOK=K
IF (K.EQ. 352) LOK=K
IF (K.EQ. 353) LOK=K
IF (K.EQ. 354) LOK=K
IF (K.EQ. 102) LOK=K
IF (K.EQ. 303) LOK=K
IF (K.EQ. 304) LOK=K
IF (K.EQ. 352) LOK=K
IF (K.EQ. 353) LOK=K
IF (K.EQ. 1002) LOK=K
IF (K.EQ. 1003) LOK=K
IF (K.EQ. 1004) LOK=K
IF (K.EQ. 1052) LOK=K
IF (K.EQ. 1053) LOK=K
IF (K.EQ. 1054) LOK=K
IF (K.EQ. 2500) LOK = K
IF (K.EQ. 3500) LOK = K
IF (K.EQ. 4500) LOK = K
IF (NC.EQ.1.AND.K.EQ.LOK) PRINT 3000,NIT,AMX(K),AMY(K),AMB(K),
1 AMC(K),A1D(K),AME(K),AMF(K),AMG(K),TEMPEN,AIX(K)
IF (AMX(K).LE.0.0) GO TO 1201
C **** TEST FOR CAPABILITY OF COMBUSTION IN CELL
IF (AMB(K).LT.0.001*AMX(K)) GO TO 1000
IF (AMG(K).GE.0.001*AMY(K)) GO TO 5
IF (AMF(K).GE.0.001*AMX(K)) GO TO 5

```

IF (AMC(K).LT.0.001*AMX(K)) GO TO 1000
C ***** COMPUTE REACTION RATES AT CELL TEMPERATURE
5 RAT12 = 1.9E+16/SQRT(TG)
RAT11 = RAT12*EXP(-5.92E04/TB)
RAT02 = 1.0E+16*EXP(-3.5E+03/(8.31E+07*TG))
RAT04 = 1.0E+19/TG
RAT06 = 3.0E+16/SQRT(TG)
C ***** COMPUTE AMOUNT OF ATOMIC OXYGEN AVAILABLE FOR REACTION
AMOLE = AMA(K)/(28.0*VOLM)
BMOLE = AMB(K)/(32.0*VOLM)
CMOLE = AMC(K)/(28.0*VOLM)
DMOLE = AMD(K)/(44.0*VOLM)
EMOLE = AME(K)/(18.0*VOLM)
FMOLE = AMF(K)/(2.0*VOLM)
GMOLE = AMG(K)/(12.0*VOLM)
TMOLE = AMOLE+BMOLE+CMOLE+DMOLE+EMOLE+FMOLE+GMOLE
DOX = 2.0*RAT11*BMOLE*TMOLE*DT
OX = VOLM*DOX*16.0
NIT = 6
IF (NC.EQ.1.AND.K.EQ.LOK) PRINT 9003,K,THETA(K),TG,RAT11,
1 RAT12,TMOLE,BMOLE,DOX,OX
IF (NC.EQ.1.AND.K.EQ.LOK) PRINT 8000,NIT,AMX(K),AMA(K),AMB(K),
1 AMC(K),AMD(K),AME(K),AMF(K),AMG(K),TEMPEN,OX
IF (OX.GT.AMB(K)) OX = AMB(K)
C ***** DETERMINE WHICH FUELS ARE IN CELL
IF (AMC(K)+AMF(K).LE.0.002*AMX(K)) GO TO 10
IF (AMC(K)+AMG(K).LE.0.002*AMX(K)) GO TO 20
IF (AMF(K)+AMG(K).LE.0.002*AMX(K)) GO TO 30
C ***** COMPUTE QUANTITY OF ATOMIC HYDROGEN
HOX = SQRT(FMOLE*EXP(-5.22E-04/TG))
OH = 1.5E-38
C ***** COMPUTE RATIOS OF PRODUCTION OF H2O,CO2, AND CO
H2O = RAT04*OH*HOX*TMOLE
CO = RAT06*GMOLE*DOX*TMOLE
COO = RAT02*CMOLE*DOX*TMOLE
C ***** TEST TO DETERMINE IF ALL THREE FUELS ARE PRESENT IN THE CELL
IF (AMG(K).LE.0.001*AMX(K)) GO TO 40
IF (AMF(K).LE.0.001*AMX(K)) GO TO 40
IF (AMC(K).LE.0.001*AMX(K)) GO TO 40
C ***** COMPUTE THE AMOUNT OF ATOMIC OXYGEN GOING TO EACH REACTION -
RSUM = H2O + CO + COO
OXC = (CO*OX)/RSUM
OXCO = (COO*OX)/RSUM
OXH = (H2O*OX)/RSUM
C ***** TEST FOR ENOUGH OF EACH FUEL TO BURN THE ABOVE OXYGEN
7 AMGG = OXC/1.334
IF (AMG(K).LE.1.0E-15) GO TO 8
IF (AMGG.GT.AMG(K)) GO TO 80
9 AMFF = OXM/8.0
IF (AMF(K).LE.1.0E-15) GO TO 9
IF (AMFF.GT.AMF(K)) GO TO 90
9 AMCC = OXCO/0.572
IF (AMC(K).LE.1.0E-15) GO TO 11
IF (AMCC.GT.AMC(K)) GO TO 120
11 NIT = ?
IF (NC.EQ.1.AND.K.EQ.LOK) PRINT 9000,NIT,AMX(K),AMA(K),AMB(K),
1 AMC(K),AMD(K),AME(K),AMF(K),AMG(K),TEMPEN,OX
C ***** ACCOMPLISH ACTUAL BURN REACTIONS

```

```

TEMPEN = TEMPEN + 9.3E10*AMGG
AMG(K) = AMG(K) - AMGG
AMB(K) = A19(K) - OXG
AMC(K) = A4X(K)-A4A(K)-AMB(K)-AMD(K)-A1E(<)-A4F(<) - AMG(<)
TEMPFN = TEMPEN + 1.429E12*AMFF
AMF(K) = A1F(K) - AMFF
AM9(K) = A19(K) - OXM
AME(K) = A4X(K)-A4A(K)-AMB(K)-AMC(K)-AMD(K)-AMF(K)-AMG(K)
TEMPEN = TEMPEN + 1.92E11*AMCC
AMC(K) = A1C(K) - AMCC
AMB(K) = A19(K) - OXCO
AMD(K) = A4X(K)-A4A(K)-AMB(K)-AME(K)-AMC(K)-AMF(K)-AMG(K)
NIT = 2
IF (NC.EQ.4.AND.K.EQ.LOK) PRINT 9000,NIT,AMX(K),AMA(<),AMB(K),
1 AMG(K),AMD(K),AME(K),AMF(K),AMG(K),TEMPEN,DX
GO TO 1100
1. IF (AMG(K).LT.OX/1.334) GO TO 12
AMGG = OX/1.334
OXIAS = OX
GO TO 14
12 AMGG = AMG(K)
OXIAS = 1.334*AMGG
14 TEMPEN = TEMPEN + 9.3E+10*AMGG
AMG(K) = A4G(K) - AMGG
AM7(K) = A19(K) - OXIAS
AMC(K) = A4X(K)-A4A(K)-AMD(K)-AME(K)-A4F(K)-AMG(K)-AMB(K)
NIT = 3
IF (NC.EQ.1.AND.K.EQ.LOK) PRINT 9000,NIT,AMX(K),AMA(<),AMB(K),
1 A1C(K),AMD(K),AME(K),AMF(K),AMG(K),TEMPEN,DX
GO TO 1100
21 IF (AMF(K).LT.OX/3.0) GO TO 22
AMFF = OX/3.0
OXIAS = OX
GO TO 24
22 AMFF = A1F(K)
OXIAS = 3.0*AMFF
24 TEMPEN = TEMPEN + 1.429E12*AMFF
AMF(K) = A1F(K) - AMFF
AM7(K) = A19(K) - OXIAS
AMC(K) = A4X(K)-A4A(K)-AMC(K)-A1D(K)-A4F(K)-AMB(K)-AMG(K)
NIT = 4
IF (NC.EQ.1.AND.K.EQ.LOK) PRINT 9000,NIT,AMX(K),AMA(<),AMB(K),
1 AMG(K),AMD(K),A1E(K),AMF(K),AMG(K),TEMPEN,DX
GO TO 1100
31 IF (A1C(K).LT.OX/3.572) GO TO 32
AMCC = OX/3.572
OXIAS = OX
GO TO 34
32 AMCC = AMC(K)
OXIAS = 0.572*AMCC
34 TEMPEN = TEMPEN + 1.92E11*AMCC
AMC(K) = A1C(K) - AMCC
AM7(K) = A19(K) - OXIAS
AMD(K) = A4X(K)-A4A(K)-AMC(K)-A1E(K)-A4D(K)-AMF(K)-AMG(K)
NIT = 5
IF (NC.EQ.4.AND.K.EQ.LOK) PRINT 9000,NIT,AMX(K),AMA(<),AMB(K),
1 AMG(K),AMD(K),AME(K),AMF(K),AMG(K),TEMPEN,DX
GO TO 1100

```

```

4. IF (AMG(K).LE.0.001*AMX(K)) GO TO 50
   IF (AMF(K).LE.0.001*AMX(K)) GO TO 60
   GO TO 70
5) RSUM = H2O + CO2
   OX2 = 0.0
   KOXC = 1
   OXCO = (CO2*OX)/RSUM
   IF (KOXC0.EQ.1) OXCO = 0.0
   OXH = (H2O*OX)/RSUM
   IF (KOXH.EQ.1) OXH = 0.0
   GO TO 7
6) RSUM = CO + CO2
   OXC = (CO*OX)/RSUM
   IF (KOC0.EQ.1) OXC = 0.0
   OXCO = (CO2*OX)/RSUM
   IF (KOC0.EQ.1) OXCO = 0.0
   OXH = 0.0
   KOXH = 1
   GO TO 7
7) RSUM = CO + H2O
   OX2 = (CO*OX)/RSUM
   IF (KOC0.EQ.1) OXC = 0.0
   OXCO = 0.0
   KOXC0 = 1
   OXH = (H2O*OX)/RSUM
   IF (KOC0.EQ.1) OXH = 0.0
   GO TO 7
8) AMGG = AMG(K)
   OXMAS = 1.334*AMGG
   TEMPEN = TEMPEI + 9.3E+10*AMGG
   AMG(K) = 0.0
   AMB(K) = AMB(K) - OXMAS
   AMC(K) = A1X(K)-AMA(K)-AMB(K)-A1D(K)-A1E(K)-AMF(K)-A1G(K)
   OX = OX - OXMAS
   GO TO 5C
9) AMFF = AMF(K)
   OXMAS = 3.3*AMFF
   TEMPEN = TEMPEI + 1.425E+12*AMFF
   AMF(K) = 0.0
   AMB(K) = AMB(K) - OXMAS
   AME(K) = A1X(K)-AMA(K)-AMB(K)-AMC(K)-A1D(K)-AMF(K)-A1G(K)
   OX = OX - OXMAS
   GO TO 6C
10) AMCC = AMC(K)
   OXMAS = 3.572*AMCC
   TEMPEN = TEMPEI + 1.02E+11*AMCC
   AMC(K) = 0.0
   AMB(K) = AMB(K) - OXMAS
   AMD(K) = A1X(K)-AMA(K)-AMB(K)-AMC(K)-A1E(K)-AMF(K)-A1G(K)
   OX = OX - OXMAS
   GO TO 7L
100) IF (NC.EQ.1.AN).K.EQ.LDK) PRINT 8001,K
   GO TO 1200
1100 AIX(K) = AIX(K) + TEMPEN
   ETH = ETH + TEMPEN
   POCSUM = POCSUM + TEMPEN
   NIT = 3
   IF (NC.EQ.1.AN).K.EQ.LDK) PRINT 9000,NIT,AMX(K),AMA(K),AMR(K),

```

```

1 AMG(K),AMD(K),AME(K),AMF(K),AMG(K),TEMPEN,AIX(K)
1200 CONTINUE
PRINT 8002,POCSUM
RETURN
8000 FORMAT (1X,I2,10(1X,E12.5))
8001 FORMAT (1X,*NO COMBUSTION IN CELL *,I5)
8002 FORMAT (2X,*POC ENERGY DEPOSITED = *,E16.8,/1)
8003 FORMAT (1X,I5,9(1X,E12.5))
END

```

SUBROUTINE STEADY

```

      D I M E N S I O N
DIMENSION AIX(6200),AMX(6200),P(6200),U(6200),V(6200),
1AMA(6200),AMR(6200),AMG(6200),AMT(6200),AME(6200),AMF(6200),
2AMG(6200),THETA(6200),DY(200),XX(101),YY(201)
DIMENSION X(101), Y(200), Z(150), IZ(150), FLEFT(200)
DIMENSION TAU(100), PL(200), UL(200), PR(200), UR(200)
DIMENSION IW1(15), YM0(200), SIG0(200), GAM0(200), IX(100)
COMMON Z ,XX ,UR ,PR ,YY
COMMON AID ,AIX ,AM ,THETA ,AMX ,AREA
COMMON BIG ,BOUNCE ,DXN ,DVK ,JKE ,DVK
COMMON DX ,DY ,E ,FD ,FS ,FX
COMMON OUT ,P ,PABOVE ,PBLO ,PIOTS ,PPABOV
COMMON PRR ,PUL ,QDT ,RC ,REZ ,RMJ
COMMON RL,RR,SIG,Q000FL,SWITCH ,TABLM
COMMON TAU ,TAUDTS ,TAUDTY ,U ,JK ,URR
COMMON UT ,UU ,UUU ,UTEF ,UVMAX ,V
COMMON VAbove ,Vold ,Vel ,VK ,VT ,VTEF
COMMON VV ,VVABOV ,VV3L0 ,W2 ,W3 ,WPS
COMMON HS ,HSA ,HSB ,HSC ,XL ,XLF
COMMON XN ,XH ,YL ,YLN ,YN ,YU
COMMON ZMAX ,I ,II ,IV ,IR ,IWS
COMMON IHSA ,IHSB ,IHSC ,IH1 ,J ,JN
COMMON JP ,JR ,K ,K4 ,KP ,KR
COMMON LR1 ,L ,L ,IA ,IB ,MC
COMMON M0 ,ME ,M2 ,V ,NK ,NKMAX
COMMON NK1 ,NO ,NR ,IH2
COMMON AMA,AM3,AMC,AM1,AME,AMF,AMG

```

E Q U I V A L E N C E

1(Z(4),PRINTS),	(Z(2),PRO3),	(Z(2),CYCLE),	(Z(3),DT),
2(Z(3),PID()),	(Z(3),PRINTL),	(Z(6),DUMPT?),	(Z(7),CSTOP),
3(Z(12),GAMX),	(Z(13),FTM),	(Z(10),GAM),	(Z(11),GAM),
4(Z(16),THDZ),	(Z(17),THXZ),	(Z(14),FFA),	(Z(15),FFB),
5(Z(20),TMAX),	(Z(21),AMD4),	(Z(18),KMAX),	(Z(19),TXMAX),
6(Z(24),DMIN),	(Z(25),FEF),	(Z(22),AMX4),	(Z(23),DNN),
7(Z(28),NPR),	(Z(29),NPRI),	(Z(26),DTNA),	(Z(27),CVIS),
8(Z(32),NRC),	(Z(33),IMAX),	(Z(30),VCP),	(Z(31),VPC),
9(Z(36),JMAXA),	(Z(37),KMAX),	(Z(34),IMAXA),	(Z(35),JMAX),
		(Z(38),KMAXA),	(Z(39),NMAX)

EQUIVALENCE	(Z(40),ND),	(Z(41),KDT),	(Z(42),INMAX),
1(Z(43),NOD),	(Z(44),NOPR),	(Z(45),VIMAX),	(Z(46),NMAX),
2(Z(47),I1),	(Z(48),I2),	(Z(49),I3),	(Z(50),I6),
3(Z(51),N1),	(Z(52),N2),	(Z(53),N3),	(Z(54),N4),
4(Z(55),N5),	(Z(56),N6),	(Z(57),N7),	(Z(58),N8),
5(Z(59),N9),	(Z(60),N10),	(Z(61),V11),	(Z(62),NRM),
6(Z(63),TRAD),	(Z(64),XNRG),	(Z(65),SN),	(Z(66),DXN),
7(Z(67),RADER),	(Z(68),RADET),	(Z(69),RADE9),	(Z(70),OTRAD),
8(Z(71),REZFCT),	(Z(72),RSTOP),	(Z(73),SHELL),	(Z(74),BBOUND),
9(Z(75),TOZONE),	(Z(76),ECK),	(Z(77),SBOUND),	(Z(78),A1)
EQUIVALENCE	(Z(79),X2),	(Z(80),V1),	(Z(81),V2),
1(Z(82),CABLN),	(Z(83),VISCV),	(Z(84),T),	(Z(85),GMAX),
2(Z(86),HSGD),	(Z(87),HSGX),	(Z(88),GMADR),	(Z(89),GMAR),
3(Z(90),S1),	(Z(91),S2),	(Z(92),S3),	(Z(93),S4),
4(Z(94),S5),	(Z(95),S6),	(Z(96),S7),	(Z(97),S8),
5(Z(98),S9),	(Z(99),S10),		
7(Z(130),NFITR),	(Z(131),NFITI),	(Z(132),NFITR),	
8(Z(133),NPART),	(Z(134),NPART),	(Z(135),NPART),	

C

EQUIVALENCE(P(200),GAMC), (P(400),YAMC)	
EQUIVALENCE(UR,UL,FLEFT),	(PR,PL,SIGC)
EQUIVALENCE(XX(2),X(1)),	(YY(2),Y(1))

C

```

VEL = 0.0
FLAG2 = 12.0
20 FLAG1 = 0.0
30 READ (4) PR(1), PR(2), N3
      WRITE (6,8106) PR(1), PR(2), N3
      IF (PR(1).EQ.555.0) 40,31
31 IF (PR(1).EQ.666.0) 32,35
32 WRITE (6,8109)
      GO TO 1000
35 FLAG1 = FLAG1 + 1.0
      IF (FLAG1 - FLAG2) 34,34,9901
34 WRITE (6,8106) FLAG1
      GO TO 3C
40 READ (4) (Z(I), I=1,3)
      WRITE (6,8104) (Z(I), I=1,3)
      READ (4) (DUM,DUM,DUM,DUM,P(I),DUM, I=1,KMAXA)
      WRITE (6,8106) (P(I), I=1,3)
      READ (4) DUM
      READ (4) DUM
      READ (4) DUM
      IF (VEL) 51,50,50
50 DO 55 I = 1,KMAX
55 AMX(I) = P(I)
      VEL = 1.0
      WRITE (6,8102)
      GO TO 30
60 SUM = 0.0
      I = 3
70 DO 75 J = ?,JMAX
      K = I + 1 + (J - 1)*IMAX
      DIFF = ABS(P(K)) - ABS(AMX(K))
75 SUM = SUM + ABS(DIFF)
80 WRITE (6,8102) PR(2), SUM

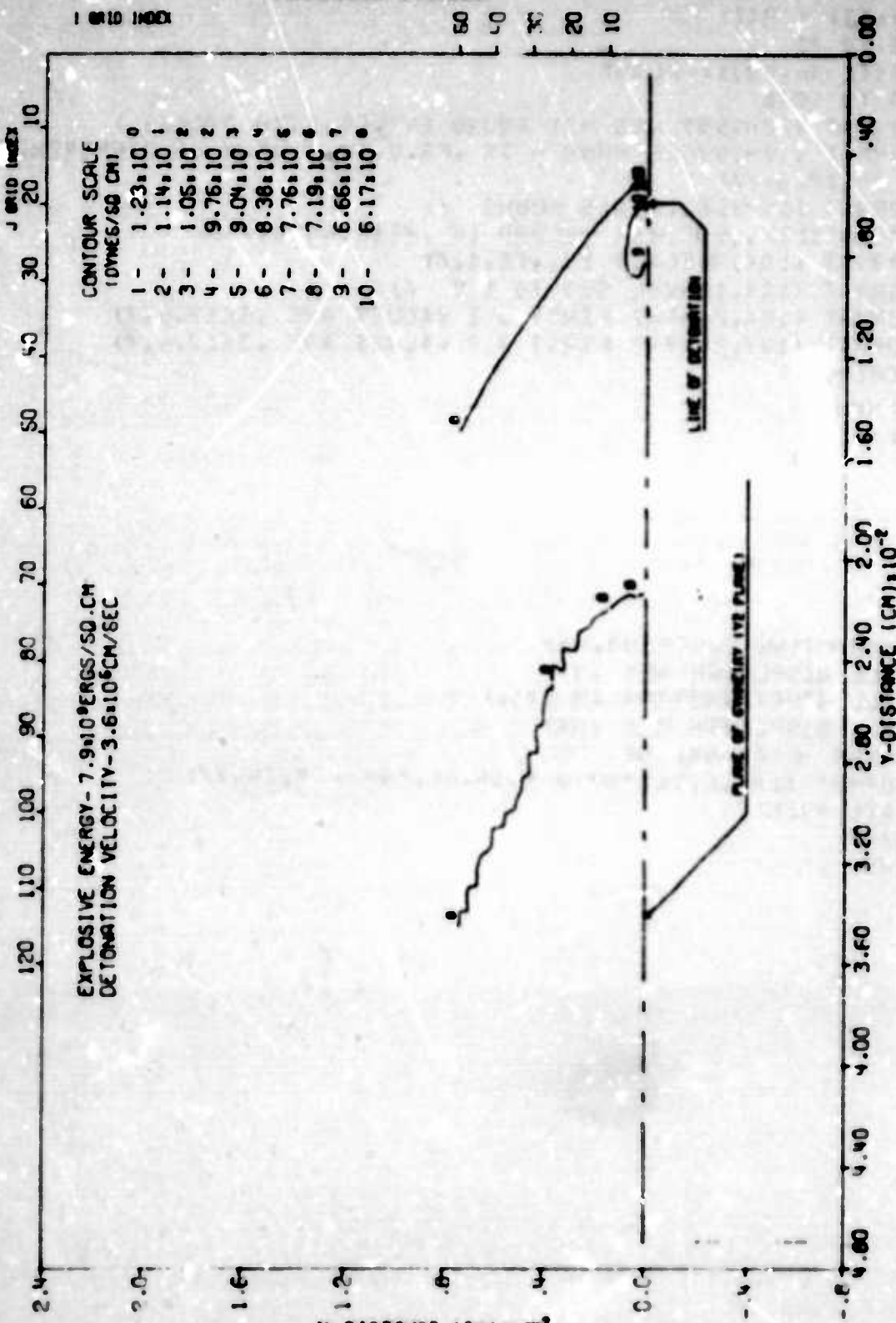
```

```
IF (CSTOP - PR(2)) 1000,1000,90
90 DO 95 I = 1,KMAX
95 AMX(I) = P(I)
GO TO 20
9901 WRITE (6,8001) FLAG2
GO TO 1000
8001 FORMAT (22H0555 WAS NOT FOUND IN ,F5.1,74 CYCLES )
8002 FORMAT (17H0C/CLE NUMBER IS ,F5.0,5X,22HSUM OF DIFFERENCES IS ,
1 0E12.6 //)
8003 FORMAT (16H0666.0 WAS FOUND /)
8006 FORMAT(10X,16HFIRST RECORD IS ,2E12.4,I6,/)
8100 FORMAT (10X,9MFLAG1 IS ,F5.1,/ )
8102 FORMAT (10X,14HVEL SET TO 1.0 /)
8104 FORMAT (10X,25HTHE FIRST 3 Z VALUES ARE ,3E12.6,/ )
8106 FORMAT (10X,25HTHE FIRST 3 P VALUES ARE ,3E12.6,/ )
1000 REWIND 4
RETURN
END
```

```
SUBROUTINE ERROR(NR,NK)
CALL DISPLAY(5H NR= ,NR)
CALL TIME(14HERROR IN SHELL )
CALL DISPLAY(5H NK= ,NK)
PRINT %00, NR, NK
8000 FORMAT (1H ,/,5X, *NR = *,I4,4X,*NK = *,I4,/)
CALL PRINTZ
STOP
END
```

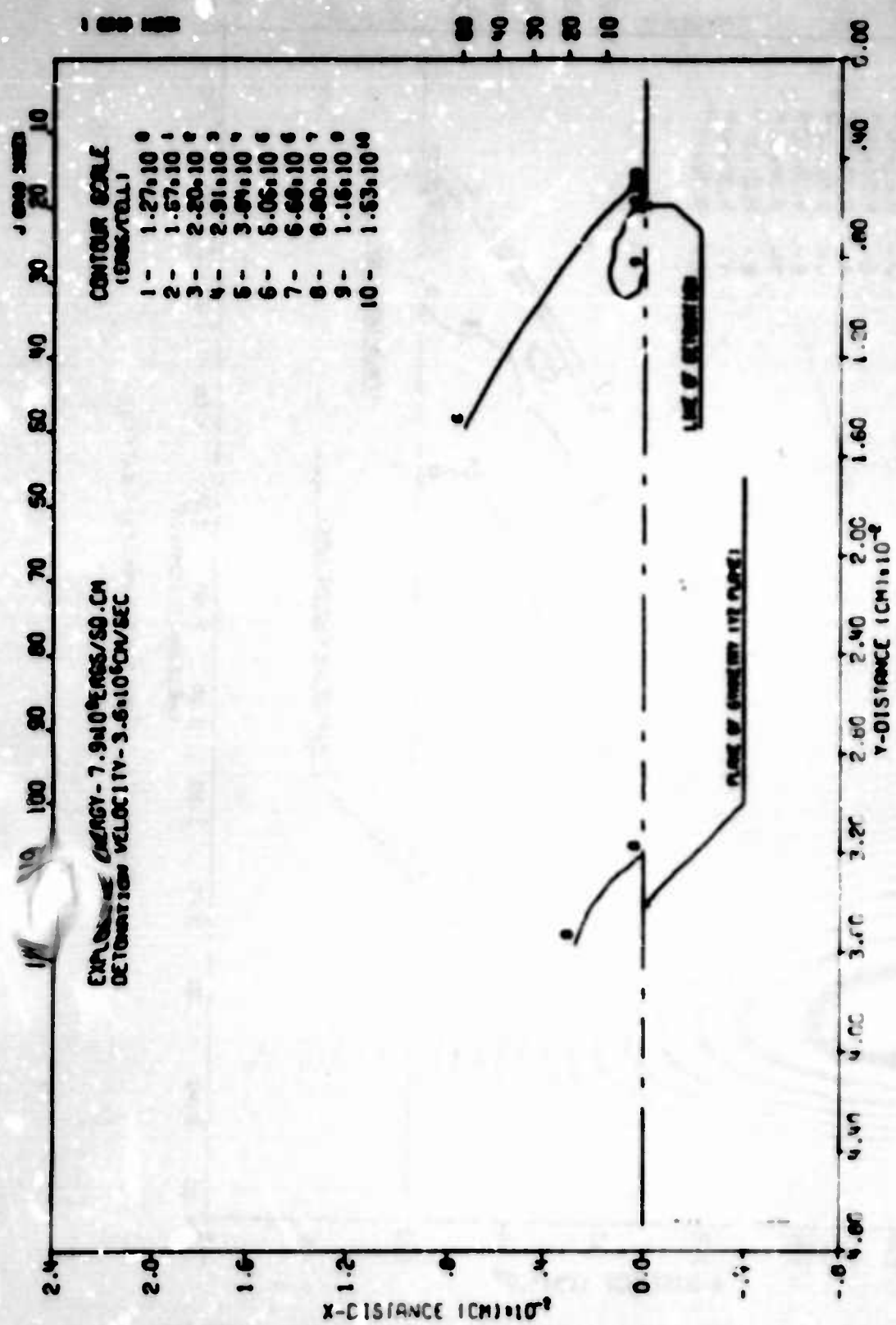
APPENDIX D

ADDITIONAL PLOTS FOR THE MASS AND ENERGY
ADDITION PROBLEM



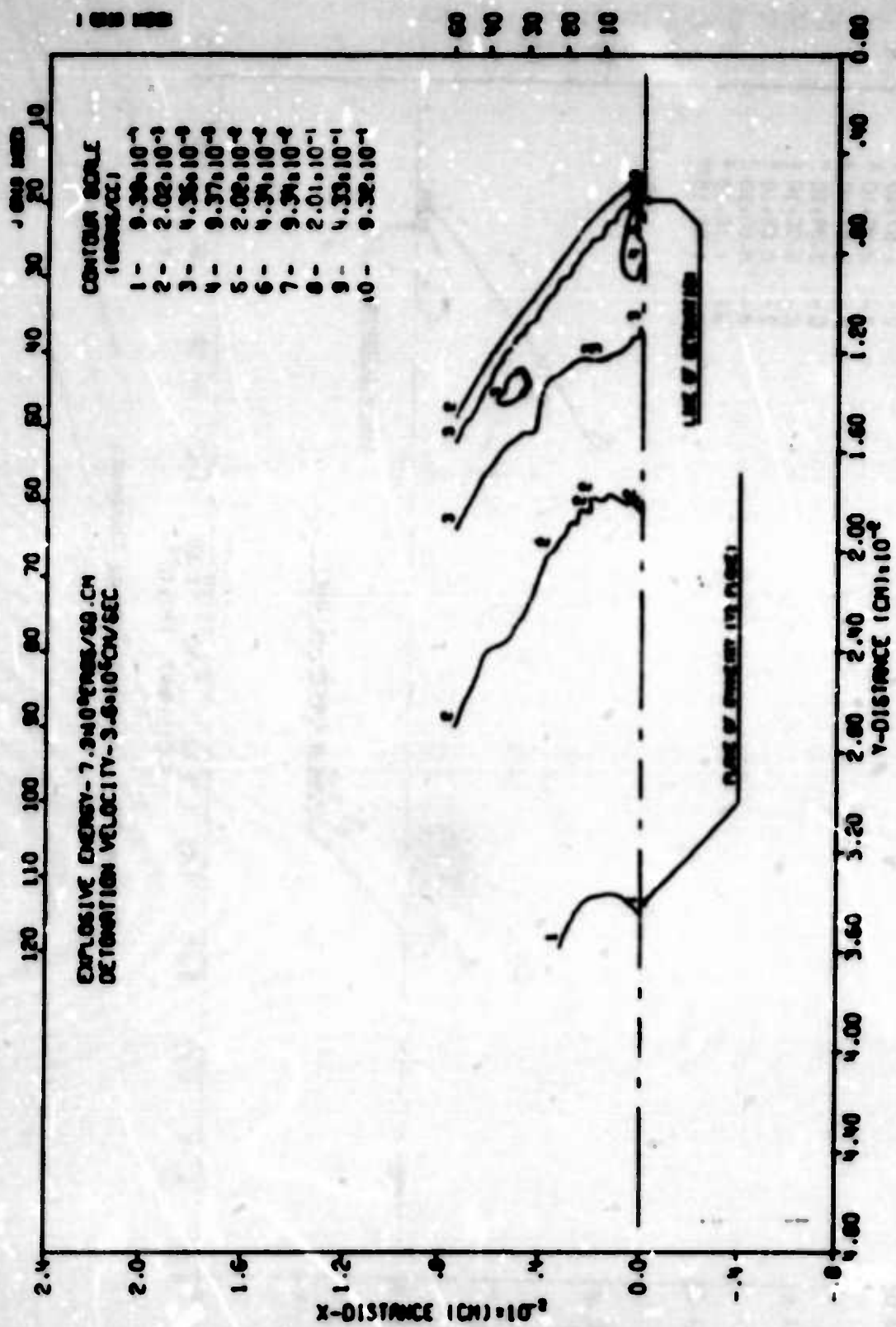
SHELTIC7 CALCULATION OF EXPLOSIVE SOURCE IN HYPERSONIC FLOW (WITH PDC)
TIME .005CM1 SEC CYCLE 1200 PROBLEM 30.1CC

Figure D1. Constant Pressure Contours (Isobars)



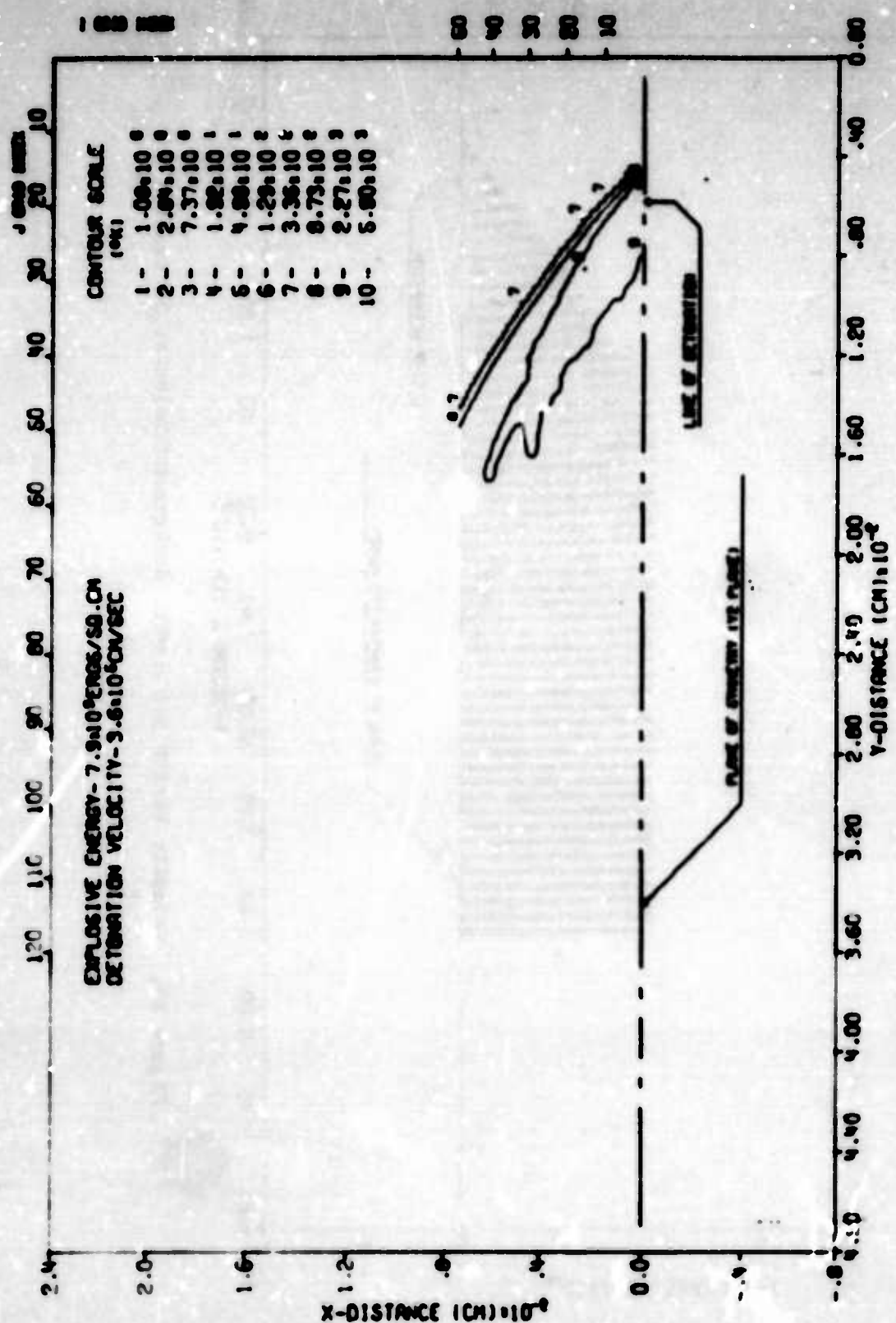
SMELTC7 CALCULATION OF EXPLOSIVE SOURCE IN HYPERSONIC FLOW (WITH PDC)
TIME .005041 SEC CYCLE 1200 PROBLEM 30.000

Figure D2. Constant Energy Contours



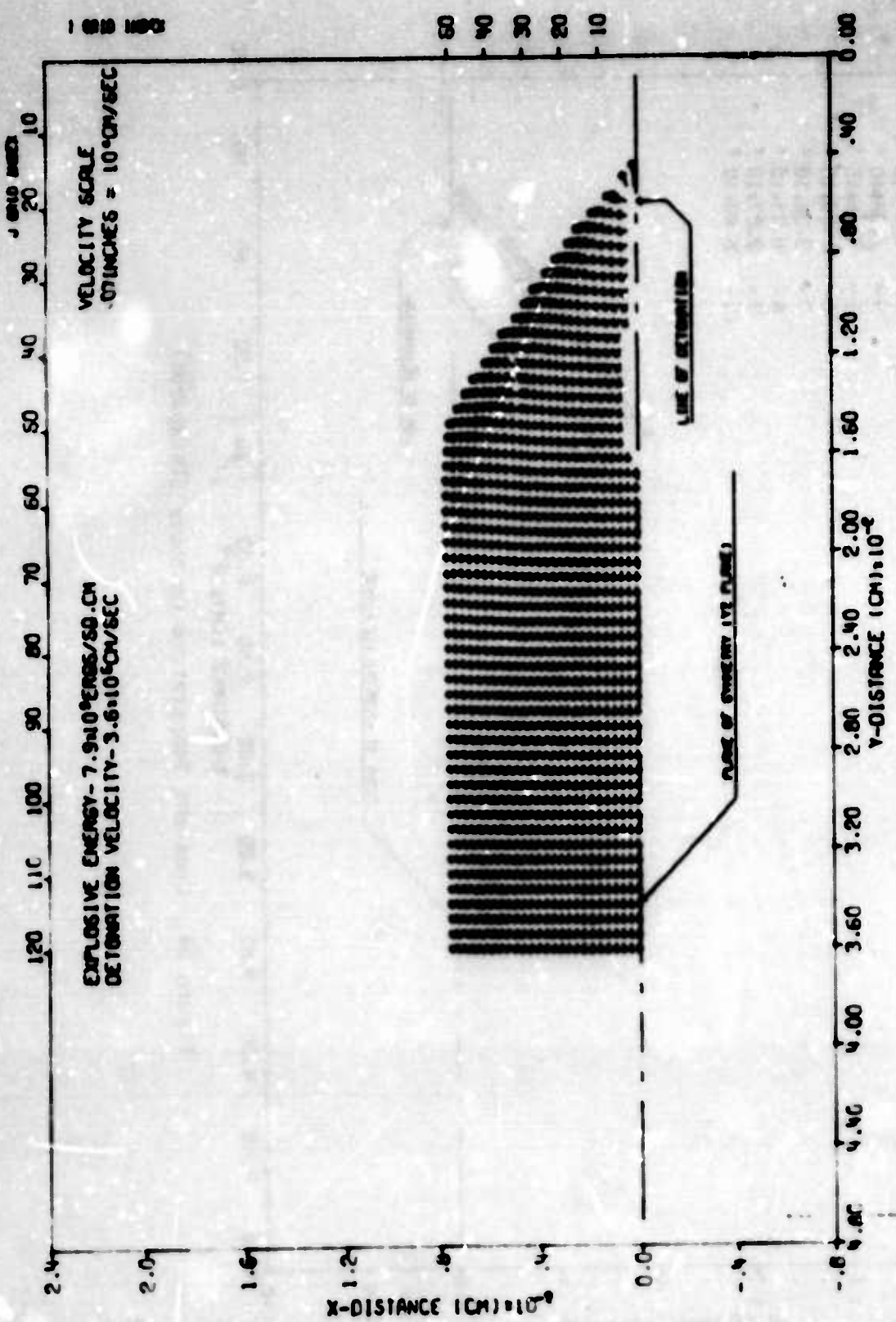
SNELLC7 CALCULATION OF EXPLOSIVE SOURCE IN HYPERSONIC FLOW (WITH POC)
 TIME .006041 SEC CYCLE 1200 PROBLEM 30.000

Figure D3. Constant Density Contours



SMELT-7 CALCULATION OF EXPLOSIVE SOURCE IN HYPERSONIC FLOW (INIT. PROB)
TIME .05541 SEC CYCLE 1200 PROBLEM 30.000

Figure D4. Constant Temperature Contours (Isotherms)



SHELTER CALCULATION OF EXPLOSIVE SOURCE IN HYPERSONIC FLOW (INITIAL PDC)
TIME .00501 SEC CYCLE 1200 PROBLEM 3C.000

Figure D5. Velocity Vector Field with Background Velocity Subtracted

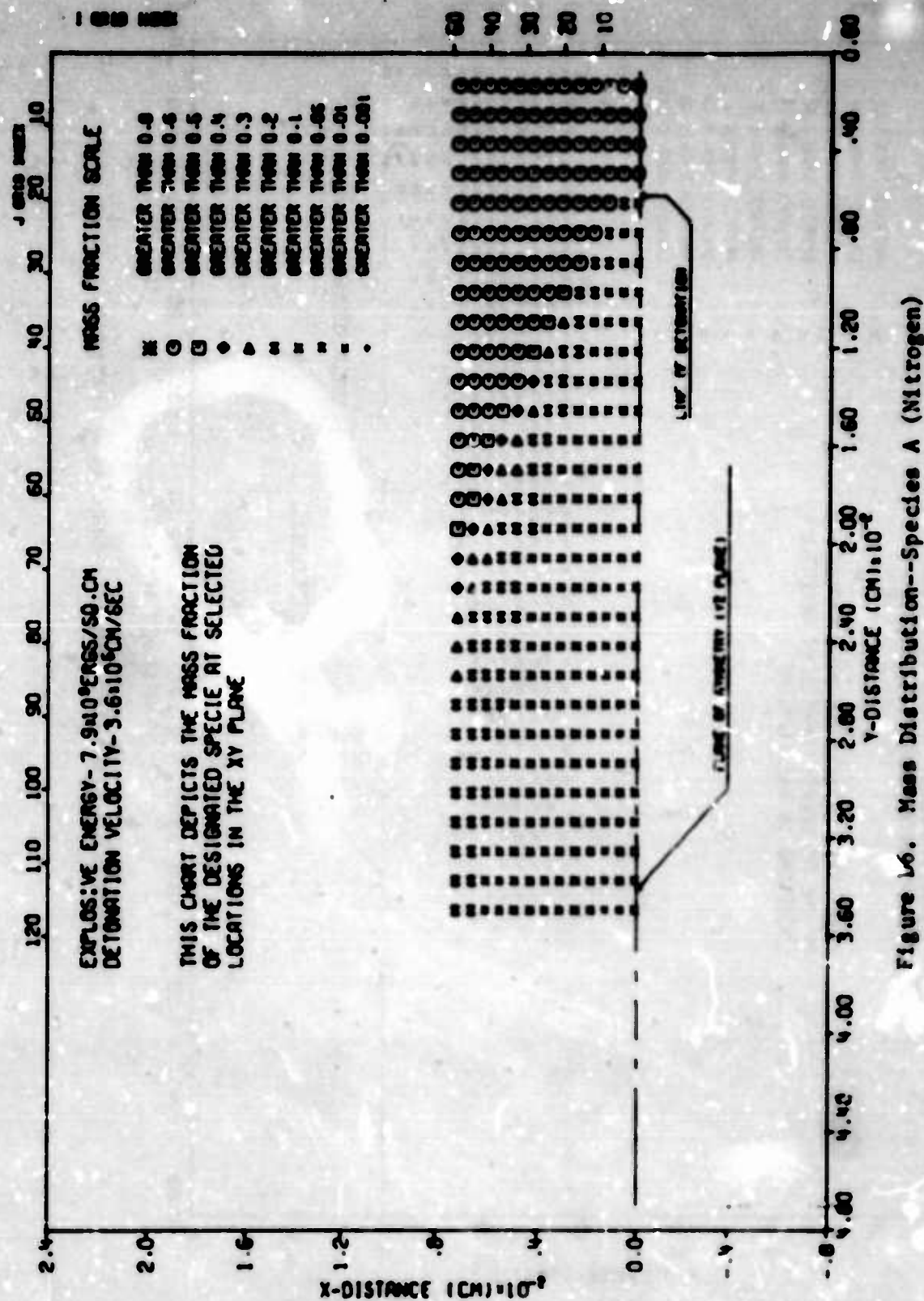
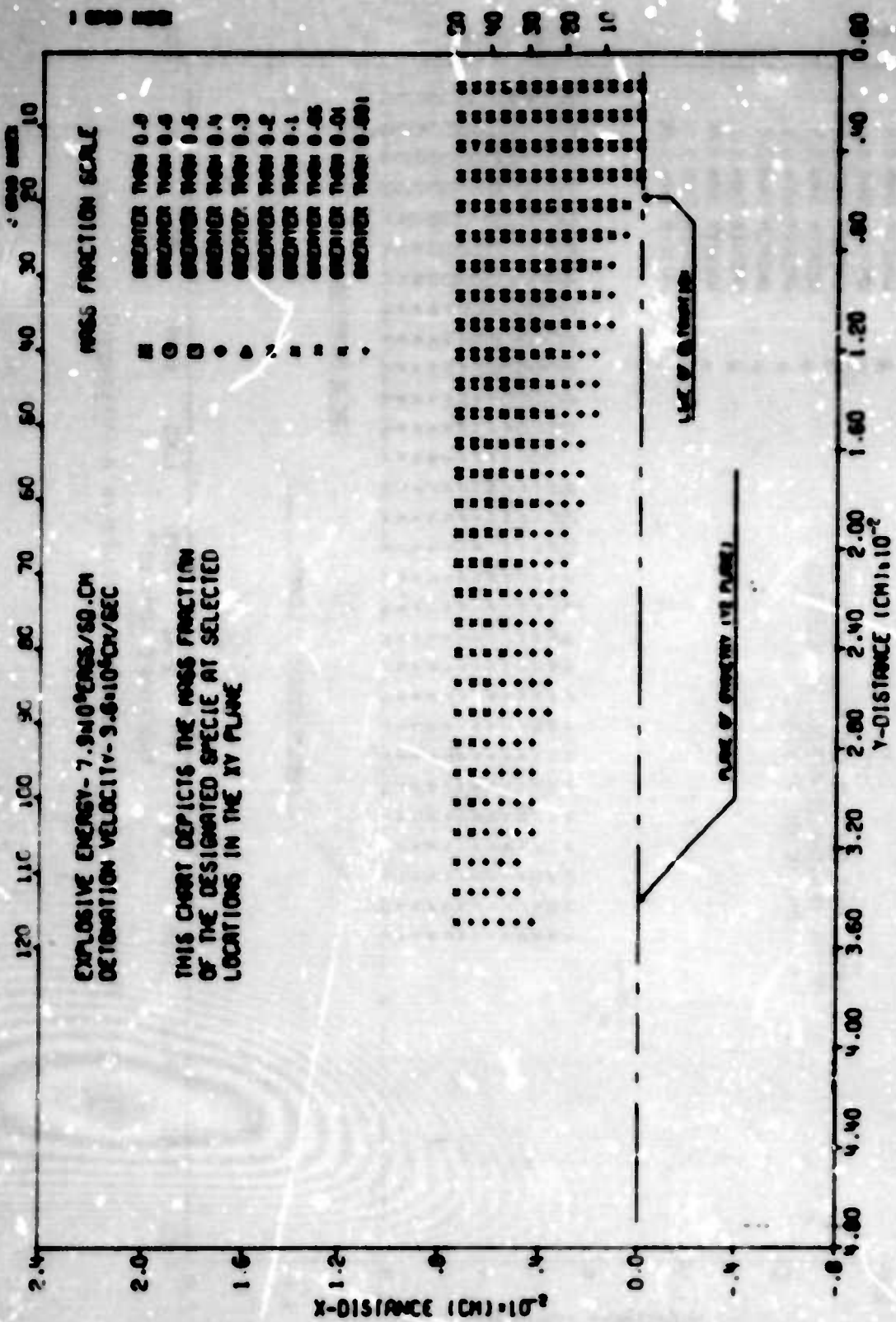


Figure 16. Mass Distribution--Species A (Nitrogen)

SMELTC7 CALCULATION OF EXPLOSIVE SOURCE IN HYPERSONIC FLOW (WITH PDC)
TIME .005041 SEC CYCLE 1200 PROBLEM 30.000



SHELTC7 CALCULATION OF EXPLOSIVE SOURCE IN HYPERSONIC FLOW (WITH POC)
TIME .00504 SEC CYCLE 1200 PROBLEM 30.000

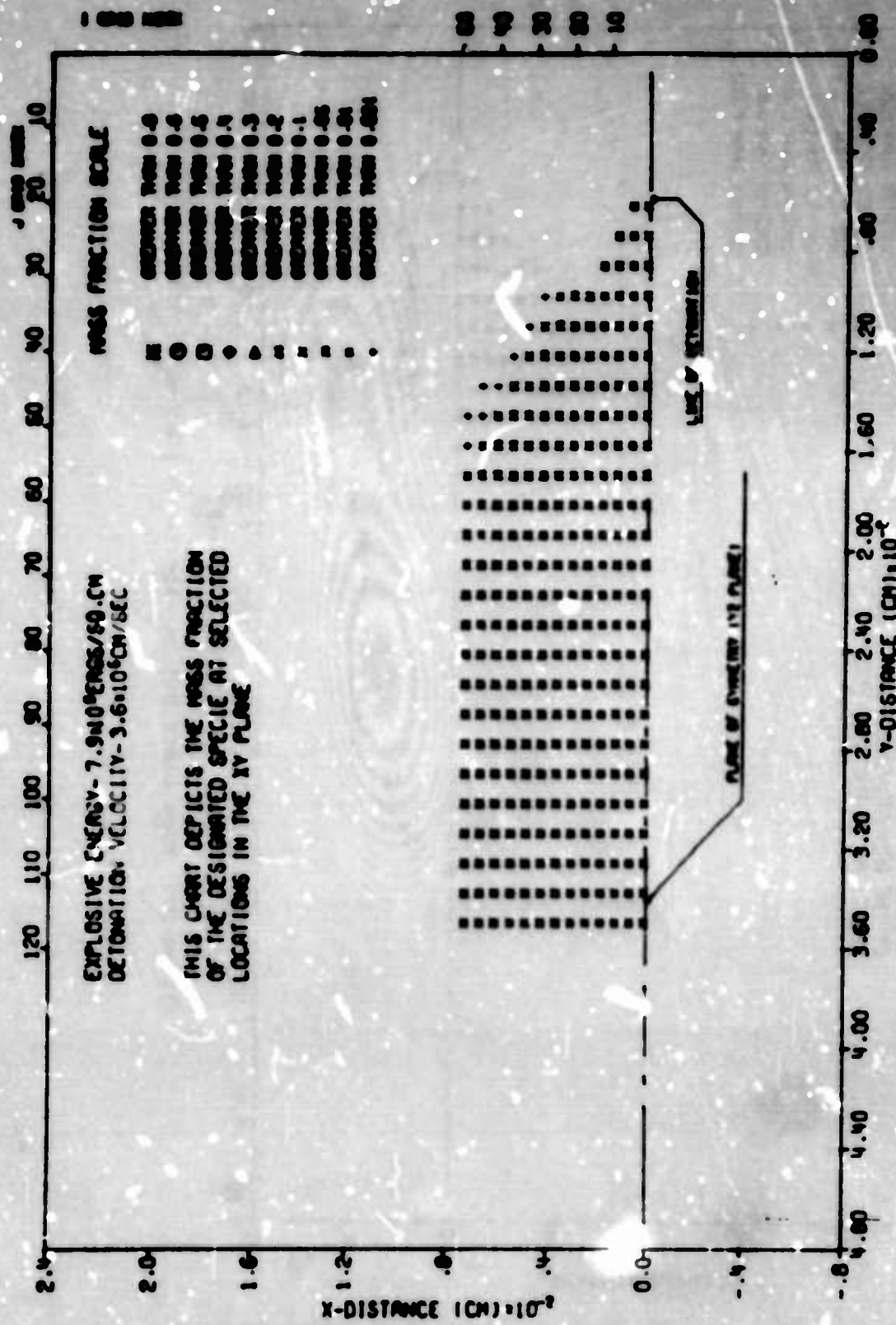
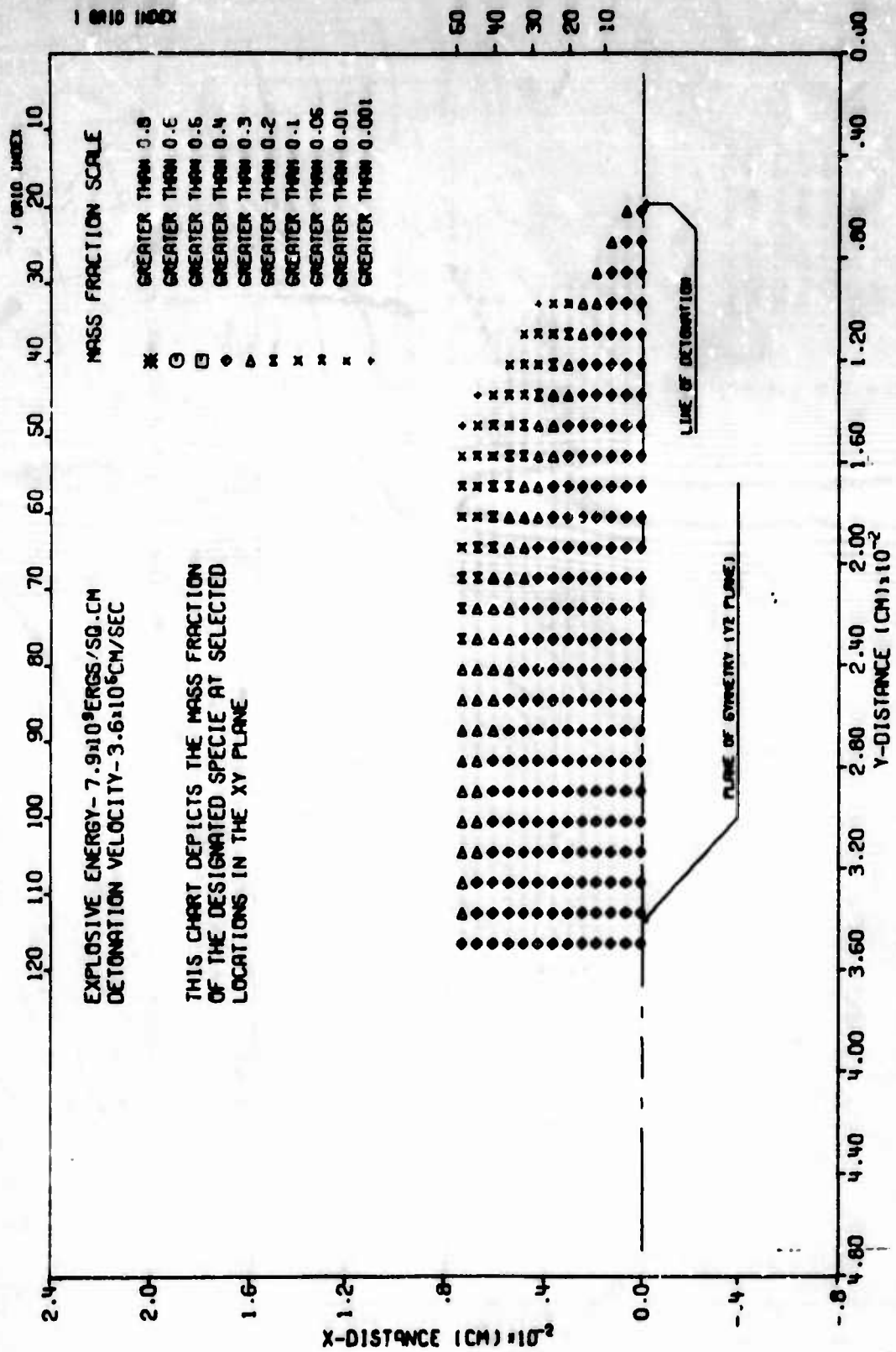
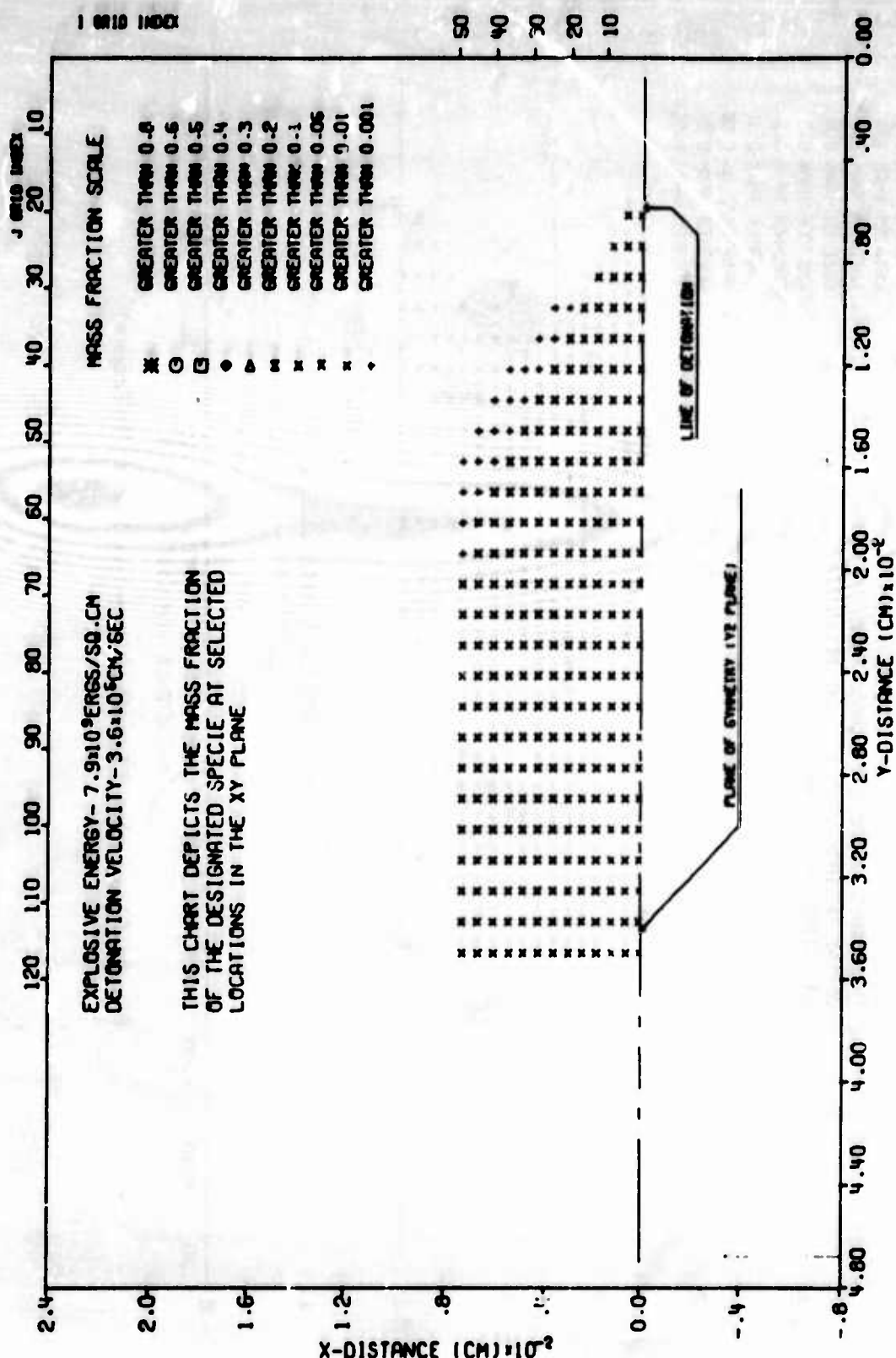


Figure D8. Mass Distribution on--Species C (Carbon Monoxide)



SHELTC7 CALCULATION OF EXPLOSIVE SOURCE IN HYPERSONIC FLOW (WITH PDC)
 TIME .005041 SEC CYCLE 1200 PROBLEM 30.000

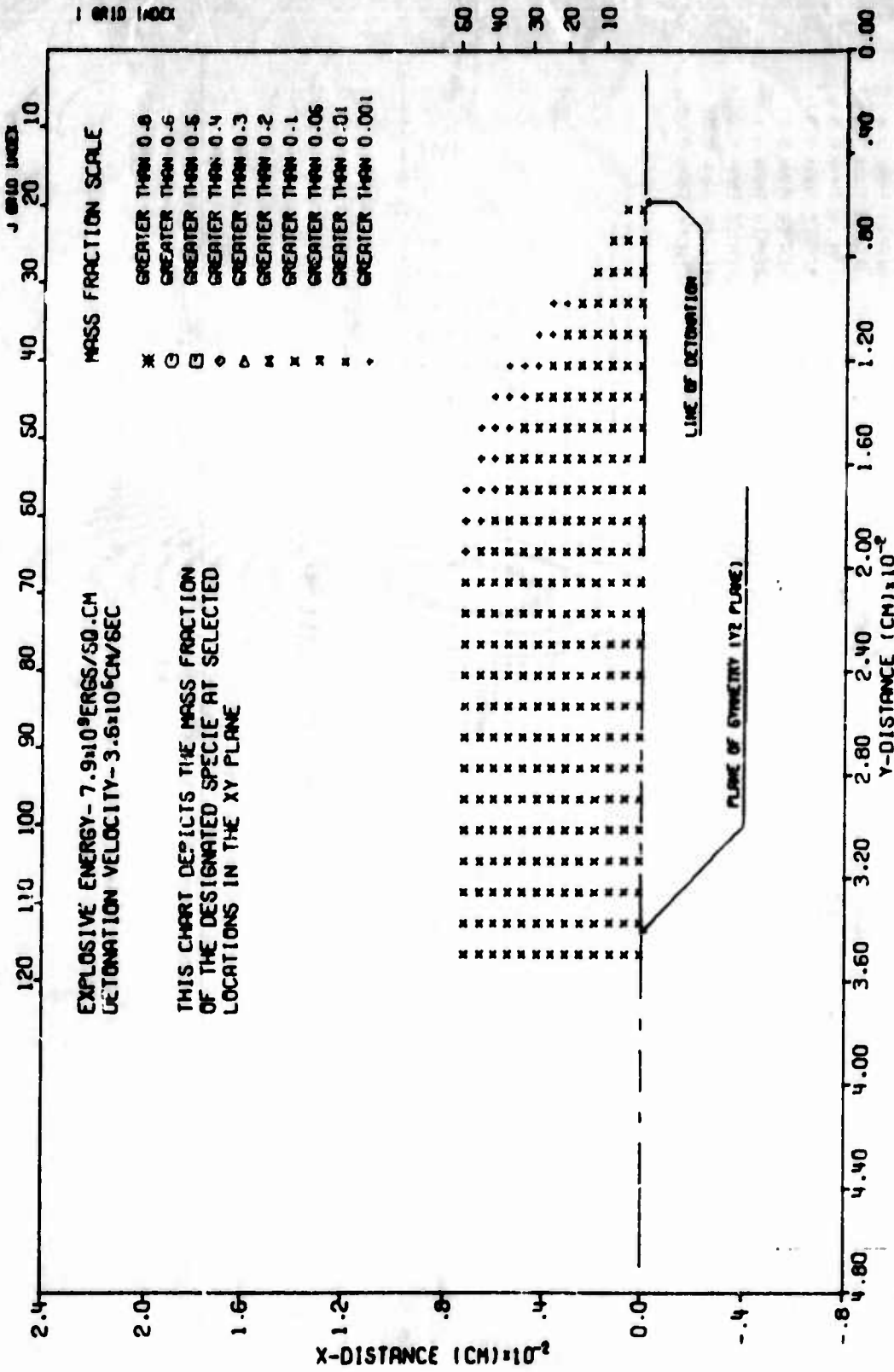
Figure D9. Mass Distribution--Species D (Carbon Dioxide)



SHELTC7 CALCULATION OF EXPLOSIVE SOURCE IN HYPERSONIC FLOW (WITH PDC)
TIME .005041 SEC CYCLE 1200 PROBLEM 30.000

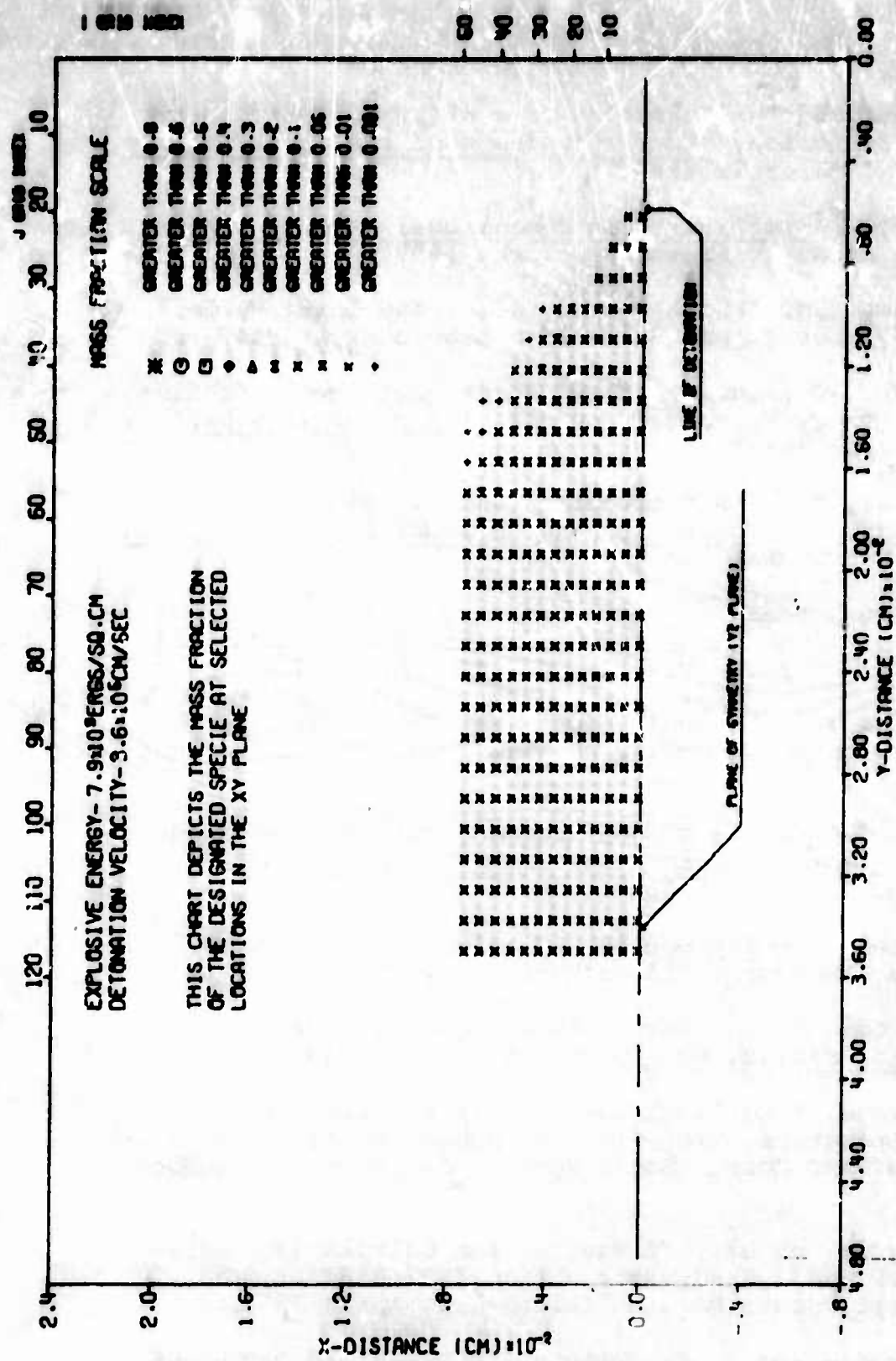
Figure D10. Mass Distribution--Species E (Water)

I GRID INDEX



SHELTC7 CALCULATION OF EXPLOSIVE SOURCE IN HYPERSONIC FLOW (WITH PDC)
TIME .005041 SEC CYCLE 1200 PROBLEM 30.000

Figure D11. Mass Distribution--Species F (Hydrogen)



SHELTC7 CALCULATION OF EXPLOSIVE SOURCE IN HYPERSONIC FLOW (WITH PDC)
TIME .005041 SEC CYCLE 1200 PROBLEM 30.000

Figure D12. Mass Distribution--Species G (Carbon).

REFERENCES

1. G. I. Taylor, "The Formation of a Blast Wave by a Very Intense Explosion," The Proceedings of the Royal Society, Vol. 201A, March 22, 1950.
2. L. I. Sedov, Similarity and Dimensional Methods in Mechanics, Academic Press, New York, 1959.
3. J. Von Neumann, "Shock Hydrodynamics and Blast Waves," AECD-2860, Los Alamos Scientific Laboratory, 1944.
4. S. C. Lin, "Cylindrical Shock Waves Produced by Instantaneous Energy Release," Journal of Applied Physics, Vol. 25, pp. 54-57, 1954.
5. A. Sakurai, "On the Propagation and Structure of the Blast Wave, I," Journal of the Physical Society of Japan, Vol. 8, No. 5, Sep.-Oct., 1953.
6. J. Von Neumann and R. D. Richtmeyer, "A Method for the Numerical Calculation of Hydrodynamic Shocks," Journal of Applied Physics, Vol. 21, p. 232, March 1950.
7. H. L. Brode, "Numerical Solution of Spherical Blast Wave," Journal of Applied Physics, Vol. 26, No. 6, June 1955.
8. H. H. Goldstine and J. Von Neumann, "Blast Wave Calculations," Communications on Pure and Applied Math, Vol. VIII, pp. 327-354, 1955.
9. H. L. Brode, "Point Source Explosion in Air," RM-1824-AEC, The RAND Corp., Santa Monica, California, 1956.
10. H. L. Brode, "Blast Wave from a Spherical Charge," The Physics of Fluids, Vol. 2, No. 2, March 1959.
11. H. L. Brode, "The Blast Wave in Air Resulting from a High Temperature, High Pressure Sphere of Air," RM-1825-AEC, The RAND Corp., Santa Monica, California, December 1956.
12. H. L. Brode, et al., "A Program for Calculating Radiation Flow and Hydrodynamic Motion," RM-5187-PR, The RAND Corp., Santa Monica, California, April 1967.
13. R. N. Brodie and J. E. Hormuth, "PUFF-66 and P-PUFF-66 Computer Programs," AFWL-TR-66-48, Air Force Weapons Laboratory, Kirtland AFB, New Mexico, June 1966.

14. M. Lutzky, "The Flow Field Behind a Spherical Detonation in TNT Using the Landau-Stanyukovich Equation of State for Detonation Products," NOLTR 64-40, U.S. Naval Ordnance Lab., White Oak, Md., Feb. 1965.
15. F. H. Harlow, "The Particle-in-Cell Computing Method for Fluid Dynamics," Methods in Computational Physics, Vol. 3, p. 319, Academic Press, New York, 1964.
16. W. A. Whittaker, et al., "Theoretical Calculations of the Phenomenology of HE Detonations," AFWL TR-66-141, Vol. I, Air Force Weapons Lab., Kirtland AFB, New Mexico, November 1966.
17. W. E. Johnson, "OIL-A Continuous Two-Dimensional Hydrodynamic Code," GAMD-5580, General Atomic/General Dynamics, San Diego, California, October 1964.
18. E. A. Nawrocki, et al., "Theoretical Calculations of the Phenomenology of the Distant Plain Event 6," AFWL TR-67-57, Air Force Weapons Lab., Kirtland AFB, New Mexico, 1967.
19. C. E. Needham, et al., "Theoretical Calculations of the Detonation of a 1000 Pound Sphere of TNT at 15 Feet Above Ground Level," AFWL TR-66-128, Air Force Weapons Lab., Kirtland AFB, New Mexico, 1966.
20. C. E. Needham and T. Burghard, "Airblast Calculation, Event MINEUNDER," AFWL TR-69-105, Air Force Weapons Lab., Kirtland A B, New Mexico, 1969.
21. J. G. Trulio, "Theory and Structure of the AFTON Codes," AFWL TR-66-19, Air Force Weapons Lab., Kirtland AFB, New Mexico, June 1966.
22. C. N. Kingery, "Air Blast Parameters Versus Distance for Hemispherical TNT Surface Bursts," BRL Report No. 1344, Ballistics Research Lab., Aberdeen, Md., 1966.
23. J. W. Reed, "Operation SAILOR HAT-Long Range Air Blast," DASA POR 4057, Defense Atomic Support Agency, Washington, D.C., 1966.
24. H. E. Auld, G. P. D'Arcy, and G. G. Leigh, "Simulation of Air-Blast-Induced Ground Motions," WLRT-65-26, Vol. I, Air Force Weapons Lab., Kir'tland AFB, New Mexico, April 1965.
25. W. S. Filler, "Explosions in Enclosed Spaces," NAVORD Report 3890, U.S. Naval Ordnance Lab., White Oak, Md., Jan. 1956.

26. V. P. Korobeynikov, et al., "The Theory of Point Explosions," JPRS:14,334-U.S. Dept. of Commerce, Office of Technical Services, Joint Publications Research Services, Washington, D.C., 1962.
27. R. J. Swigart, "Third-Order Blast Wave Theory and its Application to Hypersonic Flow Past Blunt-Nosed Cylinders," Lockheed Aircraft Corp., Space and Missile Division, Palo Alto, Calif., July 1960.
28. E. F. Roemer, "On Similar Solutions for Strong Elast Waves and Their Application to Steady Hypersonic Flow," Journal of Aerospace Sciences, June 1962.
29. W. D. Hayes and R. F. Probstein, Hypersonic Flow Theory, Vol. 1, Academic Press, New York, 1966.
30. J. Von Mises, Mathematical Theory of Compressible Flow, Academic Press, New York, 1958.
31. P. I. Chushkin and L. Li-Kan, "Determination of the Parameters of Supersonic Two-Dimensional Flows of Gas," translation of a Russian paper, FTD-HT-66-465/1+2+4, Foreign Technology Division, Wright-Patterson AFB, Ohio, Dec. 1963.
32. G. G. Leigh and J. Yagla, "A Study of Shock Structure from Hydrodynamic Codes," to be published.
33. L. Lees and T. Kubota, "Inviscid Hypersonic Flow Over Blunt-Nosed Slender Bodies," Journal of Aerospace Science, Vol. 24, pp. 195-202, 1957.
34. M. A. Cook, The Science of High Explosives, Reinhold Publishing Corp., New York, 1958.
35. R. Durrett, et al., "The INSHALLA Calculation," AFWL TR-69-85, Air Force Weapons Laboratory, Kirtland AFB, New Mexico, 1969.
36. O. A. Hougen and K. M. Watson, Chemical Process Principles, Vol. I, John Wiley and Sons, New York, 1943.
37. R. A. Strehlow, Fundamentals of Combustion, International Textbook Co., Scranton, Penn., 1968.
38. JANAF Thermochemical Tables, Clearing House for Federal Scientific and Technical Information, U.S. Dept. of Commerce, Springfield, Virginia.
39. J. A. Owczarek, Fundamentals of Gas Dynamics, International Textbook Co., Scranton, Penn., 1964.

40. R. Bork, N. Brooks, and R. Papetti, "A Numerical Technique for Solution of Multidimensional Hydrodynamic Problems," RM-2628-PR, The RAND Corp., Santa Monica, California, December 1963.
41. G. A. Hawkins and J. M. Smith, "Equilibrium Constants for Seventeen Gas Reactions," Research Series No. 108, The Engineering Experiment Station, Purdue University, Lafayette, Indiana, May 1949.
42. S. S. Cherry, et al., "Identification of Important Chemical Reactions in Liquid Propellant Rocket Engines," Pyrodynamics, Vol. 6, pp. 275-296, Gordon & Breach, Science Publishers Ltd., Northern Ireland, 1968.
43. J. M. Dewey, "The Air Velocity in Blast Waves from TNT Explosions," Proceedings of the Royal Society, A, Vol. 279, pp. 366-385, 1964.
44. T. A. McArtor, "Aerodynamic Interaction Effects Near a 2-D Sonic Jet Exhausting Normal to a Flat Plate Into a Mach 2.96 Free Stream," Masters Thesis, Arizona State U., Tempe, Ariz., Feb. 1971.

~~UNCLASSIFIED~~

Security Classification

DOCUMENT CONTROL DATA - R&D

(Security classification of title, body of abstract and indexing annotation must be entered when the overall report is classified)

1. ORIGINATING ACTIVITY (Corporate author)		2d. REPORT SECURITY CLASSIFICATION UNCLASSIFIED
Air Force Weapons Laboratory (PAZV) Kirtland Air Force Base New Mexico, 87117		2d. GROUP

3. REPORT TITLE

A CALCULATION OF THE BLAST WAVE FROM THE CONSTANT VELOCITY DETONATION OF AN EXPLOSIVE SHEET

4. DESCRIPTIVE NOTES (Type of report and inclusive dates)

July 1969-June 1971

5. AUTHOR(S) (First name, middle initial, last name)

Gerald C. Leigh, Maj, USAF

6. REPORT DATE

November 1971

7a. TOTAL NO. OF PAGES

276

7b. NO. OF REFS

44

8. CONTRACT OR GRANT NO.

9a. ORIGINATOR'S REPORT NUMBER(S)

9. PROJECT NO.

06CB

AFWL-TR-71-137

c.

9b. OTHER REPORT NO(S) (Any other numbers that may be assigned to this report)

d.

10. DISTRIBUTION STATEMENT

Distribution limited to US Government agencies only because test and evaluation information is discussed in the report (Nov 71). Other requests for this document must be referred to AFWL (DEV), Kirtland AFB, NM, 87117.

11. SUPPLEMENTARY NOTES

12. SPONSORING MILITARY ACTIVITY

AFWL (DEV)
Kirtland AFB, NM 87117

13. ABSTRACT

(Distribution Limitation Statement B)

Predictions of the blast wave from the constant velocity detonation of a thin explosive sheet have not previously considered the contribution of the postdetonation combustion of the detonation products. This problem is simplified by first considering the explosive material as releasing only energy into an ideal gas medium. This is solved for several energy densities and velocities of detonation. An expression that can predict the shape and location of the shock front from a line source of energy in a hypersonic flow is then developed. The problem is more realistically modelled by considering the explosive sheet to release six distinct mass species, as well as energy, into a mixture of nitrogen and oxygen. Results of this study shift the shock front to a position inside the previously determined shock front. Using the dissociation of molecular oxygen as the determinant for the reaction rate of combustion, and models for material mixing, the contribution of postdetonation combustion (PDC) to the total energy is determined. The mass and energy addition problems were then recomputed with PDC included. Results indicate that while significant amounts of energy are released by PDC, they are small compared to the energy released by the detonation, and there is essentially no contribution from PDC in the early time formation of the blast wave.

DD FORM 1 NOV 68 1473

~~UNCLASSIFIED~~

Security Classification

Security Classification

KEY WORDS	LINE A		LINE B		LINE C	
	ROLE	DT	ROLE	DT	ROLE	DT
Civil engineering Blast wave Explosive sheet Postdetonation combustion						

UNCLASSIFIED

Security Classification